STUDIES ON THE WATER VASCULAR SYSTEM OF REGULAR ECHINOIDS

Alan Michael Raymond

A Thesis Submitted for the Degree of PhD
at the
University of St Andrews

1979

ABSTRACT

The water vascular system is a highly modified mesocoel which is unique to the phylum Echinodermata. Hypotheses for the evolution of the water vascular system and its relationship to the mesocoel of other oligomerous animals are discussed. A scanning electron microscope survey of the skeletal structures associated with the water vascular system provides the first description of the ultrastructure of the madreporite, terminal tube foot plate, peristomial tube foot plate, tube foot (peristomial and ambulacral) disk elements.

The relationship between the structure and function of skeletal elements is discussed, with particular emphasis on the madreporite and differences between the pores and disk elements of ambulacral and peristomial tube feet.

The fine structure and innervation of the following intrathecal regions of the water vascular system were investigated: madreporite, axial organ, stone canal, circumoesophageal and radial water canals.

It is postulated that the water vascular system has an important role in the transport, processing and removal of amoebocytes. The Polian vesicles and axial organ are major sites for amoebocyte collection and the axial organ processes amoebocytes prior to their removal via the madreporite. It is proposed that the madreporite is an excretory structure and necrotic amoebocytes and waste materials are evacuated by the ciliary activity of the endothelial cells lining the madreporite canal.

On the basis of ultrastructure and fluorescence histochemistry, it is postulated that the aminergic axons of the

basiepithelial plexus have a cilio-effector role and thus respiratory currents generated by ciliated epithelial cells are under neuronal control.

The fine structure and innervation of the tube foot/ampulla complex was investigated. The three muscle groups of the complex consist of the disk levator muscle (D.L.M.), stem retractor muscles (S.R.M.) and ampulla muscles. It is proposed that the D.L.M. and ampulla muscles are structurally/functionally distinct from the S.R.M. with respect to endurance, speed of contraction and range. It is also proposed that the "changing acting partners" model for molluscan smooth muscle can also be applied to echinoderms' smooth muscle.

The innervation of the tube foot/ampulla complex is rather unusual and it is proposed that a tube foot/ampulla ganglion occurs at the base of the tube foot within the perradial pore. Modified muscle processes termed muscle tails pass into the perradial pore and are innervated by motoneurons within the tube foot/ampulla ganglion. In addition, peripheral neurons termed L.D.S.G. cells innervated S.R.M., D.L.M., and connective tissue of tube feet and the inner muscle layer and connective tissue of the axial organ and Polian vesicles.

The L.D.S.G. cells have been characterised histochemically and cytochemically and it is proposed that they elaborate a glycoprotein which has an important role in regulating cation fluxes within the connective tissue and musculature. The histochemistry and cytochemistry of tube foot connective tissue was investigated and the relationship between collagen filaments and glycoproteins and glycosaminoglycans are described.

STUDIES ON THE WATER VASCULAR SYSTEM OF REGULAR ECHINOIDS

by

ALAN MICHAEL RAYMOND

Gatty Marine Laboratory,
The University,
ST. ANDREWS,
Fife.

October, 1979.

A thesis submitted for the degree of

Doctor of Philosophy

SUPERVISOR'S CERTIFICATE

I certify that Alan Michael Raymond has fulfilled the conditions laid down under Ordinance No. 16 of the University Court, St. Andrews, and is accordingly qualified to submit this thesis for the degree of Doctor of Philosophy.

DECLARATION

I declare that the work reported in this thesis is my own and has not previously been submitted for any other degree.

VITAE

I was educated at Letchworth Grammar School (Letchworth, Hertfordshire) and I obtained a B.Sc. (Hons.) in Zoology at the University of Newcastle-upon-Tyne in July 1976. The work described in this thesis was undertaken during the period October 1976 until September 1979.

STUDIES ON THE WATER VASCULAR SYSTEM OF REGULAR ECHINOIDS

CONTENTS - PART 1

Tables (1-9) occur within the text.

Line figures (I-XXX) occur at the end of each relevant chapter. Micrographs and chart recordings (1-199) occur within PART 2.

Acknowledgements

This study was carried out with the financial support of the Science Research Council, under the supervision of Professor M.S. Laverack and I would like to express my gratitude to both for their assistance and encouragement during my postgraduate training.

I am grateful for the invaluable assistance of various people in the 'Gatty' and other departments within the University; particularly I must mention Dr. J.L.S. Cobb, Dr. D.B. Scott, Dr. C. Muir, Dr. P.A.V. Anderson, Dr. C. Evans, Professor J.W. Smith, Linda McQueen and Dr. A. Serafini-Fracassini.

I would like to thank Dr. A.C. Campbell (University of London) for the specimens of a variety of echinoids, and Dr. H.Y. Elder (University of Glasgow) for his invaluable assistance with obtaining X-ray microanalysis data. Many thanks also to Christina Lamb for deciphering my hieroglyphics so efficiently!

Last but not least, this thesis would not have been completed without the marvellous co-operation of Baby Anna and the encouragement of my wife Lynne.

CHAPTER 1

GENERAL INTRODUCTION

Why study the echinoid water vascular system?

'Why not' would, of course, be the simpler but rather negative and unconstructive answer. In order to provide a cogent explanation of the rationale for this present study it is necessary to give some perspective of the phylum Echinodermata and to discuss its relationships with other phyla.

The phylum Echinodermata consists of 5,300 known species (BARNES 1968) which are mostly marine (some inhabit brackish waters) and mainly benthic. There is some confusion over the precise taxonomic divisions of the phylum as most standard Zoology texts still use a classification based upon the mode of life of the echinoderm. In this way the sessile, attached echinoderms, including the extant crinoids and several extinct groups (e.g. eocrinoids, cystoids, blastoids etc.) were grouped under the sub-phylum Pelmatozoa. Free living echinoderms such as the echinoids, asteroids, ophiuroids and holothuroids were grouped under the sub-phylum Eleutherozoa. However, this system of classification is not corroborated by palaeontological evidence and does not take into account the comparative morphology of the various groups.

FELL (1962) has prepared a more phyletic classification which sub-divides the phylum into a number of sub-phyla: Crinozoa, Asterozoa, and Echinozoa (plus the extinct Homalozoa and Haplozoa). The only extant Crinozoans are the crinoids which comprise the sessile, stalked forms, which are mainly abyssal, and the more successful commatulids which have lost the stalk and become free living. Thus the differing habits of the crinoids were a slight embarrassment to the original classification system.

CLASS ECHINOIDEA

Sub-class Perischoechinoidea			
	Order Cidaroida		e.g. *Cidaris*
Sub-class Euechinoidea			
Regularia	(Super-order Diadematacea		e.g. 'Typical' sea-urchins
	(Super-order Echinoidea		
Irregularia	(Super-order Gnathostomata		e.g. Sea urchins, sand dollars
	Super-order Atelostomata		e.g. Heart urchins

TABLE 1

Classification of the major taxonomic divisions of the class Echinoidea. Only extant groups are shown.

The more primitive echinoid group is the Perischoechinoidea of which there is only one extant order, the Cidaridea. The sub class Echinoidea includes all other extant echinoids and is divided into two distinct groups, the Regularia and Irregularia. Regular echinoids typically possess a subspherical test. The irregular gnathostomata and Atelostomata both have bilateral symmetry secondarily superimposed upon the basic pentamerous body pattern producing a distinct antero-posterior axis. The development of the irregular body form is associated with a burrowing mode of life.

A feature unique to all extant echinoids, except the Atelostomata, is a complex calcareous feeding apparatus termed Aristotle's lantern.

The asterozoans comprise two classes, Asteroidea and Ophiuroidea, both of which have many extant species. The echinozoans comprise two extant classes, Echinoidea and Holothuroidea, which include the most successful extant echinoderms. For the purposes of this study an outline of the classification of the Echinoidea is necessary and is shown in Table 1. Characteristic features of the phylum Echinodermata are:

1. Pentamerous radial symmetry
2. Calcareous theca
3. Deuterostomatous development
4. Water vascular system

1) Pentamerous radial symmetry

This is secondarily derived and is not phyletically related to other radially symmetrical phyla such as the Porifera and Cnidaria. The only other example of possible pentamery in the animal kingdom is in *Priapulus caudatus* where the pharyngeal teeth occur in whorls of five. In some extant groups such as the Holothuroidea and the irregular echinoids there is a return to bilaterality which is associated with a burrowing mode of life. In these latter groups the basic pentameric body organisation is still clearly present. NICHOLS (1968) has discussed the various hypotheses for the origin of pentamery, none of them being entirely satisfactory. A pentagon represents the only regular polygon in which the number of sides is equal to the number of diagonals. Thus the ratio of the growth gradients of diagonals to sides will determine whether a pentagonal or stellate body is formed. This however, does not explain why pentamery arose in the first place. NICHOLS (1968) proposes that pentamery arose from mechanical factors acting upon the skeleton. After settlement, an echinoderm larva develops a calcareous theca which consists of several plates sutured together.

The development of the aboral (apical) region of the theca is very similar in all echinoderms and consists of a central plate, accommodating the arms, surrounded by a ring of five plates which later form the five genital plates. NICHOLS argues that five plates are laid down in order to obviate lines of weakness along suture lines. With a pentamerous arrangement the length and number of suture lines is kept to a minimum and not one suture is located directly opposite another.

2) <u>Calcareous theca</u>

All echinoderms possess a theca consisting of calcareous ossicles which may or may not articulate with one another. Holothuroids show a reduction in the number and size of ossicles which allows a greater degree of movement of the theca during burrowing activities. In common with the chordates and unlike other invertebrates, echinoderm skeletal ossicles are of mesodermal origin. The echinoderm skeleton is unique in structure, consisting of a fenestrate meshwork or 'stereom'.

3) <u>Deuterostomatous development</u>

Echinoderm ova are homolecithal and after fertilization, early embryology is quite uniform throughout the phylum and displays the basic features of deuterostomatous development, i.e. the blastopore forms the anus, cleavage is radial and indeterminate, and the coelomic cavities arise by enterocoelus pouching.

4) <u>Water vascular system</u>

Unique to the echinoderms is a series of coelomic canals which constitute a water vascular system. In all echinoderms pentamerous radial symmetry has a profound effect on the water vascular system and the other tubular coelomic systems (periphaemal and haemal) and also the nervous system. Each of these systems consists of a circumoesophageal ring, five radial vessels passing from it to supply the tube feet and a single axial vessel passing from the ring towards the apical side of the body.

A more detailed description of the regular echinoid water vascular system and its relationship with the nervous system is diagrammatically illustrated in Fig. I. Communicating with the exterior via the madreporite is the axial complex and passing from it to the circumoesophageal water ring is the stone canal. Arising radially from the water ring are five small evaginations termed Polian vesicles. Arising interradially are five radial water canals, each of which has a single recurrent branch which bifurcates and terminates as a pair of peristomial tubefeet protruding through the peristomial membrane. Lateral branches off the radial canals pass through ambulacral regions of the theca terminating as ambulacral tube-feet. Finally, each radial canal terminates as a terminal tube foot. Associated with each peristomial and ambulacral tube foot is a muscular sac, the ampulla, which is responsible for the extension of water vascular fluid into the tube foot thereby extending it. Each tube foot consists of a slender stem which expands distally forming a disk. Copius production of a mucoid bioadhesive by the disk epithelia enables attachment of the tube feet to the substratum. The disks of ambulacral tube feet are further modified by the development of musculature which can raise the disk surface forming a sucker. Peristomial tube feet are shorter and stouter than ambulacral tube feet and do not show the same degree of extension. Terminal tube feet are considerably reduced in size and are non-suckered.

So far, only the general structure of the water vascular system has been discussed; what of its function?

NICHOLS (1972) states that 'the function of the water vascular system is to generate, distribute and control hydrostatic pressure necessary for the operation of tube feet. Secondarily it may also serve other functions which utilise the close proximity of the water vascular fluid with the surrounding sea water...' Thus in the echinozoans and asterozoans, the prime roles of the water vascular system are locomotion and respiration. As with all generalizations there is an exception; one group of holothurians have secondarily lost the tube feet and consequently this group has been termed the Apoda. Tube foot loss in the Apoda is associated with the increased importance of the body wall in the burrowing activity of holothurians.

It is known from palaeontological evidence that the earliest and most primitive echinoderms were crinozoans. If we examine living representatives of this group, the crinoids, then we observe that the tube feet play an important role in filter feeding, not locomotion. Crinozoans are distinct from other echinoderms in that associated with the filter feeding process the mouth is directed upwards and thus 'dorsal'. NICHOLS (1960) has described a division of labour among the tube feet of the commatulid <u>Antedon</u> (a species particularly common on the west coast of Scotland) which shows a remarkable degree of complexity. The commatulids are free living but all other crinoids are sessile and in the latter the filter feeding process is essentially the same (PAUL 1977). In the Asterozoa and Echinozoa, locomotion is fundamental to all their modes of feeding. Predation, scavenging, herbivorous browsing and deposit feeding all require movement of the animal within the habitat in order to locate a fresh supply of food. Since food location occurs by the stimulation of a chemo-tactic sensory system, the oral surface of 'eleutherozoan' echinoderms becomes opposed to the substratum; i.e. the mouth is directed downwards. Thus the original crinozoan feeding orientation becomes inverted (see Fig. II) and associated with this change, the water vascular system undertakes an important role as a locomotor system. Most authors emphasise these changes in the water vascular system but do not discuss the significance of a sensory role for the system. In crinozoans the tube feet play an important role in the detection of food and the stimulation of mucous production by the epithelia in order to package particles into a food bolus which is passed down the pinnules and arm to the mouth. The sensory capacity of crinozoan tube feet is surely a significant pre-adaptation to their subsequent role in echinozoans and asterozoans. The co-ordinated locomotor activities of tube feet would not be possible without a considerable degree of sensory feedback which would in turn provide information about the external environment.

As tube feet are thin walled and protrude in great numbers from the echinoderm theca then they will provide a considerable surface area for the exchange of gases and metabolites. FARMANFARMAIAN (1966) and PAUL (197[illegible]) have shown that oxygen will diffuse into an echinoderm through the theca for a depth of 1–3 mm only. Thus the growth of the theca and its increased calcification forming a rigid test will have a potential 'suffocation' effect in the echinoids. In modern echinoids this is overcome by modifications of the tube foot/ampulla complex such that, in addition to its locomotor and sensory roles, it functions as a respiratory structure.

A major evolutionary trend among palaeozoic echinoderms is the development and increasing size of respiratory structures. A whole gamut of exothecal and endothecal pore structures evolved where gaseous exchange took place external or internal to the theca respectively. Most of these structures had their limitations and this may be an important factor responsible for the demise of these palaeozoic groups.

The functional efficiency of a respiratory surface can theoretically reach its maximum value and achieve 100% saturation of the internal fluid if a counter current convection system is in operation (PAUL 1977). Palaeontological evidence for counter current systems is difficult to substantiate but good 'indicators' are separate entrances and exits for the passage of opposing currents. Such structures first appeared quite early in echinoderm evolution, in the Middle Cambrian, with the occurrence of diplopores in a group of crinozoans, appropriately named the Diploporita. However, palaeontologists do not appear to have sufficient evidence as to determine whether water vascular fluid flowed through the diplopores (as opposed to perivisceral coelomic fluid). PAUL (1977) postulates that the lack of protection of diplopores by spines (c.f. tube feet in echinoids) may account for the extinction of the Diploporita in the Middle Devonian. It was not until the Middle Ordovician that the Echinoidea appeared with counter current convection in a tube foot/ampulla complex.

In echinoids the tube foot/ampulla connection consists of two canals which pass through two separate pores, the perradial and adradial pores. The diporous arrangement of tube feet is unique to echinoids, both extant and extinct. FENNER (1973) investigated counter current convection in the water vascular system of both regular and irregular echinoids. The results of this study are diagrammatically illustrated in Fig. III. Fluid circulation within the tube foot/ampulla complex consists of an excurrent flow of fluid passing via the adradial pore and incurrent flow via the perradial pore. (N.B. The perradial pore is nearest to the radial canal). A septum divides the proximal half of most echinoid tube feet and this separates the opposing currents within the lumen of the tube foot. Septae within the ampullae also guide the one way flow of fluid within the ampullae. Counter currents of perivisceral coelomic fluid pass across the ampullae towards the radial water canal and then pass from the canal deeper into the coelom.

The water vascular system is a tubular coelomic system and thus constitutes a rather unusual modification of a coelomic cavity. Crucial stages in the evolution of the metazoa were the appearance of secondary body cavities and metameric segmentation. Consequently a major theme in the evolution of the metazoa has been the elaboration of the coelom into a variety of hydroskeletal structures. It is therefore important to consider the water vascular system as a coelom, and to discuss its evolution in relation to the coelomic cavities of other phyla.

Comparative anatomy and embryology indicate that the echinoderm body is oligomerous; i.e. divided into three regions, the proto-, meso- and metasomes. The oligomerous phyla include all other deuterostomes (Hemichordates, Urochordates, Protochordates and Chordates) and the lophopherate protostomes (Ectoprocts, Phoronids, and Brachiopods). The oligomerous condition of echinoderms is best exemplified in the dipleurula larva, an early stage of larval development which is common to all asterozoans and echinozoans. The development of the dipleurula from a gastrula (see Fig. IV) consists of the formation of enterocoelic pouches which separate from the archenteron and then divide to form a posterior and anterior pair of cavities. On the left side of the animal the anterior cavity becomes bilobed forming a proto-/mesocoel. On the right side of the animal the anterior cavity degenerates and subsequently both posterior cavities enlarge forming the left and right metacoels. The mouth of the dipleurula is formed by an invagination of the ventral surface of the larva which opens into the archenteron. To complicate matters even more; in the developed dipleurula the pro-, meso- and metacoels are termed as the axo-hydro, and somatocoels respectively. An invagination of the dorsal surface of the larva opens into the axo/hydrocoel forming the hydropore. During subsequent development the axocoel fuses with the hydrocoel forming the water vascular system and the hydropore develops into the madreporite. The somatocoel forms the perivisceral coelom, genital sinuses, haemal and perihaemal canals.

A major problem in dealing with the evolution of the water vascular system and the interrelationships between echinoderms and other phyla, is the effect pentamerous symmetry has on late larval development and the adult forms. Notwithstanding these difficulties, it is more productive to consider the water vascular system as a mesocoel and relate it to the mesocoelic cavities of other oligomerous phyla.

Throughout the evolution of the coelomate phyla the mesocoel develops as a hydrostatic mechanism for the support and extrusion of soft tentacular structures. In a review of the functions of the coelom CLARK (1967) has discussed the various hypotheses regarding the origins of the echinoderm water vascular system and the following outline of these hypotheses is largely based on that work (see CLARK 1967 for details of the original papers).

Close similarities between the tornaria larva of enteropneusts and the bipinnaria of asteroids and auricularia of holothurians provide evidence for a close relationship between hemichordates and echinoderms. Consequently a major concept in deuterostome evolution is that the ancestral deuterostome was oligomerous, bilaterally symmetrical and akin to the echinoderm dipleurula. Thus the hypothetical ancestor was named as the Dipleurula.

The Dipleurula theory was first proposed by SÉMON in 1888 and was eagerly supported by BATHER in 1900. During the evolution of the Dipleurula the loss of the right axo/hydrocoels is supposedly associated with the adoption of a sessile mode of life. It is supposed that the right side of the anterior end of the animal became attached to the substratum and subsequent torsion of the gut produced hypertrophy on the left side and degeneration of the right axo/hydrocoels (see Fig. V). The primitive 'pelmatozoan' echinoderm thus had a dorsal mouth and dorso-lateral anus (Fig.VI). BATHER proposed that during later development three tentaculiferous grooves arose from the mouth and two subsequently divided producing a total of five. Five evaginations of the hydrocoel accompanied the grooves forming the radial canals.

However, CLARK describes serious drawbacks to this hypothesis which include:-

i) The '...strong overtones of HAECKEL's theory of recapitulation'.

ii) The Dipleurula is '...little more than the lowest common denominator of echinoderm and hemichordate larvae'

iii) The lack of any explanation for the function of the tentaculifous grooves

iv) The lack of any evidence of grooves in embryology.

An alternative hypothesis of SEMON, which was expanded by BURY in 1895 and MACBRIDE in 1896, created another hypothetical animal, the Pentactula (Fig. VII). In a free-living, bilateral symmetrical pentactula the water vascular system developed as a ring of five hollow tentacles which contained branches of the hydrocoel. In a similar manner to the dipleurula, the pentactula settled on the substratum and underwent torsion becoming radially symmetrical. However the main drawbacks of this hypothesis are:

i) The lack of explanation of the origin of the circumoesophageal ring vessel of the hydrocoel.

ii) The function of a tentacular system which is opposed to the substratum.

In order to provide a compromise between the dipleurula and pentactula theories, MACBRIDE in 1896 and 1914 proposed that the dipleurula possessed five tentacular outgrowths from each hydrocoel (Fig.VIII). After settlement and torsion the right axo/hydrocoel degenerates and the left hydrocoel develops into a circumoral ring of tentacles. However, MACBRIDE's 'compromise' does not provide any explanation of the function of the tentacular out-growths from the hydrocoel.

It is apparent that the dipleurula/pentactula theories are far from satisfactory and the whole concept of a free-living, ciliated organism does not accommodate the functions of coelomic cavities (CLARK 1967). The hydro-coel may have the function of supporting the tentacles but what of the axocoels and somatocoels? It is likely that an echinoderm ancestor is more akin to a hemichordate, particularly the pterobranchs.

The pterobranch origin of echinoderms was first proposed by GROBBEN in 1923 and is supported by HYMAN (1955) and CLARK (1967). CLARK considers that the 'modified' dipleurula of MACBRIDE is very similar to a pterobranch with a paired lophophore supporting five tentacles in each side (Fig. IX). In both the dipleurula and the pterobranch the tentacles are supported by the mesocoel (hydrocoel). It is proposed that the pterobranch ancestor underwent torsion producing a reduction of the right side of the lophophore. NICHOLS (1972) postulates that the external opening of the pterobranch mesocoel is 'equivalent' to the echinoderm hydropore. NICHOLS further proposes that the opening of the circumoral branchial canal of the brachiopod lophophore may also be 'equivalent' to the hydropore.

The essential difference between the pterobranch ancestor and the dipleurula is that the former is relatively sedentary. The coelomic cavities of the pterobranch would have accountable functions such as tentacle eversion and possible peristaltic body wall movements allowing a limited degree of locomotion.

NICHOLS (1967) has also postulated that echinoderms may have evolved from a sipunculid-like ancestor. Features such as a recurved gut, and a tentaculiferous proboscis which is in communication with a circumoral vessel are very similar to an echinoderm. NICHOLS proposed that the muscular compensation sacs from the circumoral vessel are responsible for the extension of the proboscis and tentacles, a situation apparently similar to that in echinoderms. Sipunculid features such as the tentacle arrangement, protostomatous development, trochophore larva and metanephridia show similarities to the lophophorate phyla. NICHOLS suggests that the development of a theca to support an enlarging lophophore would produce a structure quite similar to a crinoid arm.

In a later discussion, NICHOLS (1968) is more cautious about this hypothesis and mentions that similar modes of life may produce convergence, and sipunculids do have a totally different embryonic development to echinoderms and all other deuterostomes. Sipunculids are a rather enigmatic group because of their lack of segmentation. The formation of an 'annelid cross' during their early embryology indicates possible annelid affinities. It is interesting to note that NICHOLS' (1967) hypotheses of proboscis eversion do not agree with studies on Sipunculus nudus (von UEXKULL, 1903, ZUCKERKANDL 1950) and Dendrostoma zostericola (PEEBLES & FOX 1933) which show that the proboscis is everted by contraction of the posterior half of the body wall musculature.

Despite all the drawbacks of the theories regarding Echinoderm origins it is quite clear that the water vascular system represents a highly specialised and unusual modification of a mesocoelic cavity.

In this investigation echinoids were chosen as experimental material for a study of the water vascular system because of two factors:

a) They show the highest development of the tube foot/ampulla complex.

b) They have a highly developed skeletal system which forms interesting relationships with the water vascular system.

In particular, the regular echinoids were chosen because:

a) They are easy to collect and maintain in aquaria, unlike the irregular echinoids.

b) The irregular echinoids exhibit a wide spectrum of tube foot structure and function and this alone would justify a whole investigation.

Major regions of the water vascular system have been investigated using a variety of techniques and some of the results obtained provide evidence for interesting phenomena such as connective tissue plasticity and the neural control of ciliary activity. Perhaps the most significant results provide a characterisation of a novel type of neuron and evidence for an unusual mode of innervation of the tube foot musculature.

However, all the data obtained in this present investigation is applied to an interpretation of the water vascular system in the phylum Echinodermata as a whole.

Fig. I

Diagrammatic representation of the water vascular system of a regular echinoid. (Modified after NICHOLS 1968)

A	Anus	Ma	Madreporite
AL	Aristotle's Lantern	P	Polian vesicle
Ax	Axial gland	PTF	Peristomial tube foot
ATF	Ambulacral tube foot	RN	Radial nerve
CN	Circumoesophageal nerve ring	S	Stone canal
CW	" water ring	To	Tooth
E	Epidermis	TTF	Terminal tube foot
M	Mouth		

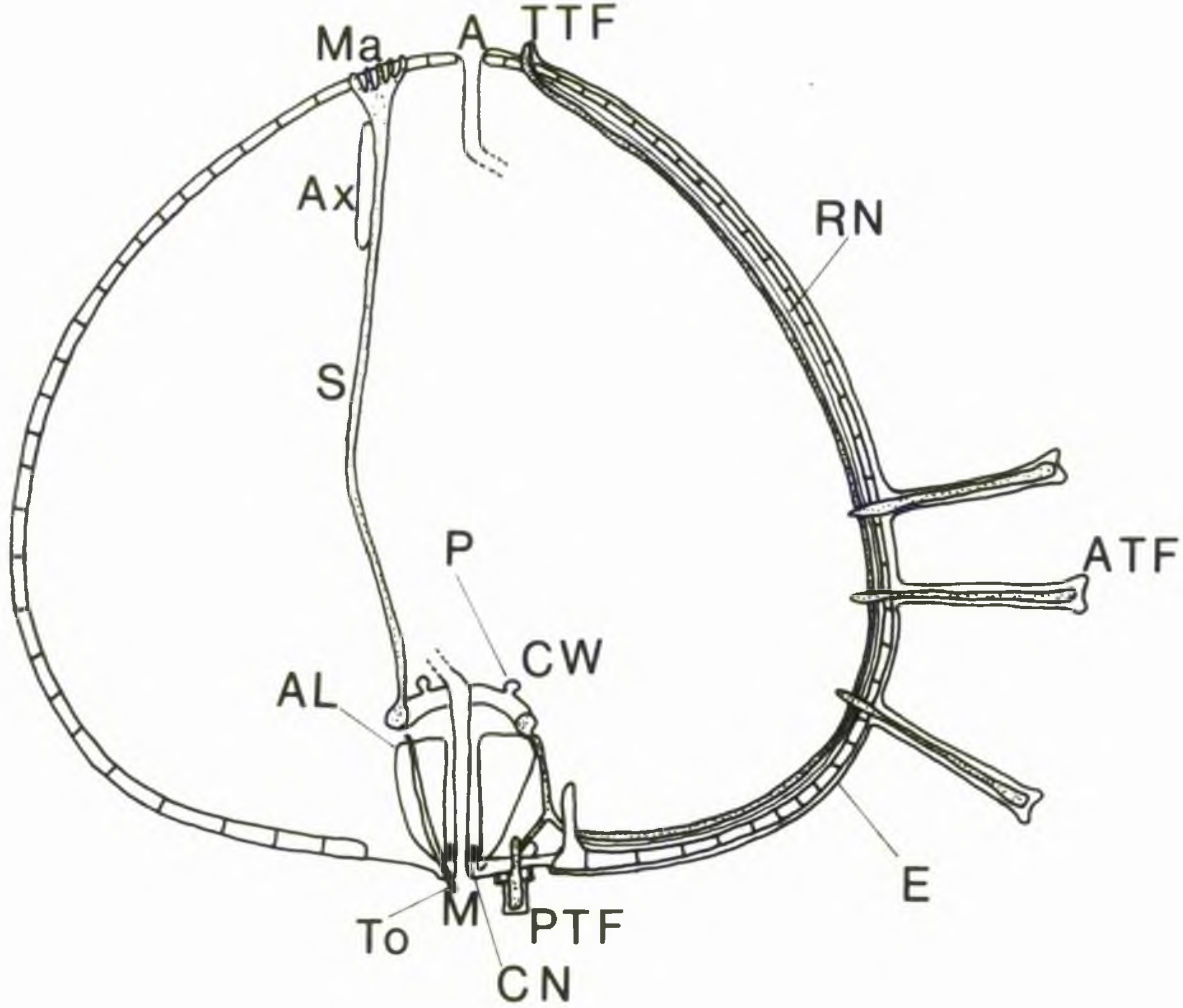

Ma
A
TTF
Ax
RN
S
P
ATF
CW
AL
E
M
PTF
To
CN

FIG. II

Evolutionary changes in the role of tube feet associated with feeding orientation

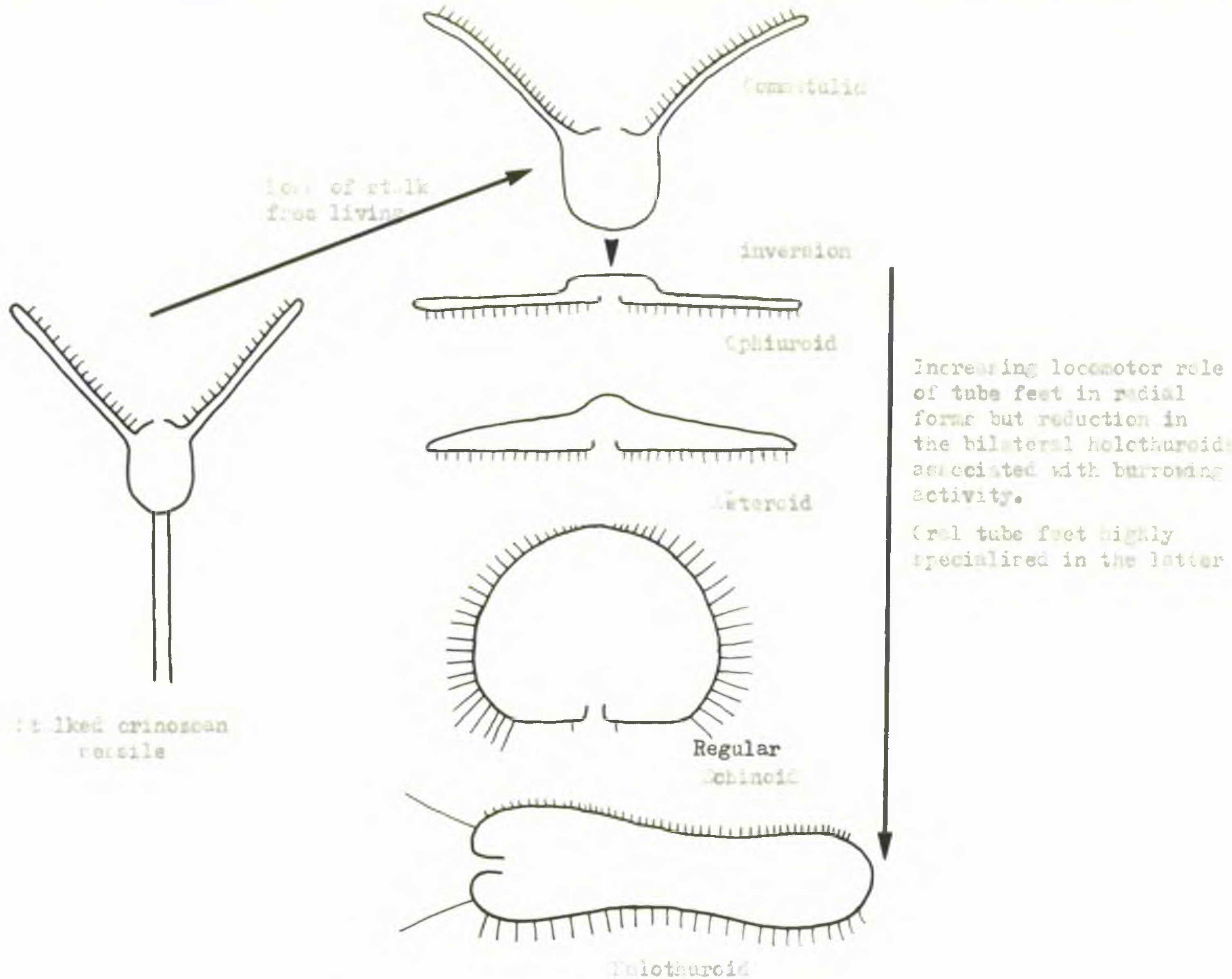
Comatulid
Loss of stalk
free living
inversion
Ophiuroid
Asteroid
Stalked crinozoan
sessile
Regular
Echinoid
Holothuroid
Increasing locomotor role of tube feet in radial forms but reduction in the bilateral holothuroids associated with burrowing activity.
Oral tube feet highly specialized in the latter

Fig. 11

FIG. III

Diagrammatic representation of counter current convection in the echinoid tube foot/ampulla complex (based upon data from FENNER 1973)

a) Current directions within tube feet/ampullae

b) Current directions across ampullae and radial water canals

a	Ampulla
l	Lateral water canal
m	Mouth
r	Radial water canal
t	Tube foot

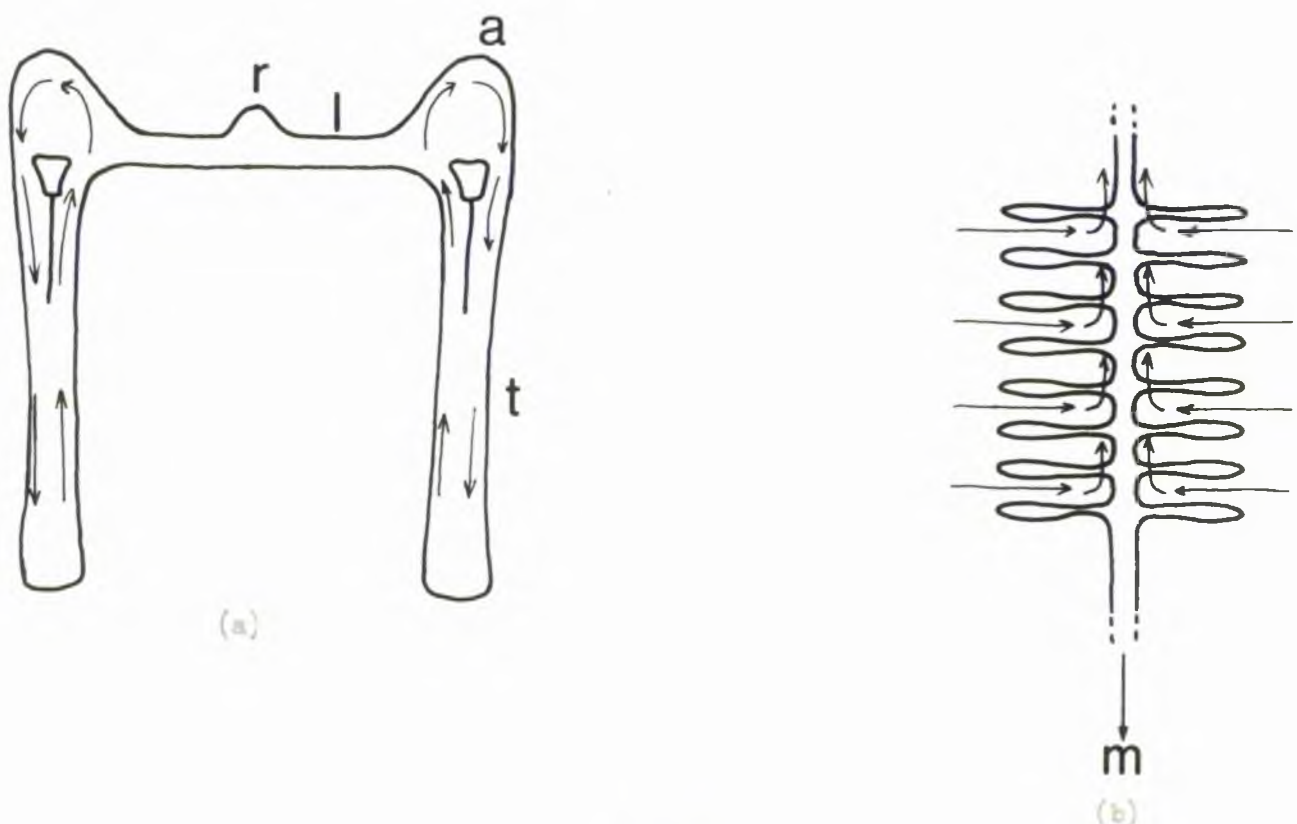

Fig. III

Fig. IV

Diagrammatic representation of the development of the dipleurula larva.

Stages 1–6 are gastrulae viewed from a ventral aspect

The dipleurula larva is viewed from the left side.

1. Blastopore formation
2. Enterocoelic pouching
3. Enterocoels
4. Enterocoels divide forming...
5. a posterior and anterior pair of cavities
6. Left anterior cavity becomes bilobed, right anterior degenerates

The left anterior cavity forms the axo/hydrocoel and the posterior cavities form the somatocoels.

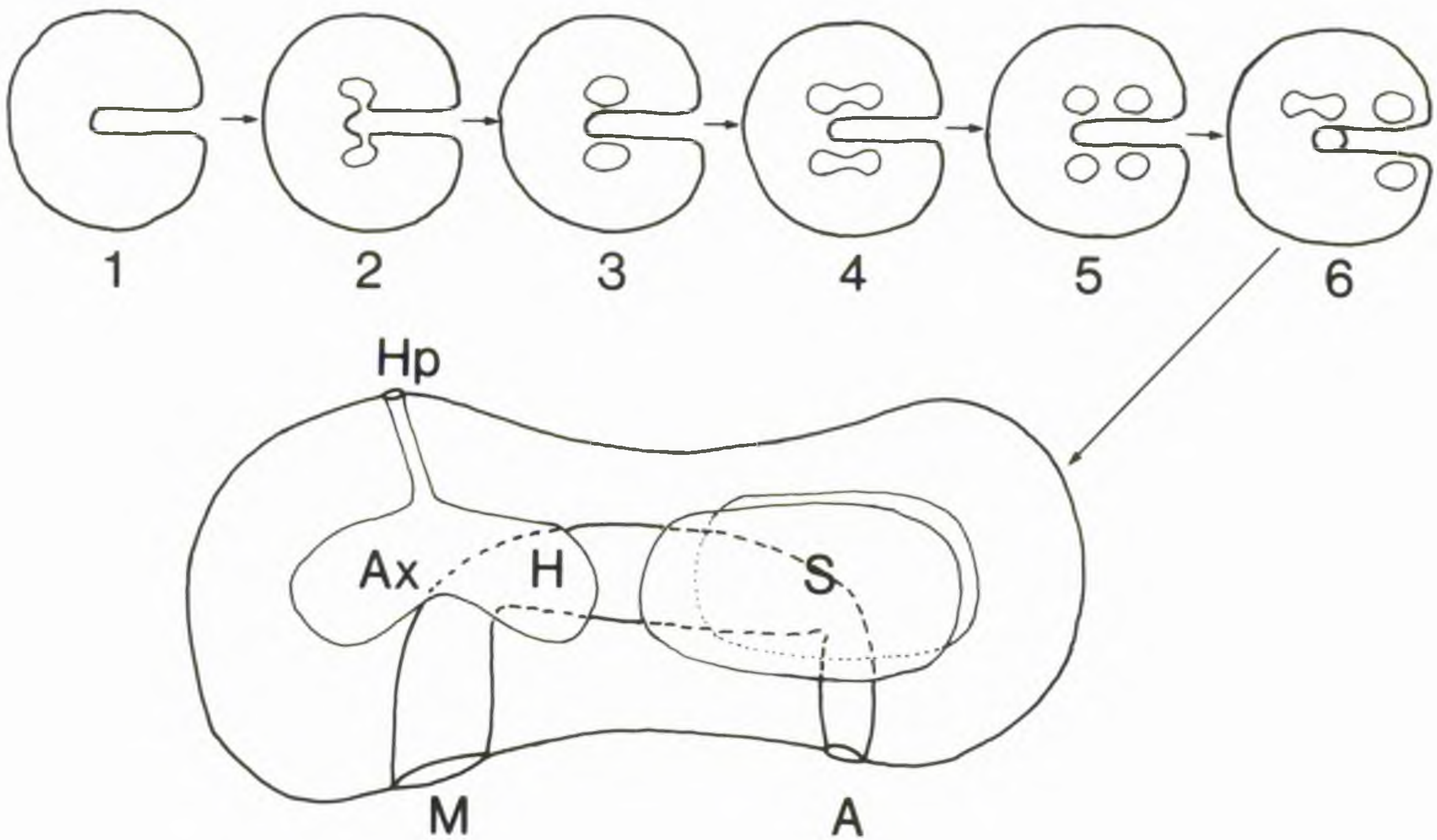
1
2
3
4
5
6
Hp
Ax
H
S
M
A

Fig. V

Diagrammatic representation of the evolution of the Dipleurula (after SEMON) showing loss of right axo/hydrocoels.

1. Ancestral, bilaterally symmetrical Dipleurula (free living)
2. Anterior end attaches to substrate, inclined on right side.
3. Torsion of gut produces 'dorsal' mouth and degeneration of right axo/hydrocoels.

a	Anus
ax	Axocoel
h	Hydrocoel
m	Mouth

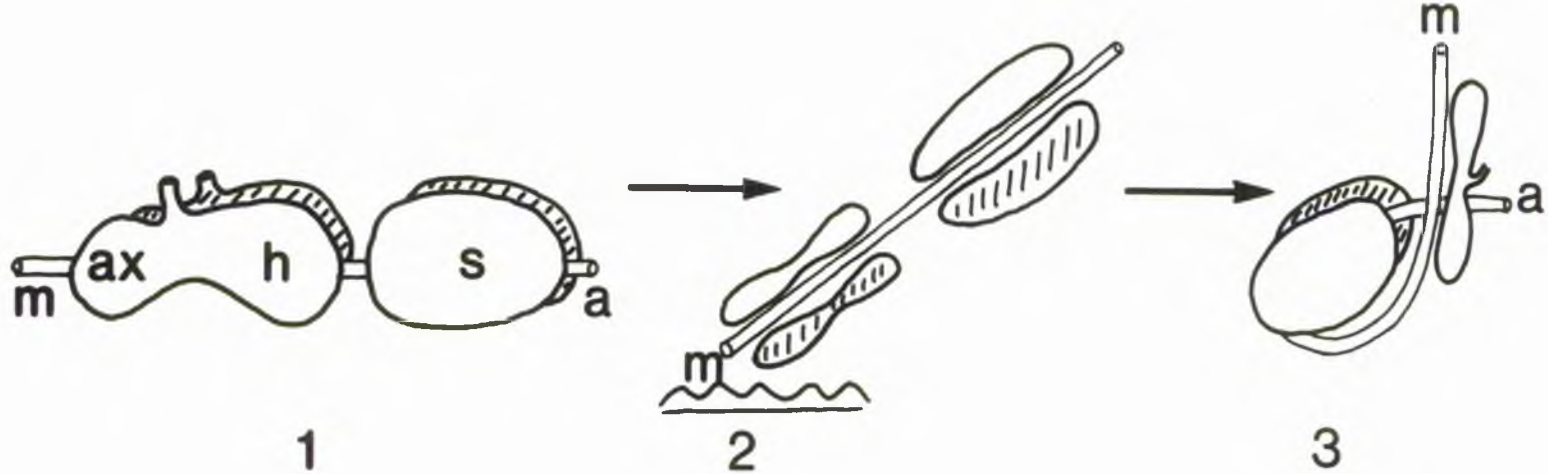
m
ax
h
s
a
m
m
a
1
2
3

Fig. VI

The dipleurula theory of the origin of echinoderms (after BATHER)

a) Free living, bilaterally symmetrical Dipleurula

b) Radially symmetrical primitive echinoderm

Figs. VI - IX are reproduced from 'Dynamics in Metazoan Evolution' (CLARK 1964) with the kind permission of Professor R.B. Clark and Clarendon Press.

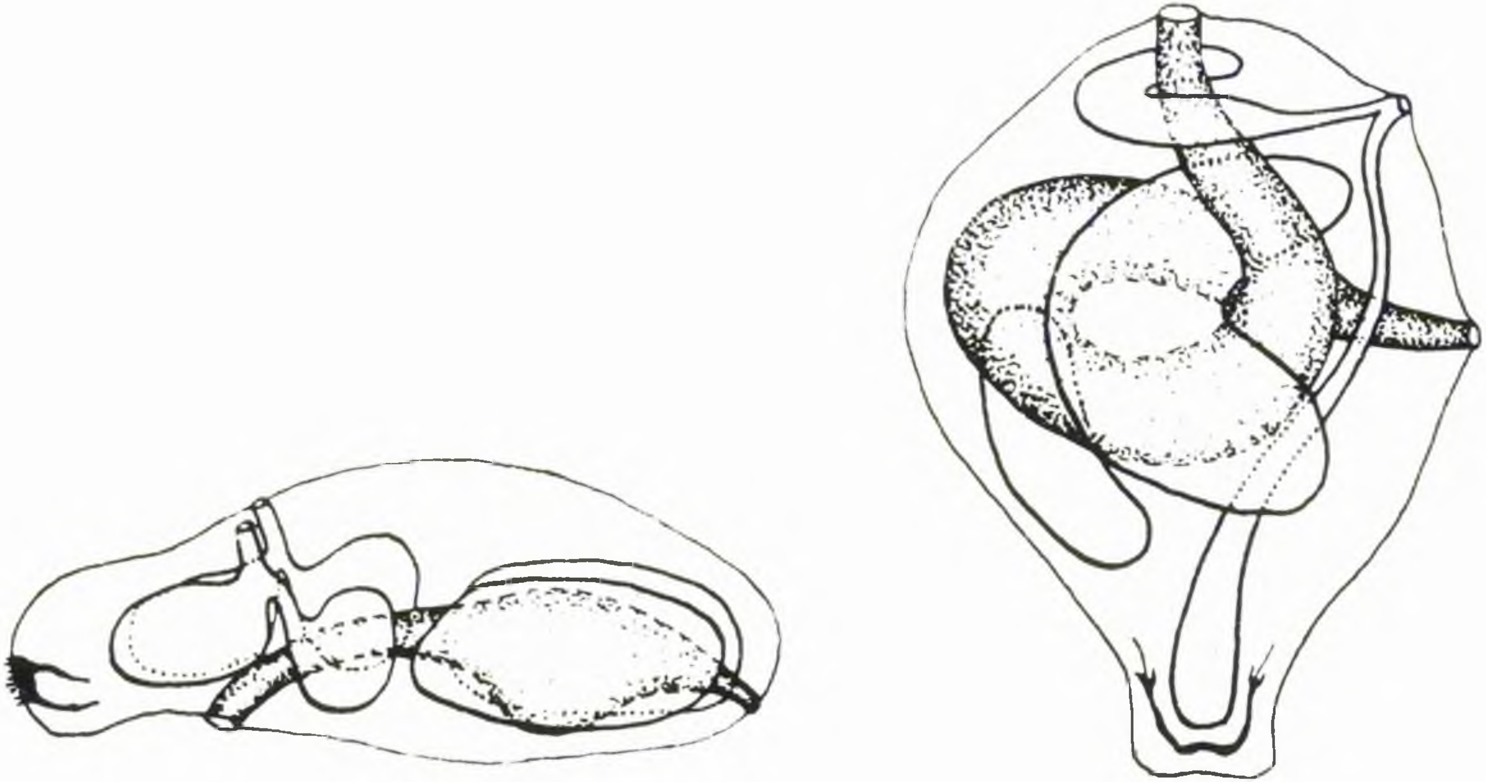

(a) (b)

Fig. VII

The Pentactula theory of the origin of echinoderms (after SEMON)

a) Free living, bilaterally symmetrical Pentactula

b), c) Settlement and torsion

d) Radially symmetrical, primitive echinoderm

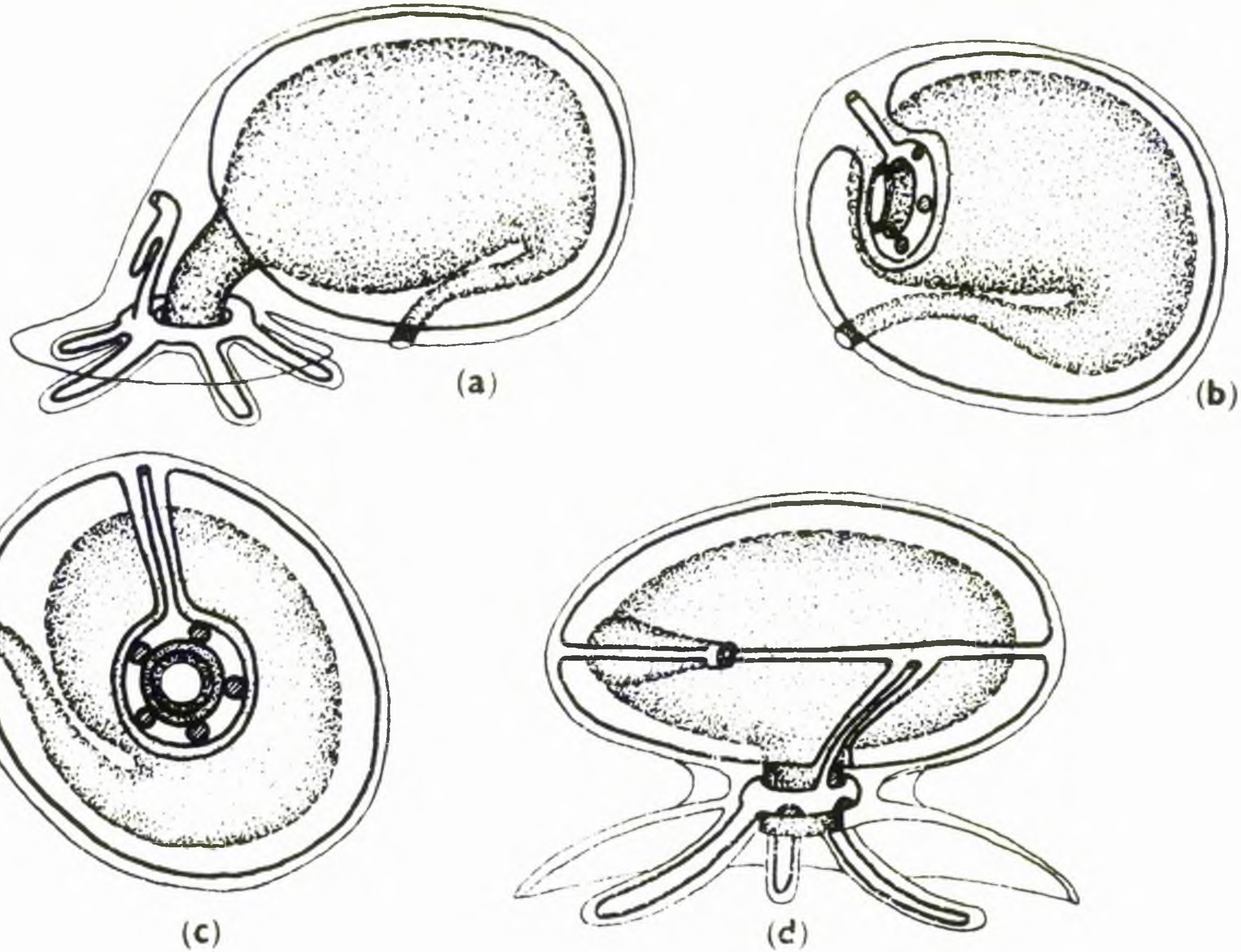
(a)
(b)
(c)
(d)

Fig. VIII

MACBRIDE'S modified dipleurula theory for the origin of echinoderms.

a) Free living, bilaterally symmetrical dipleurula with five tentacular outgrowths from each hydrocoel.

b) Sessile form after torsion.

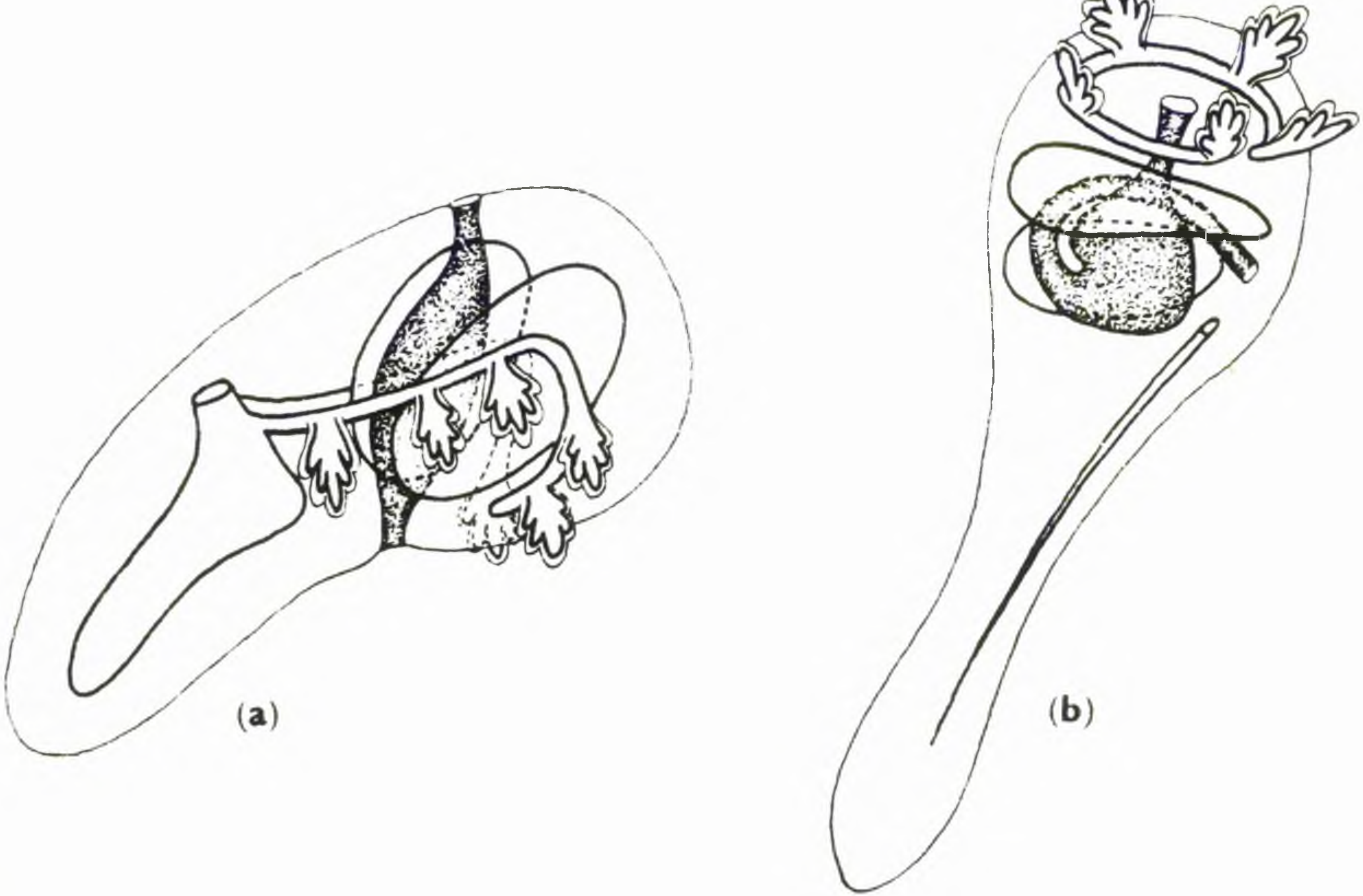

(a) (b)

__Fig. IX__

The Pterobranch theory for the origin of echinoderms (after GROBBEN)

a), b) Pterobranch-like ancestor viewed from left and ventral sides respectively. The paired lophophore supports five tentacles on each side.

c) Torsion produces a reduction in the right lophophore

d) The remaining 5 tentacles form the radial water canals

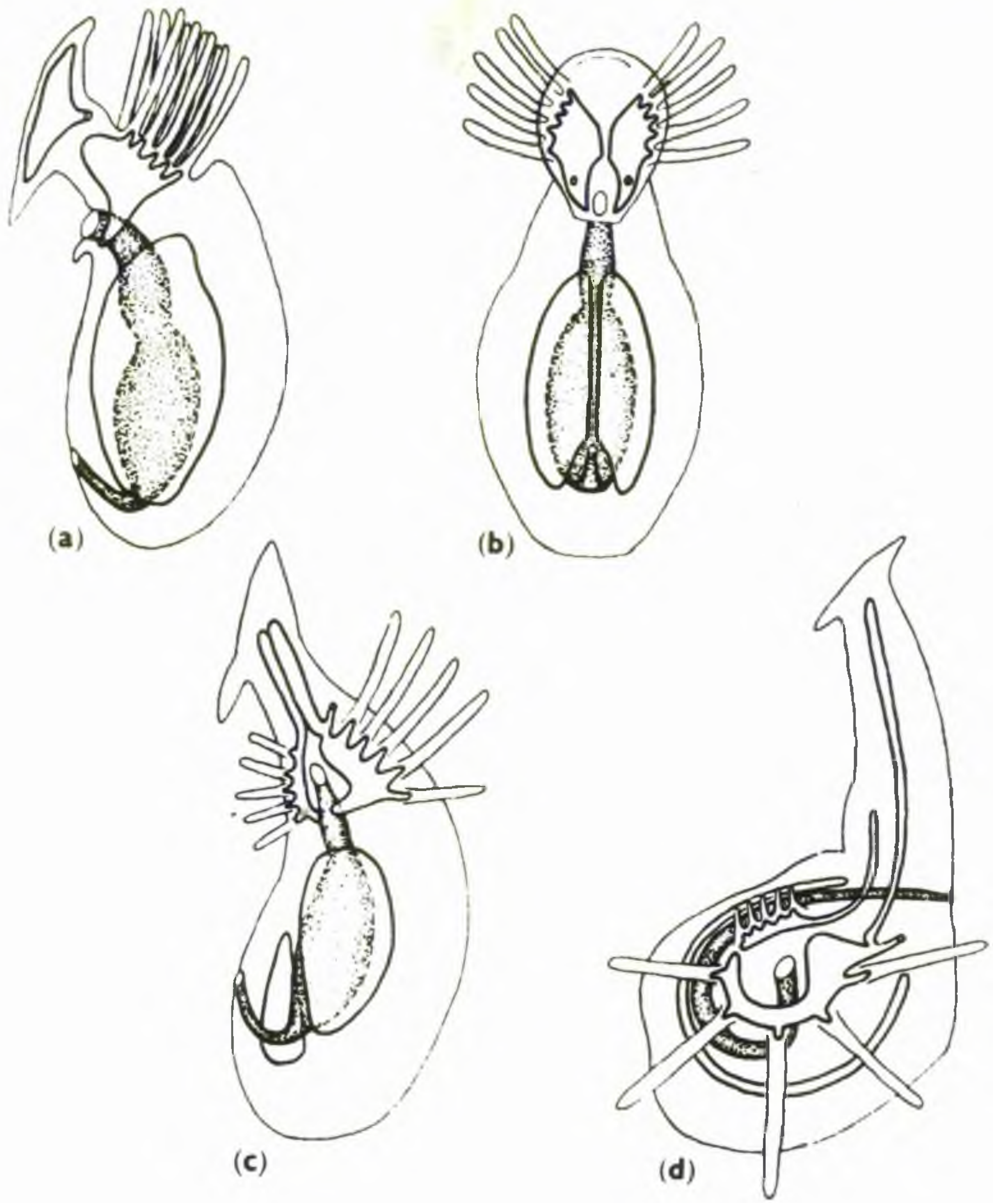
(a)
(b)
(c)
(d)

CHAPTER 2

METHODOLOGY

Sub-Class	Super Order	Order	Family	Genus
Perischoechinoidea	-	Cidaroida	Cidaridae	Cidaris cidaris
Euechinoidea	Diadematacea	Diadematoida	Diadematidae	Diadema setosum
	Echinacea	Salenioida	Saleniidae	Salenocidaris profundii
		Arbacioda	Arbaciidae	Arbacia lixula
		Temnopleurida	Temnopleuridae	Holopneustes (spp. ?)
			Toxopneustidae	Lytechinus variegatus
				Tripneustes gratilla
		Echinida	Echinidae	Psammechinus miliaris
				Echinus esculentus
			Echinometridae	Echinometra mathaei
				Evechinus chloroticus
			Strongylocentrotidae	Strongylocentrotus droebachiensis
				Strongylocentrotus purpuratus
				Strongylocentrotus pallidus

TABLE 2

Classification of the regular Echinoids used as experimental material.

METHODOLOGY

MATERIALS

Two species of regular Echinoid, Echinus esculentus and Psammechinus miliaris, were used throughout the major part of the work described in this thesis.

E. esculentus was obtained by SCUBA methods off various localities in North East Fife, in particular, the St. Andrews Bay area. Specimens were easily found most of the year, many occurring within kelp forests. During the latter part of the summer specimens were mainly found further offshore at depths exceeding 10 metres. This correlates with the migration of E. esculentus populations shorewards during winter in order to spawn.

P. miliaris was collected from rock pools in the Fife Ness area at low tides.

Both these species survived for several months after collection, in circulating seawater aquaria. Important factors influencing mortality rate were handling during collection and time of exposure to air.

For the study of the morphology of skeletal structures associated with the WVS, several species of regular Echinoid were used (listed in Table 2). Most of these specimens were alcohol fixed or dried tests.

METHODS

The following techniques were used in order to investigate the structures and function of the Echinoid WVS:

1. SEM

a) Skeletal structures.

Various regions of the test were removed and placed in a 25% solution of NaOCl for 15 minutes in order to remove the bulk the organic tissue. Following a change of NaOCl pieces of test were then placed in a sonicator for 3 minutes at 90,000 c.p.s. After sonicating again in distilled water, pieces were rinsed with absolute methanol, air dried and attached to specimen stubs with double sided 'sellotape' and carbon paint.

The process of sonication proved to be too vigorous for the small delicate structures occurring within tube foot disks and subsequently a slightly different method was used for preparing these structures.

Excised tube feet were placed in a small drop of NaOCl in a petri dish. After 15 minutes the NaOCl was replaced with distilled water and then removed using a pipette. After air drying the small skeletal structures were manipulated onto a 400 mesh TEM grid using a fine hair attached to a hypodermic needle, and then transferred to stubs covered with double sided 'sellotape'.

b) Soft Tissue

Attempts were made at SEM studies of tube foot disks. Unfortunately, conventional methods of preparation proved unsuccessful due to two factors. Firstly, the dehydration process of graded acetone series followed by critical point drying produced shrinkage of soft tissues around the skeletal structures leading to cracking of the tissue. Secondly, a mucoid bioadhesive is produced by the tube foot disk and this proved extremely difficult to remove. Placing under a stream of saline prior to fixation was ineffective. Enzymatic digestion using Hyaluronidase (Bovine testicular) or Lysozyme had deleterious effects on the soft tissue.

The most effective method, although this produced far from satisfactory results, was placing the tissue under a stream of 0.01% Ethylene-diamine-tetra acetic acid (EDTA) for approximately 5 minutes prior to fixation.

The following procedure was finally used:

i) Tube feet were excised from the test and then rinsed with a 0.01% solution of EDTA in sea water

ii) Fixation: 1 hour 0–4°C in 2% OsO_4 (0.2M Phosphate pH 7.4)

iii) Rapid rinse in buffer

iv) Dehydrate through ascending series of Ethanol (30 mins. each)

v) Pass through Ethanol/Amyl acetate; 3:1, 1:1, 1:3 (30 mins. each)

vi) 30 mins. Amyl acetate

vii) Transfer via Amyl acetate to Critical Point drying apparatus.

Pieces of tissue were attached to stubs with nail varnish and carbon paint.

All stubs were sputter coated with gold and examined in a Cambridge Stereoscan S-600 operating at 15 kV.

2. <u>TEM</u>

For TEM the following procedure was used for tissue preparation:

a) Dissection

b) Fixation

c) Decalcification

d) En bloc staining

e) Dehydration–Infiltration–Embedding

f) Ultramicrotomy and Staining

a) Dissection

In order to dissect out intrathecal regions of the WVS, the test was cut in half around the ambitus (i.e. the widest part of the test) and then the two halves carefully separated and immersed in cold sea water.

Tube feet were excised from the test in cold sea water. For fixation in an extended state, tube feet were either ligatured with cotton thread or the whole animal was narcotised with 1:1 Isotonic $MgCl_2$/Sea water (Pantin 1969). Peristomial tube foot plates were dissected out from the peristomial membrane in 2.5% Glutaraldehyde/0.2M Phosphate pH 7.6 + 0.21M NaCl.

b) Fixation

Echinoderm tissues have deservedly acquired considerable notoreity because of difficulties in producing consistently good fixation. However, systematic trials of many methods led to the use of five different methods, each of which had their faults and merits.

i. Method I (Fix I):

1 hour, 0-4°C in 2% OsO_4/0.2M Phosphate pH 7.6

5 minute rinse in distilled water

ii. Method II (Fix II):

1 hour, room temperature in

2.5% Glutaraldehyde/0.2M Phosphate pH 7.6 + 0.21M NaCl

5 minute rinse in Phosphate/NaCl

1 hour, 0-4°C in 2% OsO_4/0.2M Phosphate pH 7.6

5 minute rinse in distilled water

iii. Method III (Fix III):

1 hour, 0-4°C in the following mixture:-

1 Part 2.5% Glutaraldehyde/0.2M sym-collidine pH 7.4 + 2M NaCl

1 Part 4% OsO_4

5 minute rinse in 0.2M sym-collidine pH 7.4 + 1M NaCl

iv. Method IV (Fix IV):

1 hour, 0-4°C in the following mixture:

1 Part 2.5% Glutaraldehyde/0.2M sym-collidine pH 7.4 + 2M NaCl

1 Part 8% Paraformaldehyde

1 Part 4% OsO_4

5 minute rinse in 0.2M sym-collidine pH 7.4 + 1M NaCl.

8% Paraformaldehyde is prepared by dissolving 2g. Paraformaldehyde in 25ml. of distilled water at 60°C. The solution is cleared by adding a few drops of 1M NaOH and then allowed to cool.

v. Method V (Mix V):

1 hour, 0–4°C in the following mixture:-

1 Part 0.2M sym-collidine pH 7.4 + 2M NaCl

1 Part 8% Paraformaldehyde + 2M NaCl

1 Part 4% OsO_4

5 minute rinse in 0.2M sym-collidine pH 7.4 + 1M NaCl.

The former two fixation methods are quite conventional but the latter three are unusual in that the Aldehyde and Osmium fixatives are used simultaneously. In order to prevent rapid reduction of the Osmium tetroxide by the aldehyde it is important that the separate parts of the mixtures are not brought together until required. Also, the final mixtures must be maintained at 0–4°C.

The first published accounts of Glutaraldehyde and Osmium tetroxide being employed simultaneously are by Danneel & Weissenfels (1965) and Trump & Bulger (1966). Hirsch & Fedorko (1968) employed a Glutaraldehyde-Osmium tetroxide mixture and then 'postfixed' (i.e. en bloc stained) with Uranyl acetate. Finally, postosmication after simultaneous Glutaraldehyde-Osmium tetroxide prefixation was developed by Franke et al. (1969).

There appear to be no published accounts of Paraformaldehyde being employed simultaneously with Osmium tetroxide and Glutaraldehyde.

c) Decalcification

Another complicating factor in the preparation of echinoderm tissues for TEM is the presence of a calcareous endoskeleton.

If calcareous ossicles cannot be avoided or dissected free, then decalcification is necessary. Consequently, peristomial tube foot plates, tube foot disks and madreporites needed decalcification.

The disadvantage of decalcification is the reduction of ultra-structural preservation to varying degrees depending on type of tissue and decalcification method employed. Two methods were used and compared. EDTA (after Warshawsky & Moore 1969) and Ascorbic acid (after Dietrich & Fontaine 1975). The latter proved to be far superior in decalcification and ultrastructural preservation.

i. EDTA:

After fixation (Fix III) and rinsing, small pieces of tissue were left for 2 days at 0-4^{o}C with continuous agitation in 0.3M Na_2 (EDTA). The tonicity of the solution was increased by adding 0.1 to 1M NaCl.

ii. Ascorbic Acid:

After prolonged fixation (Fix II, double fixation times), small pieces of tissue were placed in a 500ml. beaker containing 50ml. 1M Ascorbic acid/0.17M NaCl and continuously agitated for 24-36 hours at room temperature using a Gallenkamp agitator.
The solution was changed six times (each solution is prepared freshly) and the beaker was kept in a dark bag since Ascorbic acid solution decomposes photochemically.

After decalcification tissues were quickly rinsed in distilled water prior to en bloc staining.

d) En bloc staining

Exposure of tissues to heavy metals such as Uranium before embedding can improve ultrastructural preservation and contrast of sections (Hayat 1970).

Most tissues were en bloc stained for 1–2 hours at room temperature in 2% aqueous Uranyl acetate. Decalcified tissues were en bloc stained during the dehydration schedule by the addition of 2% Uranyl acetate in the 30% Ethanol stage.

e) Dehydration–Infiltration–Embedding

Two different dehydration and infiltration schedules were used depending on the nature of the embedding medium.

i. Durcupan embedding:

30, 50, 70, 90, 2 x 100% Acetone	(5 minutes each)
Acetone/Durcupan 1:1	(30 minutes)
Acetone/Durcupan 1:3	(Overnight)
Durcupan	(1 hour)

Durcupan – polymerise for 40 hours at 60°C.

ii. Spurr embedding:

30, 50, 70, 90, 2 x 100% Ethanol	(10 minutes each)
Ethanol/Spurr 1:1	(30 minutes)
Ethanol/Spurr 1:3	(30 minutes)
Spurr	(Overnight)

Spurr – polymerise for 36 hours at 60°C

Both embedding media are easily prepared and can be stored at -18°C for several weeks. However, Spurr resin was more consistent in its cutting properties, better for trimming because of its colourlessness and produced far superior infiltration of dense tissues (e.g. decalcified plates, connective tissue sheath in tube feet etc.) due to its extremely low viscosity. The 'Standard' medium of Spurr (1969) proved most satisfactory.

f) Ultramicrotomy and Staining

Ultrathin sections were cut on an LKB ultratome using glass knives and supported on 300 mesh copper grids. Sections were stained with 2% Uranyl acetate (aqueous or in 50% methanol) followed by lead citrate (Reynolds 1963 & Venable & Coggeshall 1965).

Methanolic Uranyl acetate produced more intense staining but was more prone to contamination. Reynolds lead citrate produced more contrast, but is more difficult to prepare and less stable than the Venable & Coggeshall stain.

All sections were examined in an AEI EM6B and Zeiss EM9 operating at 60kV using 25µ and 50µ objective apertures.

3. HISTOLOGY

a) Paraffin wax sections

For routine histological studies of different regions of the WVS tissues were processed as follows:-

Fix for 48 hours in seawater Bouin

Rinse in several changes of 70% Methanol for 24 hours

Dehydrate in ascending Methanol series, clear with Xylene and embed in paraffin wax

7µ sections were dewaxed in Xylene, rehydrated in descending methanol series and stained by either Heidenhain's Azan (Grimstone & Skaer 1972) or Mallory's Rapid Trichrome (Humason 1972).

Bouin is a particularly useful fixative for echinoderm tissues since it simultaneously functions as a decalcifying agent.

	ILLUMINATION			
	KOHLER BRIGHT FIELD		ULTRA-VIOLET	
Photography	Monochrome	Colour	Monochrome	Colour
Sub-Stage Filter	Orange	Blue	-	-
Film	Ilford 'Pan F' Kodak 'Panatomic'	'Kodachrome 25'	Kodak 'Tri-X Pan'	Kodak 'Professional Photomicrography
Developer	Paterson 'Acutol'	Commercial	Kodak 'ID-11'	Commercial

Table 3

Photomicrographic methods

b) Semithin epoxy resin sections

Semithin ($\sim 1\mu$) sections of all tissues prepared for TEM were obtained and examined by conventional methods.

The following staining methods were used:

i. 0.1% Toluidine Blue in 2% Borax (Tol. Blue)

ii. Tol. Blue - Distilled water rinse-Dry-1% Azure (Tol. Blue/Azure)

iii. Azure 2-Distilled water rinse-Dry-1% Acid Fuchsin (Azure/AF)

iv. Azure 2-Distilled water rinse-Dry-1% Basic Fuchsin (Azure/BF)

v. 0.1% Methylene Blue in 2% Borax (Meth. Blue)

vi. Azure 2 - Distilled water rinse-Meth. Blue (Azure/MB)

vii. Haematoxylin - Eosin, after Chang 1972 (Haem/E)

viii. Azure 2 - Distilled water rinse - Eosin (Azure/E)

The same Eosin solution is used for Haem/E and Azure/E methods.

c) Photomicrography

Photomicrographic methods for recording histological and histochemical data are shown in Table 3.

Planachromatic and Planapochromatic objective lenses were used. X40 and X100 objectives were used under oil immersion. All films were of the 35mm format.

4. HISTOCHEMISTRY

a) Histochemical localisation of biogenic monoamines.

The technique of freezing, freeze-drying and treatment of tissue blocks with paraformaldehyde vapour was applied to all regions of the MVT in order to demonstrate the presence of aminergic neurons.

The fundamental methodology used was similar to that developed by Falck and his colleagues (Falck et al. 1962):

i. Remove tissues and immerse rapidly in liquid propane (cooled with liquid nitrogen) for 1 minute.

ii. Transfer tissues via liquid nitrogen to freeze-drying apparatus and freeze-dry for 5 days at $-40^{\circ}C$, 10^{-2} Torr.

iii. Expose tissues to paraformaldehyde equilibrated to a relative humidity of 70% for 1 hour at $80^{\circ}C$.

iv. Vacuum embed tissue blocks in paraffin wax.

v. Affix 7μ sections to albumen coated glass slides, remove excess wax with liquid paraffin and mount sections in liquid paraffin.

In addition to the above procedure, a slightly different method was attempted in order to improve the localisation of 5HT (after Fuxe & Jonsson 1967). After Stage iii, tissues were further exposed to paraformaldehyde at a relative humidity of 90% for 1 hour at $80^{\circ}C$.

All sections were examined in a Zeiss fluorescence microscope using Zeiss BG12 excitation filter and Zeiss 44 & 53 barrier filters.

The specificity of tissue fluorescence was determined by the Sodium monoborohydride reduction test (Corrodi et al. 1964).

b) Histochemical localisation of peptides

In recent years the 'Fluorescamine technique' has acquired increasing use as a method for the localisation of polypeptide secreting cells (Larsson et al. 1975). Therefore, this technique was employed to demonstrate possible peptidergic cells within tube feet.

7μ sections of tissues prepared for monoamine localisation were processed in the following manner (after Hakanson et al. 1974):

Rinse in 0.2M Phosphate pH 8.0 for 3 minutes.

Immerse in 2 mg. Fluorescamine (dissolved in 10 ml. of Acetone) for 15 seconds.

Rinse rapidly in buffer and mount with 5% Glycerol in 0.2M Phosphate pH 7.2.

Sections were examined in a Zeiss fluorescence microscope using all possible combinations of barrier and excitation filters.

c) Histochemical localisation of proteoglycans and glycoproteins

Various histochemical techniques were employed for the demonstration of different carbohydrate-protein complexes ('mucosubstances') within the connective tissue and other cellular elements of ambulacral tube feet.

Ambulacral tube feet were excised from the test of E. esculentus, freeze-dried, formaldehyde vapour fixed and vacuum embedded in paraffin wax (i.e. same procedure as monoamine localisation).

5µ sections were processed by the following methods (Pearse 1972a, Chapter 10 and Appendix 10 provides an excellent account of the methodologies):

i. Periodic Acid Schiff (PAS)

Schiff's reagent was prepared by the De Tomasi or Barger and Lamater methods, the latter proved more efficacious. Some sections were counter-stained with Heidenhain's Haematoxylin (PAS/Haem) and control sections were blocked by Acetylation.

Acetylation procedure:

Slides immersed in 2:3 Acetic Anhydride/Anhydrous Pyridine for 16 hours at room temperature.

Rinse slides well in distilled water and process for PAS.

ii. Alcian Blue - Periodic Acid Schiff (AB/PAS)

iii. Alcian Blue pH 1.0 (AB 1.0)

iv. Alcian Blue pH 2.5 (AB 2.5)

v. Alcian Blue - Critical Electrolytic Concentration (AB-CEC)

vi. Ethanolic Toluidine Blue (E.Tol.Blue)

This method was necessary in order to preserve metachromasia during dehydration and clearing.

In addition, some histochemical tests were applied to semithin sections of tissues prepared for TEM.

Epoxy resin was removed using commercially available Sodium methoxide (Aldrich Chemical Co. Ltd.). After 2-3 minutes in Sodium methoxide, slides were rinsed with Methanol followed by distilled water.

Slides were processed by the following methods:

i. PAS or PAS/Haem

After the method of Lane & Europa (1965)

Control sections: Acetylation block

ii. AB 1.0 or AB 2.5

Slides were left in the same solutions used for methods AB 1.0 and AB 2.0.

d) Histochemical localisation of neurosecretory material.

In order to demonstrate the presence of possible neurosecretory cells in tube feet, 3 classic methods of staining neurosecretory material were employed.

Ambulacral tube feet were excised from the test of E. esculentus and processed for paraffin wax histology. 7μ sections were stained by the following methods:-

i. Chrome Haematoxylin Phloxin (CHP)

Both the Gomori (Gomori 1941) and Bargmann (Pearse 1972a) methods were attempted.

ii. Paraldehyde Fuchsin (PAF)

PAF preparation from fuchsin, and subsequent methodology after Gabe (1966).

iii. Alcian Blue/Alcian Yellow (AB/AY)

The method of Wendelaar-Bonga (1970) was followed.

Since many neurosecretory materials are known to be rich in Cysteine and Cystine (Highnam & Hill 1977), methods for the fluorescent histochemical localisation of sulphydryl and disulphide groups have been used to histochemically localise neurosecretory material (Servattez & Gontcharoff 1976). Consequently, the following method after Cowden & Curtis (1970) was attempted:

i. Ambulacral tube feet were excised from the test of E. esculentus and fixed for 24 hours in 3:1 Absolute Ethanol/Acetic Acid. After routine histological processing 5µ sections were dipped in molten wax to prevent oxidation.

ii. After dewaxing with xylene, sections were rehydrated with descending series of Ethanol and stained for 48 hours in a fluorescent mercurial solution:

20 mg. Mercurichrome in 0.5 ml. deionised water, volume made up to 100 ml. with $N_1 N_1$ - Dimethylformamide (DMFA).

iii. Rinse 2 x 3 mounting in DMFA.

iv. Dehydrate in Ethanol, clear with Xylene and mount with liquid paraffin.

Control sections were treated by the Iodoacetate block (Pearse 1972a).

For the detection of disulphide groups, it is necessary to reduce them to sulphydryl groups by incubating sections for 24 hours at room temperature in 1 mM Mercaptoacetic acid in n-Propanol prior to staining.

All sections were examined using Fluorescence microscopy.

5. EM CYTOCHEMISTRY

EM cytochemistry is the application of histochemical techniques to tissues prepared for TEM thus enabling certain substances to be localised at the ultrastructural level.

The main difference between light microscope histochemistry and EM cytochemistry "... lies in the necessity that in electron microscopy the 'stain' must be electron dense rather than a dye in the ordinary sense of that word" (Serafini-Fracassini & Smith 1974).

Cytochemical techniques can be applied to tissues by either treating the whole tissues during the fixation process (indicated in the methodology as 'en bloc') or treating ultrathin sections of tissues supported by grids (indicated as 'grid').

All the following methods were applied to ambulacral tube feet of E. esculentus and P. miliaris.

a) Cytochemical localisation of biogenic monoamines

i. Glutaraldehyde - Dichromate (GD) - en bloc (Wood 1966).

A method for localising catecholamines and indoleamines.

Prefix: 4 hours, 0-4°C in 3% Glutaraldehyde/0.2 M Phosphate pH 7.5 + 3M NaCl

Postfix: 18 hours, 0-4°C in Wood's Dichromate solution

Subsequent processing as for TEM, omit uranium and lead staining

Control: Postfix in Acetate buffer.

Wood's Dichromate solution:

2.5 g Potassium dichromate

1.0 g Sodium sulphate

100 ml 0.2M Acetate buffer pH 4.1

ii. Formaldehyde-Glutaraldehyde-Dichromate (FGD) - en bloc (Wood 1967)

Preliminary fixation in formaldehyde has been shown to block the reaction of catecholamines with dichromate solutions. However, the reaction of indoleamines is not blocked by this procedure.

Block: 24 hours, 0-4°C in 8% Paraformaldehyde/ 0.2M Phosphate pH 7.5 + 0.3M NaCl

Rinse in buffer and process as for GD method

Control: As for GD control

Paraformaldehyde is prepared by dissolving 2 g Paraformaldehyde in 43 ml. of dibasic phosphate at 60°C. A few drops of 1N NaOH are added to clear the solution. 7 ml of monobasic phosphate are added and the volume made up to 100ml. with distilled water.

iii. Formaldehyde-Glutaraldehyde-Dichromate-Osmium (FGDO) - en bloc (Tranzer et al. 1969)

Krebs ringer solution is used as a buffer system for aldehyde prefixation since this has been shown to yield greater staining of the amine storage granules than phosphate or cacodylate buffers (Pearse 1972b). Postosmication has been shown to improve ultrastructural preservation.

Prefix: 1 hour, 0-4°C in the following mixture -

2 ml. 50% Glutaraldehyde

5 ml. 8% Paraformaldehyde (prepared as for TEM Fix IV)

93 ml. Krebs ringer solution

pH adjusted to 7.4 with saturated Na HCO_3

Dichromate: After rinsing in Krebs ringer tissues were incubated for 18 hours, 0-4°C in Wood's dichromate.

Postfixation: Tissues are transferred, with rinsing from Wood's dichromate to 2% OsO_4/0.2. Phosphate pH 7.4 for 1 hour at 0-4°C.

Subsequent processing as for TEM, omitting Uranium and Lead staining.

Control: Omit dichromate treatment.

iv. Formaldehyde-Glutaraldehyde-Osmium (FGO) - en bloc (Tranzer & Richards 1976).

Substitution of the low pH acetate buffer with a chromate solution of higher pH has been shown to improve ultrastructural preservation without decreasing specificity of the dichromate reaction. Also, decreasing the time of exposure to aldehydes has been shown to reduce the extraction of amines from the issue.

Prefix: 1-10 minutes, 0-4°C in 1% Glutaraldehyde/0.4% Paraformadehyde in 0.1M Sodium chromate pH 7.2.

Rinse: 18 hours, 0-4°C in 0.2M Sodium chromate pH 6.0

Postfix: 1 hour, 0-4°C in 2% OsO_4/0.1M Sodium Chromate pH 7.2.

Subsequent processing as for TEM, omitting Uranium and Lead staining.

Control: Substitute 0.2M Phosphate buffer for Chromate solution.

v. Argentaffin (Ag) and Chromaffin (Cr) - grid (Hakanson et al. 1971).

Prefix: 1 hour, room temperature in 2.5% Glutaraldehyde/ 0.2M Phosphate pH 7.6 + 0.21M NaCl.

Rinse quickly in phosphate buffer

Dehydrate in Ethanol and process for TEM, omitting Uranium and Lead staining

Ultrathin sections were mounted on Nickel grids and processed for either Argentaffin or Chromaffin methods.

v Argentaffin:

Sections were stained with Ammoniacal Silver, in the dark for 3 hours at 60°C. Grids were rinsed with distilled water and allowed to dry before examination.

Control: 'Stain' with distilled water.

Ammoniacal Silver Solution:

Ammonia 880 solution is added dropwise to 10% $AgNO_3$ until the brown precipitate first formed is dissolved. Fresh 10% $AgNO_3$ is added until the precipitate just begins to reappear. The solution appears opalescent and is dissolved with 9 volumes of distilled water before use.

Chromaffin:

As for Ag method except Wood's Dichromate solution is used as a stain.

Control: 'Stain' with 0.2M Acetate buffer pH 4.1.

All stains used for grid staining in EM cytochemistry were centrifuged at 10,000 r.p.m. for 10 minutes before use.

b) Cytochemical localisation of Glycoproteins

i. Periodic Acid - Chromic acid - Silver Methenamine (PA-Cr-Ag) - grid (Rambourg et al. 1969)

Fix, Rinse etc. as for Ag method

Ultrathin sections were supported on stainless steel grids and 'stained' with the following solutions.

1% Periodic Acid 20 minutes at room temperature

Distilled water 30 " " " "

10% Chromic acid 5 " " " "

1% Sodium bisulphite - 1 minute at room temperature

Distilled water 6 x 5 minutes at room temperature

Silver methenamine 40 minutes, in dark, at 60°C

Distilled water Rapid rinse

Control: Stain with Silver Methenamine only.

Silver Methenamine Solution:

In a darkroom, 5 ml. of 5% $AgNO_3$ are slowly added to 45 ml of 3% Methenamine (Hexamine). A white precipitate is initially formed but this dissolves by shaking. 5 ml. of 2% Sodium borate are finally added to the solution.

ii. Periodic Acid - Bismuth Oxynitrate (PA-Bi) - grid (Ainsworth et al. 1972).

Tissue processing as for PA-Cr-Ag method

Ultrathin sections are stained with the following solutions at room temperature:

1% Periodic acid 10 minutes

Thorough rinse with distilled water

Alkaline Bismuth Oxynitrate 45 minutes

Thorough rinse with distilled water

Control: Periodic reaction is blocked by incubating sections with 1M meta Aminophenol in glacial Acetic acid for 45 minutes at room temperature. After rinsing with Acetic acid sections are rinsed with distilled water and then processed for PA-Bi method.

Alkaline Bismuth Oxynitrate solution:

400 g. of Sodium tartarate are dissolved in 10 ml. of 2M NaOH. This solution is added dropwise to 200 mg of Bismuth oxynitrate with constant shaking. Initially the solution is cloudy but after the addition of 6-8 ml. it clears. The stock solution is stored at 4°C and is diluted 1:50 before use.

c) Cytochemical localisation of Proteoglycans

i. Bismuth nitrate pH 1.2 (Bi. 1.2) - grid (Smith et al. 1967)

Tissues were processed as for the PA-Cr-Ag methods. Ultrathin sections were mounted on Nickel grids and stained with the following solutions at room temperature:

0.1M Nitric acid 5 minutes

0.5% Bismuth nitrate in 0.1M Nitric acid 20 minutes

0.1M Nitric acid 3 x 1 minutes

Thorough rinse with distilled water

Control: Stain with 0.1M Nitric acid alone

ii. Tannic acid - Ferric chloride (TA-Fe) - grid (Sannes et al. 1978)

Tissues were processed as for the PA-Cr-Ag method.

Sections were stained with the following solutions at room temperature:

5% Tannic acid 10 minutes

Rapid rinse with distilled water

2% Ferric chloride 10 minutes

Rapid rinse with distilled water

Control: Stain with Tannic acid only.

iii. Colloidal Iron (Coll. Fe) - en bloc (Hayat 1970)

For this procedure it is necessary to prepare very small pieces of tissue since colloidal iron penetrates tissues very poorly.

Tissues were fixed according to Fix. II. Tube feet were then cut into 1 mm^3 blocks, rinsed with distilled water and placed in colloidal iron solution for 1 hour at room temperature under continuous agitation.

After rinsing in 0.2M Acetate buffer pH 1.7, tissues were dehydrated in Ethanol and processed for TEM, omitting uranium and lead staining.

Control: Methylation block - prior to en bloc staining tissues are incubated in acidified methanol overnight at 60°C.

Colloidal Iron Solution:

FeCl 2.75g

H_2O 10 ml.

Glycerol 4 ml.

28% NH_4OH 2.2 ml.

Ferric chloride is completely dissolved in water by boiling for 5 minutes. Glycerol is added to the filtered solution and then ammonia added dropwise.

The final, rust coloured solution is dialysed through Visking tubing against distilled water for 72 hours. The distilled water is changed 10 times during this period. After dialysis the colloidal ferric chloride solution increases in volume to approximately 25 ml. The final pH of the solution is adjusted to 1.7 using glacial Acetic acid.

iv. Colloidal Iron (Coll. Fe) - grid (Matukas et al. 1967)

Tissues were prepared as for the PA-Cr-Ag method

Ultrathin sections were mounted on Nickel grids and stained with the following solutions at room temperature:

Colloidal Iron 1 hour

12% Acetic acid 3 x 5 minutes

Thorough rinse with distilled water

d) Cytochemical localisation of cations and X-ray microanalysis

i. Lanthanum Chloride (La) - en bloc (Weihe et al. 1977)

Excised ambulacral tube feet were placed in an aerated sea-water bath at 4°C containing 10 mM $LaCl_3$.

After 45 minutes tissues were rinsed in sea water and processed for TEM using Fix. II. Unstained sections were examined.

ii. Ammonium oxalate - en bloc (Carasso & Favard 1966)

As for La method except seawater bath contains 3 mM Ammonium oxalate.

iii. Potassium Pyroantimonate (K-Ant) - en bloc

Initially the method of Bulger (1969) was followed:

Prefix: 1 hour, 0-4°C in 2.5% Glutaraldehyde/0.2M Phosphate pH 7.6 + 0.21M NaCl + 2% K-pyroantimonate.

Rinse: 5 minutes in 0.2M Phosphate pH 7.6 + 0.21M NaCl + 2% K-pyroantimonate.

Subsequent processing as for TEM, omitting uranium and lead staining.

After numerous problems with dissolving K-pyroantimonate in phosphate buffer and also poor results, the method of Klein et al. (1972) was followed and this proved to be far more efficacious.

Prefix: 1 hour, 0-4°C in 2.5% Glutaraldehyde/0.2M Phosphate pH 7.6 + 0.21M NaCl.

Rinse: Seawater 3 x 2 minutes

Postfix: 1 hour, 0-4°C in 1% OsO_4/0.01M Acetic acid pH 7.8 + 2% K-pyroantimonate.

Rinse: Distilled water 3 x 5 minutes

Subsequent processing as for TEM, omitting Uranium and Lead staining.

With some tissue samples prefixation was omitted.

Control: Postfix in 1% OsO_4/0.01M Acetic acid pH 7.8 or 1% OsO_4/0.01M Acetic acid pH 7.8 + 2% K-pyroantimonate + 3M Sucrose, or 'stain' experimental grids with 10 mM EDTA at 60°C (10 mins.) prior to rinsing.

K-pyroantimonate solution:

4 g. of K-pyroantimonate are added to 0.01M Acetic acid (200 ml.) adjusted to pH 7.4 with 0.1M NaOH. After intermittent shaking and boiling for 40 minutes all the K-pyroantimonate dissolves. Fluid loss due to evaporation is compensated by the addition of distilled water. After cooling, 1 g. of OsO_4 is dissolved in 100 ml. of the solution by shaking for 2 hours at room temperature. The final solution is adjusted to pH 7.8 with 0.05M Acetic acid and allowed to stand overnight. This solution was stored in a stoppered flask at 4°C. Just before use, 4 ml. aliquots of the solutions are centrifuged for 15 minutes at 10,000 r.p.m.

iv. X-Ray Microanalysis

In order to determine the cations present in electron dense deposits produced by the K-Ant method, 100-200nm thick sections were prepared for energy dispersive X-Ray microanalysis by Dr. H.Y. Elder at the Microprobe Unit, Institute of Physiology, University of Glasgow.

A JEOL 1000 STEM (transmission mode) in conjunction with a Link System 290 Microanalysis system was used. Data was displayed on a CRT screen and printed on a chart recorder interfaced with the Link System 290 computer.

6. <u>ELECTROPHYSIOLOGY</u>

a) Intracellular

Ampullae from the peristomial tube feet of <u>E. esculentus</u> were dissected from the WVS in cold seawater using iridectomy scissors. Each ampulla was opened up with a single incision along the longitudinal axis and pinned endothelial surface uppermost onto a 'Sylgard' filled petri dish using prickly-pear spines.

High resistance microelectrodes were filled with 1M KCl and conventional methods of DC amplification and display were used. The ampulla preparation was bathed in seawater cooled to approximately 10°C.

b) Extracellular

Peristomial or ambulacral tube foot preparation were dissected free from the test of <u>E. esculentus</u> and pinned to Sylgard filled petri dishes by steel pins. Initially conventional (i.e. plastic) extracellular suction electrodes were used for stimulating the preparation. However, better results were obtained with 'large' diameter microelectrodes attached to a 10 ml. syringe using an 'Omnifit' adaptor. Electrodes were filled with seawater and conventional methods for AC amplification and display were used.

CHAPTER 3

Morphology of skeletal structures associated with the water vascular system

Morphology of skeletal structures associated with the water vascular system

INTRODUCTION

The endoskeleton has a vital and intimate connection with some regions of the water vascular system. Thus it is important to consider its role in the structure and function of that system.

Nearly all echinoids possess a hard skeleton, and the nature of this skeleton varies from group to group but certain features appear common to all species (RAUP 1966).

The skeleton is always internal but unlike that of other invertebrates it is of mesodermal origin. Individual skeletal elements are composed of calcite and magnesium substitutes for calcium at levels generally higher than in most invertebrates. Each skeletal element, or ossicle, is crystallographically a single crystal but it is probable, however, that it consists of numerous microcrystals which have very similar crystallographic orientations. All skeletal elements except teeth and spicules have a typical fenestrate meshwork, or stereom, which is unique to echinoderms.

The most conspicuous skeletal structures associated with the echinoid water vascular system are certain regions of the test. Less conspicuous structures occur at the terminations, or disks, of ambulacral and peristomial tube feet. In addition, spicules occur randomly within the tube foot stem and the stone canal.

Three regions of the test provide exits for extra thecal terminations of the water vascular system. These regions are: (1) the apical system, (2) the coronal system, and (3) the peristomial system.

Apical System

The apical plates are among those first formed at the time of metamorphosis and mark the site of origin of coronal plates.

The apical system of regular echinoids consists of a ring of five terminal tube foot plates (TTF plates) and alternating with them are five genital plates. As their names imply, TTF plates provide exits for terminal tube feet and the genitals provide exits for the gonoducts. One of the genital plates, the madreporite, is enlarged and perforated by several hydropores which provide an exit for the axial region of the water vascular system.

The apical system is important in determining the orientation of the test according to a system devised by LOVÉN (DURHAM & MELVILLE 1966). Based on observations of irregular echinoids, the antero-posterior axis of the animal passes through the TTF plate on the left of the madreporite and through the opposite genital plate (Fig. X). The apical plates are numbered in relation to this axis, the TTF plates having Roman numerals and the genitals having Arabic numerals. In aboral view, the right posterior genital is 1 and the right posterior TTF plate is I. Numbering of the apical plates is in an anticlockwise direction, thus the anterior TTF plate which straddles the antero-posterior axis is III and the madreporite is a modified genital 2.

Utilizing the madreporite as a point of reference, the Lovénian system can also be applied to the coronal and peristomial plates.

Coronal System

Most regular echinoids possess a spherical or sub-spherical test that is composed of a rigid framework of coronal plate ossicles. An exception to this is the Echinothurids, where the coronal plates imbricate with each other forming a flexible test.

Coronal plates are arranged in ten meridional areas extending from the edge of the apical system to the edge of the peristome. The ten areas consist of five ambulacra radiating from the TTF plates and five interambulacra alternating with them and radiating from the genitals. Thus according to the Lovénian system the anterior ambulacrum is numbered III.

In most extant echinoids each meridional area consists of five columns of alternating plates. Each plate is in contact with adjacent plates by means of sutures (Fig. XI). The suture between the two columns of an ambulacrum is termed the perradial suture. The suture separating an ambulacrum from an interambulacrum is termed the adradial suture. The transverse sutures of individual plates are distinguished as apical (i.e. toward the apical system) or oral (i.e. toward the mouth).

Each ambulacral plate is perforated by two pores forming a pore-pair. A pore-pair provides the exit for a single tube foot.

All coronal plates have some form of external ornamentation usually consisting of tubercles and granules. The former structures support spines and the latter support pedicellariae.

Peristomial System

The area between the adoral margin of the corona and the mouth is covered by the peristomial membrane.

In Cidaroids the peristome is covered with imbricating plates corresponding to each area of the corona. Thus there is a continuous transition of peristomial tube feet to ambulacral tube feet. In other regular echinoids only the ambulacral areas are represented on the peristomial membrane. Five pairs of peristomial tube foot plates (PTF plates) provide exits for the ten peristomial tube feet which encircle the mouth (Fig. XII).

Disk Elements

Many regular echinoids possess skeletal structures which support the disks of ambulacral and peristomial tube feet. In ambulacral tube feet the skeleton supporting the disk consists of two parts: (1) a 'rosette' arrangement of several ossicles which form the bulk of the disk, and (2) a pentagonal array of small interlocking ossicles forming a 'frame' which surrounds the lumen of the tube foot proximal to the rosette.

Peristomial tube feet do not possess a frame and the rosette is often reduced, in development and number of ossicles.

The relationship between the endoskeleton and the water vascular system has received little attention. The classic paper of LOVEN (1883) provides the first detailed description of ambulacral pore pairs but little in the way of functional interpretation. NICHOLS (1961) described the morphology of pore pairs, peristomial tube foot plates and disk elements from Cidaris cidaris and Echinus esculentus. However, descriptions were limited to light microscope observations only. NICHOLS (1959) discussed the possible relationship between tube foot function and pore pair morphology, and utilised this to interpret the structure and function of tube feet of the Cretaceous heart urchin Micraster. Similarly, SMITH (1978a) used pore pair morphology to interpret tube foot function in two Jurassic irregular echinoids, Plesiechinus and Galeropygus. SMITH (1978b) provided a correlated SEM and histological survey of ambulacral tube feet and their associated pore pairs from a wide range of extant regular echinoids. Pore pair morphology appears to be related to various factors such as: (a) the presence or absence of a septum within the tube foot, (b) the thickness of the stem retractor muscles and connective tissue sheath, and (c) the presence or absence of a suckered disk.

The microstructure of skeletal elements associated with the water vascular system has received even less attention than the macrostructure. JENSEN (1972, 1974) provided an SEM study of Strongylocentrotid coronal plate structure. OLDFIELD (1976) published an SEM survey of coronal plates of extant regular echinoids and suggested that plate microstructure is influenced by ecological factors.

It is quite apparent, that some skeletal structures associated with the water vascular system have not been described in detail using SEM. Also, most descriptions of ambulacral plates have been: (a) not specific as to the precise location of the plate within the ambulacrum, and (b) only concerned with the external side of the plate. Similarly, variation of pore-pair morphology within an ambulacrum has been largely neglected.

Consequently, the aim of this chapter is to provide a detailed SEM study of:

(1) The Madreporite

(2) TTF plates

(3) Ambulacra

(4) PTF plates

(5) Disk elements

The relationship between the morphology of skeletal elements and functional or ecological factors will also be discussed.

RESULTS

1. Madreporite

The madreporite consists of a single plate, similar in outline to the adjacent genital plates but slightly enlarged, and more convex externally (Fig. 1). The external surface of the plate is divided into three main areas: apical area, hydroporiferous area, and ornamented area.

The apical area is characterised by a single large perforation, the gonopore, which is 500-600µ in diameter. In most species that were examined the gonopore is located centrally within the apex and is not ornamented. In Holopneustes however, the gonopore is located eccentrically within the apex and a single granule occurs centrally (Fig. 2).

Ornamentation of the madreporite is mainly restricted to the adoral margin of the plate and consists of a variable number of tubercules and granules (Figs. 1, 2, 3).

The hydroporiferous area occupies the bulk of the central area of the plate and distinguishes the madreporite from the genital plates. This area consists of a regular and close packed array of hydropores (Fig. 4). Each hydropore is approximately 100µ in diameter and is formed by a hexagonal array of skeletal trabeculae.

Examination of the internal surface of the madreporite (Fig. 5) reveals that the gonopore is of a similar diameter internally and that the hydropores pass directly through the plate. In between the hydroporiferous area and the gonopore is a depression which is occupied by the madreporic vesicle. The stereom structure of the depression area is modified by thickened trabeculae and reduced pore spaces.

In E. esculentus a ridge (Fig. 6) delineates the hydroporiferous area from the remainder of the internal surface of the plate. In this region there is a remarkable variation in stereom structure. The non-hydroporiferous area consists of trabeculae approximately 30µ in diameter and intertrabecular pores approximately 20µ in diameter. The stereom comprising the ridge is characterised by smaller diameter trabeculae (approximately 15µ). The hydroporiferous area consists of a more irregular array of trabeculae varying in diameter from 4µ to 30µ.

Internally, the hydropores appear to vary in size and do not show the same regular array as they do externally. However, in _E. chloroticus_ the regular array passes through to the internal side of the plate (Fig. 7). Comparison with the external side shows one striking difference; jagged vertical trabeculae with few interlocking struts.

2) Terminal tube foot plate

The TTF plate consists of a single ossicle (Fig. 8) perforated by a single pore (approximately 100μ in diameter) located centrally and towards the adoral margin. Recesses in the adoral margin accommodate the adapical termination of the double column of ambulacral plates. The single pore which provides passage for the terminal tube foot passes directly through the plate.

Ornamentation of the TTF plate varies greatly in the number and position of tubercules and granules. _D. setosum_, for example, shows very little ornamentation except for a single granule located adapically to the TTF pore. _E. chloroticus_, however, has a single large tubercle located adapically and several tubercles laterally (Fig. 9).

In some species, e.g. _D. setosum_ (Fig. 10) there is evidence of the passage of the terminal tube foot underneath the plate, through a canal before finally emerging through the pore. In other species, e.g. _E. chloroticus_ the terminal tube foot passes less obliquely through the plate and a canal for the radial nerve and radial water canal is absent (Fig. 11).

3) Ambulacra

Each ambulacrum consists of a double column of ambulacral plates which are perforated by pore pairs. Since each pore pair consists of equal sized pores, they are termed isopores.

Passing adapically there is a decrease in the width of an ambulacrum (Fig. 12) and there is a subsequent decrease in the size of the isopores. Examination of the apical end of an ambulacrum shows that the penultimate tube foot passes through a considerably reduced pore pair (Fig. 13). The interporal partition is poorly developed and the periporal attachment area is less extensive.

A 'typical' isopore (Fig. 14) has a slightly ridged interporal partition and consists of circular pores unlike the pyriform pores found in irregular echinoids. The pore nearest to the perradial suture of the plate is termed as the perradial pore and this always abuts onto the transverse, adoral plate suture. A lateral branch from the radial nerve passes through a canal in the perradial pore (hence termed the neural canal) and bifurcates on the external side of the plate. One branch of the nerve passes up the tube foot stem forming the longitudinal nerve and the other branch passes along a groove in the adoral suture (the neural groove), linking with the basiepithelial plexus.

Another separate connection between ampulla and tube foot passes through the pore nearest to the adradial suture and this pore is hence termed the adradial pore.

Internally, the pores diverge, and this is most noticeable when the internal side of an ambulacral plate is examined (Fig. 15). A canal passes into the perradial pore and this accommodates the lateral branches of the radial nerve and radial water canal. Both of these branches pass obliquely through the plate. However, the other connection between the ampulla and tube foot passes perpendicularly through the test via the adradial pore.

In most regular echinoids each ambulacral plate is composed of a number of primary plates combined with smaller, reduced, plates. Thus the plates are termed as compound (MELVILLE & DURHAM 1966). All the component units of a compound plate are bound together by a single tubercle which transgresses the transverse sutures of the component plates.

Three main types of compound plates were found amongst the species that were studied (Fig. XIII). Diadematoid plates are composed of three primary plates which extend from perradial to adradial sutures. Arbacoid plates are also composed of three plates but the medial plate is enlarged such that the smaller adapical and adoral plates contact only the perradial suture. The latter plates are hence termed demiplates. Echinoid plates were the most common type found and varied from simple to complex types. Simple echinoid plates consist of two primary plates, the larger of which is adoral. Intercalated between the primary plates are a few demiplates: in E. esculentus (Fig. 16) for example there is only one. Complex echinoid plates have greater numbers of demiplates, S. purpuratus for example has six (Fig. 17).

S. profundii is rather unusual because the ambulacral plates consist of uncompounded units (Fig. 18). Each plate is perforated by a single pore pair with a well developed neural canal. The periporal area for tube foot attachment is poorly developed and a neural groove is absent. The stereom structure of S. profundii is characterised by large pore spaces up to 33μ in diameter.

An interesting anomaly occurs in the ambital isopores of D. setosum (Fig. 19). The periporal area is well developed and is raised above the level of the plate forming a rostrum. A well developed neural canal is associated with the perradial pore and the neural groove is located beneath the flange of the rostrum. The longitudinal nerve which emerges from the neural groove passes via a notch in the rostrum. Passing adorally across the plate there is a progressive closure of the neural notch forming a complete foramen or neuropore.

Examination of the internal side of an ambulacrum, as in _A. lixula_ (Fig. 20), shows a difference in the stereom structure of the internal side of the plate. Skeletal trabeculae are thicker in diameter thus occluding the pore spaces. However, suture lines are composed of thinner trabeculae. Perradial and transverse sutures are more apparent towards the adapical end of the ambulacrum.

4) Peristomial tube foot plate

Examination of the PTF plates from eleven different species of regular echinoid shows that there is a wider variation of plate macrostructure (i.e. shape, size, ornamentation, and pore morphology) than in ambulacral plates.

On the basis of pore morphology it is possible to classify PTF plates into three main types; Uniporous, Anisoporous and Isoporous (Fig. XIV).

The uniporous condition is exemplified by _Holopneustes_ (Fig. 21) and consists of a single pore passing through the plate. Of all the species that were studied, _Holopneustes_ appears to have the simplest form of PTF plate, with no ornamentation and a poorly developed periporal attachment area. The pore passes obliquely through the plate and the internal side shows a canal passing into the pore (Fig. 22)

E. profundii possesses irregularly shaped PTF plates (Fig. 23) composed of a characteristically open stereom mesh. Each plate is remarkably thin in sagittal section and ornamentation is restricted to a pair of granules located adapical to the pore. The plate is essentially uniporous but on the external side there is a poorly developed interporal partition which does not form a complete division. The tube foot attachment area is well developed and consists of a rostrum which is inclined adorally. The stereom microstructure of the attachment area is modified and consists of smaller diameter trabeculae and pore spaces.

The PTF plate of an immature *E. esculentus* is essentially uniporous and ornamentation consists of granules located adoral to the pore (Fig. 24). An interesting post-larval development occurs in the PTF plate of *E. esculentus* since examination of PTF plates from mature specimens reveal an anisoporous type. It appears that during maturation an interporal partition develops by the evagination of finger-like processes (Fig. 25) which eventually fuse (Fig. 26), completely dividing the pore into a larger pore adorally and a smaller pore adapically. It is interesting to note that changes in ornamentation also occur, since each mature PTF plate possesses five tubercles in addition to several granules.

In the anisoporous condition the interporal partition does not extend through to the internal side of the plate. Thus there is still only a single pore on the internal side of the plate.

Both mature and immature specimens of *P. miliaris* possess a PTF plate which is intermediate between the uniporous and anisoporous condition (Fig. 27). Processes extend from either side of the pore, but these do not fuse. A ridge extends around the adapical margin of the tube foot attachment area and several granules occur adoral to the pore.

The PTF plate of *D. setosum* is an intermediate between the anisoporous and isoporous condition. A pair of interporal partitions appear to form externally (Fig. 28) and the adapical partition is more developed than the adoral partition, the latter of which represents the incomplete separation of a neuropore. Thus the adapical partition is homologous with those of other PTF plates. Examination of the internal side of the plate reveals that the adapical interporal partition passes completely through the plate forming an isopore internally (Fig. 29). Both pores pass obliquely through the plate and associated with the adoral pore is a slightly developed neural canal. Thus, the lateral nerve lies above the lateral branch of the water canal as it passes through the plate (N.B. this relationship is constant in all the species studied).

The isoporous condition is typified by E. chloroticus (Fig. 30) and the Stronglyocentrotidae (Fig. 31). A well developed interporal partition forms a complete pore pair, both externally and internally.

It is important at this juncture to emphasise the difference in orientation between ambulacral pore pairs and peristomial pore pairs (Fig. XV). The former are orientated perpendicularly to the radial axis of the test whereas the latter are parallel to the radial axis. Consequently, the adoral pore of peristomial pore pairs is homologous with the perradial pore of ambulacral pore pairs. Evidence for this homology is the passage of the lateral nerve, which passes via the adoral pore in peristomial pore pairs (cf. perradial pore in ambulacra).

Ornamentation of isoporous plates consists of a variable number of granules only. Variation also occurs in the degree of development of the interporal partition; hypertrophy being common in the Strongyl ocentrotidae. In A. lixula (Fig. 32) there is a marked divergence of the pores through the plate such that the adoral pore passes perpendicularly through the centre of the plate.

Isoporous plates appear to have more extensive attachment areas which completely encircle the pore pair.

5. Disk elements

The disk elements of tube feet from four different families were examined. In all species, a frame only occurred in ambulacral tube feet.

The frame consists of three layers of interlocking ossicles forming a pentagon which surrounds the lumen of the tube foot (Fig. XVI). In most species there is little variation in shape and size of the ossicles composing the frame, thus each layer is very similar. In A. lixula however, there is an increase in the size of the layers distally (Fig. 33). Subsequently, ossicles forming the most distal layer are thicker and possess enlarged terminal flanges which extend over the rosette ossicles. A similar condition also occurs in E. mathaei (Fig. 34). Ossicles from proximal layers of an Arbacia frame (Fig. 35) are similar to those from all the other species examined, e.g. E. esculentus (Fig. 36). Each ossicle is arcuate, the concave side lying adjacent to the lumen of the tube foot.

The stereom structure of a frame ossicle is highly modified. The main shaft of the ossicle is composed of a solid trabecula approximately 15μ wide and 10μ thick. The main shaft expands and flattens at each end forming terminal flanges which interlock with adjacent ossicles forming adjacent sides of the frame. Small pore spaces, approximately 3-9μ in diameter, perforate the flanges. Extending parallel and luminal to the main shaft is a smaller shaft approximately 6μ in diameter. Crosslinking the main shaft with small shaft are a number of trabeculae approximately 1μ in diameter. The length of the crosslinks varies from 5μ in the central region to 18μ in the terminal regions. The large pore spaces formed by the crosslinks provide a passage for the longitudinally arranged collagen bundles which form the bulk of the connective tissue sheath in the tube foot stem.

Rosettes from ambulacral tube feet show little variation in macrostructure. Each ATF disk is circular in outline and the supporting rosette consists of five tetrahedral ossicles which are similar in shape and size (Fig. XVII). The outer edge of each rosette ossicle is scalloped by projections of the stereom structure (Fig. 37). An extreme example of this is found in E. chloroticus (Fig. 38), where the number of projections is reduced but their individual size is increased. Each projection forms the termination of an extensively thickened trabecula, approximately 50μ in diameter, which radiates from the luminal side of the ossicle to the outer edge.

Species	Habitat & Distribution	Structures Studied
Diadema setosum	Indo Pacific: barrier and fringing reefs, mainly intertidal	M, T, A, P
Salenocidaris profundii	Tropical Atlantic: mainly abyssal	M, T, A, P
Arbacia lixula	Mediterranean: intertidal	M, T, A, P, R, F.
Lytechinus variegatus	Caribbean: lagoons, seagrass beds	A
Tripneustes gratilla	Indo Pacific: lagoons, seagrass beds and reef flat	A
Psammechinus miliaris	North Sea: littoral, rock pool	M, T, A, P, R, F.
Echinus esculentus	North Sea: sublittoral, *Laminaria* beds	M, T, A, P, R, F.
Strongylocentrotus droebachiensis	E. Pacific: littoral	M, T, A, P
Strongylocentrotus purpuratus	" "	M, T, A, P
Strongylocentrotus pallidus	" "	M, T, A, P
Echinometra mathaei	Indo Pacific: intertidal - sheltered inter-reefs	M, T, A, P, R, F.
Evechinus chloroticus	South Pacific: subtidal	M, T, A, P, R, F.
Holopneustes (spp.?)	Australia: intertidal, shallow inlets	M, T, A, P, R, F.

TABLE 4

Distribution of species studied for SEM survey of skeletal structures.

A Apical system; F Frame; M Madreporite; P PTF plate;

R Rosette; T TTF plate.

In all the ATF rosettes that were examined, the proximal side is convex (Fig. 39) and the distal is concave (Fig. 40). Also, the rosette ossicles are arranged such that the luminal side of the rosette is raised proximal to the outer edge.

PTF rosettes show a wider variation in macrostructure than ATF rosettes. PTF rosettes are oval in outline and flatter in profile than ATF rosettes (Fig. XVIII). It is interesting to note also that PTF rosette ossicles can differ considerably within a single rosette. For example, in A. lixula the largest ossicle within a PTF rosette (Fig. 41) is similar to that of E. esculentus (Fig. 42) except for the form of scalloping. The smallest ossicle appears quite different however, and it is quite rudimentary (Fig. 43). PTF rosette ossicles interlock in a manner that shows no evidence of the tube foot lumen passing through the rosette.

DISCUSSION

An SEM study of the skeletal structures associated with the water vascular system has been described in this chapter.

Thirteen species of regular echinoid from eight different families were investigated (Table 4). There have been no published SEM descriptions of skeletal structures associated with the water vascular system of extant echinoids except for studies on ambulacra.

Very little variation occurs in the morphology of the madreporite. It is essentially a genital plate which is perforated in order to provide communication between the exterior and the axial complex. The structure and function of the latter will be discussed more fully in Chapter 4. However, since the function of the madreporite appears consistent throughout the echinodermata it is not surprising therefore that little variation in its structure occurs.

Madreporite variation is mainly restricted to the number of tubercles and granules thus determining the number of spines and pedicellariae which are attached to the plate. It is quite possible that such variation is not only interspecific but also intraspecific and dependant on factors such as sex, degree of maturation etc.

An interesting feature of the madreporite is the fine structure of the hydroporiferous area. In all the species examined, hydropores are constructed by a hexagonal array of trabeculae and all the hydropores are of a similar size. In D. setosum it was observed that the inner surface of the hydroporiferous area was characterised by jagged, vertical trabeculae in contrast to the meshwork of transverse trabeculae which form the 'smooth' external surface the hydropore stereom. It is possible that the madreporite increases in size by the growth of trabeculae from the internal side of the plate. Thus, the jagged trabeculae represent growing points which have not yet become interconnected by transverse trabeculae. An analogous situation occurs in regenerating tips of Echinothrix spines (MISCHOR 1975). Consequently this raises the question of whether or not there is a continual post-larval growth of the madreporite in D. setosum or whether the specimen examined was still growing.

The structure of hydroporiferous area shows a remarkable degree of modification of the basic stereom structure and this raises the important problem of how stereom development is controlled. For instance, what factors influence the development of the stereom in this region in contrast to other regions of the plate such as a granule (Fig. 44) or a tubercle (Fig. 45). Unfortunately there is a dearth of authoritative research on the process of calcification in the echinoderm endoskeleton. This is emphasised by the fact that little further information can be added to that reviewed by RAUP in 1966 and NICHOLS and CURREY in 1968. The controversy of whether calcite is deposited intracellularly (BEVELANDER and NAKAHARA 1960) or extracellularly (OKAZAKI 1960) still persists. RAUP favours the latter hypothesis since the morphology of fully developed skeletal structures is determined by the organic matrix in the form of a skeletal sheath which surrounds the calcite crystal. During development, changes in the organic matrix precede growth of the crystal (OKAZAKI 1960). Thus, the development of the crystal is determined by a mesodermal 'influence' of unknown nature.

It is quite conceivable that there is a hierarchy of controlling factors; such mesodermal factors may in turn be controlled by the ectoderm. Subsequently, this raises the possibility of a control of the calcification process by humoral and/or neural factors.

The TTF plates of the apical system are often termed oculars because of the homology between the echinoid terminal tube foot and the asteroid terminal tube foot ('tentacle') which is associated with a photosensitive optic cushion. RAUP (1960) has shown that the amount of light passing through a skeletal plate is partially determined by the crystallographic orientation of the plate and the vibration direction of plane polarised light. Thus it has been suggested that TTF plates may function in polarised light discrimination and thus provide a basis for a '... crude system of navigation'. This has been further supported by crystallographic studies (RAUP 1965) which have shown differences in the C-axis directions of TTF plates within a single apical system.

However as RAUP (1966) later pointed out, there is no behavioural data to support this hypothesis. Similarly, there is no physiological or structural evidence for a photosensitive function of the echinoid terminal tube foot and thus the term ocular should be abandoned.

Ambulacral plates are the only skeletal structures associated with the water vascular system which have received considerable attention and SEM investigation.

There is evidence for a relationship between: a) skeletal magnesium levels and environmental factors (WEBER 1973, DAVIES et al. 1972); and b) stereom regeneration rate and temperature (HISCHOR 1975). WEBER (1969) has shown that low energy niche echinoids (e.g. those inhabiting sheltered lagoons) exhibit lower skeletal magnesium levels than high energy niche echinoids (e.g. those inhabiting exposed faces of barrier reefs). WEBER (1969) also suggests that coronal plate growth rate is dependant upon magnesium incorporation into skeletal calcite. Thus, it is apparent that there is a relationship between skeletal growth rate and niche 'energy level'. OLDFIELD (1976) found that low energy niche echinoids exhibit a distinctive ornamentation of the outer surface of the ambulacral plates. High energy niche echinoids however, are characterised by an unornamental stereom surface. Therefore, it seems that plate ornamentation may be used as a gross indicator of echinoid habitat, a particularly useful aid for palaeontologists.

Relationships between ornamentation and energy niche appear to apply to peristomial plates also. For instance, the PTP plate of D. setosum is characterised by an unornamented mesh similar to that found in the ambulacral plates.

However, it is still necessary to investigate a) the factors which determine the site of magnesium incorporation, and b) the reason for higher magnesium levels occurring in high energy niches. Another problem that also arises is the reason for the dichotomy between stereom ornamentation and plate growth. Why do low growth rate echinoids channel what magnesium that is available into surface ornamentation? It is quite possible that surface ornamentation has some other role which confers some advantage to species which inhabit low energy niches.

An extensive study of echinoid ambulacral pore pair morphology has been made by SMITH (1978a,b) and there is a correlation between pore pair morphology and the structure and function of the associated tube foot.

The size of the periporal attachment area is related to the thickness of the tube foot wall. Large periporal areas (such as in A. lixula) are associated with tube feet possessing thick connective tissue sheaths (approximately 20–30μ) and well developed musculature. Small periporal areas (e.g. adapical pore pairs of E. mathaei) are associated with thin connective tissue sheaths (approximately 5–10μ) and poorly developed musculature.

The morphology of the interporal partition is related to the length of the septum which divides the proximal half of the tube foot. An increasing size of the interporal partition occurs with adoral tube feet and this is associated with a reduction in the length of the septum. Thin walled tube feet appear to have the longest septa and thus pore pairs with small periporal areas tend to have narrow interporal partitions. In most regular echinoids there is an adapical gradient in the decrease of periporal areas and interporal partition size. This gradient is therefore associated with decreasing thickness of the tube foot wall and an increasing length of the septum. FENNER (1973) proposes that this reflects an increasing respiratory role of adapical tube feet as the development of the septum improves separation of the currents within the tube foot lumen. GILLÉN (1914) first demonstrated that a current passes into the ampulla via the perradial pore and into the tube foot via the adradial pore. SMITH (1978b) also discusses the increased respiratory role of adapical tube feet but there are no physiological studies to support this assumption. The only data for oxygen exchange via echinoid tube feet is based upon studies on whole ambulacra and not different regions within an ambulacrum. FARMANFARMAIAN (1966) describes experiments where covering of all the ambulacra of S. purpuratus produces a 40% reduction in oxygen uptake.

There is further cause for scepticism regarding the 'proposed' respiratory role of adapical tube feet. In an elegant study on the effect of various parameters on the respiration rates of palaeozoic echinoderms, PAUL (1976) utilised computer programs in order to calculate the effect of exchange surface thickness on oxygen exchange rate. Using KROGH's (1919) value for oxygen diffusion through connective tissue, it was calculated that almost 100% transfer occurs with thicknesses less than 100µ. Beyond 100µ however, exchange rate decreases rapidly and drops to 66% of its original value at 200µ. Tube foot walls of extant echinoids range up to 60µ and very rarely exceed 100µ (FENNER 1973). Thus, according to the calculations of PAUL there would be no difference in oxygen exchange rate between adapical and adoral tube feet. None of these studies appear to take into account two other factors.

Firstly, many regular echinoids cover the adapical half of the test with shell fragments and vegetation (LAWRENCE 1976); amongst the living specimens investigated in this present study, P. miliaris in particular, shows this habit. The covering response is brought about by the activities of adapical tube feet and it would seem likely that oxygen diffusion via the adapical tube feet would not be facilitated by their contracted state and the debris attached to them.

Secondly, the thickness of the tube foot wall varies considerably between the extended and contracted state (Chapter 5). Thus arguments based on wall thickness would also apply to individual tube feet depending on their degree of extension.

At present, all that can be stated with any degree of certainty is that passing adapically within an ambulacrum there is a decrease in the degree of muscularization and size of tube feet. This is reflected in pore pair morphology and the functional correlate is a decreased locomotory role. Observations of E. esculentus grazing on Laminaria (RAYMOND unpub. obs.) show that most individuals are attached to the stipe by means of adoral tube feet only. Also, it is interesting to note that non-grazing echinoids such as the abyssal echinothuroids, which feed by swallowing bottom ooze (LAWRENCE 1975), do not possess highly muscularized adoral tube feet.

It was observed that ambulacral isopores of _D. setosum_ were rather unusual because of the raised periporal area and the subsequent development of a neuropore. SMITH (1978b) observed a similar raised periporal area in another diadematid, _Centrostephanus longispinus_, but the neuropore was absent. The function of the raised periporal area is rather enigmatic; it is possible that it may increase the range of movement of the tube foot relative to the test. There appear to be no other published reports of an echinoid neuropore except a description of neuropores in some Antarctic species of cidarids (HYMAN 1955).

Most standard texts state that in all known echinoderms, except the Echinoidea, tube feet pass through a single pore which passes between adjacent ossicles. Echinoids however are characterised by a pore pair which passes through a single plate or ossicle.

Nevertheless, amongst the echinoids are examples of tube feet passing through a single pore, e.g. in the phyllodes of Spatangoids and some peristomial tube foot plates (e.g. _Heliocidaris_). Most peristomial tube-feet pass through a pore pair which may be isoporous or anisoporous. This study has shown a development of the anisoporous condition from the uniporous condition in _E. esculentus_. It is therefore suggested that pore pair formation occurs in a similar manner in other peristomial and ambulacral pore pairs. The development of a pore pair for each tube foot arises by the intra-luminal growth of two processes which subsequently meet and fuse, forming a complete separation of perradial and adradial pores. Formation of the interporal partition initially occurs in the external side of the plate and then extends inwards until a pore pair is formed internally.

Since most of the specimens examined were mature, judging by the size of the test, it appears that there are phyletic differences in the degree of development of the interporal partition in peristomial plates. The Strongylocentrotidae possess well developed interporal partitions and the Arbaciodae (if. _A. lixula_ is representative) are characterized by hypertrophy of the partition. The Echinidae are characterised by a poorly developed partition since evidence of fusion of the two processes is still remaining and in _P. miliaris_ the pores are not completely divided. It would be interesting to determine whether all the Temnopluridae are characterised by a uniporous peristomial plate similar to that in _Holopneustes_. It is quite important to emphasize that as in ambulacral pore pairs (SMITH 1978b), peristomial pore pairs cannot be subdivided into distinct groups since there is a continuum of variation and the different categories merely describe major types.

The present investigation has been the first SEM study of peristomial plates and since there are only a few published light microscope studies, it is difficult to make comparisons with other echinoid groups. GORDON (1929) described the development of skeletal elements associated with PTF plates in Arbacia and that each primordial plate appears before the peristomial tube foot and that subsequently a perforation develops which permits emergence of the developing peristomial tube foot. Peristomial tube feet are the first to appear and subsequent tube feet (i.e. those forming ambulacral tube feet) develop separately from the primordial plates and then migrate across and into the plates. It is apparent that processes of skeletal resorption are occurring during these developmental changes, and, the mechanisms and control of such processes await investigation.

NICHOLS (1961) described only a single pore through the peristomial plate of E. esculentus. However, the description that it '...is nearly subdivided into three by ridges projecting from two opposite sides' shows a remarkable similarity to the condition found in D. setosum. Numerous PTF plates were examined in this present study and none of the type described by NICHOLS were found in E. esculentus.

In all the species examined it was found that the orientation of peristomial and ambulacral pore pairs differ. Peristomial pore pairs are orientated parallel to the radial axis whereas ambulacral pore pairs are perpendicular to the axis. Associated with these differences are changes in the tube foot/ampulla complex and its relationship with the rest of the water vascular system (Fig. XIX). Each radial water canal has a single recurrent branch which bifurcates into two lateral branches which terminate in a pair of peristomial tube feet. Lateral branches which supply ambulacral tube feet branch off perpendicularly from the radial canal. A transition from peristomial to ambulacral tube feet would occur by the adapical migration of the lateral branches and a corresponding abradial rotation of the ampullae which produces an abradial rotation of the pore pairs. In addition to these changes in orientation, ampulla morphology also changes. ROMANES and EWART (1881) commented on differences between the peristomial and ambulacral ampullae of regular echinoids but did not provide an explanation of the functional significance of these differences. In E. esculentus and P. miliaris peristomial ampullae are tubular with a small distal constriction; ambulacral ampullae are flattened, but possess a similar constriction. Tube feet passing through the perignathic girdle (i.e. the apophyses) show a gradation from the peristomial type to the ambulacral. FENNER (1973) proposed that ambulacral ampullae are modified for a respiratory function since a flattened shape would provide a greater surface area to volume ratio for gaseous exchange. However, it is also important to consider other structural factors. If the peristomial pore pair orientation was retained during subsequent development of the tube feet then this would impose a lower limit to the number of tube feet which would be accommodated within a single ambulacral plate. Ambulacral pore orientation provides a more efficient packing of the ampullae thus increasing the locomotory ability of the animal in addition to increasing the area for gaseous exchange between ampullae and the perivisceral coelom.

A continuous transition of peristomial pores to ambulacral pores occurs in cidaroids, where the ambulacral plates continue over the peristomial membrane. NICHOLS (1961) described a gradual increase in the size of the adradial pore adapically across the peristome and an associated abradial migration of the adradial pore. However, no description of the peristomial ampullae of cidaroids was provided. The Cidaroidea represent a more primitive group of regular echinoids and thus it is interesting to discuss the possible reasons for the loss of most peristomial plates and the subsequent development of a flexible peristomial membrane. Since the latter would produce a more prone area it must have a significantly advantageous function. The evolution of a flexible peristome appears to correlate with an increased development of the perignathic girdle and Aristotle's lantern. Thus it is possible that a flexible peristome allows an increased mobility of the Aristotle's lantern which probably provides an improvement in feeding strategies. It is also possible that a flexible peristome may play some role in regulating internal coelomic pressure. Aristotle's lantern mobility may have another function: ROMANES and EWART (1881) make an interesting comment on the role of the lantern in echinoid locomotion and observed that protruded teeth can act as a fulcrum for the lever action of spines. It was also noted that spine removal resulted in an increased use of the lantern as a 'rocker'.

In all the species examined, some form of skeletal elements were found within the disk of peristomial and ambulacral tube feet.

Disks of ambulacral tube feet possess a proximal frame and a distal rosette. NICHOLS (1961) described the frame of E. esculentus as consisting of four layers of interlocking ossicles but later (NICHOLS 1966) describes only three, similar to that observed in this study. It is possible that intraspecific differences in frame structure do occur, but it seems unlikely since few interspecific differences in frame structure were observed.

The first description of the frame appears to be that of LOVÉN (1883) in which the complete pentagonal ring of ossicles was termed as the "psellion". The present study reveals that the microstructure of frame ossicles is highly modified such that each ossicle consists of a large arcuate trabecula forming a flattened main shaft. Each end of the main shaft is laterally expanded forming terminal flanges which interlock with flanges from adjacent layers and sides of the frame. LOVÉN (1883) and NICHOLS (1961, 1966) both observed that proximally the disk levator muscles are inserted into the connective tissue sheath at the level of the frame but neither fully discuss the function of the frame. It is apparent that frame function is closely associated with suckered disks as non-suckered disks (e.g. in peristomial tube feet) do not possess a frame. The pentagonal ring of the frame provides a rigid support for the distal end of the connective tissue sheath, in which it is embedded. Thus, contraction of the disk levator muscles raises the central zone of the disk without distortion of the tube foot wall.

The rosette plays an important role in the function of the disk, in both peristomial and ambulacral tube feet, by maintaining the shape of the disk during contact with an object. In ambulacral tube feet, the rosette ossicles are modified such that they form a circular rosette which has a concave distal surface. Thus when a disk comes into contact with an object, the disk surface can be raised by the levator muscles into the concavity formed by the rosette. Ambulacral rosette ossicles may also transmit pressure to the edge of the disk, keeping only the periphery of the 'sucker' in contact with the substratum. It is interesting to note that in some species such as E. chloroticus, the radially projecting trabeculae within a rosette ossicle are thickened, thus improving the strength of the rosette and probably providing a more efficient transmission of compressive forces. In addition to transmitting pressure, ambulacral rosette ossicles may conversely transmit tension (NICHOLS 1966). During tube foot retraction it is probable that the disk levator muscles relax (see Chapter 5) before the stem retractor muscles contract. Tension would be transmitted via the rosette ossicles, lifting the edge of the disk away from the substratum.

In peristomial tube feet, the absence of a foramen allowing passage of the lumen through the rosette correlates with the absence of disk levator muscles. Also, the flatter and more oval profile of peristomial rosettes correlates with the lack of a suckered disk. The reduced functional role of peristomial rosettes is reflected in their more varied structure and reduction in development in many species.

Fig. X

The apical system of a regular echinoid - numbered according to the Lovénian system.

Roman numerals	:	TTF plates
Arabic	:	Genital plates

The antero-posterior axis passes through TTF III and Genital 5

IA	Interambulacrum
A	Ambulacrum

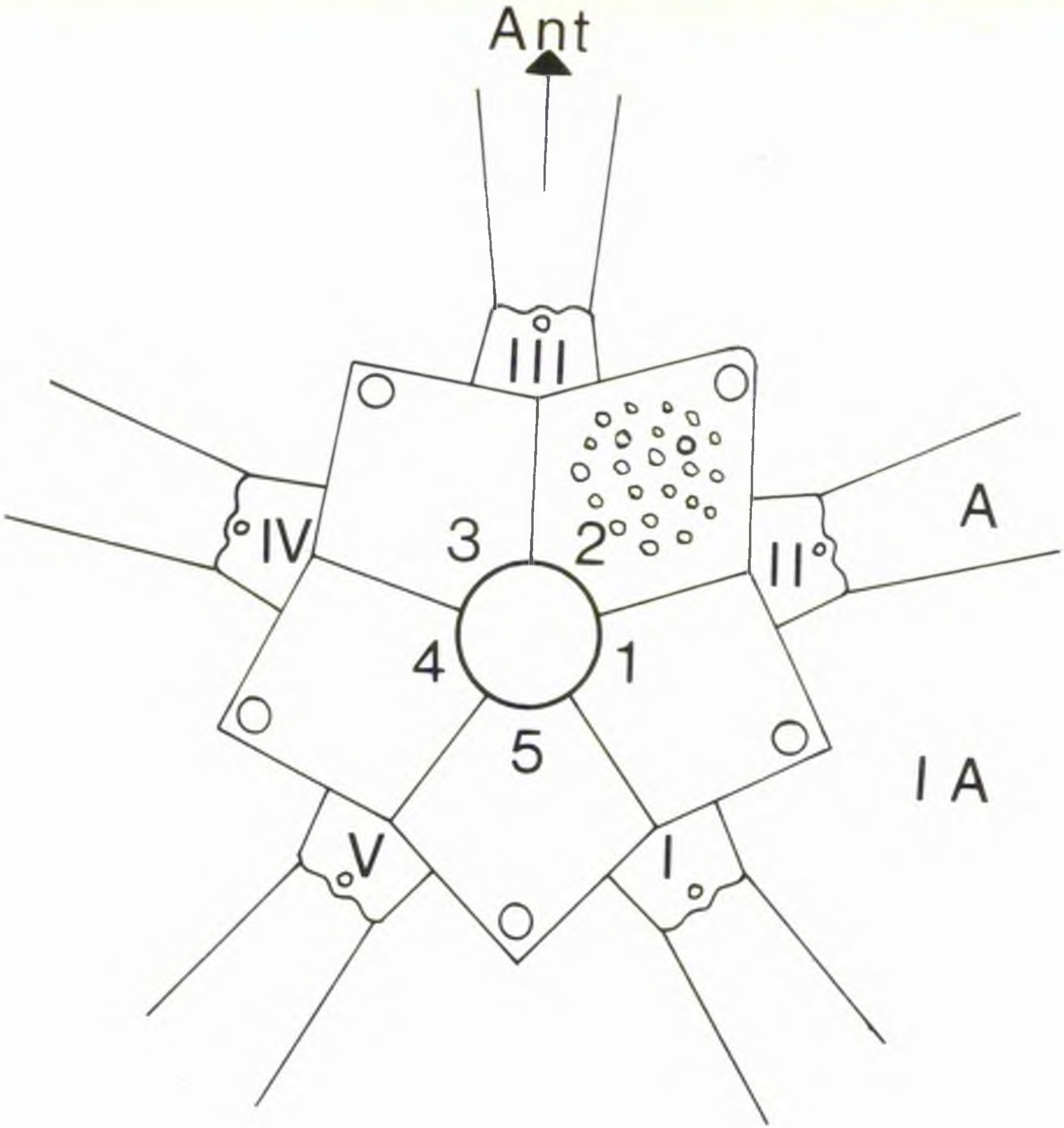

Ant
III
IV
3
2
II
A
4
1
5
V
I
I A

Fig. XI

The apical region of a single ambulacrum

In regular echinoids EDCC ambulacrum consists of a double column of plates perforated by pore pairs.

a Adradial suture (between ambulacrum and inter-ambulacrum)

p Perradial suture (between two columns of ambulacral plates)

pp Pore pairs

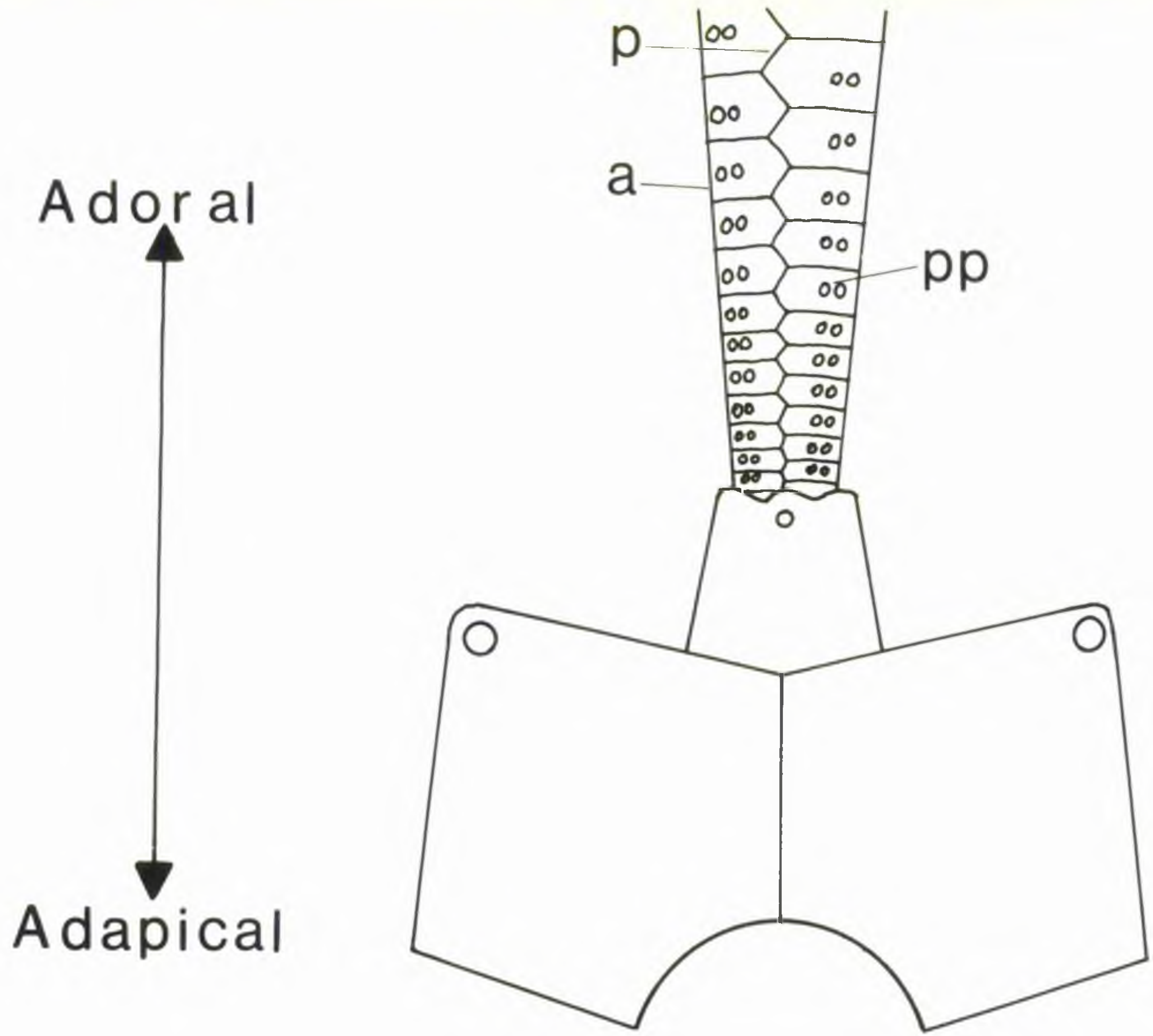
Adoral
Adapical
p
a
pp

Fig. XII

The peristomial system of regular echinoids.

The antero-posterior axis and Lovénian numerals are shown.

p   PTP plate

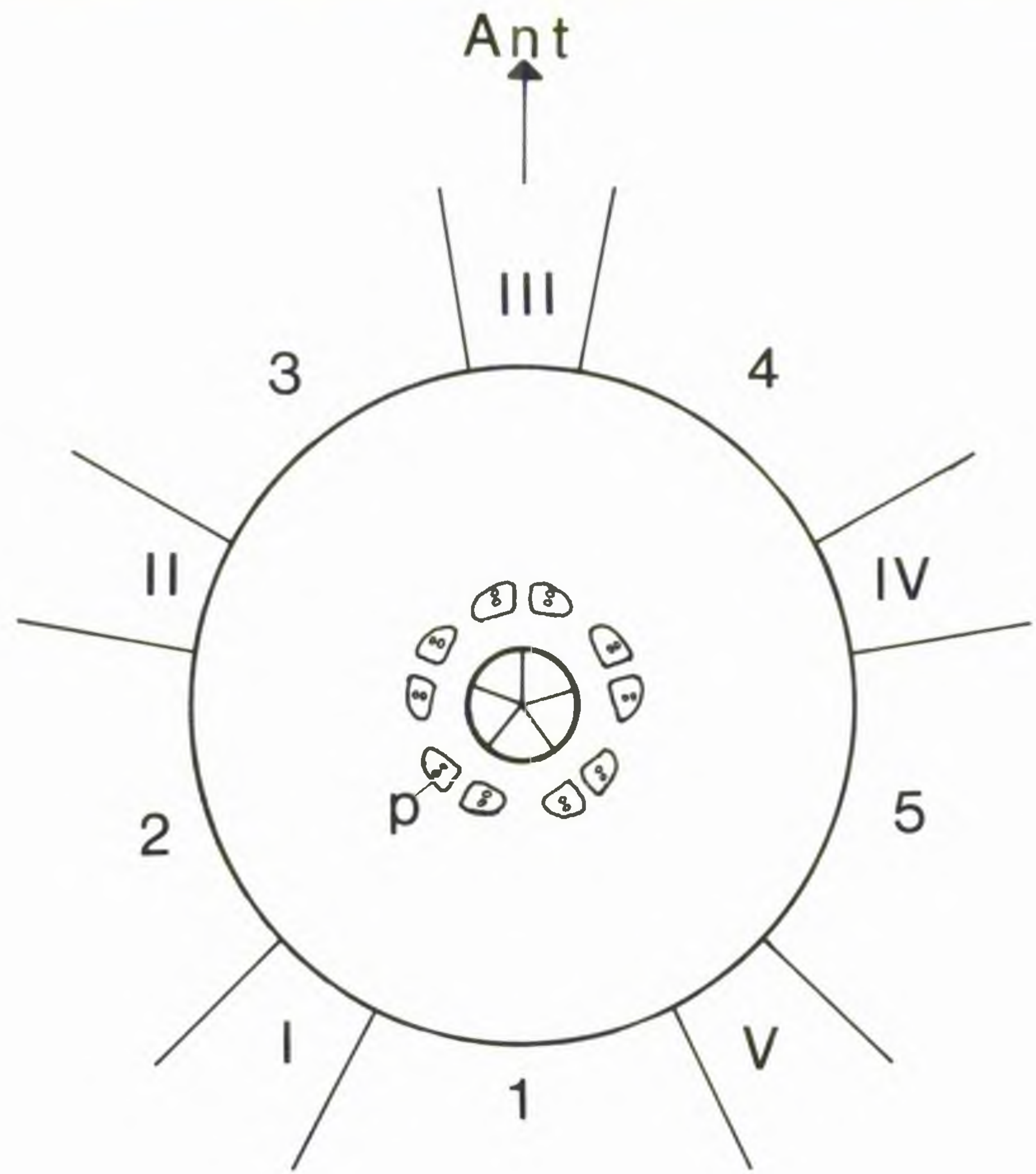
Ant
III
3
4
II
IV
p
2
5
I
V
1

Fig. XIII

Variation in ambulacral plate morphology amongst the 12 species studied.

p   Perradial suture

a   Adradial suture

3 main types were observed:

1. 3 primary plates (each extends from the perradial suture to the adradial suture).

2. Arbacioid - 3 primary plates (only the medial extends from the perradial suture to the adradial suture).

3. Echinoid - 2 primary plates with a variable number of demiplates intercalated between them.

Plate Type		Examples
Diadematoid		D. setosum
Arbacioid		A. lixula
Echinoid (simple)		E. esculentus, P. miliaris
		Holopneustes, E. mathaei, H. chloroticus T. gratilla, L. variegatus
Echinoid (complex)		S. pallidus, S. purpuratus, S. droebachiensis

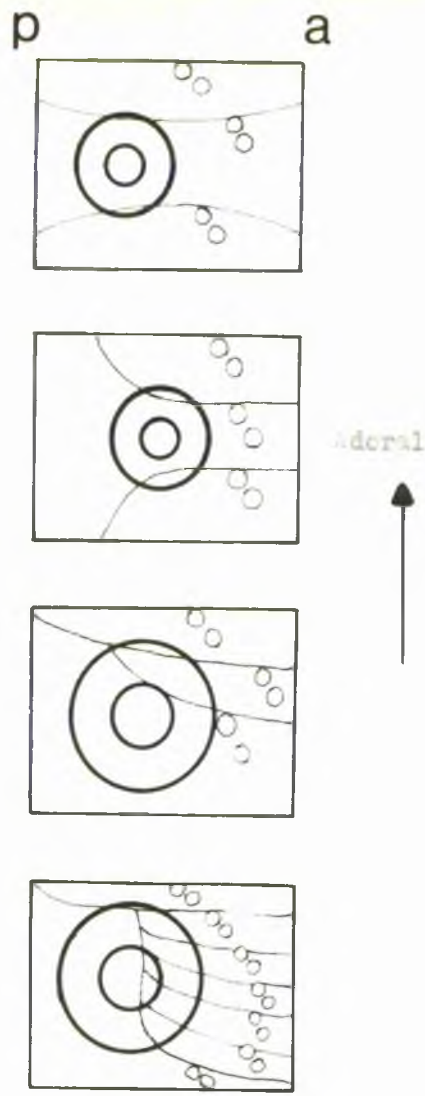

Fig. XIII

Fig. XIV

Variation in PTF plate morphology among the 11 species studied.

Ada	Adapical
Ado	Adoral
Int	Internal side of PTF plate

The passage of the lateral nerve through the PTF plate is indicated and in all three types it remains adoral in position.

The development of an adapical pore (homologous to the adradial pore in ATP plates) provides a separate connection between tube foot and ampulla.

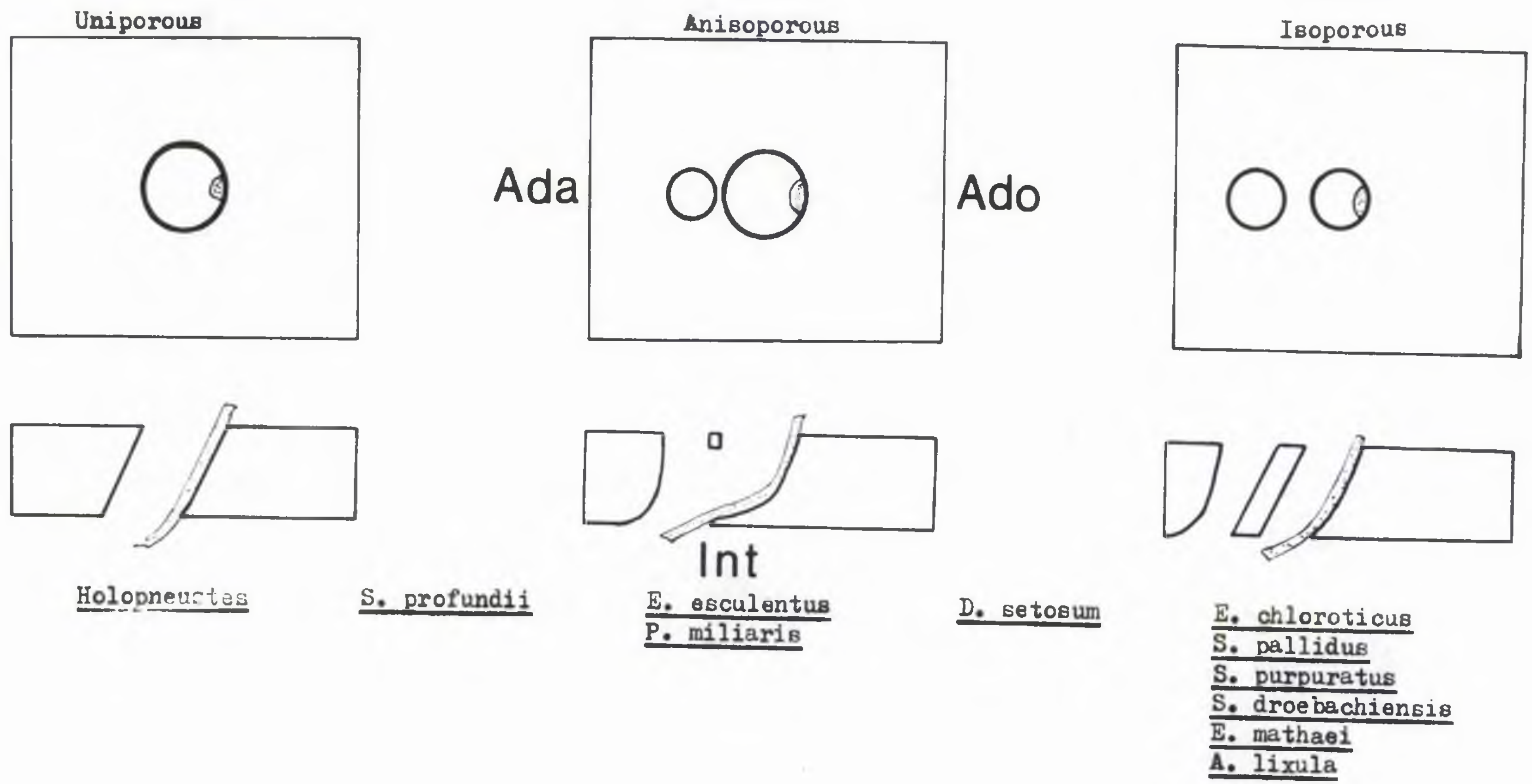
Uniporous
Anisoporous
Isoporous
Ada
Ado
Int
Holopneustes
S. profundii
E. esculentus
P. miliaris
D. setosum
E. chloroticus
S. pallidus
S. purpuratus
S. droebachiensis
E. mathaei
A. lixula

Fig. XV

Differences in orientation between ambulacral pore pairs (a) and peristomial pore pairs (p)

Stippling indicates passage of the lateral nerve.

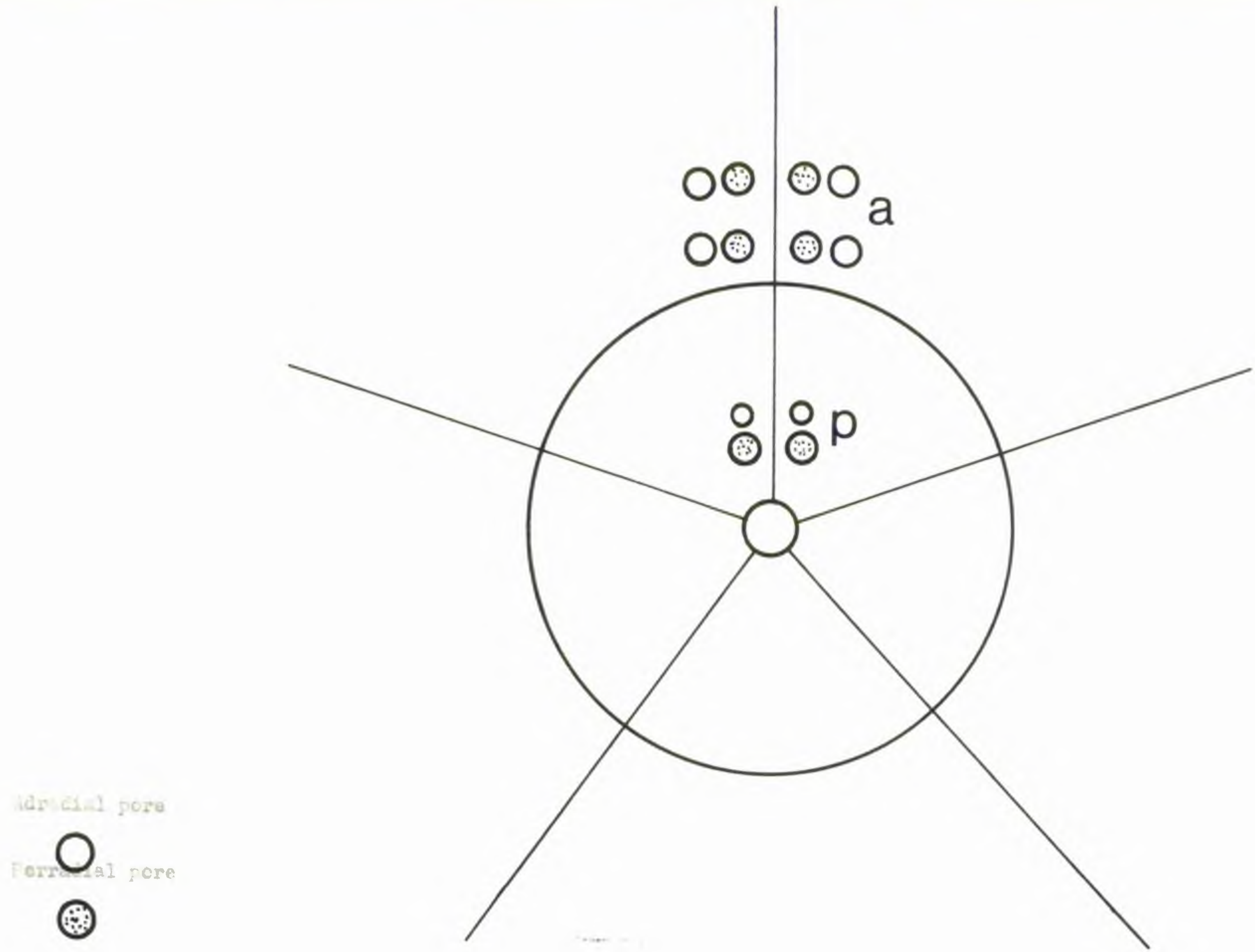
a
p
Adradial pore
Perradial pore

Fig. XVI

The frame structure of ambulacral tube feet

a) Plan view of one layer

m	Main shaft
s	Small shaft
t	Terminal flange

b) Side view (schematic) of three layers

Arrow indicates interlocking terminal flanges

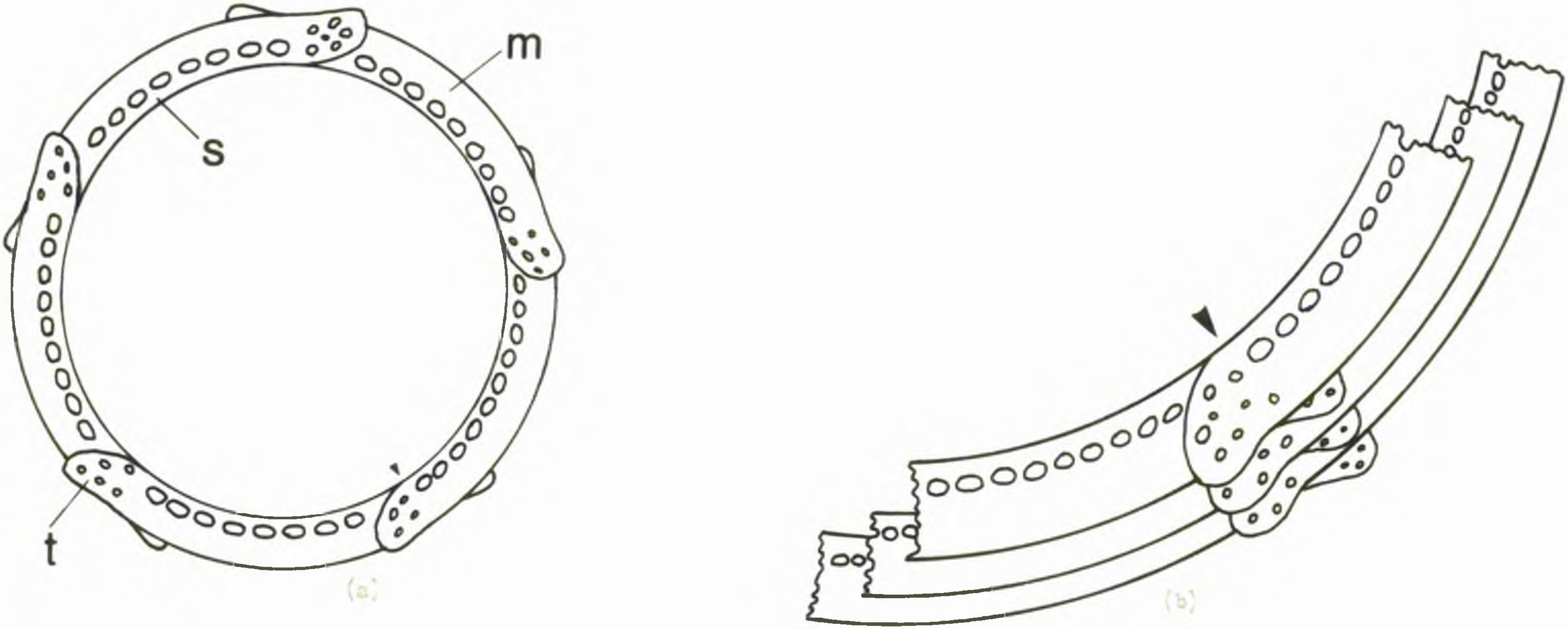
m
s
t
(a)
(b)

Fig. XVII

ATP rosette structure

a) Plan view - proximal surface + frame

f — Foramen for lumen of tube foot

b) Side view

P — Proximal

D — Distal

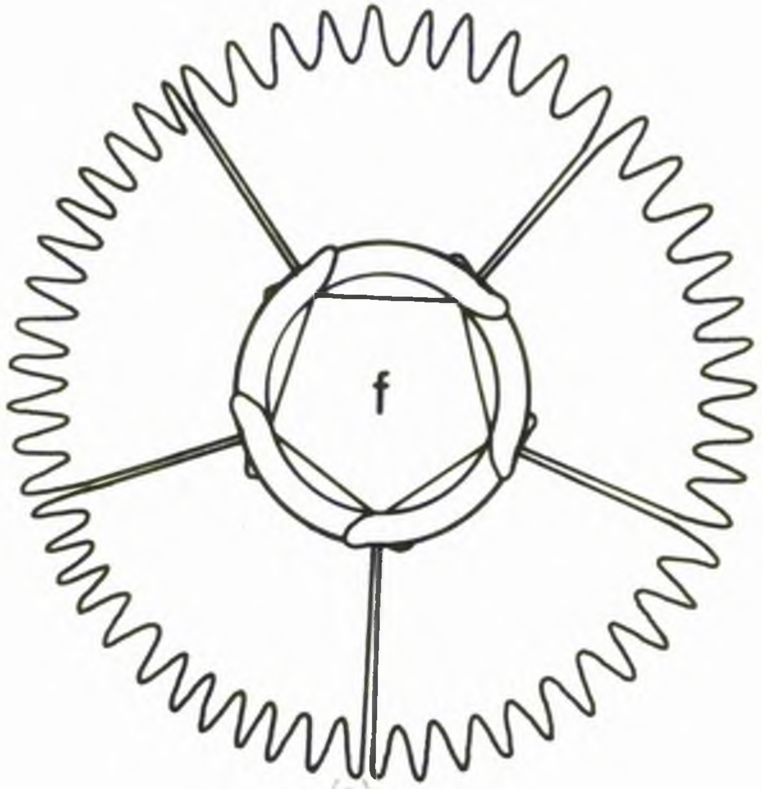

(a)

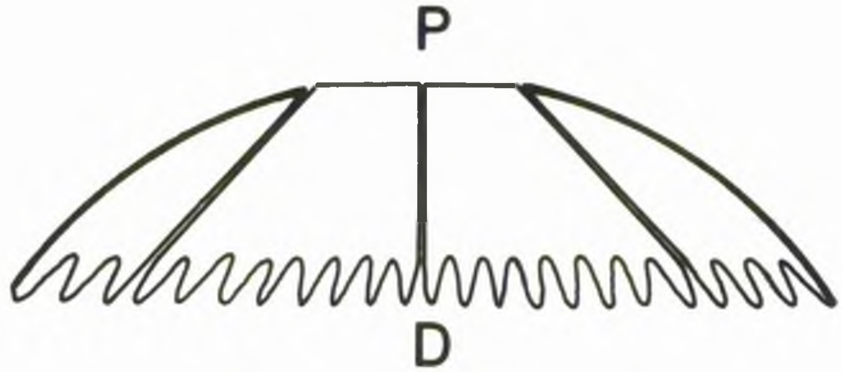

(b)

Fig. XVIII

PTF rosette structure

a) Plan view - proximal surface

X Rudimentary foramen - often absent

b) Side view

P Proximal

D Distal

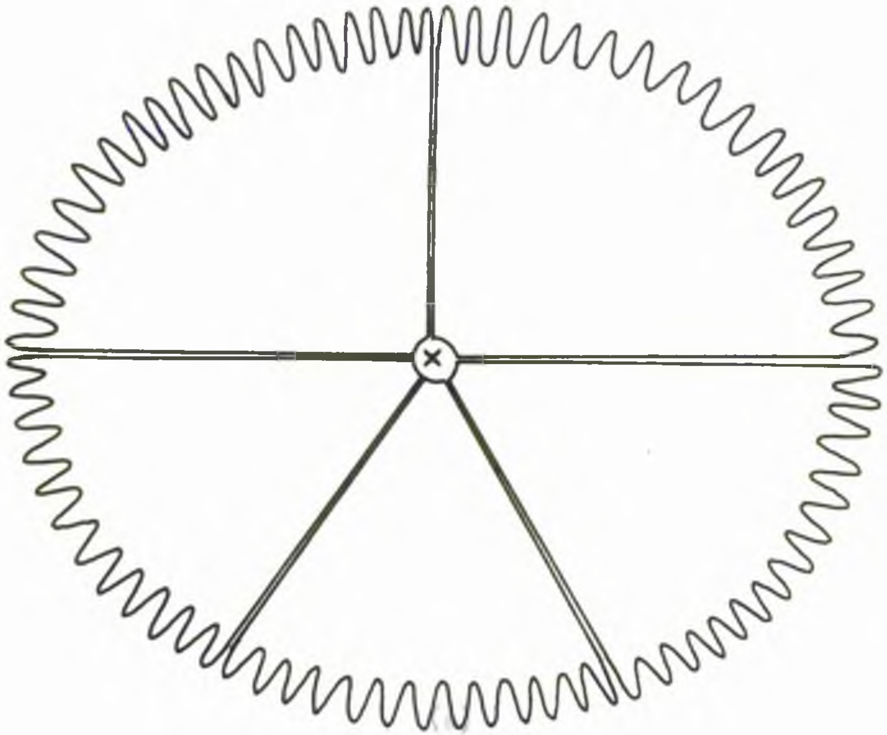

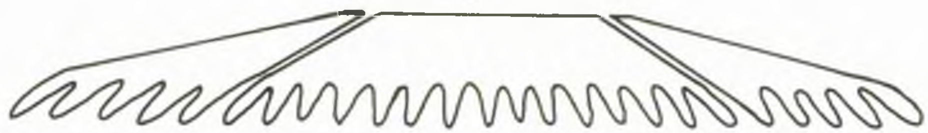

(b)

Fig. XIX a

Relationships of the peristomial and ambulacral tube foot/ampulla systems to the rest of the water vascular system. Sagittal sections (schematic) of the pore pairs are shown.

Note differences in the orientation of the pore pairs and ampulla morphology.

ATF	Ambulacral tube foot/ampulla complex
Cn	Circumoesophageal nerve ring
Cw	" water ring
Dw	Descending branch off water ring
Lw	Lateral water canal
Ln	Longitudinal (tube foot) nerve
PTF	Peristomial tube foot/ampulla complex
Rw	Radial water canal

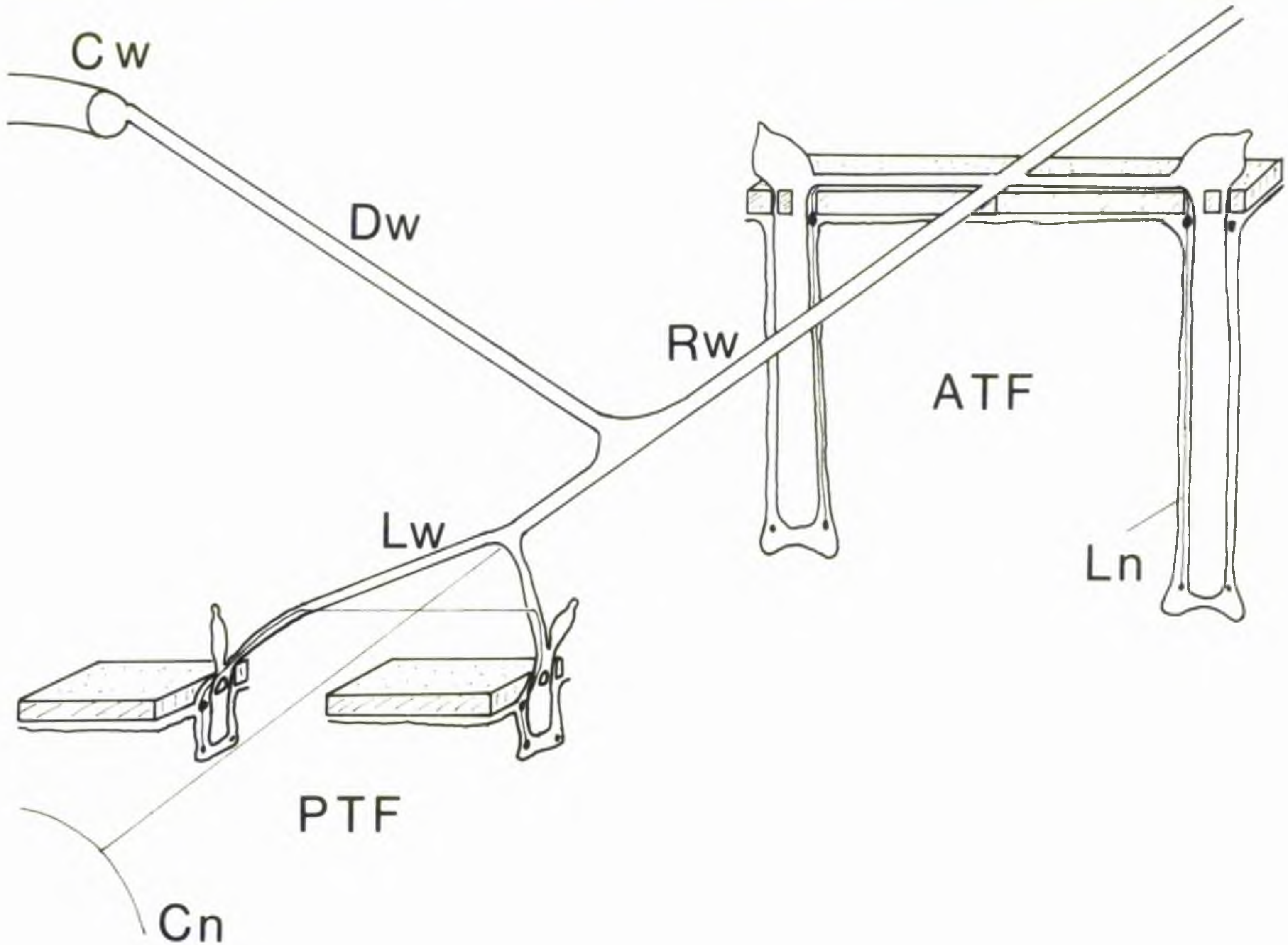
Cw
Dw
Rw
ATF
Lw
Ln
PTF
Cn

CHAPTER 4

FINE STRUCTURE AND INNERVATION OF INTRATHECAL REGIONS OF THE WVS: EVIDENCE FOR THE NEURONAL CONTROL OF CILIARY ACTIVITY

Page

FINE STRUCTURE AND INNERVATION OF INTRATHECAL REGIONS OF THE WVS: EVIDENCE FOR THE NEURONAL CONTROL OF CILIARY ACTIVITY

INTRODUCTION

Intrathecal regions of the echinoid water vascular system comprise: 1) the axial complex, consisting of an axial organ and a madreporite 2) the stone canal, 3) the circumoesophageal water ring and five polian vesicles, and 4) five radial water canals.

Of these regions, the axial complex appears to have attracted the most attention from physiologists and anatomists particularly in the nineteenth and early twentieth centuries. NICHOLS (1966) has provided a review of these studies by the British and European 'Schools' which consisted of eminent authors such as SHARPEY, HUXLEY, GEMMILL, TIEDEMANN, HAMANN and CUÉNOT to name but a few.

The madreporite of various echinoderm classes, and its connections with the haemal and water vascular systems, has formed the basis of considerable speculation, since these early studies. The term 'madreporic plate' originated from the superficial resemblance of the plate to madreporarian corals and it was HUXLEY in 1887 who later coined the term 'madreporite'. During this period, most workers were pre-occupied with the problem of fluid flow through the madreporite and a classic dichotomy of ideas developed. The European 'school' of HARTOG, LUDWIG and CUÉNOT favoured the notion of currents passing inwards from the exterior and into the madreporite. However, the British 'school' of BAMBER, GEMMILL and BUDINGTON provided more substantial evidence of ciliary currents producing an outward flow from the madreporite. To this day speculation persists regarding the function of the madreporite and the associated axial gland.

In vivo observations of the echinoid axial complex show that several parts contract rhythmically (BOOLOOTIAN & CAMPBELL 1964, MILLOTT 1967, JANGOUX & SCHALTIN 1977). Similar observations in an asteroid axial complex (BARGMANN & VON HEHN 1968) led to the conclusion by some authors that the axial complex of echinoids and asteroids functions as a 'primitive heart' (BOOLOOTIAN & CAMPBELL 1964, BARGMANN & VON HEHN 1968). However echinoderms do not possess a closed circulatory system and thus the role of a 'heart' would seem rather dubious.

VEVERS (1967) has reviewed histochemical studies of the axial complex and following these studies an endocrine and immunodefensive role has been proposed (MILLOTT & VEVERS 1964, MILLOTT 1966, 1967, 1969). LECLERG (1974) has observed an antibody reaction in asteroid axial organs and also supports the immune function hypothesis.

BACHMANN and GOLDSCHMID (1978a) have recently reviewed the structure and function of the echinoid axial complex and on the basis of ultrastructural data propose that contractility of the complex is associated with the removal of amoebocytes and other waste products.

Only three studies have described the innervation of the axial complex and these have dealt with the asteroid *Asterias rubens* (BARGMANN and VON HEHN 1968); and the echinoids *Psammechinus miliaris* (JANGOUX & SCHALTIN 1977) and *Sphaerechinus granularis* (BACHMANN & GOLDSCHMID 1978b).

The stone canal, which passes from the axial complex to the circumoesophageal water ring, is named as such, after the translation of TIEDEMANN's expression 'Steinkanal'. In 1816 he observed that the stone canal of *Astropecten aurantiacus* contained calcareous spicules which could be detected by squeezing the canal with a pair of forceps. In echinoids however, there are far fewer spicules in the stone canal (a considerable advantage for tissue processing for TEM) but the terminology remains the same. Most early studies on the stone canal (see NICHOLS 1966 for a review) were concerned with the direction of ciliary currents within the lumen of the canal, and unlike the madreporite most workers seemed to agree upon the presence of strong orally directed currents (i.e. currents down the stone canal). In a classic experiment by GEMMILL (1914) the apical end of an Echinus stone canal was ligatured and it was observed that the canal collapsed due to a complete removal of the water vascular fluid.

There have been no published studies on the ultrastructure of the stone canal from any class of echinoderm.

The polian vesicles have been described as 'muscular sacs arising interradially from the water ring' (NICHOLS 1966). The only comparatively recent study on these organs is an ultrastructural study of the polian vesicles of Holothuria tubulosa (BACCETTI & ROSATI 1968). The lack of any studies on these organs is emphasised by the fact that reviews by HYMAN (1955) and NICHOLS (1966) are mainly based upon the histological studies on holothurians by JOURDAN in 1883.

The circumoesophageal water ring and radial water canals of all classes of echinoderms have been the subject of a few histological and functional morphological studies (see review by NICHOLS 1966). Most of these studies have been concerned with the role of the water canal in tube foot extension, particularly in the ophiuroids (BUCHANAN & WOODLEY 1963, WOODLEY 1967) and crinoids (NICHOLS 1960). There have been no published ultrastructural studies on the water ring or water canals.

It is therefore the purpose of this chapter to describe studies on intrathecal regions of the echinoid water vascular system but with a particular emphasis on their innervation and muscle structure. From these studies, histochemical and ultrastructural evidence will be described in order to support a hypothesis that some ciliary activity is under neuronal control

in the echinoid water vascular system and possibly other echinoderm viscera

RESULTS

1. Madreporite and axial organ

Since the general ultrastructure of the echinoid axial complex has been described recently in Psammechinus miliaris (JANGOUX & SCHALTIN 1974) and Sphaerechinus granularis (BACHMANN & GOLDSCHMID 1978a) it is unnecessary to repeat their findings as the axial complex of Echinus esculentus is very similar in structure.

For the purposes of this study the axial complex can be divided into five main regions (Fig. XIá):

i) the madreporite which communicates with the exterior.

ii) the ampulla of the stone canal which opens into the madreporic canals (hydropores).

iii) the labyrinthine axial organ which contains the pulsatile vessel.

iv) the termination of the pulsatile vessel which abuts onto a cavity within the madreporite.

v) the stone canal which communicates with the circumoesophageal water ring.

The morphology of the madreporic plate or madreporite has been previously described in Chapter 3. The poriferous region of the plate consists of a longitudinal array of canals, the madreporic canals, passing through the plate. Light microscopy and electron microscopy show that the canals are continuous with the ampulla of the stone canal and thus lined by cells which are homologous to the endothelial cells lining all regions of the water vascular system. However, the endothelia lining the madreporic canals show a distinct zonal variation along the length of the canal (Fig. XIb). The proximal half of the canal is lined by a simple squamous endothelium (Fig. 46) similar to other regions of the water vascular system. Passing distally along the canal the endothelium becomes thicker and more extensively ciliated (Fig. 47). The distal half of the canal is lined by a columnar endothelium characterised by long microvillous projections similar in appearance to brush-border epithelia. Extending from the distal endothelial cells into the lumen of the canal are long cilia (~10μ) which bend through 90° and project towards the external opening of the canal (Figs. 48 and 49). Amoebocytes, granular inclusions and assorted vacuolar structures appear within the canals. Also occurring within the distal endothelia of the canals are numerous spindle-shaped and globular secretory cells, many of which show intense β or γ metachromasia with Azure 2 and Methylene blue (Fig. 49). It is therefore probable that these cells are secreting acid mucopolysaccharides with high degrees of sulphation.

No musculature or innervation of the madreporic canals was observed. A rather anomalous precipitation of uranyl acetate occurred over the endothelial microvilli and some vacuolar structures within the madreporic canals (Fig. 48). The reasons for this are unknown; it is possible however that uranyl precipitation may be intensified over sites of highly polyanionic substances such as the acid mucopolysaccharides produced by the secretory cells.

Unfortunately, difficulties with embedding media infiltration (even with Spurr) hindered this present ultrastructural study of the madreporite.

The axial organ can be divided into three main layers (Fig. XX):

i) an outer ciliated epithelium containing a few, small, longitudinally orientated muscle cells and underlain by an extensive basiepithelial plexus,

ii) a middle connective tissue layer which is extensively muscularized by mainly circularly orientated muscle cells,

iii) a ciliated endothelium which lines the axial sinus.

The apparently complex structure of the axial organ is due to extensive labyrinthine evaginations of the axial sinus. The outer layer of the axial organ is similar in structure to that of the stone canal and water canals i.e.

an epithelium underlain by an extensive basiepithelial nerve plexus.

Interspersed within the connective tissue layer are numerous non-striated muscle cells of irregular shape and size forming an inner muscle layer. Unlike the outer muscle layer the inner muscle cells are orientated in a variety of directions (Fig. 50) but the majority are arranged in a circular array. A characteristic feature of the inner muscle cells are their extensive interdigitations within the basal lamina of the connective tissue (Fig. 51). Most of the villiform interdigitations pass radially throughout the connective tissue and are approximately 100nm wide and up to 3µ long. The contents of the interdigitations are mainly granular sarcoplasm although some of the larger interdigitations are accompanied by myofilaments extending from the main contractile region of the cell body. Many of the muscle cells bifurcate within the connective tissue (Fig. 51). Some areas of contact between muscle cells and the basal lamina are characterised by hemidesmosomes (Fig. 51).

The basal lamina which separates the musculature from the rest of the connective tissue is approximately 100nm to 1µ wide and is composed of a meshwork of fine filaments (Fig. 52). Each filament is 10-15nm in diameter and up to 600nm long.

The fine filaments comprising the basal lamina are similar to those occurring throughout the connective tissue and associated with collagen filaments. Ramifying within the connective tissue are a variety of cellular elements and processes. Some processes are characterised by the presence of large dense storage granules (LDSG) approximately 150nm in diameter. The LDSGs are membrane bound and show a variety of profiles from ovoid to spherical.

Other fine processes ramifying throughout the connective tissue are pseudopodia extending for several microns from phagocytic cells (Fig. 53). The pseudopodia are approximately 100nm wide at their narrowest region and up to 800nm wide in varicose regions. Apart from the possession of pseudopodia phagocytes are characterised by large accumulations of vacuoles in the peri-nuclear region of the cell body and in pseudopodal varicosities. The vacuoles are approximately 200-500nm in diameter and contain an electron opaque precipitate. Other processes probably represent fragments of necrotic amoebocytes (Fig. 54) and contain large vacuoles, many of which are ruptured (probably a fixation artefact). An electron dense granular material surrounds the vacuoles, which may be as large as 1µ in diameter. The necrotic cells often possess lytic bodies of various types ranging from membrane bound electron dense granules approximately 480nm in diameter to small multivesicular bodies 100-180nm in diameter. Most phagocytes and necrotic amoebocytes appear to be passing into the lumen of the numerous evaginations of the axial sinus.

LMG processes similar to those in the connective tissue innervate the inner muscle layer (Fig. 55). Varicosities contain LMGs, small clear vesicles (approximately 50nm in diameter) and neurotubules (approximately 16nm in diameter). Sites of innervation of the musculature are non-specialized and mainly consist of simple abutments of LMG axons against the sarcolemma. Some interesting modifications of the LMG/sarcolemma junction do occur and these consist of lamellar sarcolemmal extensions 'wrapping' over LMG varicosities (Fig. 55). Within the sarcoplasm of sarcolemmal extensions are sub-surface cisternae which constitute regions of a simple sarcoplasmic reticulum. Sub-surface cisternae are also juxtaposed with the sarcolemma along contacts between adjacent muscle cells.

Each muscle fibre contains two types of myofilaments; thin filaments (less than 10nm in diameter) and thick filaments (approximately 30nm in diameter). Non-contractile regions of the muscle cell bodies are characterised by clusters of unusual mitochondria (Fig. 56) containing lamellar cristae. The lumen of the mitochondrial cristae is electron lucent in contrast to the electron dense intramitochondrial space.

Numerous LDCG axons form an extensive plexus within the inner muscle layer (Fig. 56) and it is apparent that LDCGs vary considerably in shape and size within an individual LDCG process. In most LDCGs the electron dense core fills the granule, particularly in the larger examples. However, smaller LDCGs tend to have a reduced core separated from the granule membrane by a distinct electron lucent halo. Similar variations in LDCG structure also occur within LDCG processes ramifying within the connective tissue (Fig. 57).

Fluorescence histochemistry according to the FALCK-HILLARP method indicates that catecholamine containing neurones occur within the basiepithelial plexus of the whole axial complex. The small size of the neurones, in addition to their close packing and large numbers, produces a fluorescent plexus within which individual axons cannot be distinguished (Fig. 58). With monochrome photomicrography it can be difficult to distinguish the specific fluorescence of the outer basiepithelial plexus from the non-specific fluorescence of the endothelia and epithelia. However, colour photomicrography enables a distinction to be made between specific and non-specific fluorescence (Fig. 59). After reduction with sodium monoborohydride in 95% Propan-2-ol only non-specific fluorescence or autofluorescence is observed (Fig. 60). Unfortunately, the spectral sensitivity of colour film can produce a colour shift such that non-specific bluish fluorescence is shifted to blue-green and specific apple-green fluorescence is shifted to yellow. Specific fluorescence was only observed in the basiepithelial plexus in all of the intrathecal regions of the water vascular system. Also, all the specific fluorescence observed was apple-green in colour indicating the presence of dopamine and/or noradrenaline. Numerous orange autofluorescent bodies, presumably the phagocytes observed with TEM, occur within the axial organ (Fig. 61). Also, the basiepithelial plexus greatly thickens in the region of the stone canal (Fig. 61). Occasionally in some transverse sections of the axial organ it was possible to distinguish individual fluorescing axon bundles within the outer epithelia (Fig. 62).

2. Stone Canal

The axial organ narrows into the axial haemal vessel which extends down to the circumoral haemal vessel. Adjacent to the axial haemal vessel is the more conspicuous stone canal. Fluorescence histochemistry indicates that an extensive aminergic nerve plexus occurs within the outer layer of the axial haemal vessel and the stone canal (Fig. 63). The nerve plexus is particularly thickened on one side of the stone canal forming a nerve tract.

The ultrastructure of the stone canal is very similar to that of the water canals and consists of an epithelium, basiepithelia nerve plexus, connective tissue layer and an endothelium which lines the lumen of the canal (Fig. XII). The stone canal differs from the water canals in the presence of small muscle cells which are longitudinally orientated between the endothelium and connective tissue layer (Fig. 64). Some of the muscle cells appear to be degenerating and in the process of expulsion into the lumen of the stone canal (Fig. 65). Degenerating muscle cells have a reduced number of thick filaments, assorted lytic bodies and a more opaque cytoplasm.

3. Polian vesicles and circumoesophageal water ring

Preliminary TEM studies show that the polian vesicle are muscularized evaginations of the circumoesophageal water ring. The circumoesophageal water ring is similar in ultrastructure to the radial water canals. Polian vesicles possess an inner muscle layer similar to that of the stone canal and there is an extensive basiepithelial nerve plexus (Fig. 66). A further distinguishing feature of polian vesicles are the abundance of a variety of amoebocytes which appear to pass through the connective tissue (Figs. 67, 68) and into the labyrinthine evaginations of the lumen (Fig. 69).

4. Radial water canal

The ultrastructure of the epithelia and basiepithelial plexus of the radial water canal is the basic organisation found throughout the intrathecal regions of the water vascular system. The following more detailed description also applies to the epithelia and nerve plexus of other intrathecal regions, such as the axial organ, stone canal and polian vesicles.

The water canals consist of; an outer epithelium overlying a basiepithelial nerve plexus, a thin connective tissue sheath (approximately 13μ), and an endothelium which lines the lumen of the canal.

Epithelial and endothelial cells are very similar in ultrastructure and possess a large nucleus which occupies most of the cell body. Each epithelial and endothelial cell possesses a single cilium which is surrounded by a distinctive collar structure around its base (Fig. XXII). The collar consists of a cylinder of lamellae projecting from the plasma membrane (Fig. 70). The collar is approximately 1.3μ long and 1μ in diameter distally and 1.7μ proximally. The proximal portion of each lamella is extensively vacuolated, but the distal portion is non-vacuolated and tapers into a microvillous ending (Fig. 71). Lining the interior of the collar is an electron opaque 'fuzz' coat which forms a cylindrical sheath 0.8 - 1.2μ in diameter. The fuzz coat varies in thickness from 90nm distally to 100nm proximally at the base of the collar. Surrounding the ciliary shaft is a less extensive 'fuzz' coat from which lateral filaments radiate into the collar coat (Fig. 70). Lateral filaments appear to be of a similar composition to the fuzz coats and occur at all levels through the collar (Fig. 72). The cilium contains a 'typical' 9 x 2 + 2 array of filaments and the shaft diameter varies from 270nm distally to 360nm proximally. Since longitudinal sections of a complete cilium were not obtained, estimates of the length of cilia can only be approximations. The longest section observed shows a minimum length of 2.3μ (Inset Fig. 72).

The ciliary basal apparatus consists of the following regions:

i) transition zone

ii) basal collar

iii) basal rootlet

The transition zone represents the sites of origin of the central axonemal tubules and consists of a transverse basal plate spanning the lumen of the ciliary shaft and closely apposed to the peripheral doublet tubules. The region of the basal plate corresponds with a constriction of the shaft membrane (Inset Fig. 72) and this may represent the point of 'articulation' of the cilium. The basal plate occurs in a position approximately 130nm above the base of the ciliary shaft and projecting past the edges of the plate are the peripheral tubules which enter into the basal rootlet (Fig. 72).

At the base of the ciliary shaft is a basal collar consisting of a ring of electron dense material which encircles the peripheral doublets (Fig. 70). At the level of the basal collar an electron dense filament or 'spoke' radiates from each peripheral doublet and terminates as an electron dense body internal to the collar (Fig. 70). Each spoke is 90nm long and 10-15nm in diameter.

The basal rootlet is approximately 800nm long and tapers from a maximum width of 175nm. The rootlet is composed of longitudinal filaments and is characterised by an electron dense striation with a repeat period of 60nm. Orientated perpendicular to the basal rootlet is a single centriole. Extending laterally from the distal end of the rootlet, and on the same side as the centriole is a basal foot. Usually associated with the basal apparatus is a Golgi complex consisting of flattened cisternae and numerous Golgi vesicles (Fig. 72).

The basiepithelial nerve plexus of the water canals consists of bundles of several axons ramifying between epithelial cells and the basal lamina (Fig.73).

Many of the axon bundles are separated by fine processes which extend from epithelial cell bodies and terminate as enlarged 'feet' apposed to the basal lamina (Fig. 74). Axons can be readily distinguished from epithelial processes on the basis of three criteria:

i) the absence of an electron opaque granular cytoplasm

ii) the presence of neurotubules

iii) the presence of vesicles and membrane bound granules

Basiepithelial axons are small and can narrow down to 23nm in diameter in some regions (Fig. 75), which accounts for the inability to localise single axons using the FALCK-HILLARP method. Axonal varicosities contain two main types of vesicles; small clear vesicles 40-50nm in diameter and dense core vesicles 80-120nm in diameter. A distinct electron lucent halo separates the core of dense core vesicles from the limiting membrane. Some varicosities reach up to 1.2μ in diameter and the axonal lumen can be completely occluded with numerous dense core vesicles and small clear vesicles (Fig. 76-79). Such varicosities abut against epithelial plasma membranes forming simple synaptoid contacts. However, some epithelial cells extend small processes which wrap around the varicosity (Fig. 79).

Fluorescence histochemistry of the water canal shows similar results to those obtained in the axial organ and stone canal, i.e. specific apple-green fluorescence occurs only within the basiepithelial plexus.

Evidence for electrotonic coupling between axons and epithelial cells was not observed but a characteristic feature of interepithelial junctions is a septate junction which occurs proximal to a desmosome (Fig. 80). The septate junction consists of approximately five transverse links between the adjacent plasma membranes. Each link is 20nm long and 11nm in diameter (assuming it is a tubular structure) and the inter-link distance is 13-17nm.

Occurring within the connective tissue sheath of the water canal are a variety of amoebocytes similar to those found in other regions of the water vascular system. In addition, large morula cells up to 24μ long and 10u wide appear to pass through the connective tissue (Fig. 81). Morula cells are characterised by a cell body which is totally occluded with large membrane bound spherules containing granular material varying in electron capacity. The tight packing of the spherules is such that the nuclear membrane is distorted.

Another cell type found in the connective tissue is fibrocytic since fibrillar elements occur within the cytoplasm and in the connective tissue ground substance adjacent to the cell (Fig. 82).

LDSG processes were not observed in any layer of the water canal.

Within the connective tissue, collagen filaments occur in a variety of diameters, ranging from 27nm to 182nm (Fig. 83). Each filament has the same typical cross-striation consisting of alternating electron dense and electron lucent bands. Each dense band contains a light interband (Fig. XXIII) and the repeat period of the main electron dense band is approximately 54nm. Variations in the width of the filament along its length correlate with the cross-striation, such that the main dense band comprises the widest region.

The water canals are devoid of any musculature, however, non-striated muscle cells occur in the mesenteric sheet which supports the radial water canal as it passes from the circumoesophageal water ring down through the auricle of the perignathic girdle. The epithelia on both sides of the mesentery are continuous with the outer epithelia of the radial canal.

The muscle cells are longitudinally orientated between the epithelia and the connective tissue sheath of the mesentery (Fig. 84). Hemidesmosomes occur along the junction between the sarcolemma and the basal lamina. Fine epithelial processes extend over the muscle cell bodies which do not appear to be exposed to the coelomic space. Passing through the connective tissue layer of the mesenteric sheet are small bundles of axons (Fig. 85) similar in ultrastructure to basiepithelial axons. However, basiepithelial axons between the epithelia and the basal lamina were not observed.

DISCUSSION

The results of this investigation of intrathecal regions of the water vascular system provide evidence for functions which have been underestimated or completely undescribed.

SEM, TEM and light microscopy indicate that canals passing through the madreporite provide communication between the exterior and the water vascular and haemal systems. The zonal differentiation of the endothelia lining the madreporic canals provides evidence for:

a) the outward beating of long cilia at the distal end of the canal

b) the secretion of mucosubstances into the lumen of the canal

c) an extensive brush-border modification of the distal endothelia

The orientation of the cilia at the distal end of the canal indicates that water vascular fluid may pass through the madreporite to the exterior. However, the volume of fluid is probably small due to the small size of the canals. More importantly, the presence of necrotic amoebocytes and vacuolar membranous arrays within the canals indicates that the madreporite is an excretory structure. Using light microscopy, BACHMANN & GOLDSCHMID (1978a) observed similar excretory products within the madreporic canals of Sphaerechinus granularis.

Apart from simply providing an exit for waste products passing from the axial complex, it is also possible that the madreporite may secrete waste products and resorb certain metabolites and ions. The mucosubstances secreted by cells at the distal end of the madreporic canals may be excretory as the positioning of the cells would facilitate an efficient removal of their secretions. Alternatively, the mucosubstances may not be excretory products but substances which lubricate and protect the lining of the canals. The endothelial mucosubstances show strong γ metachromasia with thiazine dyes such as Methylene blue and Azure 2 which indicates the presence of highly sulphated acid mucopolysaccharides (or glycosaminoglycans to use more modern nomenclature). Similar substances are known to have a bacteriostat function in addition to their lubricatory role (HUNT 1970). A protective function seems quite probable since the direct opening of the water vascular system to the exterior would provide undesirable access for a variety of bacterial and fungal infections. It is also possible that mucosubstances may facilitate ciliary activity in the removal of waste products from the madreporic canals.

The brush-border modification of the endothelia at the distal end of the canals raises an intriguing possibility. The development of long microvilli by the endothelial cells provides an increase in surface area for the exchange of substances between the lumen of the canal and the endothelial cytoplasm. Ions and small organic molecules may be resorbed from the canal fluid and recycled back into the coelom. However, the nature of the recycling mechanism, if it occurs, is unknown. Perhaps resorbed molecules and ions diffuse through the connective tissue supporting the madreporite.

Ultrastructural studies of the axial organ support the hypothesis that the axial complex is an excretory structure. The axial organ is a point of confluence between the haemal and water vascular systems as shown by the distribution of dyes injected into the axial sinus (BOOLOOTIAN & CAMPBELL 1964). The opening of both systems into the madreporite would correlate with the development of a single specialized exit for the removal of necrotic cells and amoebocytes since two exits performing the same function would be superfluous. JANGOUX & SCHALTIN (1977) have suggested that the axial organ functions in the collection and preparation of waste material since amoebocytes pass from the perivisceral coelomic fluid into the axial gland via the thin epithelia , a process which was termed 'diapedesis' ('... les coelomocytes le traversement facilement par diapedese...'). Diapedesis was followed by the intracoelomic injection of ferritin and it was observed that ferritin was rapidly endocytosed by amoebocytes within the perivisceral fluid. Shortly afterwards amoebocytes containing ferritin occurred within the evaginations of the axial sinus (termed canaliculi). The subsequent fate of the ferritin was not described.

BACHMANN & GOLDSCHMID (1978a) also propose an excretory function and observed phagocytosis of whole cells and amoebocytes passing through transformational stages. Many of the amoebocytes were remarkably similar in ultrastructure to those observed in this study indicating that there are few interspecific differences in the structure of echinoid amoebocytes. Similarly, few differences in the structure of the axial complex occur.

The presence of an extensive musculature within the axial organ agrees with in vivo observations of alternating and periodic contractions of the axial complex of both echinoids (BOOLOOTIAN & CAMPBELL 1964, MILLOTT 1967, JANGOUX & SCHALTIN 1977) and asteroids (BARGMANN & VON HEHN 1968). The data obtained in this study favours the argument that contractions of the axial organ enable the exit of waste materials into the ampullae of the stone canal. In addition, ciliary activity by endothelial cells would facilitate the movement of fluid from the axial organ through the madreporic canals.

Preparations of the axial complex of E. esculentus showed occasional contractions but any form of rhythmicity was not observed. It is possible that any pacemaker activity is sensitive to small differences in the external saline (which was sea-water).

A muscular axial organ functioning as a 'primitive heart' has been the alternative hypothesis favoured by studies in the nineteenth century (see BACHMANN & GOLDSCHMID 1978a) and more recently by BOOLOOTIAN & CAMPBELL (1964) and BARGMANN & VON HEHN (1968). This is most unlikely since neither the haemal nor the water vascular systems are true circulatory systems. The ultrastructure of the axial organ indicates that it is unlikely that fluid passes up to the axial complex via the axial haemal vessel and stone canal; and then back along the same vessels. BURTON (1964) has shown that the 'ebb and flow' movement of fluid within haemal vessels 'supplying' the echinoid stomach does not constitute a true circulatory system. Instead BURTON proposes that the ebb and flow movement may aid diffusion of nutrients into the coelom. It would be interesting to determine whether the haemal vessels provide a direct passage for amoebocytes and waste materials from the stomach to the axial complex.

The present study of the axial complex indicates that a glandular function is unlikely. Glandular cells were not observed within the axial complex; furthermore an endocrine function as proposed by MILLOTT & VEVERS (1964) seems unlikely because of the lack of a true circulatory flow would not assist the distribution of the hypothetical endocrine secretions. Despite the endocrine proposals, MILLOT & VEVERS (1964) agree that amoebocytes accummulate and degenerate within the axial organ.

HOLLAND (1970) has proposed that the axial organ of the crinoid Nemaster rubiginosa functions as a neurohaemal structure. TEM studies indicated that neurosecretory axons terminated against the axial sinus. However, the property of neurosecretion cannot be inferred from ultrastructural evidence alone. Histochemical and histophysiological tests are required to confirm the presence of neurosecretory material. Similar neurosecretory cells were not observed in the present studies.

Another hypothetical function for the madreporite and stone canal has been the suggestion that it functions as a 'topping up' structure maintaining the fluid volume of the water vascular system. The structure of the madreporic plate is presumed to act as a sieve preventing foreign particles from entering and only allowing sea water through. Significant increases in hydrostatic pressure within the tube foot/ampulla complexes would produce a loss of water and salts by ultrafiltration. Perhaps such losses are compensated for by fluid entering the madreporite?

BINYON (1964) calculated that fluid loss from a 50g. starfish to be about 0.48 ml. h^{-1}. This estimate was based upon the external surface area of tube feet but more accurate estimates based upon the internal surface area produced a revised value of 0.75 ml.h^{-1} (BINYON 1976). On hydromechanical grounds, FECHTER (1965) has calculated that a maximal flow rate through the madreporite of E. esculentus is 0.4 ml.S^{-1} (i.e. 1.44 l. h^{-1}). Thus on a theoretical basis it would appear that the madreporite may have a 'topping up' function. However, there are five important factors which do not support this hypothesis:-

1. Water vascular fluid is not the same composition as sea water (see Reviews by ROBERTSON 1949 and BINYON 1972). In addition to the presence of protein (approximately 1.5g.l^{-1}), water vascular fluid also contains numerous amoebocytes and has an elevated potassium content (approximately 6mM greater). PRUSCH (1977) has shown that the chloride content of water vascular fluid is 8mM greater than that of sea water. The potassium and chloride content of perivisceral coelomic fluid is similar to that of sea water (BINYON 1972).

2. FECHTER (1965) could not obtain experimental evidence to support his theoretical assumptions. Two experiments were performed in which an animal, just covered with sea water, either had a manometer attached to the

madreporite or the madreporite was sealed with wax. In either case tube foot movement was usual but fluid movement did not occur in the manometer. Two other experiments produced rather curious results.

One animal was immersed in 20 cm. of sea water with the madreporite sealed; tube foot extension did not occur. Another animal was just covered with sea water but had a 20 cm long glass tube, containing sea water, attached to its madreporite; tube feet extended maximally but were unable to retract.

NICHOLS (1972) was unable to repeat these results with P.miliaris but postulates that the madreporite functions as a pressure equalizing device.

3. In asteroids it has been calculated that the volume of fluid within intrathecal regions of the water vascular system is only 1-2% that contained by the ambulacral systems (SMITH 1946).

4. BINYON (1976) has observed that isolated arms of A. rubens, in which the radial canal is blocked by vaseline or mercury, can still move for several days despite a fluid loss which would have totally emptied the whole ambulacral system. Similarly, fragments of echinoid test containing only a few tube feet can survive and function adequately for several days.

5. It has been shown that exogenous radiolabelled compounds such as ^{14}C-amino acids and ^{14}C-polyethylene glycol do not pass through the madreporite of different asteroid species (FERGUSON 1967 and PRUSCH 1977). Therefore, it is quite unlikely that fluid loss, via ultrafiltration by tube feet, is compensated for by the madreporite.

An alternative hypothesis for fluid maintenance is the process of solute secretion by the tube feet epithelia. ROBERTSON (1949) first suggested that the elevated K^+ content of water vascular fluid is due to the active pumping of K^+ by the tube foot epithelia. Using flame photometry BINYON (1964, 1972, 1976) has demonstrated the accumulation of K^+ within the lumen of asteroid tube feet. In addition, BINYON has calculated that the increased hyperosmicity of the water vascular fluid would generate a sufficient osmotic influx of water to counterbalance the hydrostatic efflux. BINYON (1979) has also calculated that the oxygen requirement for a K^+ pump is only 0.69% of the total O_2 consumption of a 50 g A. rubens. Unfortunately, BINYON (1976) found that in vitro experiments were 'erratic and unpredictable', and that metabolic inhibitors such as 2-4, dinitrophenol and sodium acetate had no effect on K^+ accumulation. Using a tube foot 'sac' preparation ligatured onto a hypodermic needle, PRUSCH (1977) has obtained convincing evidence of K^+ accumulation by monitoring ^{42}K levels. The use of ^{42}K enables measurement of unidirectional K^+ fluxes and not only net accumulation rates. The measured K^+ influx was 4.2 x 10^{-9} moles. cm^{-2} min^{-1} and efflux was 3.4 x 10^{-9} moles. cm^{-2} min^{-1}. Furthermore PRUSCH (1977) has shown that K^+ influx demonstrates Michaelis-Menten kinetics with increasing external K^+ concentration. The active pumping of K^+ by the epithelia was further confirmed by the elimination of the possibility of an electrochemical gradient since the transepithelial potential was only 0.1mV. In addition, CN^- inhibited the secretion of K^+.

On the basis of the evidence available it is proposed that the madreporite and axial complex has an excretory role in the transport, processing and removal of amoebocytes and waste products. The 'topping up' function of the madreporite is unnecessary since fluid loss through ultrafiltration can be compensated for by the passive diffusion of water through the tube foot epithelia following the maintenance of a K^+ concentration gradient.

The stone canal which passes from the axial complex to the circumoesophageal water ring is very similar in structure to the water canals, differing only in the presence of an inner musculature and a slightly thicker connective tissue sheath.

The initial studies made on Polian vesicles indicate that they are similar in ultrastructure to those of holothurians (BACCETTI & ROSATI 1968a). The polian vesicles show the same organization as the stone canal but possess a more extensive endothelium due to evaginations of the Polian sinus. Thus they are similar to the axial organ. A characteristic feature of the stone canal and the Polian vesicles are the presence of numerous amoebocytes, passing into the hydrocoel from the perivisceral coelom. NICHOLS (1966) has suggested three possible functions for Polian vesicles:

i) they function as reservoirs for water vascular fluid when several tube feet contract suddenly

ii) they maintain turgor in the peristomial tube feet

iii) they function as low pressure reservoirs for fluid en route from the stone canal to the ambulacral system; NICHOLS favoured the latter.

All three possibilities are common in the assumption that Polian vesicles have a hydrostatic function. This seems unlikely because:

i) the tube foot/ampulla complex is known to function as a hydraulic unit independent of the rest of the water vascular system

ii) in echinoids, peristomial tube feet possess ampullae and do not arise directly from the circumoesophageal water ring,

iii) the volume of the hydrocoel within the Polian vesicles is too small to function as a 'reservoir' (BACCETTI & ROSATI 1968a).

The ultrastructural and histochemical studies of BACCETTI and ROSATI provide evidence for amoebocytes, rich in mucosubstances, passing through the wall of the Polian vesicles and apparently releasing their contents into the hydrocoel. It is possible that the numerous vacuolar structures observed within the lumen of echinoid Polian vesicles are released from amoebocytes in a similar manner to that in holothurians.

EPITHELIA	GENUS	REFERENCE	
Coelomic	Mesothuria		Lamellar Choanocytes
	Stichopus	Nørrevang & Wingstrand (1970)	
Ampulla	Porania		
Axial complex	Sphaerechinus	Bachmann & Goldschmid (1978a)	
Dorsal haemal vessel	Parastichopus	Jensen (1975)	
Gill	Echinus	Cobb & Sneddon (1977)	Microvillous choanocytes
Tridentate pedicellariae	Echinus	Cobb (1969)	
Papulae	Asterias	Cobb (1978)	
Ciliary band	P. miliaris plutei	Ryberg (1977)	
	S. purpuratus	Burke (1978)	
	Asteroid brachiolaria (various)	Nørrevang & Wingstrand (1970)	
Ampulla	Asteroid (various)	" "	

Table 5

Occurrence of choanocyte cells in echinoderms

Thus the data obtained in this study supports the evidence of BACCETTI and ROSATI and indicates that Polian vesicles have an excretory function. In a similar manner to the axial organ, the inner musculature of Polian vesicles would facilitate ciliary activity (of endothelial cells) in the extrusion of waste products into the circumoesophageal water ring. This hypothesis is by no means recent since it was put forward by JOURDAN in 1883 and is quoted in all subsequent reviews.

A feature common to the ciliated epithelial and endothelial cells of most intrathecal regions of the water vascular system is the development of a collar of radial lamellae around the base of the cilium. Collars composed of lamellae or microvilli have been observed in the epithelia of other echinoderm tissues (see Table 5). NØRREVANG & WINGSTRAND (1970) have termed such modified epithelia as choanocytes due to their similarity to choanoflagellates. The functional significance of the collar structure is unknown. Variation within choanocyte cells is great and it does not appear that they have a unique function. A sensory role is likely in some structures such as the sensory hillock of Echinus pedicellariae (COBB 1968). Similar choanocytes occur throughout the invertebrates (see NØRREVANG & WINGSTRAND 1970) and sensory roles are likely in cnidarian statocysts and the cnidocil apparatus. The choanocyte cells of the water vascular system are motile and do not appear to have a sensory function (further evidence is discussed later).

Ultrastructural studies of the collar structure show that the base of the ciliary shaft is covered by a mesh of fine filaments which extend laterally into the 'fuzz' coat which is supported by the lamellae. It is possible that the choanocyte modification has a structural role in supporting the point of 'articulation' of the ciliary shaft (i.e. the transition zone). The collar may be quite rigid due to the turgor exerted by vacuolation of the lamellae and the 'fuzz' coat may be quite viscous, providing support for the cilium but not hindering its movement. An identification of the material comprising the 'fuzz' coat would be useful in determining its function.

In most of the examples quoted (Table 5), choanocytes have an important role in the movement of coelomic, haemal or water vascular fluid and it is probable that the collar structure is associated with a motile role. Furthermore, cells possessing non-motile cilia such as the external epithelium of tube feet (see Chapter 5) are not choanocytic.

The innervation of intrathecal regions of the water vascular system consists of two main components; the basiepithelial plexus and the LDSG plexus. The former occurs between the outer epithelia and connective tissue whereas the latter occurs within the connective tissue and inner muscle layer. Fluorescence histochemistry and TEM show that catecholaminergic axons are abundant within the basiepithelial plexus. Ultrastructural studies show varicose axons contain numerous dense core vesicles (DCVs) and small clear vesicles (SCVs).

Previous studies on the water vascular system have not described or emphasised the presence of two distinct components to the innervation. Indeed a characteristic of these and other echinoderm studies is marked confusion due to differences in the nomenclature of the outer epithelia (somatocoelic, coelomic) and the endothelia (axocoelic, coelomic, inner). For the purposes of clarity it seems logical to term the outer epithelia as such and the inner epithelial lining the lumen of the canal, or organ, as endothelia.

JANGOUX & SCHALTIN (1977) termed the basiepithelial plexus as 'intra-epithelial' and comment on its particular thickening in the stone canal region. The data obtained in this study confirms this and it is proposed that the thickened nerve tract represents an axial nerve which passes from the circumoesophageal water ring to the axial complex.

The function of an extensive basiepithelial plexus in the water vascular system has not been fully discussed in other studies. BACHMANN & GOLDSCHMID (1978b) propose that aminergic neurones innervate the outer muscle layer of the axial complex since '...neuromuscular junctions with small dense core vesicles are found at sites possessing amine fluorescence'. The outer muscle layer was not investigated in this study but the latter study does confirm the present observations of amine fluorescence in the basiepithelial plexus only. In addition, microspectrofluorimetric analysis indicated that the fluorescence spectra were characteristic of dopamine. Unfortunately, similar analysis could not be undertaken in the present study.

An outer muscle layer is absent from the stone canal, Polian vesicles and water canals. Thus a muscle control function for basiepithelial axons in these regions is unlikely. Consequently, the basiepithelial plexus may have four possible functions (Fig. XXIV). Firstly, axons may terminate between outer epithelial cells and release their contents into the perivisceral coelom. Secondly, choanocyte cells may be sensory and terminate as axons which enter into the plexus. Thirdly, basiepithelial axons may be interneurones connecting sensory and motor neurones in other remote regions. Fourthly, basiepithelial axons may be innervating choanocyte cells.

The results obtained in this study indicate that the first two possibilities are unlikely. There is no ultrastructural evidence for a neuroendocrine release of catecholamines into the perivisceral coelom. JANGOUX & SCHALTIN (1977) supposed that the intraepithelial plexus would be a neurosecretory centre because the vesicular contents of the axons resembled elementary neurosecretory granules; '...prolongements axoniques riches en grains de forte densite electronique (neurosecretion?)'. Vesicles and granules within axons are quite variable in ultrastructure and fixation methods can considerably alter their appearance (see Chapter 6 for effects of fixation on LNSG axons). The LCVs of basiepithelial axons resemble amine storage granules far more than elementary neurosecretory granules which tend to be larger in diameter (see GOLDING 1974 for review). Similarly, there is no ultrastructural evidence that outer epithelial cells are sensory. Epithelial processes differ quite clearly from axons in the presence of a granular, electron opaque cytoplasm. Also, epithelial cell bodies differ in ultrastructure from aminergic nerve somata (see Chapter 5) and there is no evidence of the production of amine storage granules. Epithelial processes appear to have an anchoring role in attaching the cell body to the basal lamina. An interneuronal role for basiepithelial axons cannot be dismissed and it is quite likely that many longitudinally orientated tracts of axons represent interneurones. PENTREATH & COBB (1972) have proposed that aminergic neurones in echinoderms function as interneurones because amines do not occur in sensory structures nor in motoneurones. However, subsequent work has shown that aminergic axons innervate the outer muscle layer of the axial complex (BACHMANN & GOLDSCHMID 1978b). Also, the data obtained in this study indicates that aminergic axons innervate the outer epithelial cells and thus have a cilioeffector role. The presence of CVs in addition to LCVs within varicosities abutting against epithelial cells are indicative of synaptic release.

Ciliary activity of epithelial cells is responsible for the generation of currents which may aid the exchange of respiratory gases (FENNER 1973) and possibly waste products. The neuronal control of ciliary activity which is associated with a respiratory function is a similar phenomenon to that in the molluscan gill epithelium (see AIELLO 1974 for review).

Evidence for the control of ciliary study in echinoderms has been described by only a few authors, MACKIE et al (1969) observed that ciliary reversal in the arms of *Strongylocentrotus* plutei was associated with 20mV monophasic potentials recorded extracellularly from the ciliary band. However, axons were not detected in that study and it was therefore suggested that neuroid conduction occurred via the epithelium or mesenchymal cells. RYBERG (1977), however observed neurones in the pluteus of *P. miliaris* and described the presence of 'axon-like' strands containing DCVs, adjacent to ciliated cells in the arm. It was postulated that neurones may innervate larval effector organs such as the ciliated epithelia. BURKE (1978) also observed varicosities containing DCVs and CVs abutting against ciliated cells in the pluteus of *Strongylocentrotus*. Such contacts were described as synapses. RYBERG (1974) described fluorescence histochemical evidence for the presence of catecholamines in the basiepithelial plexus of the main ciliated band of *P. miliaris* plutei but a cilioeffector role was not discussed. Recent studies (COBB & RAYMOND in press) show that an aminergic control of ciliary activity also occurs within the rectal caecae of *A. rubens*.

The neuronal control of ciliary activity has been most extensively studied in the bivalve molluscs, where structural, electrophysiological, and pharmacological evidence has been obtained. AIELLO (1960) observed that lateral cilia of *Mytilus* are under neuronal control and that 5HT has a potent cilioexcitatory effect. AIELLO and GUIDERI (1965) observed that axons from the branchial nerve penetrate gill filaments and ramify beneath the lateral epithelial cells in a manner similar to that described in the present study.

Dopamine was detected in the nerve tissue innervating the molluscan gill (SWEENEY 1963) and it has been shown to have a cilioexcitatory effect on frontal cilia (MALANGA 1974, 1975) but a cilioinhibitory effect on lateral cilia (PAPARO & AIELLO 1970, MALANGA 1974). Further evidence for the cilio-effector role of dopamine is the demonstration of mechanisms for the metabolic degradation of dopamine to inactive metabolites (such as dihydroxyphenylacetic acid or DOPAC) in the gill epithelium of *Mytilus* and *Modiolus* (MALANGA & YOUNG 1978).

The neuronal control of ciliary activity occurs throughout the metazoa (see AIELLO 1974 for review) and it occurs in other deuterostomes apart from echinoderms, for example: frog oropharyngeal cavity, *Amphioxus* gill slits, *Saccoglossus* trunk cilia, and tunicate pharyngeal baskets.

The mechanism by which neurotransmitters control ciliary activity are not fully understood. Recent studies indicate that ciliary arrest in the gills of *Elliptio complanatus* is initiated by an increase of intracellular calcium (WALTER & SATIR 1978). This mechanism is similar to that in protozoa where ciliary reversal in *Paramecium* is associated with calcium influx during membrane depolarization (see review by NAITOH & ECKERT 1974). The calcium sensitive site is possibly localized within the basal apparatus (WALTER & SATIR 1978).

The second component of the innervation of the water vascular system is a less well defined plexus of axons termed LDCG axons due to their content of LDCGs approximately 150nm in diameter. LECLERC & DELAVAULT (1971) have postulated that some cells within the LDCG plexus of the asteroid axial complex are glial in nature thus constituting a glio-interstitial system. BACHMANN & GOLDSCHMID (1978b) referred to the LDCG plexus as an intraepithelial plexus and made erroneous comparisons of neurosecretion with the intraepithelial plexus of JANGOUX & SCHALTIN (1977) which in fact referred to the basiepithelial plexus.

On the basis of vesicle type, BACHMANN & GOLDSCHMID (1978b) state that three types of axons occur within the LDCG plexus and the type with '... large dense core vesicles measuring 110-160nm may well represent neurosecretory material'. BACHMANN & VON HAHN (1969) ascribed a neurosecretory function to similar axons in the asteroid axial organ. However, there is no evidence for the release of neurosecretory material into the axial sinus of asteroids and echinoids (as BACHMANN & GOLDSCHMID also observed). Also, present observations indicate the LDSG axons cannot be subdivided on the basis of vesicle type since a variety of vesicles occur within individual LDSG axons. All that can be stated with any certainty is that LDSG axons within the axial complex do not contain a biogenic amine which forms a fluorophore with paraformaldehyde.

In addition to innervating the inner muscle layer of the axial organ; LDSG axons also occur within the connective tissue, and throughout the connective tissues and musculature of other structures in echinoderms.

An investigation of the nature and function of LDSG axons in the Echinodermata is discussed in Chapter 6.

Finally, the description of the innervation of the water vascular system is complicated by the observation of tracts of axons passing through the connective tissue of the mesentery supporting the radial water canal. Unfortunately fluorescence histochemistry of this mesentery was not attempted but the mesenteric axons are similar in ultrastructure to basiepithelial axons (particularly in their size). Further studies are required to determine whether the tracts are aminergic and whether they innervate the water canal or the musculature/epithelia of the mesentery itself.

Fig. XIX'

a) Diagrammatic representation of the echinoid axial complex.

A	Ampulla of Stone canal	Mc	Madreporic canal
Ao	Axial organ	Pv	Pulsatile vessel
As	Axial sinus	S	Stone canal
F	Foramen	Tp	Terminal process
M	Madreporite		

b) Zonal variation of endothelia lining a madreporic canal

A	Ampulla of Stone canal
Bb	Brush border-like region
Sc	Squamous cell
Se	Squamous epithelia

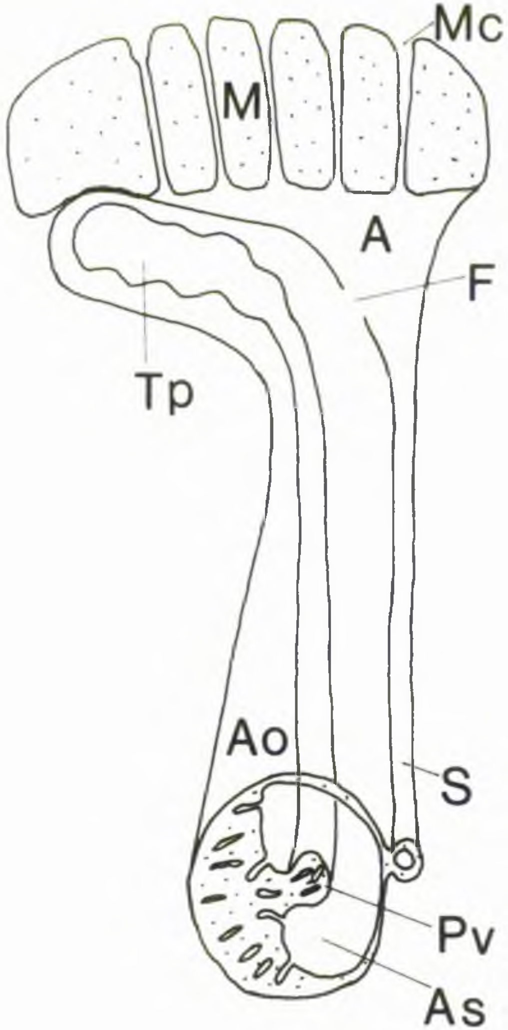

(a)

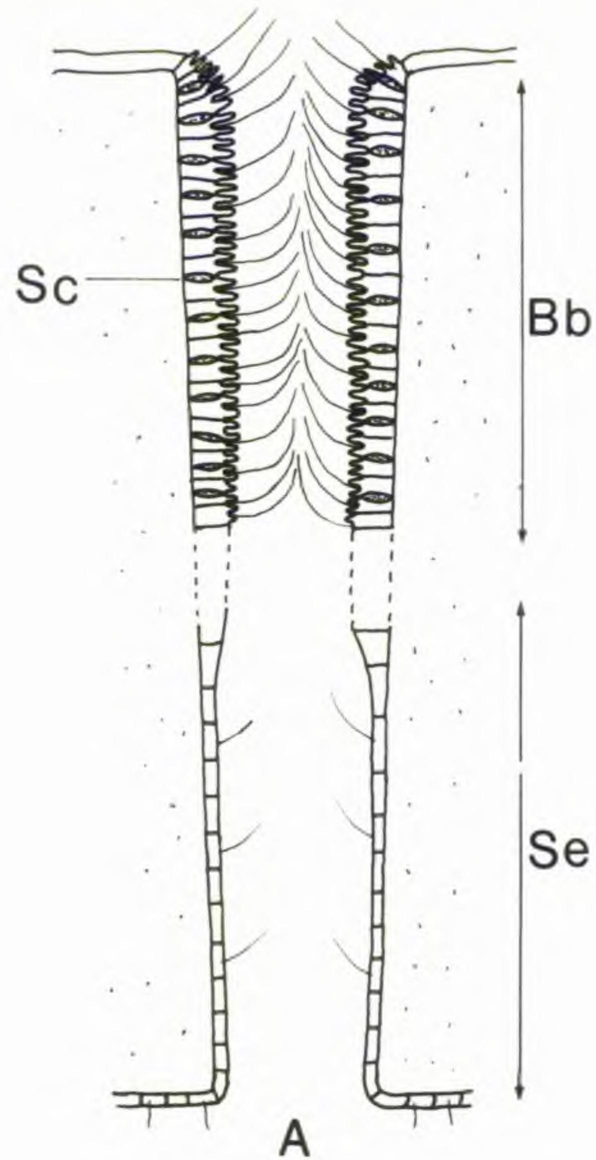

(b)

Fig. XX

Schematic T.S. of an echinoid axial organ

As	Axial sinus	f	Filaments
Ba	Basiepithelial axons	Im	Inner muscle
Bl	Basal lamina	La	LDSG axon
c	Collagen	Om	Outer muscle
En	Endothelia	Pc	Perivisceral coelom
Ep	Epithelia		

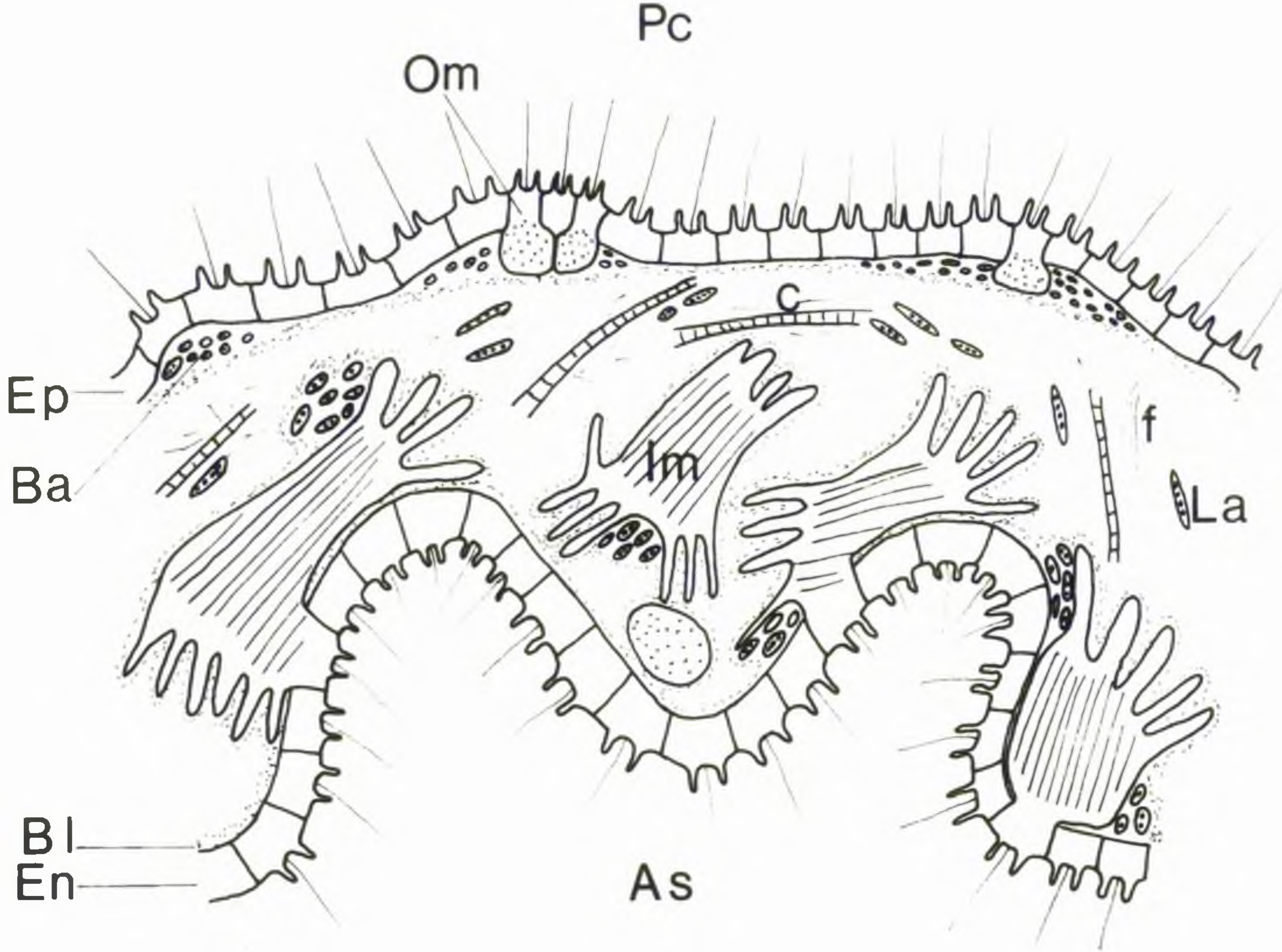

Pc
Om
Ep
Ba
C
Im
f
La
Bl
En
As

Fig. XXI

Schematic T.S. of the echinoid Stone canal

A	Axon bundle	Ep	Epithelia
h	Axial haemal vessel	H	Hydrocoel
m	Axial mesentery	M	Muscle
Ba	Basiepithelial plexus	Pc	Perivisceral coelom
En	Endothelia		

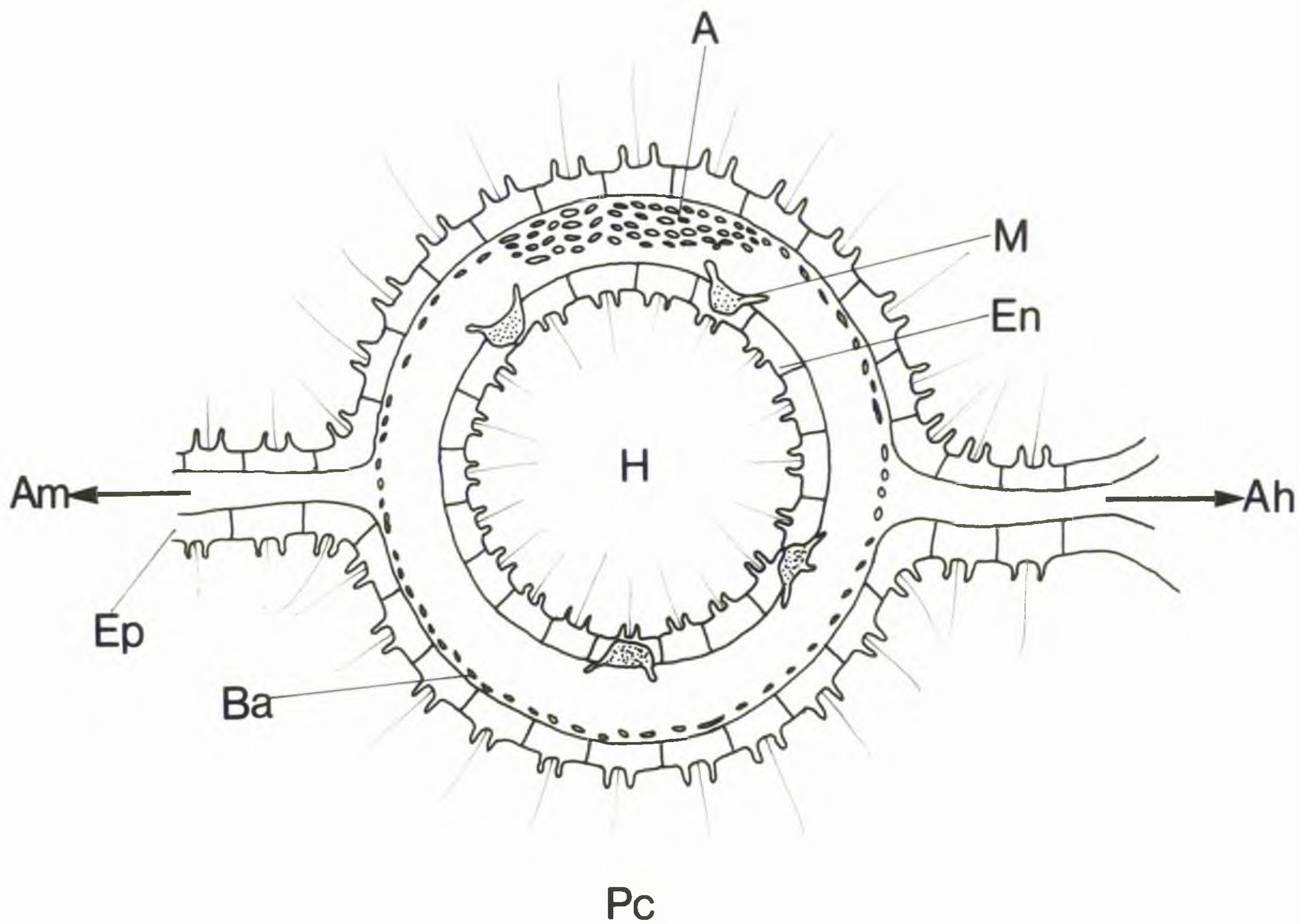
A
M
En
Am
H
Ah
Ep
Ba
Pc

Fig. XXII

Schematic T.S. and L.S. of the 'choanocyte' cell characteristic to epithelia and endothelia of the WVS.

Transverse sections are shown at three different levels through the collar structure

A	Axon	F	Fuzz coat
Bc	Basal collar	G	Golgi body
Br	Basal rootlet	l	Length of collar = 1.3μ
C	Collar	N	Nucleus
Ce	Centriole	S	Spoke
Ci	Cilium	Sj	Septate junction
D	Desmosome	V	Vacuole
Db	Dense body	W	Width of collar = 1μ

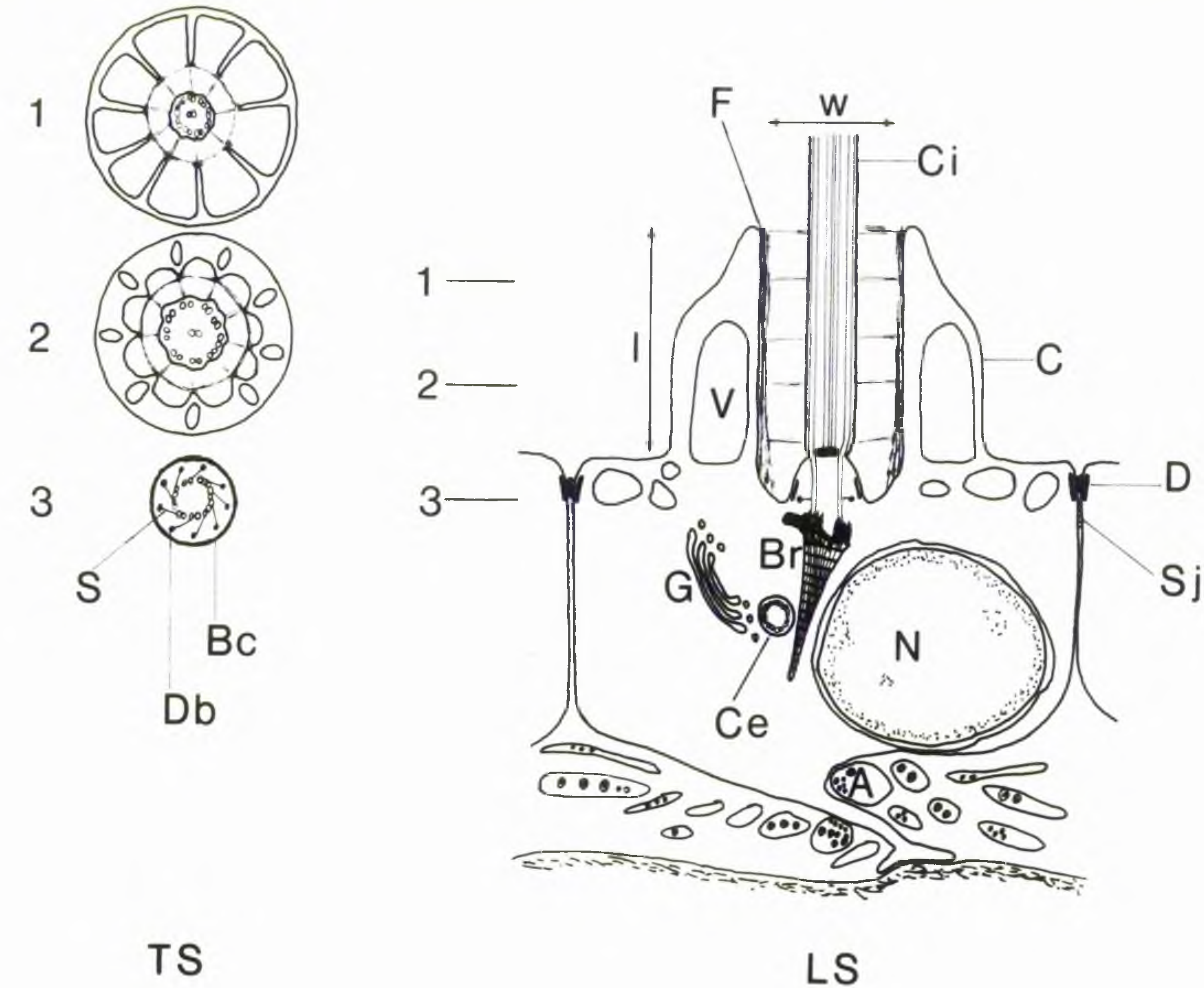
1
2
3
S
Bc
Db
TS
F
w
Ci
1
2
3
I
V
C
D
Sj
Br
G
N
Ce
A
LS

Fig. XXIII

Periodic striation of a collagen filament

Each dense band has a light band on each side and a light interband occurs within the dense band.

Figures - nanometres

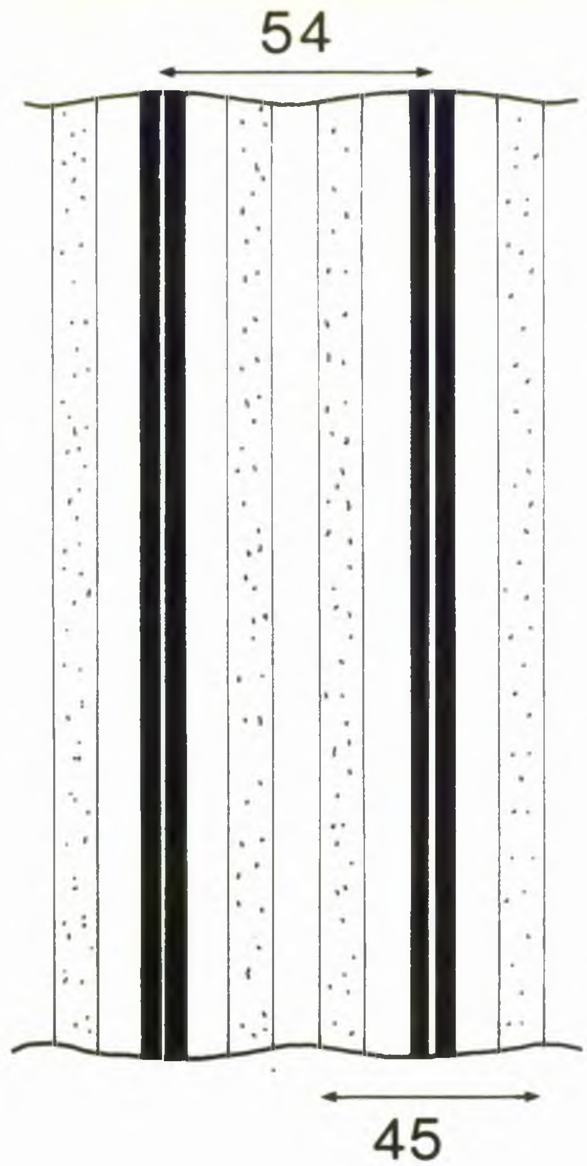
54
45

Fig. XXIV

Diagrammatic representation of the four possible functions of the basiepithelial plexus in the WVS.

1. Neuroendocrine release of catecholamines
2. Interneurones receiving sensory input from choanocyte cells
3. Interneurones connecting sensory and motor neurones in other remote regions
4. Innervating choanocyte cells (i.e. cilioeffectors)

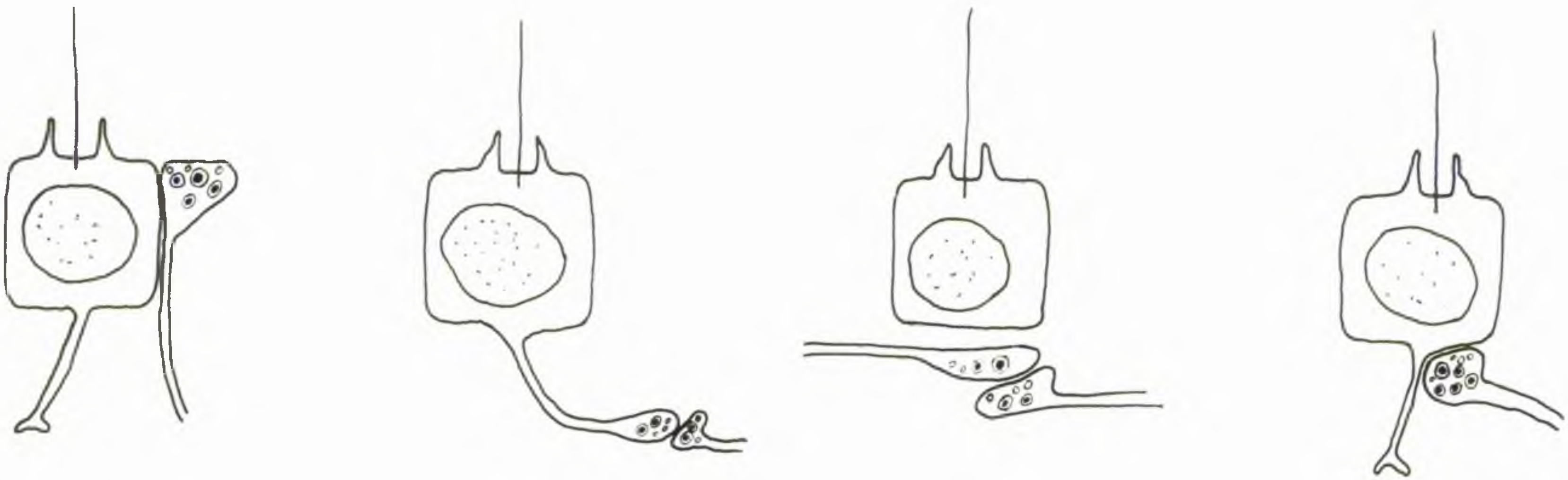

1 2 3 4

CHAPTER 5

MYONEURAL ANATOMY AND PHYSIOLOGY OF THE TUBE FOOT/AMPULLA COMPLEX

THE NEURAL ANATOMY AND PHYSIOLOGY OF THE TUBE FOOT/AMPULLA COMPLEX

INTRODUCTION

The tube foot/ampulla complex forms a highly organized functional unit within the water vascular system and it has been accredited with a variety of functions including respiration, locomotion and sensory capacity.

Studies on the tube foot/ampulla complex of all classes of echinoderms can be divided into four main groups:-

The first group includes studies on the general histology and functional morphology of tube feet (NICHOLS 1966 provides review of the early literature and see Chapter 1). SMITH (1978b) has recently provided an extensive histological survey of the ambulacral tube feet of most echinoid orders and describes a good correlation between structural variation and the relative importance of respiratory and locomotory roles. In all classes of echinoderms, the gross histological organization of tube feet is essentially the same and consists of five concentric layers: an outer epithelium, basiepithelial nerve plexus, connective tissue sheath, longitudinal muscle, and an endothelium which lines the lumen of the tube foot.

The second group includes studies concerned with the mucous producing cells in the epithelia of tube feet from: Asteroidea (CHAET & PHILPOTT 1960, SOUZA SANTOS 1966a,b, SOUZA SANTOS & SILVA SASSO 1968, 1970, 1973 and 1974). Echinoidea (COLEMAN 1969a), Ophiuroidea (MARTINEZ 1976), Crinoidea (HOLLAND 1969) and Holothuroidea (HARRISON 1968, MENTEN & EISEN 1970). All these studies indicate that the mucous granules contain an association of neutral and acid mucopolysaccharides which confer adhesive and lubricating properties to the mucous. The mucous granules show a wide degree of ultrastructural organization and ENGSTER & BROWN (1972) propose that this is proportional to the type of environment in which the echinoderm lives. Thus, species inhabiting hard rocky substrates tend to have highly organized granules whereas species inhabiting sandy or muddy substrates have less organized granules.

The third group of studies includes those on the myoneural anatomy of the tube foot/ampulla complex. Asteroids appear to have provided the most popular preparation for study, presumably due to the impetus given by the work of SMITH (1946, 1947, 1950a, 1965) which identified a group of axons, termed 'ribbon axons', innervating the musculature of both the ampulla and the tube foot. Subsequent ultrastructural studies on the ampulla of asteroids (BARGMANN & BEHRENS 1963, COBB 1967, COBB & LAVERACK 1967) and echinoids (COBB 1970) have shown that the ribbon axons identified by vital methylene blue staining are not axons but modified muscle processes termed 'muscle tails'. However an ultrastructural study of the ampulla of another echinoid species (KAWAGUTI 1965c) failed to describe the presence of structures akin to muscle tails. Similarly, ultrastructural studies on the tube feet of; echinoids (KAWAGUTI 1964a, COLEMAN 1969b, FLOREY & CAHILL 1977), ophiuroids ([illegible] 1977c,d), asteroids and holothuroids (COLEMAN 1972, 1975) have not described any muscle tails, nor any other ultrastructural correlate of ribbon axons.

The fourth group of studies includes those concerned with the myoneural physiology of the tube foot/ampulla complex. The pharmacology of various echinoderm nerve-muscle preparations has been exhaustively reviewed by [illegible] (1966), [illegible] (1969) and PENTREATH & COBB (1972). Histochemical localization of acetyl cholinesterase provides some evidence that asteroid tube foot musculature is cholinoreceptive (PENTREATH & COTTRELL 1968). In addition, FLOREY et al (1975) have demonstrated acetyl choline (A.Ch.) and gamma amino butyric acid (GABA) in tube foot extracts and have shown that the musculature of isolated echinoid tube feet will contract in response to ACh. and GABA.

The control and co-ordination of echinoderm tube feet has been intensively investigated in the Asteroidea. An excellent discussion of these studies by KERKUT (1954) reflects the dichotomous attitudes of behaviourists at that time and provides a sagacious criticism of the classic 'peripheral versus central control' hypotheses. Authors such as HAMILTON, MAGEN and SCHEREMKLA (see KERKUT 1954 for references) supported the peripheral control hypothesis but COLE (see KERKUT 1954) and SMITH (1945, 1950b) provided evidence for a central control of tube foot activity.

The only published account of electrophysiological studies on the tube foot/ampulla complex is that of SANDEMAN (1965) where extracellular stimulation of the radial nerve caused contraction of ampullae in the same ambulacrum, and rather interestingly, contraction also in other ambulacra. Complex potentials were recorded extracellularly from the ampullae but recordings from tube feet were not attempted.

It is quite apparent from all the aforementioned studies that a number of important questions regarding the structure and function of the echinoid tube foot/ampulla complex remain unresolved.

Dealing firstly with the ambulacral tube foot disk, there has been only one ultrastructural study of this region (COLEMAN 1969a) but the structure of the disk levator muscles (DLM) was not described and the only evidence provided for the presumed sensory nature of the disk was an observation that the basiepithelial plexus is in '...direct contact with epithelial cells of the sucker...'. There appear to be no published ultrastructural studies of any region of the peristomial tube foot/ampulla complex and yet it is known from light microscope studies that the peristomial tube foot disk is more extensively innervated and ciliated than the ambulacral tube foot. Is this associated with an increased sensory role of the peristomial tube foot ?

It is interesting to note that all ultrastructural studies of tube feet have been concerned with the tube foot stem. There have not been any investigations of the region communicating between the ampulla and the tube foot, i.e. the intraporal region. Presumably the difficulty in preparing this area for EM, due to the calcareous test, has discouraged its investigation. The most recent study of echinoid tube feet (FLOREY & CAHILL 1977) observed the absence of neuro-muscular synapses and thus proposed that neurotransmitters are released from motoneurones in the basiepithelial plexus and diffuse through the connective tissue of the stem before acting upon the musculature. Thus the innervation of tube foot muscle appears to occur in a manner similar to the autonomic innervation of vertebrate blood vessels. An attractive analogy, especially because of the possible phylogenetic link between echinoderms and chordates. However, a serious drawback to this hypothesis is that vertebrate blood vessels only undergo rhythmic contractions; they do not exhibit the same kind of co-ordinated postural movements that occur in tube feet.

In order to clarify some of these problems and to contribute to a further understanding of the myoneural anatomy and physiology of echinoderms; the fine structure and innervation of the following regions was investigated.

1. Ambulacral tube foot disk
2. Peristomial tube foot disk
3. Tube foot: a) Stem
   b) Intraporal region
4. Ampulla

In addition, extracellular and intracellular electrophysiological techniques were attempted on isolated tube foot/ampulla preparations.

RESULTS

PTF Disk

The general structure of the peristomial tube foot disk (Fig. XXV) consists of: an outer epithelium underlain by an extensive basiepithelial plexus, secretory cells which communicate with the epithelial surface, and a well developed connective sheath which surrounds the rosette ossicles (described in Chapter 3).

The basiepithelial plexus of the disk extends from the distal side to the proximal (Fig. 86), where it thickens into a nerve tract forming the tube foot nerve (Fig. 87).

TEM shows a distinct ultrastructural difference between the proximal and distal epithelia of the disk. Both epithelia consist of extensively vacuolated microvillus cells, and extending between the epithelial cells are glandular processes releasing secretory granules amongst the microvilli. However, the distal epithelia (Fig. 88) differ from the proximal (Fig. 89) in the presence of more secretory processes which contain secretory granules of an unusual ultrastructure. Proximal secretory cells produce membrane bound granules (approximately 200nm in diameter) consisting of a homogeneously electron dense core. During extrusion of the granules, the limiting membranes break down as they pass along fine processes (approximately 390nm wide) which extend between epithelial microvilli (Fig. 90). The secretory granules produced by distal secretory cells are similar in size to proximal granules but show a more complex ultrastructural organization. The granules are membrane bound, and consist of a small highly electron dense core (usually eccentric) surrounded by electron opaque granular material. One half of the granules is more electron lucent and contains filamentous material which is transversely striated by opaque material from the rest of the granule (Fig. 91). In a similar manner to proximal secretory granules, distal granules pass along slender processes which extend into the epithelium (Fig. 92).

Azure 2 and Methylene blue staining of semi-thin sections shows that the proximal and distal secretory cells differ in their staining properties (Fig. 93). The distal epithelium is intensely basophilic and does not appear to be metachromatic. The proximal epithelium shows purple (β) metachromasia in addition to a non-metachromatic basophilic band passing along the outer edge of the microvilli. The latter band probably corresponds with the electron dense band observed in TEM studies (Figs. 89 & 90).

Characteristic features of the proximal epithelial cells are the presence of numerous vacuoles, well developed golgi complexes and large lytic bodies approximately 0.5μ in diameter. However, a distinguishing feature is small processes which extend from adjacent cells and ramify among each other. The processes are up to 3.5μ long, approximately 200nm wide and contain cisternae of rough endoplasmic reticulum and small mitochondria. Intermediate junctions occur in some regions of apposition between processes and these consist of a narrowing of the intercellular space (20nm) along a straight or slightly curved region. Intermediate junctions extend for up to 1μ in length. Some zones between intermediate junctions appear to form intercellular channels approximately 140nm in diameter (Fig. 94).

In addition to glandular processes, other processes quite different in ultrastructure terminate within both distal and proximal epithelia (Fig. 95). The latter processes contain numerous neurotubules and neurofilaments and terminate with a single cilium which projects from the epithelium. It is probable that these processes represent dendrites of neurosensory cells.

SEM studies of the peristomial tube foot disk were hindered by the copious production of mucous which obscured details of the epithelial surface and cilia distribution (Fig. 96). (EDTA) rinsing removed some of the superficial mucous and it appears that the cilia are $4-5\mu$ long (Fig. 97).

Sensory neurone somata are clustered between projections of the rosette ossicles and occur below the epithelial cell bodies (Fig. 98). The neurone somata are elongate (approximately 4μ x 2μ), possess little perinuclear cytoplasm and appear to be bipolar (Fig. 99). Axons extending from the somata contain small mitochondria, cisternae of rough endoplasmic reticulum and dense clusters of neurotubules and electron opaque granular material. Processes from secretory cells can be distinguished from axons by their content of secretory granules; also, cell body regions of secretory cells are characterised by the abundance of secretory granules.

Axons from sensory neurone somata extend into the basiepithelial plexus and ramify among basiepithelial axons (Fig. 100). Specialised synaptic contacts between sensory axons and basiepithelial axons were not observed. However, intermediate type junctions are common between sensory axons and other axons (Fig. 100). Sensory axons within the basiepithelial plexus can be distinguished from other axons by their content of dense clusters of neurotubules and granular material (Fig. 101). Some sensory axons contain CV approximately 50nm in diameter. In some regions, sensory axons narrow down to 100nm in diameter and may contain cisternae of rough endoplasmic reticulum only (inset Fig. 101). Sensory axons may come into close contact with the basal lamina but do not form any junctions with it.

Unfortunately, fluorescence histochemistry for biogenic amines would not be undertaken due to the calcareous rosette preventing sectioning and the lability of specific fluorophores in aqueous media.

The basiepithelial plexus of the distal surface of the disk forms well developed circumferential tracts which produce radial branches extending to the edge of the disk (Fig. 102). It appears that radial branches of the distal disk plexus pass between projections of the rosette ossicles and enter into the proximal disk plexus.

ATF disk

The general structure of the ambulacral tube foot disk is similar to that of peristomial tube feet, except for two factors. First, the distal epithelia appear to be less extensively ciliated and fewer neurosensory somata and axons were observed. Secondly, the lumen of the tube foot extends deeper into the disk, through the rosette structure (see Chapter 3), and the inner longitudinal muscle layer inserts into the disk constituting the Disk Levator Muscles (Fig. XXVI). The central zone of the disk is raised into the lumen of the tube foot to such an extent that tranverse sections of that region (Figs. XXVI & 103) pass through the walls of the tube foot stem and the disk. Disk levator muscles appear to pass obliquely from the stem retractor muscles and attach to the connective tissue sheath of the central zone of the disk.

The distal epithelium and connective tissue layer of ambulacral disks is thinner than that of peristomial disks, measuring approximately 10μ in depth. Basiepithelial axons are separated from the disk levator muscles by a connective tissue sheath approximately 2.5μ thick (Fig. 104). Varicosities of basiepithelial axons contain numerous DCV (approximately 80nm in diameter) and CV (approximately 50nm in diameter).

The disk levator muscles are attached to the connective tissue sheath of the disk by extensions of the basal lamina which penetrate deeply within the muscle fibres (Fig. 105). Regions of the muscle fibre in contact with attachment processes of the connective tissue are characterised by the presence of hemidesmosomes. The mode of attachment of disk levator muscles to the stem wall differs because extensions of the connective tissue pass between muscle cells and penetrate into muscle fibres to a lesser extent (Fig. 106). Similarly though, attachment points are characterised by hemidesmosomes. The connective tissue sheath of the stem wall is more organised than that of the disk and consists of bundles of longitudinally orientated collagen filaments in addition to an inner circular layer.

Ramifying among disk levator muscles fibres are axons containing LDSCs (similar to those observed in the axial complex), mitochondria, free ribosomes, rough endoplasmic reticulum and neurotubules (Figs. 106, 107, 108) LDSC axons were observed more frequently at the junction of the connective tissue and the musculature. LDSC cells were the only neurones observed within the disk levator musculature.

There appear to be two types of muscle fibre within the disk elevator muscles (Fig. 106). Type I fibres contain thin filaments approximately 8nm in diameter and thick filaments approximately 23nm in diameter. Type I centre thick to centre thick spacing is approximately 23nm in diameter. Type II fibres contain thin filaments approximately 8nm in diameter and thick filaments varying in diameter from 20nm to 70nm (Fig. 107). Type II centre thick to centre thick spacing is less uniform than that of Type I fibres and ranges from 50nm to 125nm. Type I and Type II fibres contain well developed mitochondria. Intramitochondrial dense bodies, approximately 10nm in diameter, were observed in many muscle and LDSG mitochondria and especially in glutaraldehyde pre-fixed tissues (Figs. 106, 108).

Sarcoplasmic reticulum is not extensive but consists of subsurface cisternae juxtaposed to the sarcolemma and separated by a sarcoplasmic space of approximately 10nm.

Sarcolemmal extensions of muscle cells form sinuous processes which ramify across the muscle layer. Sarcolemmal extensions vary in diameter from 30nm to 800nm. The smallest may contain only sarcoplasm, but rough endoplasmic reticulum is usually present, larger extensions may also contain mitochondria. Subsurface cisternae are particularly well developed in larger sarcolemmal extensions and may run parallel to the sarcolemma for lengths of up to 3.5μ (Fig. 108).

Enveloping membranes forming a sheath around some LDSG processes (Fig. 108) may originate from sarcolemmal extensions.

TEM shows that secretory granule ultrastructure varies in ambulacral tube foot disks in a similar manner to peristomial tube foot disks.

Tube foot: a) Stem

The general structure of the tube foot stem consists of six concentric layers: outer epithelium, basiepithelial plexus, longitudinal connective tissue, circular connective tissue, longitudinal stem retractor muscles and endothelium (Fig. XXVII).

The peristomial tube foot stem is similar to that of ambulacral tube feet but is shorter and thicker and possess a relatively larger tube foot nerve.

The outer epithelium consists of microvillous, vacuolated cells which are anchored to the connective tissue sheath by long processes (Fig. 109). Epithelial processes pass through the basiepithelial plexus and can be distinguished from axons by their content of tonofilaments (approximately 9nm in diameter).

Projecting from the epithelium of the tube foot stem are circumferential rows of cilia (Fig. 110) which extend from processes extending from cells differing in ultrastructure from typical epithelial cells (Figs. 111, 112). Such cells are non-vacuolated, unlike epithelial cells, and possess a granular cytoplasm containing numerous cisternae of rough endoplasmic reticulum and a variety of lytic bodies, lipid droplets, neurotubules and rosettes of glycogen. It is probable that these cells are neurosensory and that the ciliated processes represent sensory dendrites. The neurone somata (approximately 7μ x 10μ) may possess more than one dendrite (Fig. 111) and this may explain the fewer neurosensory somata observed in relation to the number of cilia. Only a single axon per neurosensory soma was observed, but unfortunately, their small size and numbers prevented an analysis of their relationship with the basiepithelial plexus.

The basiepithelial plexus consists of several small axons (less than 1μ in diameter) containing DCV (50-80nm in diameter) and/or CV (approximately 50nm in diameter). Pre- and post-synaptic specializations were not observed within the basiepithelial plexus. However, some synaptoid contacts contain aggregations of electron dense material in the interaxonal space and adjacent to the 'pre-synaptic' membrane (Fig. 113).

The basiepithelial plexus thickens on one side of the tube foot (perradial - ambulacral, adoral-peristomial) forming the tube foot nerve (Fig. 114). The ultrastructure of basiepithelial axons differed with different fixations methods and it was observed that glutaraldehyde considerably improves the ultrastructural preservation of neurotubules (compare Figs. 115 and 116). Axons within the tube foot nerve are small, most are approximately 400nm in diameter and the largest do not exceed 2.5μ. Within the stem region of the tube foot, neurone somata were not observed in the tube foot nerve. A characteristic feature of basiepithelial axons are close packing and the absence of glial investment. Non-neuronal elements within the tube foot nerve are amoebocytes (typical of those found throughout the water vascular system) and epithelial processes containing tonofilaments.

DCV within basiepithelial axons probably represent amine storage granules since fluorescence histochemistry produces apple-green specific fluorescence in the tube foot nerve and basiepithelial plexus (Fig. 117) which is completely quenched by sodium monoborohydride reduction (Fig. 118), indicating the presence of primary catecholamines such as dopamine or noradrenaline. Primary catecholamine fluorescence was only observed in the basiepithelial plexus and the tube foot nerve.

Orange autofluorescence was observed in all layers of the tube foot, particularly the epithelia and endothelia. Borohydride reduction often reduced the intensity of orange autofluorescence but never completely quenched it, unlike specific fluorescence.

The connective tissue sheath shows the same organization in peristomial and ambulacral tube feet and consists of an outer longitudinal and inner circular layer (Figs. 119, 120). The longitudinal layer varies in thickness from 10µ in extended tube feet to 25µ in contracted tube feet. The longitudinal layer consists of an external amorphous region containing amoebocytes, fibrocytes and randomly arranged collagen filaments and fine filaments. The inner region of the longitudinal layer consists of bundles of closely packed collagen filaments which are helically coiled and the degree of coiling is dependant upon the degree of tube foot extension. Thus, in tranverse sections of tube feet; the 'longitudinal' filaments appear in tranverse section in the extended condition (Fig. 120), but in more oblique section in the contracted condition (Fig. 122).

Passing between bundles of longitudinal collagen filaments are radial filaments extending from the inner circular layer (Figs, 120, 121). The circular layer varies in thickness from 1µ in the extended condition to 4µ in the contracted; the orientation of the filaments remains constant however. The circular layer of connective tissue also contains a more extensive arrangement of fine electron dense filaments, approximately 15nm in diameter, which interweave among the collagen filaments (Fig. 121).

Collagen filaments of both longitudinal and circular layers are similar in ultrastructure and vary in diameter from 40nm to 250nm (Fig. 123). Periodic striation of collagen filaments is similar to that of filaments occurring in the water canal, but the repeat period differs slightly and is approximately 60nm.

The muscle layer of tube feet consists of longitudinally orientated, unstriated muscle fibres (stem retractor muscles) and varies in thickness from 65µ in the contracted condition (Fig. 124) to 2µ in the extended condition (inset Fig. 124). The thinnest region of the muscle layer is adjacent to the tube foot nerve (Fig. 125). It is also in this region that the connective tissue sheath decreases in thickness to 1-2µ, due to the absence of the longitudinal connective tissue layer.

The stem retractor muscles are attached to the connective tissue sheath by means of small lateral evaginations which penetrate into the circular connective tissue layer (Fig. 126). Hemidesmosomes occur in some regions of contact between the sarcolemma and the basal lamina.

A characteristic feature of the muscle cells are sarcolemmal extensions which interdigitate with each other (Fig. 127). Sarcolemmal extensions are similar to those found in the disk levator muscles and are devoid of myofilaments, containing only sarcoplasm and subsurface cisternae of sarcoplasmic reticulum (Fig. 128). Occurring between subsurface cisternae and the adjacent sarcolemma are clusters of electron dense material. Subsurface cisternae also occur within contractile regions of the muscle cells.

Stem retractor muscles are composed of only one type of muscle fibre, which contains thin filaments approximately 8nm in diameter and thick filaments 20 - 60nm in diameter. Thick and thin filaments do not show a regular, ordered array and most thick filaments appear to pass out of the plane of section thus preventing accurate estimates of filament length. However, thick filaments appear to be quite long and lengths up to 4µ were observed. Muscle fibres are thin (approximately 2-4µ) and very long (greater than 80µ).

Glutaraldehyde prefixation improves the ultrastructural preservation of thin filaments (compare Figs. 127, 128, 129), showing that regular groupings of thin filaments are not evident; many thin filaments are not parallel to each other, and complete orbits of thin filaments around a central thick filament are scarce (Fig. 128). Organization of thick and thin filaments shows little difference in relaxed and contracted muscles. Centre thick to centre thick spacing is quite variable (30 - 90nm) and centre thick to centre thin spacing varies to a lesser extent (25 - 35nm).

Occurring randomly throughout the contractile regions of muscle fibres are Z-bodies, which consist of clusters of electron dense material. Extending from opposite sides of a Z-body are numerous thin filaments (Fig. 130).

Junctions between muscle cells are characterized by straight (Fig. 131) or irregular (Fig. 132) desmosomes; usually with electron opaque material in the intercellular space (approximately 20nm wide). Occurring adjacent to some desmosomes are intermediate junctions (Fig. 133), which can be distinguished by the conspicuous absence of a densification of the subsequent sarcoplasmic matrix and a narrower intercellular space (approximately 10nm wide).

Occurring between muscle cells and endothelial processes are hemidesmosomes (Fig. 134). Densification only occurs in the muscle cell and a laminar structure occurs in the intercellular space, close to the endothelial plasma membrane.

In addition to desmosomal structures and intermediate junctions are septate junctions, which occur in muscle-muscle contacts (inset Fig. 135) and muscle-endothelial process contacts (Fig. 135). Septate junctions in the tube foot musculature are similar to those previously described in the water canal epithelium, but it was observed in the tube foot that the subjacent cytoplasmic matrix associated with septate junctions contained small granular aggregations which appear to be associated with the transverse links (Fig. 135). The number of transverse links in a septate junction varies from three to more than thirty.

Ramifying throughout the connective tissue layer and the stem retractor muscles are LDSG cells similar to those previously described in the axial complex (Figs. 120, 130, 135). A more detailed description of LDSG cells is given in Chapter 6.

The lumen of the tube foot is lined with choanocyte-like endothelial cells which are similar to those found in other regions of the water vascular system.

Tube foot: b) Intraporal area

The general structure of the proximal region of the tube foot shows one major difference to the stem region; transverse sections of the tube foot at a level close to the periporal area reveal the presence of modified muscle fibres, termed muscle tails (Fig. 136).

Muscle tails are clustered in closely packed bundles and the width of the intercellular space between muscle tails is remarkably constant, remaining at approximately 30nm. Muscle tails are irregular in outline and bundles of several muscle tails form a characteristic mosaic. At levels distal to the periporal area muscle tails contain a central mass of thick and thin filaments surrounded by clear cytoplasm often containing several mitochondria. At this level however, muscle tails differ from unmodified muscle fibres in the presence of numerous microtubules orientated in the same direction as the myofilaments (Fig. 136). In addition, the thick filaments appear to decrease in size and number and eventually disappear at levels more proximal to the periporal area (Fig. 137). The minimum width of muscle tails varies from 2µ to 100nm.

A conspicuous feature of muscle tail bundles is the absence of LDCG processes and endothelial processes ramifying between the muscle tails. Muscle tails also differ from unmodified muscle fibres in the absence of small sarcolemmal processes.

Bundles of muscle tails only occur in the region of the muscle layer which is adjacent to the tube foot nerve. The distribution of bundles can be observed at the light microscope level using semi-thin sections stained with Methylene blue. Muscle tail bundles stain in a similar manner to basiepithelial axons and quite distinctly from other unmodified muscle fibres (Fig. 138). Bundles observed with the light microscope correlate with clusters of muscle tails observed using TEM (compare bundles a and b in Fig. 138 with Figs. 139 and 140 respectively). Each bundle is quite variable in size and shape, and the number of constituent muscle tails may vary from five to fifteen.

The presence of a sinus between the tube foot nerve and the circular connective tissue layer is likely to be an artefact produced during tissue processing. In some tissue specimens a sinus is not present and the tube foot nerve is closely apposed to the circular connective tissue layer (Fig. 141). TEM shows that the thickness of the circular connective tissue layer in this region decreases to approximately 2μ and always separates the muscle tails from basiepithelial axons containing SV (Fig. 142).

Passing further into the pore-pair, bundles of muscle tails become smaller and more diffuse (Fig. 143). Sections passing through the perradial and adradial pores show that the musculature only extends into the perradial pore and is still separated from the tube foot nerve by a thin circular connective tissue layer (Fig. 144). The adradial pore (or adapical in peristomial tube feet) is lined by a vacuolated endothelium only.

Morula-type amoebocytes pass between the tube foot nerve and the connective tissue (Fig. 145) thus increasing the distance between basiepithelial axons and the muscle layer. However, vesicle-containing varicosities still occur in these regions and form synaptoid contacts against the basal lamina.

In addition to the significant differences in the musculature of the periporal region, it was observed that tube foot nerve also differed due to the presence of bipolar neurone somata. Two main types of neurone can be distinguished; Type I contains numerous DCV (Fig. 146) and Type II is characterised by well developed Golgi complex (Fig. 147).

Type II neurones are smaller (approximately 4μ x 3μ) and contain vacuoles which probably represent swollen cisternae of smooth endoplasmic reticulum. Type I neurones contain a well developed rough endoplasmic reticulum (Fig. 148) and also vacuoles similar to those found in Type II neurones. Type I neurone somata measure approximately 11μ x 3μ.

There appear to be two sub-types of Type I neurone somata. Most somata contain DCVs approximately 100nm in diameter; however some somata contain vesicles of a similar size but they differ in the presence of an electron lucent halo separating the limiting membrane from the core (Fig. 149).

Ampullae

The peristomial and ambulacral ampullae of echinoids are similar in structure to asteroid ampullae, consisting of: outer epithelium, basiepithelial plexus, thin circular connective tissue, circularly and obliquely orientated muscle fibres, endothelium.

A detailed description of the ampullae will not be given since similar results to other studies (e.g. BARGMANN & BEHRENS 1963, COBB 1967, COBB & LAVERACK 1967, and COBB 1970) were obtained.

However, it is important to emphasise the following observations:

a) LNSC axons do not occur within the connective tissue, nor the musculature,

b) ampulla muscle cells are much shorter than tube foot muscle cells (lengths of up to 20µ were observed),

c) muscle fibres are attached to the connective tissue by small evaginations of the basal lamina (Fig. 150),

d) ampulla muscle fibres contain more mitochondria than the tube foot muscle, and clusters of tightly packed mitochondria frequently occur within central regions of the muscle fibre (Fig. 151).

e) ampulla muscle thick filaments are approximately 23nm in diameter.

Electrophysiology

Attempts at intracellular or extracellular recording from tube feet or ampullae were unsuccessful.

Intracellular recording from the muscle layer of opened tube foot/ampulla preparations produced negative results except for transient depolarizations (approximately −15mV) when the electrode tip entered the tissue. Similar negative results were obtained with either glass or plastic extracellular suction electrodes.

Extracellular stimulation of tube foot/ampulla preparations with glass suction electrodes produced inconsistent results. Stimulation of the lateral nerve innervating an isolated tube foot/ampulla preparation induced tube foot contraction. Ampulla contraction occurred very rarely. Ampulla contraction could only be induced repeatedly by direct stimulation of the ampulla itself. It was observed that contraction only occurred within a small radius (approximately 1mm) from the electrode tip.

DISCUSSION

An ultrastructural study of the tube foot/ampulla complex would not have been possible without the prior decalcification of the disk and peri-poral regions. The ascorbic acid method of DIETRICH & FONTAINE (1975) was quite satisfactory and had only one disadvantage. It was observed that decalcified tissues often developed a low affinity for stains and sufficient contrast was only obtained after prolonged staining, preferably in methanolic uranyl acetate. A consequence of prolonged staining however, was increased levels of contamination. Thus a compromise between sufficient contrast and tolerable levels of contamination had to be achieved.

The tube foot disk of eleutherozoan echinoderms functions as an adhesive organ due to the production of copius amounts of bioadhesive by secretory cells within the epithelia. However, adhesion in the suckered tube feet of asteroids, echinoids and holothuroids is also due to suction (SMITH 1937). The relative contributions of suction and bioadhesive were analysed by PAINE (1926) and it was calculated that 56% is due to suction and 44% due to other causes, mainly '...some sort of sticky secretion'. The contribution of a bioadhesive must be considerably larger in non-suckered tube feet such as those occurring in all ophiuroids, crinoids and in some species of the remaining classes.

ENGSTER & BROWN (1972) have reviewed the ultrastructural and histochemical studies of tube foot secretory cells and little information has been obtained subsequent to that work. MARTINEZ (1977a) observed six morphologically different secretory cells in ophiuroid tube feet, of which one type ('Type B') was thought to be ciliated and supposedly has a sensory-glandular function. Similarly, BARKER (1978) observed that many of the secretory cells in the adhesive papillae of brachiolariae larvae terminate with a single cilium. However, neither of these studies provide ultrastructural evidence (e.g. basal apparatus) for the origin of a cilium from a distinct secretory cell.

The present study in _E. esculentus_ and _P. miliaris_ shows that the distal disk epithelia contain secretory cells which produce secretory granules of an unusual ultrastructure, unlike the ultrastructurally homogeneous granules occurring in the proximal epithelium. Two distinct types of secretory cell in echinoid tube feet have not previously been described. It is probable that distal secretory granules contain a mucosubstance which has more adhesive properties than the proximal (since the former are in contact with the substratum). The proximal granules may contain a mucosubstance which has lubricating or protective function.

The data obtained in this study supports the proposition of ENGSTER & BROWN (1972) that the ultrastructural complexity of secretory granules correlates with the type of substratum upon which the echinoderm lives. Both _E. esculentus_ and _P. miliaris_ live on rocky substrates; similarly they both produce secretory granules which have the same degree of ultrastructural complexity as other echinoids living on similar substrates, e.g. _Arbacia_ (ENGSTER & BROWN 1972). The secretory granules of _D. antillarum_, which lives in coral sands, are ultrastructurally simpler (COBB 1969a) and more similar to the proximal secretory cells of _E. esculentus_ and _P. miliaris_.

Further histochemical and biochemical tests are necessary in order to determine whether ultrastructural similarities correlate with biochemical similarities.

Evidence obtained in this study indicates that cilia in the tube foot disk and stem have a sensory function. The cilia are short (less than 5μ), and project from dendritic processes extending from neurone somata. The cilia are particularly abundant in regions which have been assumed to be sensory, such as the tube foot disk, and in particular, the peristomial tube foot disk. The extensive development of neurosensory cells within the peristomial disk enabled an analysis of their relationship with the basiepithelial plexus. The distinctive dense clusters of neurotubules in sensory axons and their large numbers, show that they form synaptoid contacts with other non-sensory basiepithelial axons. Neurosensory somata appear to produce one axon only but may produce more than one dendrite, which has not previously been described in any echinoderm.

The peristomial tube feet of echinoids and their homologues in other classes (there is some confusion over the nomenclature of peristomial tube feet and the terms oral or buccal have also been used) have been accredited with a sensory and/or feeding role (NICHOLS 1966), but with little evidence of neurosensory cells with an input into the basiepithelial plexus.

As early as 1881 ROMANES & EWART observed that the tube foot nerve ('podial nerve') of peristomial tube feet was 'darker and thicker' than that of ambulacral tube feet and comment that this may be associated with an increased sensory role. On the basis of light microscope observations, NICHOLS (1961) proposed that peristomial tube feet of _Cidaris_ and _Echinus_ have a sensory role and states that '...most of the cells in the epithelium have an appearance consistent with their having a sensory function, possibly both tactile and chemoreception'. The present study indicates that tube foot cilia are probably chemosensory but electrophysiological evidence is required to confirm this. NICHOLS (1959a) observed that the 'buccal' tube feet of _Echinocyamus pusillus_ '...function only while the animal is feeding' and '...touched particles of the substratum...', and commented on a possible gustatory role. STOTT (1955) observed that in _E. esculentus_ the 'buccal' tube feet and pedicellariae took no mechanical part in the feeding process. However, during the course of this study, it had been observed that the peristomial tube feet of *E. esculentus* and *P. miliaris* have a mechanical role in 'holding' fragments of *Fucus* and *Laminaria* during feeding. QUINN (1965) observed an interesting example of cannibalism amongst *Astropyga* and noted that the 'buccal' tube feet were into contact with the food, '... perhaps acting in a feeding capacity'.

GOODBODY (1960) has observed that in *Mellita sexiesperforata*, the 'oral' tube feet probe the sand and collect food particles. In another sand doller, *Dendraster excentricus*, CHIA (1969) has observed that the 'buccal' tube feet and 'oral' spines are responsible for pushing mucous strings (containing food particles) towards the mouth. CHIA (1975) also observed that juvenile *D. excentricus* selectively ingest heavy sand particles and proposes that 'buccal' tube feet and 'peristomial' spines are the sites of selection. CAMPBELL et al. (1973) observed that the 'oral' tube feet of *Echinostrophus molaris* hold onto pieces of food which are ready for mastication.

Thus, the feeding and sensory role of peristomial tube feet is particularly well documented especially also in the irregular echinoids (NICHOLS 1959b, BUCHANAN 1966). The data obtained in this study provides ultrastructural evidence for the presence of monociliated neurosensory cells in the tube foot; since the number of neurosensory cells is greatly increased within the peristomial tube foot disk then this supports the hypothesis that peristomial tube feet are specialised for a sensory role in the feeding process.

In general, the pentameric symmetry of echinoderms has imposed restrictions upon the degree of cephalization and the evolution of highly organised sensory structures (REESE 1966). PENTREATH & COBB (1972) have reviewed studies on echinoderm sensory cells and conclude that the evidence available '...confirms the hypothesis that epithelial cells are in part sensory in function, only rarely showing even the simplest specialization, and that they are receptive to most stimuli...'. However, the sensory role of epithelial cells in echinoderms is still the cause of some debate, and unfortunately many of the arguments are based upon comparisons between different tissues from different species. TEM studies of monociliated epithelial sensory cells have been described in; the adhesive papillae of asteroid brachiolariae (BURKE (1978), plutei of *S. purpuratus* (BURKE 1978), integument of *D. setosum* (KAWAGUTI & KAMISHIMA 1964b) radial nerve of asteroids (COBB 1970), tridentate pedicellariae of *E. esculentus* (COBB 1968b), and tube feet of *H. pulcherrimus* (KAWAGUTI 1964a). However, studies on the tube feet of *D. antillarum* (COLEMAN 1969b); and *S. franciscanus*, *A. lixula*, and *E. esculentus* (FLOREY & CAHILL 1977) indicate that there is no evidence that epithelial cells have a sensory function. It is interesting to note that COLEMAN (1969a) also argues that the sucker of the tube foot is sensory because the basiepithelial plexus is in '...direct contact with epithelial cells...'. In addition, STOREY & CAHILL (1977) based their assumptions upon the ultrastructure of vacuolated epithelial cells and mucous cells; monociliated dendritic processes were not described.

The present study of echinoid tube feet has shown that three types of epithelial cell occur: vacuolated cells, secretory cells, and monociliated neurosensory cells. It is only the latter type of cell which forms axons that make synaptoid contact with basiepithelial interneurones. WEBER & GROSMANN (1977) reach a similar conclusion after studies on the spine base epithelia of *Centrostephanus longispinus*.

It is probable that quite different interpretations of the sensory role of epithelia are due to two main factors: an erroneous assumption of the singularity of epithelial cell types, and confusion between epithelial processes containing tonofilaments and axons. In the present study it was noted that sensory axons containing dense clusters of neurotubules and granular material (glycogen?) could be confused with tonofilament containing epithelial processes. Unfortunately this error was made in some earlier TEM studies of the ampullae and tube feet of H. pulcherrimus (KAWAGUTI 1964, KAWAGUTI 1965c).

This study and others (COBB & LAVERACK 1966b, COBB 1970, FLOREY & CAHILL 1977, and WEBER & GROSMANN 1977) has shown that tonofilament-containing processes are not axons but anchoring processes which attach to the connective tissue by means of terminal expansions. Filamentous epithelial processes are particularly well developed within the tube foot nerve and appear to bind the axons between the outer epithelium and the circular connective tissue layer. A remarkably similar phenomenon has been observed in the ventral nerve cord of nereid polychaetes (BASKIN 1971a, 1971b) where 'fibrous glial processes' bind the axons to the epidermis. BASKIN (1971b) proposes that glial filaments are rigid and resilient enabling a dissipation of the stresses produced during body wall movements. It was observed that various muscles, in particular the parapodial musculature, are anchored to the connective tissue sheath surrounding the nerve cord and that during contraction tensile forces are continuously transmitted to the nervous tissue. Similar stresses must be transmitted through the tube foot nerve, particularly during extension. Thus the glial processes of polychaetes and epithelial processes of echinoids are interesting examples of the parallel evolution of similar structures performing similar functions.

The connective tissue sheath of the tube foot exhibits a high degree of organisation into amorphous, longitudinal and circular layers. Only the present TEM study has observed the helical coiling of the longitudinal collagen filaments in echinoid tube feet. It is probable that the bundles of helically coiled longitudinal filaments provide increased rigidity to the tube foot wall thus preventing buckling during contraction and swelling during extension.

The longitudinal layer may also play an important role in facilitating muscle activity during extension and contraction due to its visco-elastic properties (discussed more fully in Chapter 6).

It is rather unusual that previous TEM studies of tube feet failed to describe the helical coiling of the longitudinal collagen filaments since this was described in an earlier light microscope study by SMITH (1947), who observed that they '...are seen to be much convoluted...' in the contracted condition.

The general ultrastructure of the tube foot/ampulla musculature of E. esculentus and P. miliaris is similar to that of other echinoderms.

The contractile apparatus is similar to that of other invertebrate smooth muscles consisting of thin/actin and thick/myosin-paramyosin filaments. There is only one report of the biochemical identification of actin in echinoderm muscle: OBINATA et al. (1974) isolated actin filaments from the lantern musculature of Lytechinus variegatus and Arbacia punctulata. A characteristic feature of the actin was the absence of a calcium sensitive regulatory system (i.e. troponin) and it was therefore concluded that a myosin-linked regulatory system occurred in echinoderms. If this is the case, then echinoderm muscles are similar to that of molluscs, sipunculids, nemerteans, and brachiopods; and unlike annelids, vertebrates and arthropods (which contain troponin).

Estimates of thin filament diameter in echinoid muscles vary from 5nm (COBB 1968a, HOLLAND 1971, DOLDER 1972) to 10nm (FLOREY & CAHILL 1977, BACHMANN & GOLDSCHMID 1978a). It is probable that these small differences may be due to factors such as fixation and magnification calibration.

Thick filaments of echinoderm smooth muscles show a larger and probably representative difference in size, varying from 20nm (most studies) to 100nm (OBINATA et al. 1974). The large diameter of echinoderm thick filaments (smooth muscle only) provides some evidence that they are of the myosin-paramyosin type. Other ultrastructural studies of echinoderm muscle have also implicated the occurrence of paramyosinic filaments in: holothuroid polian vesicles (BACCETTI and ROSATI 1968a), asteroid and holothuroid tube feet (DOLDER 1972), and asteroid axial organ (BACHMANN & VON HEHN 1968). However, the confirmation of the presence of paramyosin requires biochemical and biophysical analysis. The experimental techniques for isolating and identifying paramyosin (described in WINKELMAN 1976) essentially consist of extraction by homogenization in salt solutions and alcohol-ether followed by procedures for the removal of myosin and tropomyosin contaminants. The paramyosin extract is subsequently dissolved in salt solutions and dialysed against a buffer at pH 6.0 where it forms a paracrystalline precipitate. The precipitate is mounted on grids, negatively stained and examined using TEM. The precipitate consists of striated fibrous elements which are termed tactoids. Many α-fibrous proteins form tactoids in a similar manner, but each protein forms tactoids with characteristic axial periodicities e.g. 39.5nm for rabbit tropomyosin, and 72.5 or 14.5nm for paramyosin (KENDRICK-JONES et al. 1969). Unfortunately, 14.5nm axial periodicity is also exhibited by light meromyosin and myosinrod tactoids (WINKELMAN 1976). Other methods of identification include sodium dodecyl-sulphate (SDS) gel electrophoresis and immunodiffusion (ELFVIN et al. 1976).

Echinoderm paramyosin tactoids have been obtained from: holothuroid body wall and polian vesicles (BACCETTI & ROSATI 1968b) and echinoid lantern musculature (OBINATA et al. 1975). In addition to tactoid identification, WINKELMAN (1976) has also determined the paramyosin-myosin weight ratio and amino acid composition of holothuroid longitudinal muscle bands. WINKELMAN analysed paramyosins from seven invertebrate phyla and found that holothuroids

Phylum	Class/Species
PLATYHELMINTHES	Cestoda (S)
NEMATODA	*Ascaris* (O)
NEMATOMORPHA	
SIPUNCULOIDEA	*Phascolosoma* (O)
ANNELIDA	Polychaeta (O), Oligochaeta (O), Hirudinea (O)
MOLLUSCA	Bivalvia (S, O, C)
ARTHROPODA	Merostomata (C), Crustacea (C), Insecta (C)
BRACHIOPODA	*Terebratulina*
ECHINODERMATA	Echinoidea (S), Holothuroidea (S)

TABLE 6

Biochemical/Biophysical Identification of Paramyosin in the invertebrates (after Baccetti & Rosati 1968b, Winkelman 1976, Elfvin et al. 1976)

S = Smooth muscle
O = Obliquely striated muscle
C = Cross striated muscle

have a very high paramyosin-myosin ratio (1.0 in Cucumaria lactea compared with the maximum of 2.2 in Pecten maximus abductor muscle). The amino acid composition of holothuroid paramyosin was found to be typical of paramyosin in having a lysine/arginine ratio less than 1.

The properties and functional significance of paramyosin in invertebrate muscles has received considerable attention since its initial discovery in molluscan catch muscle by BEAN in 1944 and subsequent isolation by BAILEY in 1956 (see WINKELMAN 1976, ELFVIN et al. 1976). Paramyosin has a widespread distribution in the invertebrates (Table 6) and occurs in a wide variety of muscles ranging from insect flight muscle to molluscan catch muscle. Paramyosin-myosin weight ratios are quite variable, ranging from 0.065 in Aequipecten striated adductor to 5.5 in Mercenaria opaque adductor (LEVINE et al. 1976).

There appear to be slight differences in estimates of the size of paramyosin molecules after SDS-gel electrophoresis. WINKELMAN obtained a range of 93,000 daltons (P. maximus) to 123,000 Daltons (Holothuria forskali and Homarus vulgaris) but noted that '...some degradation of the paramyosin had occurred...' in some instances. ELFVIN et al. (1976) obtained similar chain weights (115,000 $\pm$ 4000 Daltons) for the paramyosins they studied (Bivalve, Crustacean and Limulus) and argue that the lower estimates obtained in other studies were due to proteolysis during preparation. The technique of ELFVIN et al. (1976) differed from WINKELMAN (1976) in the addition of a glycerination process prior to homogenization and it is suggested that this minimized proteolysis. ELFVIN et al. provide further evidence for the uniformity of the paramyosin molecule by showing that rabbit anti-Limulus paramyosin forms a precipitin reaction with other invertebrate paramyosins. In addition, immunofluorescence localized paramyosin in the A band of striated muscles (i.e. associated with thick filaments) and throughout the entire fibre of smooth muscles such as Mytilus ABRM.

In order to obtain an understanding of the functional significance of paramyosin in the echinoderm tube foot/ampulla complex it is necessary to examine evidence that is available from studies on other invertebrates.

A model for the structure of paramyosinic filaments has been described by SQUIRE (1971) and it is suggested that paramyosin is the core inside a myosin sheath. Paramyosinic filaments show a striking variation in diameter and length when compared with non-paramyosinic filaments. Molluscan thick filaments can vary from 8nm (KAWAGUTI & IKEMOTO 1958) to 150nm (PHILPOTT et al. 1960); vertebrate thick filaments (striated muscle) only vary from 10-15nm (HUXLEY 1966). LEVINE et al. (1976) have demonstrated that paramyosinic filaments show a similar large variation in length, ranging from 1.8μ in molluscan striated muscle to 40μ in molluscan catch muscle. Most vertebrate thick striated filaments are approximately 1.5μ in length.

It thus appears that the paramyosin core may provide increased stability resulting in filament lengths that are impossible with myosin alone. Consequently there is some relationship between paramyosin-myosin ratio and filament size. WINKELMAN (1976) found that there is no direct correlation between filament size and paramyosin-myosin ratio but states that '...the amount of paramyosin synthesized in a muscle may be one factor determining filament width and/or length.' However, the failure of WINKELMAN to obtain a direct correlation may be due to some loss of paramyosin by proteolysis since LEVINE et al. (1976) obtained a linear correlation between paramyosin-myosin ratio and thick filament length. A similar correlation does not occur with filament diameter; the largest diameter filaments (molluscan catch muscle) do have the highest paramyosin-myosin ratios but these filaments are also the longest.

LOWY et al (1964) proposed that increased filament length provides a greater number of actomyosin cross-bridges and therefore develops greater tension. LEVINE et al. (1976) subdivided invertebrate muscles into three classes on the basis of paramyosin-myosin ratio and found that thick filament length correlated with maximum tension development but only when the three classes were compared with one another. 'Class I' muscles (filament length up to 2.4µ, filament diameter up to 21nm) developed tensions up to 1.2Kg.cm^{-2}; 'Class II' muscles (6µ x 22nm) developed up to 5.2Kg.cm^{-2}; and 'Class III' muscles (catch muscles) developed tensions up to 14Kg.cm^{-2}. However, variations in tension development within individual classes would not be directly correlated with filament length. Also, 'Class I' muscles (molluscan and insect striated) attained lower tension development than vertebrate skeletal muscle (approximately 2.3Kg.cm^{-2}) despite having larger filaments. Clearly, there are other factors (such as the number of filaments) in addition to filament length which are responsible for increasing tension development. Similarly, there is no direct correlation between tension development and filament diameter except for the observation that catch muscles develop the greatest tensions. Molluscan catch muscles (see TWAROG 1976 for review) are quite unusual in their ability to maintain a sustained contraction for long periods of time without fatigue.

Using the criteria of thick filament size, tube foot/ampulla muscles are intermediate between 'Class II' and 'Class III' muscles. Rather interestingly, the paramyosin-myosin ratio of holothuroid body muscles (WINKELMAN 1976) is also intermediate between 'Class II' and 'Class III'. It is unfortunate that there are no estimates of the maximum active tension developed by echinoderm muscles.

LEVINE et al. have also observed that 'Class II' muscles can '...undergo extreme, reversible length changes'. Tube foot musculature undergoes similar changes and it is possible that this is also due to thick filament shortening as proposed for 'Class II' muscles by LEVINE et al.

The ultrastructural data obtained in this study indicates that there are two types of muscle in the tube foot/ampulla complex; however, does this correlate with functional differences? The physiological functions of muscles can be classified by the following criteria: speed of shortening, speed of relaxation, maximum force generation (tension development), endurance (stamina) and range. JOSEPHSON (1975) has reviewed the morphological correlations of these criteria in cross-striated muscle and they may also be applicable to smooth muscle.

Speed of shortening is affected by the number of contractile units that are arranged in series. Thus short filament lengths enable more contractile units and thus faster contraction.

Speed of relaxation is affected by calcium resequestration rate and is thus dependant upon the volume of sarcoplasmic reticulum (this criterion may not necessarily apply to echinoderm muscles discussed later).

Maximum force generation is affected by the number of actomyosin bridges which can be formed and thus the number of thick and thin filaments per unit area of muscle fibre and the length of filaments.

Endurance is affected by energy production and thus the number of mitochondria.

Range is the extent over which muscle can operate and is affected by the degree of overlap between thick and thin filaments and thus the length of thick filaments. Range is also affected by the degree of order exhibited by the myofilaments. Consequently highly developed muscles (cross - striated) have fixed Z-lines or rows of Z-bodies which limit the degree of contraction and stretch. Intermediately ordered muscles (obliquely-striated) have rows of Z-bodies which can move with respect to the longitudinal axis and thus increase range. Less ordered muscles (smooth) have no form of sarcomere organization since Z-bodies occur throughout the cell thus increasing range.

It is possible that Type II disk levator muscles are in fact the distal regions of stem retractor muscles since they have extremely similar ultrastructure and thick filament diameters (20-70nm in Type II DLM and 20-60nm in stem retractors). Type I disk levator muscles are similar to ampulla muscles in having thick filament diameters of approximately 23nm and shorter muscle fibres. Applying JOSEPHSON's criteria; the ampulla and disk levator muscles will exhibit faster shortening and greater endurance than stem retractors due to shorter thick filaments, shorter muscle fibres, and a larger relative volume of mitochondria. However, stem retractors will generate more force and operate over a far greater range due to having a larger fibre volume, thicker and longer filaments. Comparisons of the speed of relaxation are difficult to make since sarcoplasmic reticulum occupies a low relative volume in all echinoderm muscles, thus apparently indicating low speeds of relaxation. However it is possible that calcium is resequestered in sites other than sarcoplasmic reticulum such as the sarcolemma or extra-muscular sites; this phenomenon is discussed more fully in Chapter 6.

Behavioural observations confirm these findings of structural/functional diversity since: a) tube foot muscle operates over a much wider range than ampullae or disk levator muscles, b) faster shortening in ampulla and disk levator muscles is necessary for rapid tube foot extension and attachment of the disk to the substrate, c) ampulla and disk levator muscles remain contracted for longer periods than stem retractors in order to maintain tube foot extension and suction.

It appears that JOSEPHSON's criteria can be applied to echinoderm muscles in a similar manner to other invertebrate smooth muscles such as the body wall musculature of gastropods (PLESCH 1977a).

In addition, these criteria can also be applied to the only known example of striated muscle in echinoderms. GEDDES & BEDDARD (1881) and KIERNICK (1906) described striated muscle in echinoid pedicellariae and COBB (1968a) showed that the tridentate pedicellariae of E. esculentus contain smooth and striated muscles. The striated muscle shows sarcomeric organization with distinct Z-lines similar to that in other cross-striated muscle. Striated muscle thick filaments were smaller than smooth muscle thick filaments and measured approximately 15nm in diameter. The striated muscles function in the rapid closure of the pedicellariae but smooth muscles are involved in maintaining closure and opening. COBB (1968a) found that the striated muscle did not contain a sarcoplasmic reticulum but had a well developed T-system in the region of the Z-lines.

Echinoderm smooth muscles do not exhibit the same degree of sarcomeric organization and the myofilaments have a characteristic lack of alignment. Z-material usually occurs randomly throughout the fibre, in the form of Z-bodies (termed J granules by KAWAGUTI et al.) and this has been observed in: echinoid spine muscle (KAWAGUTI & KAMISHIMA 1965), echinoid tube foot (KAWAGUTI 1964a, FLOREY & CAHILL 1977, present study), holothuroid and asteroid tube feet (DOLDER 1972), echinoid ampulla (KAWAGUTI 1965c, present study), asteroid ampulla (BARGMANN & BEHRENS 1963), holothuroid intestine (KAWAGUTI 1964b), holothuroid body wall (HILL et al. 1978), asteroid axial gland (BARGMANN & VON HEHN 1968) and echinoid axial complex (present study). The absence of Z-material, in any form, has been described in crinoid ovary (HOLLAND 1971), echinoid ovary (KAWAGUTI 1965b), holothuroid dorsal haemal vessel (JENSEN 1975), echinoid axial complex (BACHMANN & GOLDSCHMID 1978a) and ophiuroid tube feet (MARTINEZ 1977d).

The apparent absence of Z-material in some studies may be due to the lability of Z-material (similar to the labile actin filaments) and their irregular distribution throughout the longitudinal axis of the muscle fibre.

In this study, Z-bodies were more commonly observed in longitudinal sections of muscle fibres and they were not frequently observed in transverse sections.

Echinoderm smooth muscle fibres, particularly the stem retractors of the tube foot, exhibit features such as: irregular arrays of Z-bodies, lack of filament alignment, irregular arrays of thin filaments around thick filaments, variable thick filament diameters and no ultrastructural differences in filament organization between the inactive and active condition. All of these features provide evidence of a loosely organized muscle where it is possible that thick filaments may not have specific thin filament partners. Thus, actomyosin bridges can be formed between any thick and thin filaments that happen to be 'close' enough for linking to occur. Consequently the range of the muscle will be greatly increased (particularly advantageous for tube foot function).

Such a 'changing actin partners' model has been proposed for molluscan smooth muscles and is supported by physiological and X-ray diffraction evidence in molluscan and vertebrate smooth muscle (PLESCH 1977a).

Whether loosely organized smooth muscles represent an early grade in muscle evolution remains to be answered.

The innervation of the tube foot/ampulla complex shows rather unusual and interesting features, and the present ultrastructural study reveals some inconsistencies in the conclusions reached by other studies of echinoderm myoneural anatomy and physiology.

There is pharmacological evidence for a cholinergic control of tube foot musculature: PENTREATH & COTTRELL (1968) found high levels of acetyl cholinesterase (A.Ch.E) activity in the basiepithelial plexus and musculature of asteroid tube feet, and FLOREY et al. (1975) found that echinoid tube feet contracted in response to A.Ch. and GABA but not to catecholamines, 5-HT, nor glycine. In the latter study it was proposed that tube foot muscle cholinoreceptors '...cannot be classified as either muscarinic or nicotinic...' since M-cholinolytics (e.g. atropine, banthine) and N-cholinolytics (demethonium, mytolon) were both effective antagonists to A.Ch. In addition M-cholinomimetics and N-cholinomimetics both induced contraction.

A cholinergic motor innervation is ubiquitous among echinoderm muscles (see reviews by WELSH 1966, PENTREATH & COBB 1972) and in addition to the work of FLOREY et al. (1975), the presence of M- and N-cholinoreceptors on the same muscle has been observed in: echinoid lantern muscle (MENDES et al. 1970, SHELKOVNIKOV et al. 1977), and holothuroid pharynx protractor (SHELKOVNIKOV et al. 1977). The occurrence of both M- and N-cholinoreceptors on the same muscle fibre is fully discussed in the study of SHELKOVNIKOV et al. and it appears that natural transmitter A.Ch. predominantly binds to N-cholinoreceptors (like vertebrate skeletal muscle) and the role of M-cholinoreceptors '...is not yet clear'.

In a study of the radial muscle of an echinothuriid (N.B. echinothuroids possess a flexible test which can be contracted by the radial muscles), TSUCHIYA & AMEMIYA (1977) found that only N-cholinoreceptors are present. It thus appears cholinergic neuromuscular transmission is not necessarily uniform throughout echinoderm muscles.

COBB (1978) states that 'there is no evidence that echinoderm muscle is sensitive to any transmitter except acetylcholine...' and yet COBB (unpublished observations quoted in PENTREATH & COBB 1972) has observed that echinoid lantern retractor muscle is rapidly relaxed by low concentrations of either noradrenaline or adrenaline. There is further evidence that biogenic amines have various effects on echinoderm muscle (early studies are discussed by HILL 1970): LAVERACK (unpublished observations) has found that adrenaline and noradrenaline relax the gut of _E. esculentus_. HILL (1970) found that tryptamine relaxed the holothurian cloaca and tyramine blocked delayed tonic responses produced by electrical stimulation. In addition, SHELKOVNIKOV et al. (1977) found that dopamine produced slow contractions of the pharynx protractor muscle of Cucumaria; an excitatory effect of biogenic amines has also been found in holothuroid intestinal haemal vessels (WYMAN & LUTZ 1930, PROSSER & JUDSON 1952). Thus, from the pharmacological studies on other echinoderm muscles it is not necessary that the tube foot musculature receives only a cholinergic innervation. It is important to consider this since the present ultrastructural study provides evidence for a dual innervation of the tube foot musculature.

The mode of innervation of the tube foot/ampulla complex is unusual because: a) synaptoid contacts occur between centrally derived motoneurones (i.e. lateral nerve) and modified muscle processes termed muscle tails; and b) connective tissue always separates motoneurones from muscle tails.

Muscle tails were first described in the ampulla of Astropecten by COBB (1967) and COBB & LAVERACK (1967). It was observed that large groups of muscle tails pass down the ampulla 'seam' into the lateral and medial 'bulbs' which are characteristic of asteroid tube feet. Ampulla muscle tails are characterized by: a) central clusters of myofilaments surrounded by an area of clear cytoplasm; and b) a tesselated outline in transverse section. The muscle-tails of the ampulla represent the so-called 'ribbon' axons which were described in the earlier studies of SMITH. COBB (1967) and COBB & LAVERACK (1967) described neuromuscular junctions in the ampulla as consisting of an intermingling of muscle processes and axons within the bulb. However, subsequent studies by COBB (1970) on asteroid and echinoid ampullae showed that axons do not pass through the connective tissue sheath and synaptoid contacts occur across a basement membrane which separates the muscle tails from the lateral (podial) nerve. It is probable that in earlier studies, 'muscle tails' identified within the nervous tissue were confused with filamentous epithelial processes.

The innervation of the tube foot was not investigated in earlier TEM studies but COBB (1970) suspected that processes arose '...from the muscles of the ampulla and probably the tube foot'. The present ultrastructural study of echinoid tube feet confirms the latter suspicion to a certain extent. Clusters of muscle tails pass from the proximal region of the stem retractor muscles (close to the site of attachment to the periporal area) and extend into the perradial/adoral pore of ambulacral/peristomial tube feet. Tube foot muscle tails do not extend completely through the pore-pair and do not therefore intermingle with ampulla muscle tails. The size of individual muscle tails makes it unlikely that they represent ribbon axons identified by SMITH. It is probable that the characteristic bundles of muscle tails may correspond with individual ribbon axons. It is interesting to note that in Methylene blue stained semi-thin sections, muscle tails showed similar staining affinities to axons in the tube foot nerve.

The ultrastructure of tube foot muscle tails is quite characteristic and similar to that of ampulla muscle tails in asteroids and echinoids. Significant modifications of the muscle ultrastructure are:

a) reduction in size of the fibre,

b) reduction in volume of the myofilaments and relative increase in volume of sarcoplasm,

c) larger numbers of mitochondria (appearing in the condensed state after aldehyde fixation),

d) appearance of microtubules.

The latter two modifications have not previously been described in echinoderm muscle tails.

The phenomenon of muscle processes extending towards motoneurone is by no means unique to echinoderms since similar structures have been found in other groups of invertebrates such as the 'muscle arms' in nematodes (ROSENBLUTH 1965) and 'root fibres' in cephalochordates (FLOOD 1966). Similar muscle processes have also been observed in other invertebrates too, e.g. 'sarcoplasmic extensions' in turbellaria (MacRAE 1963, CHIEN & KOOPOWITZ 1972), 'prolongements de fibres' in polychaetes (WISSOCQ 1970), 'muscle tails' in oligochaetes (MILL & KNAPP 1970), and 'muscle pillars' in insects (HAMORI 1963, ATWOOD et al. 1967). CHIEN & KOOPOWITZ (1972) propose that all muscle processes described in different invertebrates have a similar function in the transmission of excitation toward contractile regions of the muscle fibre and thus somewhat analogous to neuronal dendrites. It was also proposed that muscular junctions between muscle processes and motoneurones should be termed 'sarconeural junctions' in order to distinguish them '...from the more usual neuromuscular junctions'.

Echinoid tube foot muscle tails characteristically contain numerous microtubules, which also have been observed in turbellaria sarcoplasmic extensions' (CHIEN & KOOPOWITZ 1972). Non-tubular filamentous structures were observed in muscle processes of Branchiostoma (FLOOD 1966), Ascaris (ROSENBLUTH 1965) and Syllis (WISSOCQ 1970). The role of microtubules or microfilaments within muscle processes is unknown but their similarity to neurotubules and neurofilaments within axons is intriguing and may correlate with an adaptation for the rapid transmission of excitation.

It is interesting to note that muscle fibres which are modified for the through conduction of excitation also occur in the vertebrates. Fibres within the atrioventricular bundle (Bundle of His) of the mammalian heart are of a highly distinctive appearance and are termed Purkinje fibres. The ultrastructure of Purkinje fibres is similar in all mammals but they have been extensively studied in the ungulates due to their large size (in Chapter 11 BLOOM & FAWCETT 1968) and they show some remarkable similarities to echinoderm muscle tails. Purkinje fibres have a reduced complement of myofilaments, clear sarcoplasm containing numerous mitochondria, and a tesselated outline in transverse section. They differ however, in being much larger (up to 50µ in diameter in bovine heart) and in the presence of close junctions between adjacent fibres.

Thus, the ultrastructure of echinoderm muscle tails correlates with a role in the rapid conduction of excitation from the distal site of innervation to the contractile region of the muscle. This role would apply also to the other known examples of 'sarconeural' innervation. It would be interesting to investigate the factors which determine this peculiar mode of innervation, and whether they are similar in all known cases.

The innervation of echinoid tube foot muscle tails occurs in a discrete region at the base of the tube foot, within the perradial pore. The echinoderm 'sarconeural junction' differs from others in the presence of a thin connective tissue layer between motoneurones and muscle. The thickness of the connective tissue can vary from 100nm in the ampulla to 2µ in the tube foot. For reasons which will be discussed later it is unlikely that these thicknesses of connective tissue present a barrier for the diffusion of neurotransmitters.

The structural arrangement of muscle tails into well defined clusters may represent a degree of functional architecture. Each muscle tail bundle may originate from discrete muscle blocks and thus different areas of the tube foot musculature may contract producing bending in different directions. It is also possible that processes from disk levator muscles may be grouped into one cluster. Unfortunately the tube foot preparation is not amenable to electrophysiological analysis since this would ultimately determine whether any form of functional architecture does occur within the muscle tail clusters.

The present study of echinoid tube foot muscle tails leaves one particular question unanswered; do all tube foot/ampulla muscle cells produce muscle tails? In any transverse section, the total number of tube foot muscle tails is far less than the number of muscle cells. It is therefore possible that within each muscle block (distinct groupings of muscle fibres are particularly apparent in the extended condition) only one cell is innervated and excitation is subsequently spread to other non-innervated cells within the group. The extent of coupling must be small since electrical stimulation of the ampulla produced only local contractions in the region of the electrode tip. There is no ultrastructural evidence for coupling between muscle cells (i.e. gap junctions) but since synaptic transmission is rather unusual in echinoderms (PENTREATH & COBB 1972, COBB & PENTREATH 1976, 1977) then it is possible that coupling may occur by a hitherto unidentified mechanism (discussed in Chapter 6).

The two types of muscle in the tube foot/ampulla complex are both innervated via muscle tails and this finding does not support hypotheses regarding echinoderm musculature and its innervation. Firstly, there is no evidence for endothelial processes innervating the tube foot muscle as proposed by KAWAGUTI (1964a). Such processes have a role in 'anchoring' endothelial cells to the connective tissue sheath. Secondly, it is unlikely that the tube foot musculature is innervated by the basiepithelial plexus in a manner similar to the autonomic innervation of vertebrate blood vessels as proposed by FLOREY & CAHILL (1977). The latter mechanism cannot account for the bending of tube feet by the contraction of specific blocks of fibres, nor does it correlate with the integrated activities of the ampulla, stem retractors and disk levators. It is more likely that integration of the activities of these three muscle groups occurs within the neuropile of the lateral nerve innervating the tube foot/ampulla complex. This correlates with: a) the ability of an isolated tube foot/ampulla complex to function normally and b) evidence that each echinoderm effector organ (pedicellariae, spines etc.) is associated with a discrete area of neuropile or 'ganglion' (COBB 1970, PENTREATH & COBB 1972). It is interesting to note that the present study provides ultrastructural evidence for a tube foot/ampulla ganglion since clusters of neurone somata (one type is probably aminergic) were observed within the proximal region of the tube foot nerve. Neurone somata only occur in the intraporal region (except for neurosensory somata) and this explains the assumption of FLOREY & CAHILL (1977) that neurones within the tube foot stem '...must have their cell bodies within the radial nerve or in the ganglionic region at the distal end of the tube foot'.

Thirdly, there is no evidence that echinoderm muscles can be divided into a 'skeletal' and 'visceral' type (COBB & LAVERACK 1977, COBB 1978). After comparing the ultrastucture and innervation of echinoderm muscles, COBB (1978) proposed that muscle in the: tube feet, gut, gills, and circular muscle of papulae is of a 'visceral' type and is characteristically innervated by LGVC axons (large granular vesicle containing axons) similar to those observed in this study. Lantern retractor and ampulla muscles however, are of the 'skeletal' type and are innervated by hyponeural axons (indirectly via muscle tails in the ampulla), and LGVC axons are not present. From the evidence obtained in this study, it is apparent that tube foot muscles are neither 'skeletal' nor 'visceral' since they are innervated by means of muscle tails and are associated with an extensive LGVC plexus. As COBB (1978) has stated '...the proposed hypothesis is at present a simplification since there are several inconsistencies'.

The present study has classified the tube foot/ampulla musculature according to the criteria used for other muscles and thus provides functional correlates of ultrastructural differences.

The presence of LDSG axons within the tube foot connective tissue and musculature indicates that a dual innervation may occur; a central control via muscle tails which is responsible for the co-ordinated activities of tube feet, and a peripheral control via LDSG axons. The nature of the LDSG innervation is discussed in Chapter 6.

Fig. XXV

Schematic section of the PTF disk passing through the plane A-B

Ba	Basiepithelial axons
Ct	Connective tissue
De	Distal epithelia
N	Neurosensory cell
Pe	Proximal epithelia
R	Rosette projection
S	Secretory cell

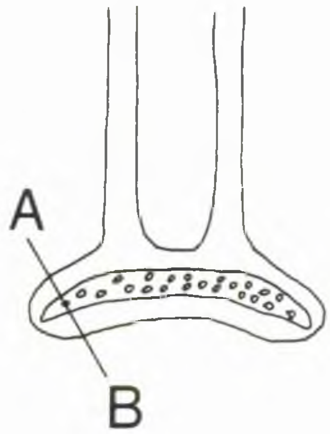

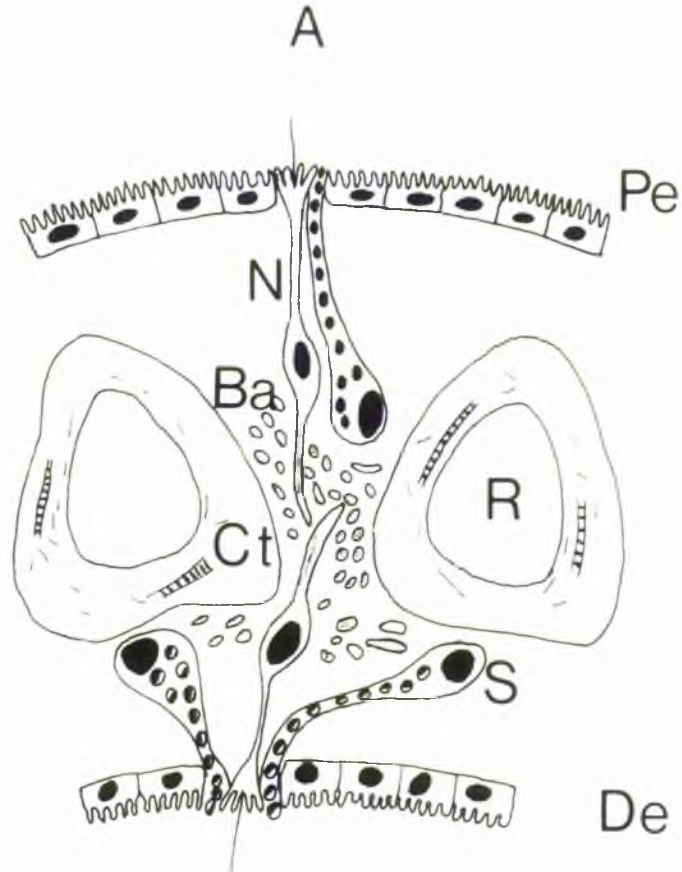

B

Fig. XXVI

Schematic L.S. of the [illegible]TF disk

D Disk Levator Muscle

F Frame

R Rosette

Bar indicates level of T.S. shown in Fig. 103.

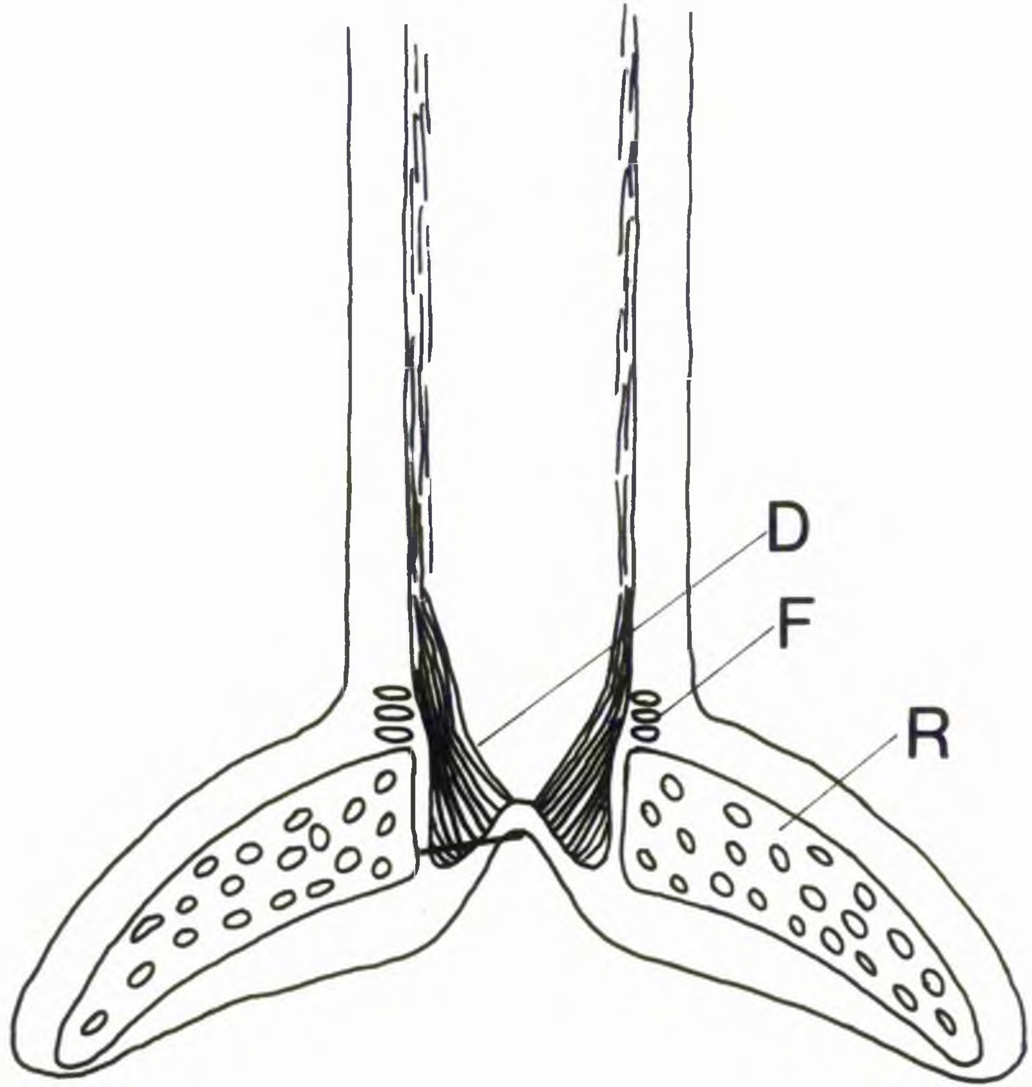
D
F
R

Fig. XXVII

Schematic T.S. of the tube foot wall

Bp	Basiepithelial plexus
C	Circular connective tissue
En	Endothelium
Ep	Epithelium
L	Longitudinal connective tissue
M	Muscle

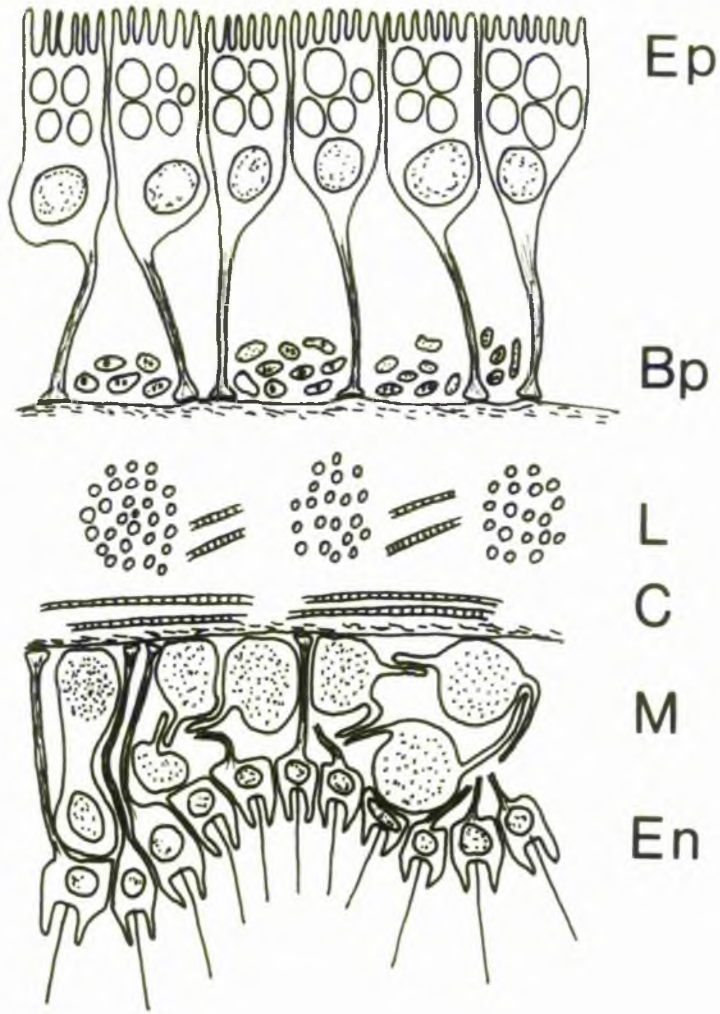
Ep
Bp
L
C
M
En

CHAPTER 6

HISTOCHEMICAL AND EM CYTOCHEMICAL STUDIES ON TUBE FOOT CONNECTIVE TISSUE, LDSG CELLS AND MUSCULATURE: THE PHENOMENON OF CONNECTIVE TISSUE PLASTICITY IN ECHINODERMS

HISTOCHEMICAL AND EM CYTOCHEMICAL STUDIES IN AMBULACRAL TUBE FEET : THE PHENOMENON OF CONNECTIVE TISSUE PLASTICITY IN ECHINODERMS

INTRODUCTION

For the purposes of this chapter, three interesting points emerge from studies concerned with the structure and function of echinoderm tube feet.

First, FLOREY and CAHILL (1977) postulated that during contraction of echinoid tube feet there are changes in the 'plastic properties' of the connective tissue by an alteration in the number of cross-linkages between collagen filaments. There have been few studies on the connective tissues of echinoderms and only one of these has dealt with the connective tissue sheath of tube feet. MARTINEZ (1977b) described the ultrastructure of collagen filaments and non-collagenous fibrils within the tube feet of *Ophiothrix fragilis*. However, no histochemical techniques were utilised and cross-links between collagen filaments were not observed or discussed.

Secondly, TEM studies have revealed the existence of neuron-like cells which form fine processes ramifying amongst the connective tissue and musculature. A characteristic feature of the ultrastructure of these cells is the presence of numerous, membrane bound, electron dense storage granules approximately 150nm in diameter. For convenience, such cells have been termed 'Large dense storage granule' containing cells or LDSG cells. The role of LDSG cells is the subject of considerable speculation by various authors. Cells of similar ultrastructure have been found within the tissues of all classes of echinoderms (PENTREATH and COBB 1972). Most authors ascribe a neurosecretory function to LDSG cells on the basis of ultrastructural evidence alone and without the support of histochemical or experimental evidence. On the basis of negative fluorescence histochemical results, COBB (1969a) proposes that LDSG cells in the oesophagus of Heliocidaris erythrogramme are neurons which contain '...a transmitter of unknown chemical composition but not a monoamine'. DOLDER (1975), however, provides EM cytochemical evidence for the presence of 5HT in LDSG cells in the tube feet of *Pentacta petersoni*, but unfortunately does not provide any form of control for the specificity of the cytochemical tests that were employed. To extend the speculation even further, FLOREY and CAHILL (1977) consider that LDSG cells in echinoid tube feet are '...more akin to Mast cells than to neurosecretory cells'.

Thirdly, ultrastructural studies of tube foot musculature have failed to reveal the presence of a well developed sarcoplasmic reticulum and thus it might be expected that such cells would be deficient in calcium storage sites for excitation-contraction coupling. Since echinoderms have the tendency to adopt rather unusual and novel methods for solving various biological problems it is possible that calcium storage is accomplished by a different manner and thus other sites within the musculature may sequester calcium.

It is therefore the purpose of this chapter to describe histochemical and EM cytochemical techniques which were employed in order to fulfil the following aims:

1. Determine the relationship between collagen and other connective tissue elements.

2. Characterise LDSG cells by their ultrastructure, histochemistry and EM cytochemistry.

3. Determine whether LDSG cells occur within a structure known to exhibit connective tissue plasticity e.g. spine catch apparatus (TAKAHASHI 1967b).

4. Determine the site of calcium storage in the tube foot musculature.

Test	Reaction
Semithin sections:	
Azure/AF	Azure +
Azure/BF	BF ++
Meth. Blue	γ metachromasia
Azure/MB	γ metachromasia
Haem/E	Haem ++
Azure/E	Azure ++
Tol. Blue	γ metachromasia
Paraffin sections:	
AB 2.5	++
AB 1.0	++
AB/PAS	AB + /PAS +
AB-CEC	All tissue alcianophilic at 0.0M [$MgCl_2$]. Alcianophilia persists in endothelia, epithelia and connective tissue (particularly inner layer) until 1.0M [$MgCl_2$]

\+ Moderate positive reaction

++ Strong positive reaction

Table 7

Histochemistry of the tube foot connective tissue

RESULTS

1. Connective tissue histochemistry and EM cytochemistry

The histochemical reactions of the tube foot connective tissue are summarized in Table 7.

Reactions such as γ metachromasia, basic fuchsinophilia and alcianophilia persisting at high levels of $MgCl_2$ (see Figs. 152-154) indicate that highly sulphated proteoglycans occur within the connective tissue. Alcianophilia at pH 2.5 and pH 1.0 indicates that both weakly and strongly acidic proteoglycans occur. The purple staining of the connective tissue with AB/PAS indicates that periodate-reactive mucosubstances occur within the connective tissue, in addition to non-periodate-reactive proteoglycans.

Unfortunately, all EM cytochemical methods for the localization of proteoglycans were unsuccessful. Bismuth nitrate treatment at pH 1.2 produced completely negative results. Tannic acid-ferric chloride appeared to be completely non-specific and little difference occurred between TA-Fe treated grids and TA treated grids. The en bloc colloidal iron procedure was unsuccessful due to poor penetration; a distinct surface precipitate of iron occurred around the periphery of the tissue block despite the use of small tissue blocks. Grid staining with colloidal iron produced a complete precipitate film over the tissue section.

Both the PA-Cr-Ag and PA-Bi methods for the EM cytochemical localization of periodate-reactive sites were successful. However, the finer precipitate formed by Bi provided more detailed and consistent results. Periodate reactive mucosubstances form a specific relationship with collagen filaments and consist of three discrete elements (Fig. XXIX):

1. Outer coat
2. Transverse belts
3. Fine lateral filaments (FLFs)

The outer coat appears to cover the whole length of the collagen filament and shows little variation in thickness, remaining at approximately 20nm (Fig. 155). Transverse belts are of a similar thickness to the outer coat and exhibit a regular axial periodicity of 100nm (Figs. 155, 156). Extending from the transverse belts are FLFs approximately 150nm long. There is some variation in the appearance of FLFs with respect to their relative orientation to the longitudinal axis of the collagen filament and in some sections they were not abserved at all. This indicates that FLFs only occur at specific loci around the collagen filament and do not radiate from the complete circumference of the transverse belt. Thus if the plane of section does not pass through a specific locus then FLFs will not be observed. Control sections treated with m-aminophenol completely blocked PA-Bi staining of the collagen filaments (Fig. 157). No other connective tissue elements showed periodate reactivity with the Pa-Cr-Ag or PA-Bi methods.

2. Connective tissue - stereom relationship

Azure/BF staining of semithin sections of decalcified PTF plate shows that collagen bundles exhibit intense fuchsinophilia (Fig. 158) similar to tube foot collagen.

TEM shows that other cellular elements in addition to connective tissue also occur within the stroma pervading the stereom (Fig. 159). A variety of amoebocytes and fibrocytes were observed in addition to LDSG cells similar to those previously described. The ultrastructure of collagen filaments appears more granular after decalcification and the characteristic axial striation is less apparent.

Collegen filaments are clustered into distinct bundles which wrap around skeletal trabeculae (Fig. 160). The collagen filaments are separated from the trabecula (which has a smooth surface) by an electron dense layer (approximately 200nm thick) which may represent a basal lamina.

The terminations of collagen filaments taper to approximately 65nm in diameter and attach to discrete areas of the skeletal trabecula (Fig. 161) Collagen attachment areas are characterised by the irregular outline of the trabecula and the presence of interweaving electron dense fibrils approximately 18nm in diameter. The fibrillar layer is approximately 900nm thick and probably binds the collagen filaments to the surface of the skeletal trabeculae.

3. LDSG cell ultrastructure

LDSG processes and somata have been observed in certain regions of the water vascular system (axial organ and polian vesicles) and are particularly extensive within the connective tissue and musculature of the tube foot stem and disk.

Tube foot LDSG cells are similar in ultrastructure to those occurring in other regions of the water vascular system and thus the following description applies to all LDSG cells unless stated otherwise.

LDSG cells do not possess dendrites but may produce more than one axon/process. LDSG somata (Fig. 162) are elongate (approximately 7 x 3μ) and contain numerous LDSGs of a variety of shapes and sizes. Elongate granules can reach up to 400nm in length but rarely exceed 250nm. LDSG diameters vary from 80-200nm but most are approximately 150nm. The variety of LDSG profiles indicates that an LDSG is not spherical but an ellipsoid. Thus sections at different angles through the ellipsoid will produce oval to circular profiles. Similarly transverse sections of an LDSG will exhibit different diameters depending on which level the section passes through.

An LDSG soma contains one golgi complex and few cisternae of smooth endoplasmic reticulum. Free ribosomes, α glycogen, small mitochondria and neurotubules occur within the perinuclear cytoplasm. A distinctive feature of LDSG cells is an extensive rough endoplasmic reticulum which consists of several cisternae, often stacked parallel to the nuclear membrane (Fig. 162).

Few differences in LDSG ultrastructure occur between tissues fixed simultaneously with glut./OsO_4 or prefixed with glut. Tissues fixed in OsO_4 alone show distinct differences in LDSG cell ultrastructure (Fig. 163). LDSGs are similar except for an increased electron density but somata show considerable disruption of the rough endoplasmic reticulum. In addition, the perinuclear cytoplasm is agranular and neurotubules are no longer apparent.

LDSG somata may occur throughout the musculature and connective tissue of the tube foot but within the musculature most somata occur subjacent to the endothelia. Such somata centrifugally project LDSG processes through the musculature and terminate against the connective tissue sheath.

LDSG processes are small in diameter, rarely exceeding 1μ. In addition to ramifying between muscle cells, LDSG processes appear to tunnel into non-contractile regions of muscle cells. Whether LDSG processes pass completely through a muscle cell is not known. In some profiles of 'tunnelling' LDSG processes it was observed that a sheath occurred between the LDSG process and the sarcolemma (Fig. 164). It is possible that the sheath is formed by a small collar-like evagination of a sarcolemmal pit which envelopes the termination of the LDSG process.

Most LDSG processes terminate at the junction of the connective tissue and muscle layers (Fig. 165). LDSG terminations are varicose and contain LDSGs, CVs and neurotubules.

Typical synaptic modifications between LDSG cells and muscle cells were not observed. As previously described, septate junctions appear to be the only form of specialised contact between LDSG cells and either muscle cells or endothelial cells. Specialised junctions between adjacent LDSG cells were not observed.

Test	Reaction
MUCOSUBSTANCES	
1) Semithin sections:	
Tol. Blue	Basophilic
Meth. Blue	"
Azure/MB	"
Azure/AF	Azure +
Azure/BF	Azure +
PAS/Haem (Control)	PAS + (-)
2) Paraffin sections:	
PAS (Control)	+ (-)
AB/PAS (Control)	PAS + (-)
3) EM Cytochemistry:	
PA-Cr-Ag (Control)	+ (-)
PA-Bi (Control)	+ (-)
NEUROSECRETORY MATERIAL/PEPTIDES	
CHP	-
PAF	-
AB/AY	-
Fluorescent mercurial	-
Fluorescamine	-
MONOAMINES	
1) Fluorescence histochemistry	
Falck et al. method	-
Fuxe & Jonsson method for 5HT	-
2) EM Cytochemistry	
All en bloc and grid methods	-

Table 8

LIEG cell histochemistry and cytochemistry

Evidence for any form of neuronal control of LDSG cells is lacking. However, some contacts between basiepithelial axons and LDSG processes within the tube foot connective tissue could be interpreted as synaptoid (Fig. 166). A thin layer of connective tissue (approximately 150nm) separates the basiepithelial axons from the LDSG processes and several CV occur within the 'presynaptic' terminal of the axon.

In the connective tissue LDSG processes ramify the matrix surrounding collagen filaments. LDSG somata occur randomly and there is no evidence for LDSG processes cummunicating from the muscle layer into the connective tissue or vice-versa.

In longitudinal sections of tube feet it is quite apparent that LDSG processes accompany lateral evaginations of muscle cells into the circular connective tissue layer and terminate against the basal lamina (Fig. 167).

4. <u>LDSG Histochemistry & Cytochemistry</u>

The histochemical and cytochemical reactions of LDSG cells within the tube foot are summarized in Table 8.

Negative results were obtained with tests for neurosecretory material or peptides. Fluorescence histochemistry failed to reveal any specific fluorescence within the connective tissue or musculature. EM cytochemical methods for biogenic amines were either negative in en bloc methods or completely non-specific in grid methods.

Semithin sections proved to be the most effective method of visualising LDSG cells in the light microscope. LDSG processes are basophilic and non-metachromatic when stained with Tol. Blue, Meth. Blue, or Azure/M.B. LDSG processes are most noticeable at the connective tissue-muscle boundary (Fig. 168). LDSG somata within the connective tissue and musculature (Fig. 169) contain a clear cytoplasm with numerous basophilic granules. The basophilia of LDSG cells is particularly demonstrated in sections stained with Azure 2 and counterstained with an acid stain such as Acid fuchsin (Fig. 170).

Correlation of paraffin and semithin section histochemistry with EM cytochemistry indicates that LDSG cells contain periodate reactive mucosubstances. The AB/PAS method reveals PAS positive somata within the musculature (Fig. 171). A network of fine PAS + processes within the musculature can be observed in paraffin sections (Fig. 172). All PAS reaction within the tube foot is specific since it is blocked by acetylation (Fig. 173). PAS/Haem stained semithin sections provide better resolution of PAS reactive sites within the tube foot (Fig. 174). PAS positive LDSG somata and proximal regions of LDSG processes are observed within the inner region of the musculature (Fig. 175). The finer distal regions of LDSG processes are also PAS positive (Fig. 176).

At the ultrastructural level, periodate reactivity is demonstrated by both the PA-Cr-Ag and PA-Bi methods. Within LDSG somata periodate reactivity occurs in the nuclear material, LDSGs and free or attached ribosomes (Fig. 177). Within the musculature there is little precipitation of Ag or Bi over muscle cells (due to glycogen?) but intense precipitation occurs over LDSGs within LDSG processes (Fig. 178). Similar precipitation occurs over LDSGs within the connective tissue (Fig. 179). The PA-Bi method (Fig. 180) produced similar results to the PA-Cr-Ag.

Control grids (either omission of periodic acid or blocking with m-aminophenol) exhibited a marked reduction in precipitation over LDSGs using either Pa-Cr-Ag (Fig. 181) or PA-Bi (Fig. 182) methods.

In addition to the cytochemical localisation of periodate reactivity in the connective tissue and LDSG cells, intense precipitation also occurs around epithelial microvilli (Fig. 183). This correlates with epithelial PAS reactivity observed in semithin sections.

5. LDSG cell-connective tissue relationship/The spine catch apparatus

In addition to the aforementioned observations of LDSG cells within the water vascular system, it was observed that LDSG cells formed a well developed plexus within the connective tissue matrix of the ATF rosette (Fig. 184), and within the spine catch apparatus (Figs. 185, 186). LDSG processes in the catch apparatus ramify between bundles of collagen filaments and show basophilia in contrast to the metachromasia of collagen (inset Fig. 186). Also occurring within the connective tissue matrix are small muscle processes which frequently occur adjacent to LDSG processes (Fig. 185).

The LDSG plexus of the catch apparatus differed in the presence of bundles of axons (containing neurotubules and CV) lying adjacent to LDSG processes (Fig. 187). It is possible that the axons may be LDSG processes since it was observed that LDSG processes can contain few LDSGs (Fig. 188). LDSG somata were observed within the catch apparatus and within the stroma of the spine tubercle (Fig. 189). Small axons containing neurotubules and CV occur adjacent to LDSG somata.

6. Cation localisation in tube foot musculature and X-ray microanalysis

The K-Ant method for the localisation of cations produced the most consistent results when glutaraldehyde prefixation was omitted.

Concentrations of cations localised by dense Sb precipitates occurred in the following regions:

1) Muscle - sarcolemma (Fig. 190)
2) Muscle - mitochondria (Fig. 191)
3) Muscle - vacuolar cisternae (Fig. 192)
4) Muscle - subsurface/tubular cisternae (Fig. 193)
5) LDSG cell - degranulating LDSGs and cytoplasm (Fig. 194)

Very little Sb precipitation occurred within myofilaments and sarcoplasm and Sb precipitation does not occur within endothelial and LDSG cell plasma membranes.

Except for LDSGs, most Sb precipitation is in association with a membrane.

Addition of sucrose or omission of K-Ant from the fixative prevented any form of precipitation. EDTA Treatment of ultrathin sections of K-Ant prepared tissues removed the Sb precipitate (inset Fig. 193).

X-ray microanalysis of the Sb precipitates produced by the K-Ant method reveals some of the inconsistencies of that method since other cations apart from Ca^{2+} can occur. X-ray microanalysis provides a qualitative estimate of the elements present in the Sb precipitate but one difficulty arises: the X-ray emission spectrum (i.e. peak) of the $Sb_{L\alpha}$ line (3.6 KeV) is quite close to the $Ca_{K\alpha}$ line (3.7 KeV) and frequently obscures it if low Ca levels occur.

(N.B. $K\alpha$, $L\alpha$, and $L\beta_1$ denote X-ray lines from different electron energy levels).

X-ray emission spectra of Sb precipitates in muscle cisternae (all varieties) and LDSG cells reveal quite distinct $Ca_{K\alpha}$ and $Sb_{L\alpha}$ peaks (Figs. 195-198). A $Cl_{K\alpha}$ peak is dominant in the X-ray spectra of all Sb precipitates (e.g. Fig. 197) and indicates the high Cl^- content of tube foot tissues. Spectra of LDSG precipitates indicate high concentrations of Os, S and K (Fig. 197). The high Os level correlates with the intense osmiophilia of LDSGs.

X-ray emission spectra of Sb precipitates in muscle sarcolemma (Fig. 199) reveal only one peak in the 3.6 KeV region. A $Ca_{K\alpha}$ peak cannot be distinguished (subjectively) thus indicating the absence of Ca concentrations. Thus Sb precipitation in the muscle sarcolemma is due to cations other than Ca.

DISCUSSION

As previously described in Chapter 5, the connective tissue of tube feet is a highly ordered structure which plays an important role in supporting the tube foot wall.

Histochemistry and EM cytochemistry indicate that tube foot connective tissue is by no means unusual since collagen filaments occur in a matrix composed of proteoglycans. Strong γ metachromasia and alcianophilia at high electrolyte levels indicate the matrix contains sulphated glycosaminoglycans. It is probable that the glycosaminoglycans are linked to protein forming high molecular weight proteoglycans similar to the chondroitin sulphate-protein complexes of vertebrates.

It is necessary at this juncture to emphasise the statement of HUNT (1970) that one cannot regard that '...histochemical and cytochemical studies as a means of identifying molecules, are sufficient unto themselves'. Thus the localisation of sulphated glycosaminoglycans does not infer the presence of chondroitin sulphate. Highly sulphated glycosaminoglycans have been isolated from tube feet (see review by MATHEWS 1975) and from the body wall of the holothurian Cucumaria japonica (MOTOHIRO 1960). The latter compound was found to be similar to chondroitin sulphate.

Chondroitin sulphates act as organisers of highly ordered networks of collagen filaments in connective tissue and are involved in the calcification process in vertebrate cartilage (HUNT 1970). Chondroitin sulphates closely resemble ion exchange resins and this coupled with molecular seiving properties and heavy hydration of the connective tissue matrix confers a significant role in the exchange and diffusion of many types of metabolite. Thus the connective tissue sheath of tube feet may have important physiological functions in addition to its structural role. It is possible that the thin connective tissue layer separating basiepithelial axons from muscle tails may facilitate diffusion of neurotransmitters over a distance ...

of approximately 2µ in tube feet.

Histochemistry and LM cytochemistry have localised periodate reactive mucosubstances in association with tube foot collagen filaments and thus provide the first cytochemical study of echinoderm connective tissue. Periodate reactivity is due to the presence of vicinal (vic) - glycols (PEARSE 1972a) and these occur in glycogens, starches, cellulose, glycoproteins and phospholipids. Periodic acid oxidation breaks C-C bonds within vic-glycols forming dialdehydes. Dialdehydes reduce Schiff's reagent to a red dye or precipitate silver/bismuth from silver/bismuth salts. During control procedures acetylation blocks vic-glycols thus preventing their oxidation, and m-aminophenol blocks dialdehydes thus preventing their reduction of Schiff or metal solutions.

It is probable that vic-glycols localised on collagen filaments represent glycoproteins which have a filament stabilising role since they form an intimate association consisting of: an outer coat, transverse belts and fine lateral filaments. Such a filament stabilizing role for glycoproteins occurs in vertebrate tendon and cartilage (see reviews by JACKSON & BENTLEY 1966 and MATHEWS 1975). The short carbohydrate side chains of glycoproteins allow a closer spatial organization of collagen aggregates (which constitute a single filament) than would be possible with the longer carbohydrate side chains of proteoglycans. Thus glycoproteins have a cementing role at a lower order of collagen filament organization. Similar associations of mucosubstances (i.e. outer coat, transverse belts and fine lateral filaments) with collagen have been described in human synovium using the Ruthenium red technique (MYERS et al. 1969). The specificity of the latter technique is open to question since it has been used for localising a variety of polyanionic mucosubstances including glycoproteins and glycosaminoglycans. In a later study by MYERS et al. (1973) Ruthenium red-positive filaments were described as '...linear aggregates of glycoproteins and proteoglycans'. Collagen/mucosubstance associations have been recently investigated in the sponges Chondrilla nucula and Hippospongia communis (see review by GARRONE 1978) where the Ruthenium red and Phosphotungstic acid - low pH techniques localised an outer coat and transverse belts similar to those previously described in echinoids and humans. Thus despite the use of different techniques, the remarkable similarity between the outer coat, transverse belts and fine lateral filaments of echinoid, sponge and human collagen indicates that the fundamental organisation of the collagen filaments is similar.

It is unfortunate that the methods for the EM cytochemistry of proteoglycans were unsuccessful since the interaction between glycoproteins and proteoglycans may have been ultrastructurally 'visualised'. Proteoglycans have a major cementing role at a higher order of collagen filament organization and networks of proteoglycan molecules form an 'interaction complex' with collagen filaments due to ionic and hydrogen bounding. This form of binding provides short term mechanical linkages between collagen filaments. Thus the degree of interaction (i.e. the physiochemical state of the connective tissue matrix) will affect the mechanical properties of the connective tissue.

On the basis of hitherto unpublished evidence, FLOREY and CAHILL (1977) suggest the connective tissue sheath of tube feet, '...can undergo reversible changes in stress-strain behaviour and that these drastic changes in mechanical properties depend on the function of the nerve plexus'. FLOREY (1974) observed that in its resting stage, the connective tissue sheath resists extension with a force that is one to two orders of magnitude greater than that developed b the contraction of ampulla muscles. Thus connective tissue plasticity may have an important role during tube foot extension and contraction. In addition, stiffening of the connective tissue may have an important role

CLASS	EXAMPLE	REFERENCE
Crinoidea	Arm & cirri ligaments	MEYER 1971
Asteroidea	Body wall connective tissue	EYLERS 1976a
	Arm autotomy	ANDERSON 1956
Ophiuroidea	Arm ligaments and autotomy	WILKIE 1978a,b 1979
Echinoidea	Spine catch apparatus	TAKAHASHI 1967a,b.
	Pedicellaria valve ligaments	HILGERS & SPLECHTNA 1976
	Tube foot	FLOREY & CAHILL 1977
Holothuroidea	Body wall	JORDAN 1914, 1917
	" "	STOTT et al. 1974
	" "	EYLERS 1976b
	Evisceration response	SMITH & GREENBERG 1973

Table 9

Studies describing the mechano-effector role of connective tissue in Echinodermata.

in tube feet which are extended for long periods of time such as during attachment to the substratum.

Connective tissue plasticity is by no means unique to tube feet and the phenomenon has been investigated in more detail in several other examples. (see Table 9). The role of connective tissue plasticity in autotomy will not be discussed here as it will be the subject of a forthcoming review (WILKIE & EMSON pers. comm.). Investigations of the physiological mechanisms involved in connective tissue plasticity have only recently commenced. EYLERS (1976b) described changes in the mechanical properties of the body wall of Thyone roscovita and observed that reduction in salinity of a bathing medium increased compliance of the body wall (i.e. reduced resistance to stress). EYLERS proposed that the matrix of the body wall, '...is a cross-linked polymeric gel structure with inorganic ions playing a role in the maintenance of viscosity'. The compliance changes in the body wall occurred within 2-5 seconds and thus EYLERS suspected a neuronal control of connective tissue plasticity.

The effects of neurotransmitters on connective tissue compliance changes have been investigated in the spine catch apparatus by TAKAHASHI (1967a,b); adrenaline and noradrenaline induced compliance. A.Ch, 5HT and high K concentrations had an antagonistic effect. In an elegant study of the intervertebral ligaments of Ophiocomina nigra WILKIE (1978a) observed that the mechanical behaviour of the ligament is sensitive to ambient pH and divalent cations. High pH, Ca^{2+} chelation, and high K^{+} concentration produced an abrupt decrease in viscosity of the ligament. Unlike the data of TAKAHASHI (1967b), adrenaline, noradrenaline, A.Ch and 5HT had no effect on the ligament. In addition, GABA, Na-L-glutamate and glycine had no effect. WILKIE observed that removal of the radial nerve did not prevent connective tissue plasticity but the rate of plasticisation was slower. Thus WILKIE postulated, '...that more peripherally located nerve elements are involved'.

From the little data that is available it is apparent that connective tissue plasticity is due to the effects of peripheral neurones modulating cation fluxes within the proteoglycan/glycoprotein matrix. It is probable that calcium ions link adjacent anionic groups of polyanionic molecules (i.e. proteoglycans) thus increasing the viscosity of the connective tissue matrix. In addition, calcium links probably occur between the glycoproteins directly associated with collagen filaments (perhaps via fine lateral filaments?) and matrix proteoglycans. Under certain conditions, the calcium links are chelated thus decreasing intramatrix and matrix-collagen interaction and consequently decreasing the viscosity of the connective tissue. In this way, collagen filaments may flow past each other such that the connective tissue behaves as a viscous fluid.

Echinoderm connective tissue is therefore visco-elastic since it contains two elements: 1) viscosity due to the matrix, and 2) elasticity due to collagen.

The behaviour of visco-elastic materials can be described by two models: 1) the Voigt model where viscous elements act in parallel with elastic elements and 2) the Maxwell model where viscous elements act in series with elastic elements.

In a study of the visco-elastic properties of rat skin, VOGEL (1975) describes an interesting "spring and dashpot" analogy for the Voigt-Maxwell models (spring = elasticity, dashpot = viscosity). Thus, if a load is applied to a dashpot and spring in parallel (i.e. Voigt model) then there is a fixed final strain and strain rate decreases with time. If a load is applied to a dashpot and spring in series (i.e. Maxwell model) then there is no fixed final strain and the strain rate remains constant.

EYLERS (1976b) succintly described the plasticisation of the holothurian body wall as involving, '...a transformation from a Voigt to a Maxwell element'. It is probable therefore that calcium links are necessary for the maintenance of Voigt behaviour.

It is important to emphasise that connective tissue plasticity is due to changes in the collagen-matrix interaction and not changes in the collagen filaments themselves (e.g. due to collagenases). X-ray diffraction, biochemistry, TEM indicate that echinoderm collagen is not unusual and is more similar to vertebrate collagen than other invertebrate collagens (BACCETTI 1967, PUCCI-MINAFRA et al. 1978). In the present study it was observed that collagen filaments which were inserted onto skeletal trabeculae have tapered ends. Similar observations have been described in a study of isolated collagen filaments from holothurian body wall (MATSUMURA 1974) where complete filaments were shown to be 'spindle shaped'.

From the data obtained in this study it is postulated that the LDSG cell described in various regions of the water vascular system is a novel type of peripheral neurone which is implicated in modulating cation fluxes within echinoderm connective tissues and certain types of muscle.

LDSG cells within the connective tissue and musculature are similar in ultrastructure, histochemistry and EM cytochemistry. The ultrastructure of LDSG cells indicates the production of a proteinaceous compound (extensive rough ER, numerous ribosomes and storage granules) and its release by a synaptoid mechanism into the connective tissue matrix or onto adjacent muscle cells. A direct correlation of light microscope histochemistry and EM cytochemistry indicates that LDSGs contain a periodate-reactive, basophilic mucosubstance, probably a glycoprotein. From light microscope histochemistry WILKIE (1979) also proposes that 'juxtaligamental cells' in ophiuroid intervertebral ligament produce a glycoprotein.

The K-Ant method for the cytochemical localisation of cations indicates that LDSG cells (LDSGs & cytoplasm) contain high levels of cations. WILKIE (1979) obtained similar histochemical results with juxtaligamental cells. Energy dispersive X-ray microanalysis confirms the K-Ant data since distinct K and Ca peaks are present in LDSG spectra. It is tempting to postulate that LDSG-calcium is released extracellularly and subsequently affects muscle or connective tissue physiology. However, it is important to consider the role of calcium in excitation secretion coupling (see RUBIN 1974 for review) and that the calcium in LDSGs may be involved in binding the unknown LDSG factor to a carrier molecule, or associated with the secretion of the LDSG factor. (It was observed that calcium was particularly localised in degranulating LDSGs). Calcium has been localised by cytochemistry and X-ray microanalysis in neuroendocrine cells of the rat pars distalis by CRAMER et al. (1978). In the latter study the K-Ant method produced precipitation on elementary neurosecretory granules in a similar manner to LDSGs.

In most descriptions of LDSG-like cells the main consideration has been whether LDSG cells are neurosecretory. The productivity of this line of reasoning seems limited since if it is established that LDSG cells are neurosecretory then this gives no further information as to the mechanisms of LDSG control of connective tissue and muscle physiology. It is more productive to consider:

a) the nature of LDSG factor,

b) its effect on connective tissue and muscle and

c) the relationship between LDSG cells and more central nervous elements.

On the basis of little more than histological and ultrastructural evidence LDSG-like cells have been described as neurosecretory in all classes of Echinodermata (Table 10). As GOLDING (1974) has stated, histophysiological and experimental evidence is necessary to establish the occurrence of

CLASS/SPECIES	TISSUE	GRANULES SIZE	EVIDENCE/REMARKS	REFERENCE
CRINOIDEA				
Florometra seratissima	Chambered organ	-	LM	WELSH 1966
Nemaster rubiginosa	Axial organ	Two classes: 100nm & 200–400nm	TEM. Proposes release of NSM into axial sinus	HOLLAND 1970
-"-	Ovary	50–100nm	TEM. Axons within BEP of ovarian wall*	HOLLAND 1971
ASTEROIDEA				
Marthasterias glacialis	Nerve ring and radial nerve	-	LM	UNGER 1962
Asterias rubens	Hyponeural tissue	100–450nm	TEM	von HEHN 1970
-"-	Axial organ - musc.	100–200nm	TEM	BARGMANN & von HEHN 1968
-"-	Pyloric caecum musc.	120–160nm	TEM	BARGMANN & BEHRENS 1968
-"-	Dermal papulae - musc.	100–300nm	TEM but no pictorial evid.	COBB 1978
Asterias forbesi	Radial nerve	-	LM	UNGER 1962 IMLAY & CHAET 1967
-"-	Coelomic lining and haemal vessel	-	LM	-"-
Asterina gibbosa	Genital tract and gonad wall	Two classes: 100–120nm & 300nm	TEM Axons within BEP*	BRUSLÉ 1969
-"-	Axial organ	100–300nm	TEM Axons within BEP and sinus wall*	LECLERC & DELAVAULT 1971
Asterina stellifera	Longitudinal musculature	100–250nm	TEM EM cytochem. indicates presence of 5HT	DOLDER 1975
Stichaster australis	Brachiolaria larvae-adhesive papillae	60–100nm	TEM Axons within BEP*	BARKER 1978
Coscinasterias calamaria				
Echinaster patiria	Radial nerve	1–2u	LM Granules are rather large?	ATWOOD & SIMON 1971
OPHIUROIDEA				
Ophiopholis aculeata	Disk & arm	-	LM	FONTAINE 1962
Ophiothrix fragilis	Hyponeural tissue	800–200nm	TEM	PENTREATH & COTTRELL 1971
Ophiocomina nigra	Intervertebral ligament	Two classes: Ellipsoid † Circular ††	TEM, LM	WILKIE 1979
Ophioderma panamensis	Pharynx oesophagus		TEM, but LDSGs described as occurring in muscle processes.	SCHLECHTER & LUCERO 1968

† < 750 x 250nm Cells termed 'Juxtaligamental'. †† < 400nm Cells - NSY role proposed.

ECHINOIDEA				
Echinus esculentus	Hyponeural tissue	70–100nm	TEM	COBB & LAVERACK 1966
–"– +	Tube foot connective tissue and musculature	110–200nm	TEM, cells described as 'akin to Mast cells'	FLOREY & CAHILL 1977
S. franciscanus +				
A. lixula				
E. esculentus	Gill musculature	70–150nm	TEM	COBB & SNEDDON 1977
Heliocidaris erythrogramma	Oesophagus-musculature	80–200nm	TEM. Cells described as producing an unknown neuro-transmitter	COBB 1969a
Diadema antillarum	Tube foot musculature	280nm	TEM	COLEMAN 1969b
Hemicentrotus pulcherrimus	–"–	100nm	TEM Cells described as endothelial processes	KAWAGUTI 1964a
–"–	Intestine musculature	100nm	TEM unknown role	KAWAGUTI 1964b
Centrostephanus longispinus	Spine base	100nm	TEM Axons in BEP *	WEBER & GROSMANN 1977
Anthrocidaris crassispina	Spine muscle	?	TEM unknown role	KAWAGUTI & KAMISHIMA 1965
Sphaerechinus granularis	Axial complex: musculature	160nm	TEM	BACHMANN & GOLDSCHMID 1978b
P. miliaris	Axial complex		TEM Axons in BEP of stone canal *	JANGOUX & SCHALTIN 1977
HOLOTHUROIDEA				
Pentacta peterseni	Tube foot musculature	100–250nm	TEM EM cytochemistry indicates presence of 5HT	DOLDER 1975
Cucumaria frondosa	Haemal vessel musculature	300nm	TEM	DOYLE 1967
Parastichopus tiemulus	Dorsal haemal vessel musculature	100–300nm	TEM	JENSEN 1975

Table 10

Survey of literature describing neurosecretory cells or cells similar to LDSG cells.

N.B. BEP – Basiepithelial plexus
NSY – Neurosecretory

* Granules are more likely to be catecholamine storage granules

neurosecretion. It is quite apparent that in many studies, the presence of dense core vesicles in axons is assumed to be indicative of neurosecretion. There is evidence for neurosecretory phenomena in echinoderm reproduction (see review by GOLDING 1974) but little evidence elsewhere in echinoderms. In some reports of elementary neurosecretory granules within the basiepithelial plexus (see Table 10) it is more likely that these represent catecholamine storage granules because of,

a) their smaller size,

b) the presence of an electron lucent halo between core and limiting membrane.

c) histochemical evidence for high concentrations of catecholamines in the basiepithelial plexus (COBB 1969b, PENTREATH and COBB 1972, COBB and RAYMOND in press). Apart from the observations in hyponeural tissue, most other reports of neurosecretory/LDSG cells are in musculature and connective tissue. Although LDSG cells were not described in the body wall of Leptosynapta tenuis by ELDER (1973), it is interesting to note in electromicrograph figure 2d that the "fibrocyte" is remarkably similar to LDSG cells.

It is probable that LDSG cells within echinoderm connective tissue and musculature constitute a nervous element which is quite distinct from the ectoneural and hyponeural nervous systems of echinoderms.

If LDSG cells are peripheral neurosecretory cells then they possess certain similarities to the neurosecretory control of muscle in other animals (SCHLOTE 1963, SILK and SPENCE 1969, OSBORNE et al. 1971, ANWYL and FINLAYSON 1973, PLESCH 1977b).

In contrast to the "neurosecretory school", FLOREY and CAHILL (1977) propose that LDSG cells in tube feet are similar to Mast cells because of their peripheral nature, lack of synaptic input and granule content. However, no other evidence for the presence of Mast cells was provided. The Mast cell is typical of vertebrate connective tissues and two of its characteristic histochemical properties are metachromasia (due to hepain) and 5HT fluorescence (see SELYE 1965 for review and ENERBACK and GUSTAFSSON 1977). From the histochemical data obtained in this study it is quite apparent that LDSG cells are not Mast cells since they do not exhibit metachromasia nor 5HT fluorescence.

Using EM cytochemical methods based upon dichromate methods, DOLDER (1975) localised 5HT in LDSGs from various holothurian tissues. This evidence for 5HT in LDSGs is quite dubious because of the following reasons:

1) no control procedures were used by DOLDER,

2) the lack of specificity of the dichromate methods in echinoderm tissues (present study)

3) the lack of fluorescence histochemical evidence for 5HT in adult echinoderms (COTTRELL & PENTREATH 1970, COBB, 1969, PENTREATH and COBB 1972, present study).

4) the lack of biochemical and pharmacological evidence for 5HT in adult echinoderm tissues (ROBERTSON and JUORIO 1976, JUORIO and ROBERTSON 1977).

The absence of 5HT from adult echinoderm tissues is enigmatic since GUSTAFSSON and his colleagues have substantial histochemical and pharmacological evidence that 5HT plays an important role in echinoderm larval development and motility (GUSTAFSSON & TONEBY 1970, 1971, GUSTAFSSON et al. 1972a,b, RYBERG 1974, TONEBY 1977a,b). The disappearance of 5HT from echinoderm tissues during development is a phenomenon which seems to have escaped the attentions of echinoderm developmental biologists and neurobiologists alike.

In a detailed study of monoamines in Pycnopodia helianthoides, JUORIO and ROBERTSON (1977) detected high concentrations of tryptamine (1251 ng/g in radial nerves, 109 ng/g in tube feet) and made the interesting proposition that in asteroids 5HT is substituted by tryptamine. JUORIO & ROBERTSON also detected various catecholamines (β-phenylethylamine, p-tyramine, m-tyramine, octopamine, dopamine and noradrenaline) within radial nerves and tube feet. It is interesting to note that octopamine occurred in relatively high concentrations in tube feet (157 ng/g) in relation to the radial nerve (260 ng/g). Unfortunately, monoamines such as tryptamine and octopamine do not form fluorophores with paraformaldehyde and thus cannot be localised using the FALCK-HILLARP method. Taking this factor into account, it is possible that the apparent lack of histochemical evidence for monoamines in LDSG cells only indicates the absence of fluorophore-forming monoamines. Assuming that the pharmacology of echinoid tube feet is similar to asteroid tube feet, it is therefore possible that LDSG cells are aminergic and produce a catecholamine such as octopamine or an indoleamine such as tryptamine.

The detection of a glycoprotein within LDSGs thus raises two possibilities: firstly, the glycoprotein is an active factor and LDSG cells are not aminergic (unless they produce more than one neurotransmitter?) and secondly, LDSG cells are aminergic and the glycoprotein functions as a carrier molecule.

Throughout this discussion it has been assumed that LDSG cells are neurones. However, it is possible to make comparisons between LDSG cells and the glio-interstitial system (GIS) of molluscs (see review by NICAISE 1973). The GIS of molluscs has the following characteristics which are similar to LDSG cells:

1) small processes ramifying through musculature and connective tissue,
2) membrane bound electron dense gliosomes (200-600nm, in diameter),
3) infrequent occurrence of somata,
4) microtubules in somata and processes,
5) high levels of cations in gliosomes,
6) presence of glycoprotein in gliosomes.

In contrast, significant differences between the GIS and LDSG cells are:

1) LDSG cells do not have a glial relationship with nervous tissue,

2) LDSGs are smaller than gliosomes,

3) there is little evidence for specialised junctions between LDSG cells and other neurones and muscle cells.

It is probable that LDSG cells have functional similarities to the GIS of molluscs since NICAISE describes evidence for "gliosecretory" activity and proposes that gliointerstitial cells have a humoral/trophic influence on neurones and muscle cells. Similarly, GILLOTEAUX (1975) proposes that the gliointestitial cells do not store cations but are involved in the '...control of ionic and metabolic exchanges between the interstitial spaces and the neural compartment'.

Evidence for gliosecretory activity in vertebrate glial cells is reviewed by ORKAND (1976) and it is interesting to note that PAS positive granules have been described in astrocytes and ependymal cells. The ependymal secretion is implicated in cerebrospinal fluid homeostasis and buffering local ionic changes.

One of the main proposals in this discussion is that LDSG cells regulate cation fluxes in connective tissue plasticity and muscle activity. One of the main weaknesses of this argument is the lack of experimental evidence for connective tissue plasticity in tube feet. Experiments similar to those conducted by WILKIE (1978a) on ophiuroid intervertebral ligament were attempted on tube feet. Unfortunately, the tube foot preparation was inconsistent due to its small size and tissue damage. Isolated, ligatured tube feet were loaded with small weights and bathed in various saline media. Some correlation between rupturing and absence of calcium occurred but in most trials tube feet ruptured at the ligature probably due to tissue damage.

In order to provide some further evidence for the role of LDSG cells in connective tissue plasticity the following investigation was undertaken: was there ultrastructural evidence for LDSG cells in a connective tissue known to exhibit plasticisation, e.g. the spine catch apparatus. Fortunately, LDSG cells do occur within the catch apparatus and form a well developed plexus throughout the connective tissue matrix. The LDSG plexus of the catch apparatus differs from the tube foot in the presence of discrete bundles of LDSG processes and possibly other non-LDSG axons.

Thus LDSG cells occur in connective tissues where there is experimental evidence for plasticisation, i.e. the catch apparatus (TAKAHASI 1967a,b) and ophiuroid intervertebral ligament (WILKIE 1978a, 1979). Further pharmacological and biochemical studies are necessary to fully elucidate the role of LDSG cells in connective tissue and muscle physiology.

Finally, during the present investigation of LDSG cells and cation accumulations it was observed that cations were sequestered within specific sites in tube foot muscle cells. This study provides the first description of calcium storage sites in echinoderm muscle cells. X-ray microanalysis revealed inconsistencies in the K-Ant method (discussed fully by KLEIN et al. 1972 and BURGER & MATHEWS 1978) since not all antimony precipitates were associated with calcium. The apparent lack of sarcoplasmic reticulum in echinoderm muscle and the presence of numerous sarcoplasmic extensions seemed to indicate an increased sarcolemmal area for calcium storage sites as proposed by HILL et al. (1978). However, the combination of cytochemistry and X-ray microanalysis indicates that low levels of calcium occur in the sarcolemma of tube foot muscle cells. Instead, it appears that calcium sequestration is within the membranes of vacuolar and tubular cisternae (subsurface cisternae) occurring subjacent to the sarcolemma.

It is therefore proposed that subsurface cisternae within tube foot muscle cells function as a sarcoplasmic reticulum in the sequestration of calcium for excitation - contraction coupling. Thus in tube foot muscle cells, calcium sequestration occurs in a similar manner to vertebrate skeletal and smooth muscles (see reviews by EBASHI & ENDO 1968, SOMLYO & SOMLYO 1976), and molluscan smooth muscle (SUGI & SUZUKI 1978, SUZUKI & SUGI 1978). Further studies are required to determine whether calcium sequestration occurs in a similar manner in all echinoderm smooth muscles and the striated muscles of echinoid pedicellariae.

Fig. XXIX

Diagrammatic representation of periodate reactive mucosubstances associated with a collagen filament.

C	Collagen
Flf	Fine lateral filament
Oc	Outer coat
Tb	Transverse belt

Dimensions are in nm.

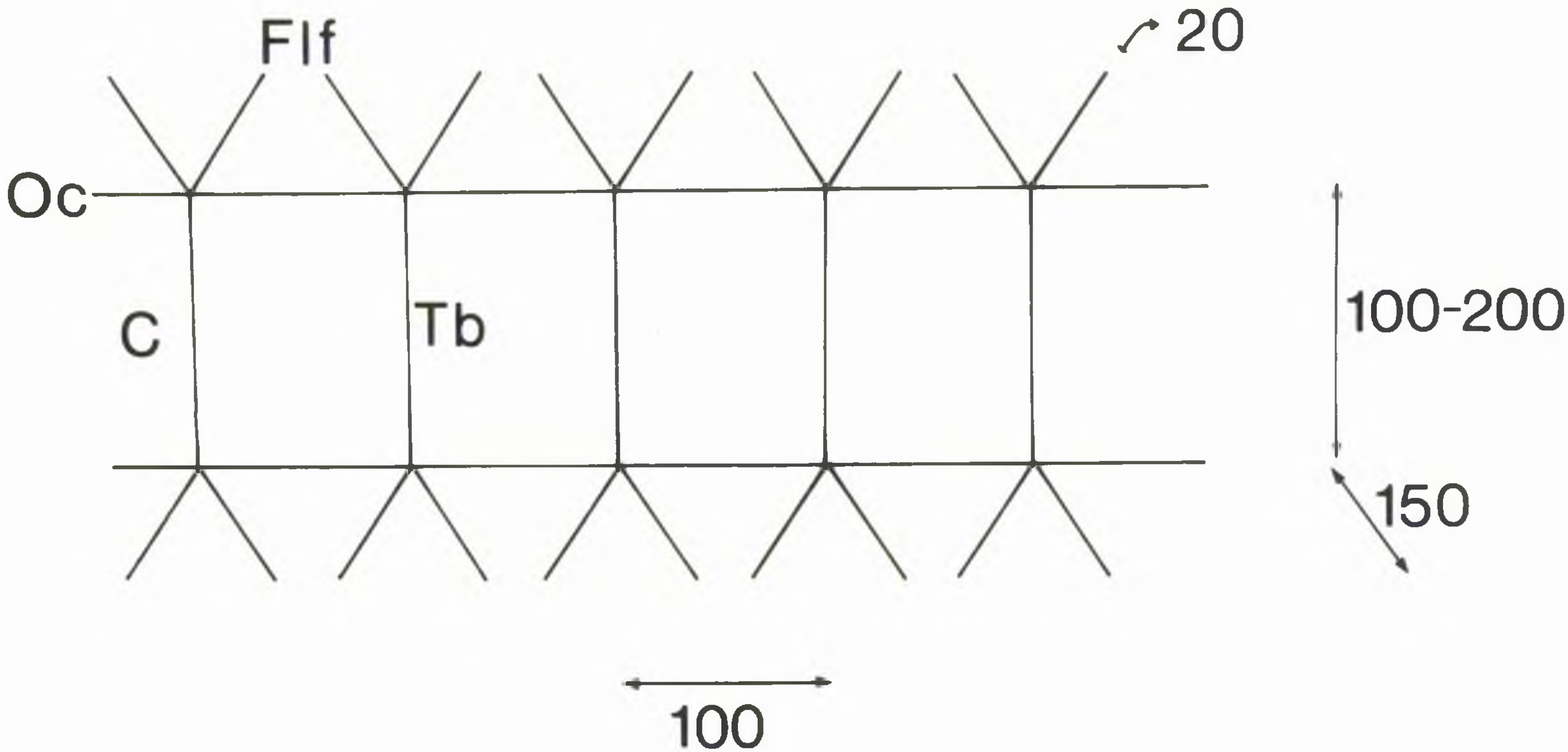

Flf
20
Oc
C
Tb
100-200
150
100

CHAPTER 7

FINALE

THE FINALE

Summary

The main points discussed in this dissertation on the echinoid water vascular system can be summarized as follows:

1. The water vascular system is unique to the phylum Echinodermata and represents a highly modified mesocoel.
2. The relationships between the water vascular system and the mesocoels of other oligomerous phyla are discussed.
3. A comparative SEM study of skeletal structures associated with the water vascular system exhibits that the madreporite and TTF plate shows little structural variation.
4. ATF pore-pair morphology shows a direct correlation with ATF form and function both intraspecifically and interspecifically.
5. PTF plate morphology shows interspecific variation and three basic types of PTF plate have been identified (Uniporous, Anisporous and Isoporous).
6. ATF disk elements consist of a frame and rosette structure which show remarkable modifications of the stereom structure unique to echinoderms.
7. ATF disk elements show little interspecific variation.
8. PTF disks only possess a rosette which shows considerable variation due to reduction in size and number of the component ossicles.
9. The greater development of disk elements in ATF correlates with their role in sucker action
10. The ultrastructure of intrathecal regions of the water vascular system indicates that it is an important organ system for the transport, processing, and removal of amoebocytes and waste material.

11. It is proposed that the madreporite is an excretory structure, providing an exit for the removal of necrotic amoebocytes and other waste products.

12. The innervation of the axial complex, stone canal, and polian vesicles consists of an outer basiepithelial plexus and an inner LDSG plexus (Large Dense Storage Granule-containing cells) which occurs in the musculature and connective tissue.

13. The circumoesophageal water ring and water canals are not muscularized and are only innervated by a basiepithelial plexus.

14. The basiepithelial plexus of the whole water vascular system is catecholaminergic.

15. In addition to an interneuronal function, ultrastructural and histochemical evidence indicates that catecholaminergic axons in the basiepithelial plexus may have a cilio-effector role. Thus, the current-generating choanocyte cells of the epithelia are neurally controlled.

16. The ultrastructure and innervation of the following regions of the tube foot/ampulla complex is described: disk, stem, intraporal region and ampulla.

17. The PTF disk epithelium contains numerous monociliated neurosensory dendrites.

18. Neurosensory somata were identified and sensory axons form synaptoid contacts with basiepithelial axons of the disk. This evidence confirms prior hypotheses regarding the sensory function of PTF.

19. The ATF disk contains fewer neurosensory cells and also differs from the PTF disk in the development of disk levator muscles responsible for sucker action.

20. TEM, histochemistry and EM cytochemistry reveal that the musculature of the tube foot is dually innervated in a rather unusual way.

21. Modified muscle process, termed muscle tails, pass from proximal regions of the tube foot musculature into the perradial pore of the pore-pair. The lateral nerve innervating the tube foot ampulla complex passes through the perradial pore and is separated from the musculature by a thin connective tissue sheath.

22. Motoneurons within the lateral nerve form synaptoid contacts against the connective tissue adjacent to muscle tails.

23. Neurone somata of two types (one aminergic, one non-aminergic, probably cholinergic) were identified within the intraporal region of the lateral nerve. Neurone somata (apart from neurosensory cells) do not occur within the tube foot nerve.

24. It is therefore proposed that the intraporal region of the lateral nerve is tube foot/ampulla ganglion which are responsible for central control of the tube foot ampulla complex.

25. Central innervation via muscle tails only occurs within a discrete region at the base of the tube foot. Throughout the stem and disk the musculature is peripherally innervated by LDSG cells.

26. It is proposed that LDSG cells are a novel type of neurone which regulate cation fluxes within some connective tissues and muscle cells.

27. It is proposed that the nervous system of echinoderms thus consists of ectoneural, hyponeural and LDSG elements.

28. Histochemistry, EM cytochemistry and X-ray microanalysis indicates that LDSG cells contain a periodate-reactive mucosubstance (probably a glycoprotein) and high levels of calcium and potassium.

29. Various hypotheses for the nature of LDSG cells and LDSG factor are discussed.

30. It is proposed that LDSG cells are involved in connective tissue plasticisation, a phenomenon which is unusually well developed in echinoderms.

31. The ultrastructure of the musculature of the tube foot/ampulla complex indicates that stem retractor muscles differ from ampulla and disk levator muscles and these differences correlate with functional differences such as range, speed of contraction and endurance.

32. EM Cytochemistry and X-ray microanalysis indicate that stem retractor muscles sequester calcium in subsurface cisternae and not the sarcolemma. It is proposed that the subsurface cisternae constitute a functional sarcoplasmic reticulum.

33. Histochemistry and EM Cytochemistry indicate that tube foot collagen is associated with glycoproteins similar to vertebrate collagen and is embedded in a matrix composed of sulphated proteoglycans.

Suggestions for further work

Throughout the course of this present investigation it is hoped that some questions regarding the structure and function of an organ system unique to echinoderms may have been answered. However, many questions remain unanswered and most answers have created more questions.

Some of the more important questions which perhaps deserve further investigation can be summarised as follows:

1. What factors control the development of the stereom? Although the basic organisation of the stereom is similar in all structures, differences in the diameter of skeletal trabeculae, arrangement of trabeculae and pore spaces confer different physical properties to the structure. Possible systems for investigation are spine tubercles, pedicellariae or the madreporite.

2. The mechanism of skeletal resorption is unknown and yet it is an important factor in skeletal development and the turnover of calcium.

3. The role of tube feet in respiration requires detailed physiological examination and comparisons of respiration rate between extended/contracted tube feet and tube feet in various regions of an ambulacrum is necessary.

4. The excretory role of the madreporite could be investigated by a variety of methods such as:

  a) injecting radiolabelled compounds into the axial organ and determining whether they pass through the madreporite,

  b) following the passage of ferritin-labelled amoebocytes through the axial complex and determining whether they are ejected via the madreporite.

  c) measuring the composition of fluid in madreporic canals in relation to water vascular fluid.

5. The role of tube feet in maintaining hydrostatic pressure within the water vascular system needs further investigation. It may be possible to turn large tube feet inside-out and thus measure K^+ fluxes into a bathing medium.

6. The probable neural control of ciliary activity in the water canal epithelia needs further pharmacological and electrophysiological investigation.

7. The bioadhesive secreted by the tube foot disk has only been characterised by histochemical methods. A biochemical study may identify a compound which is unique to echinoderms and has unusual properties.

8. The bioadhesive of the tube foot disk hindered an SEM study of sensory cilia. It is possible that more recently developed mucolytics such as n-acetyl-cysteine may remove the bioadhesive and thus morphology and distribution of sensory cilia could be investigated.

9. Tactoid isolation, SDS-gel electrophoresis, and immunodiffusion are necessary in order to determine the presence of paramyosin in tube foot/ampulla musculature.

10. Estimates of isolated thick filament lengths from ampulla, stem retractor and disk levator muscles are necessary since estimates from ultrastructure alone are inaccurate.

11. The proposition that tube foot stem retractors are functionally different to ampulla muscles requires further investigation such as measurements of maximum force generation and endurance.

12. The role of LDSG cells in echinoderm connective tissue and muscle physiology is enigmatic and could be investigated using a suitable preparation.

It is interesting to note that: a) high proportions of LDSG cells have been found in Holothurian haemal tissue (DOYLE 1967), and b) extracts of the haemal tissue of Sclerodactyla briareus contain a plasticising factor which also has a potent effect on pharyngeal retractor muscles by producing tonic contractions (SMITH & GREENBERG 1973).

Holothurians thus appear to provide a suitable preparation for an investigation of the role of LDSG cells. They show a variety of behavioural responses which show connective tissue plasticity changes, e.g. evisceration, Cuverian tubule ejection and body wall softening during locomotion.

The production of plasticising agent by LDSG cells could be determined by:

a) obtaining haemal extracts and a LDSG rich fraction using density gradient ultracentrifugation and TEM.

b) assaying the LDSG rich fraction in various preparations suspected of showing plasticity changes.

c) investigating whether high proportions of LDSG cells correlate with high levels of plasticising factor.

The role of LDSG cells in controlling muscle physiology could be determined by:

a) investigating the effect of LDSG rich fractions on pharyngeal retractor muscle and longitudinal retractor muscle preparations.

b) investigating the effect of various ions such as Ca^{2+}, Mg^{2+} and Na^{+} on any LDSG mediated response.

c) investigating the effect of cholinomimetics, A.Ch. and monoamines on any LDSG mediated response.

The nature of 'LDSG factor' may be determined by biochemical analysis of LDSG rich fractions for monoamines, glycoproteins and peptides. A further understanding of the role of LDSG cells in connective tissue and muscle physiology may have important implications in medical research since changes in the viscosity and behaviour of human connective tissues have been reported. For instance, during pregnancy the connective tissue of the reproductive tract and pelvic girdle alters in extensibility (see review by JACKSON & BENTLEY 1968). Also, a pathological condition of the skin, termed Ehlers-Danlos syndrome is characterised by extraordinary elasticity due to changes in the matrix.

It is probable that connective tissue plasticity is not unique to echinoderms and may represent a primitive feature of all connective tissues which is particularly exploited by the echinoderms.

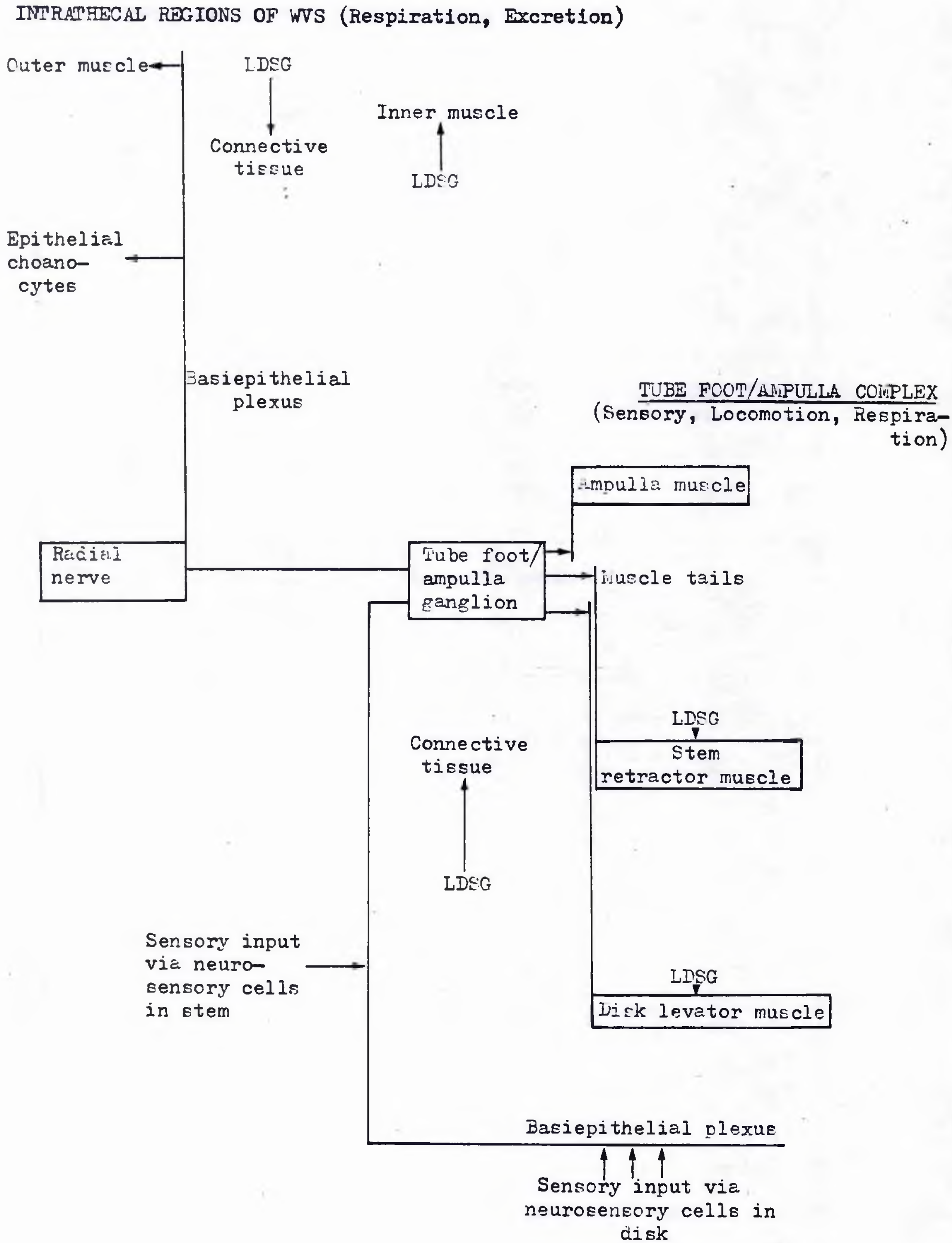

Fig. XXX

Diagrammatic representation of the innervation of the water vascular system

Conclusion

The introduction to this dissertation stated that the water vascular system has been accredited with a variety of functions including respiration, locomotion and sensory capacity.

In order to provide an understanding of these functions the innervation of the water vascular system (see Fig. XXX) was investigated. Evidence for the neural control of muscle, connective tissue and ciliary respiratory activity is described.

Hypotheses for the sensory capacity of the water vascular system are corroborated by the description of neurosensory cells within the tube foot and evidence for their input with the ectoneural nervous system.

The structure/function relationships of skeletal structures and musculature within the water vascular system are discussed.

Finally, it is proposed that the water vascular system also has an important excretory function in the transport, processing and elimination of amoebocytes.

BIBLIOGRAPHY

AIELLO, E. 1960. Factors affecting ciliary activity in the gill of the mussel, Mytilus edulis. Physiol. Zool. 33, 120-135.

AIELLO, E.L. 1974. Control of ciliary activity in metazoa. In Cilia and Flagella (M.A. Sleigh, Ed.) pp 353-378. Academic Press, London.

AIELLO, E.L. & GUIDERI, G. 1965. Distribution and function of the branchial nerve in the mussel. Biol. Bull. 129, 431-438.

AINSWORTH, S.K., ITO, S. & KARNOVSKY, M.J. 1972. Alkaline Bismuth reagent for high resolution ultrastructural demonstration of Periodate reactive sites. J. Histochem. Cytochem. 20, 995-1005.

ANDERSON, J.M. 1956. Observations on autotomy in the starfish, Asterias forbesi. Biol. Bull. 111, 297.

ANWYL, R. & FINLAYSON, L.H. 1973. The ultrastructure of neurons with both motor and a neurosecretory function in the insect, Rhodnius prolixus. Z. Zellforsch. 146, 367-374.

ATWOOD, D.G. 1973a. Ultrastructure of the gonadal wall of the Sea Cucumber, Leptosynapta clarki (Echinodermata. Holothuroidea). Z. Zellforsch. 141, 319-330.

ATWOOD, D.G. 1973b. Correlation of gamete shedding with presence of Neurosecretory gametes in Asteroids (Echinodermata). Gen. Comp. Endocr. 20, 347-350.

ATWOOD, D.G. & SIMON, J.L. 1971. Correlation of gamete shedding with presence of neurosecretory gametes in Echinaster and Patiria (Echinodermata; Asteroidea). Am. Zool. 11, 701-702.

ATWOOD, H.L., SMYTH, T., and JOHNSTON, H.S. 1967. Neuromuscular synapses in cockroach extensor tibiae muscle. J. Insect Physiol. 15, 529-535.

BACCETTI, B. 1967. High resolutions on collagen of echinodermata. Monitore Zool. Ital. (N.S.), 1, 201-206.

BACCETTI, B. & ROSATI, F. 1968a. The fine structure of the polian vesicles of holothurians. Z. Zellforsch., 90, 148-160.

BACCETTI, B., & ROSATI, F. 1968b. On the thick filaments of Holothurian muscles. J. Microscopic., 7, 455-458.

BACHMANN, S., & GOLDSCHMID, A. 1978a. Fine structure of the axial complex of Sphaerechinus granularis (Lam.) (Echinodermata: Echinoidea). Cell Tiss. Res. 193, 107-123.

BACHMANN, S. & GOLDSCHMID, A. 1978b. Ultrastructural, Fluorescence microscopic and microfluorimetric study of the innervation of the Axial complex in the Sea Urchin Sphaerechinus granularis (Lam.). Cell Tiss. Res., 194, 315-326.

BARANY, M. 1967. ATPase activity of myosin correlated with speed of muscle shortening. J. Gen. Physiol., 50, 197-218.

BARGMANN, W., von HARNACK, M. & JACOB, Y. 1962. Über den feinbau des nervensystems des seesterns (*Asterias rubens* L.). I. Mitteilung ein beitrag zur vergleichenden morfologie der glia. Z. Zellforsch., 56, 333-345.

BARGMANN, W. & BEHRENS, Br. 1963. Über den feinbau des nervensystems des seesterns (*Asterias rubens* L.). II. Mitt. (Zur frage des baues und der innervation der ampullen). Z. Zellforsch., 59, 746-770.

BARGMANN, W. & BEHRENS, B. 1964. Über die Tiedemannschen Organe des Seesternes (*Asterias rubens* L.). Z. Zellforsch., 63, 120-133.

BARGMANN, W. & BEHRENS, Br. 1968. Über die Pylorusanhänge des Seesternes (*Asterias rubens* L.), insbesondere ihre Innervation. Z. Zellforsch., 84, 536-584.

BARGMANN, W. & von HEHN, G. 1968. Über des Axialorgan (mysterious gland) von *Asterias rubens*. Z. Zellforsch. Mikrosk. Anat., 88, 262-277.

BARKER, M.F. 1978. Structure of the organs of attachment of brachiolaria larvae of *Stichaster australis* (Verrill) and *Coscinasterias calamaria* (Gray) (Echinodermata: Asteroidea). J. exp. mar. Biol. Ecol. 33, 1-36.

BARNES, R.D. 1968. Invertebrate Zoology. W.B. Saunders Co. London.

BASKIN, D.G. 1971a. The fine structure of neuroglia in the central nervous system of nereid polychaetes. Z. Zellforsch. 119, 295-308.

BASKIN, D.G. 1971b. Fine structure, functional organization and supportive role of neuroglia in *Nereis*. Tissue & Cell 3, 579-588.

DeBELL, J.T. 1965. A long look at neuromuscular junctions in nematodes. Quart. Rev. Biol. 40, 233-251.

BEVELANDER, G. & NAKAHARA, H. 1960. Development of the skeleton of the sand dollar (*Echinarachnius parma*). Publ. Amer. Assoc. Adv. Sci. 64, 41-56.

BINYON, J. 1964. On the mode of functioning of the water vascular system of the starfish *Asterias rubens* L. J. mar. biol. Ass. U.K., 44, 577-588.

BINYON, J. 1972. Physiology of Echinoderms. Pergamon Press, Oxford.

BINYON, J. 1976. The permeability of the asteroid podial wall to water and potassium ions. J. mar. biol. Ass. U.K., 56, 639-647.

BINYON, J. 1978. Some observations upon the chemical composition of the starfish *Asterias rubens* L., with particular reference to strontium uptake. J. mar. biol. Ass. U.K., 58, 441-449.

BINYON, J. 1979. Ion movements and oxygen requirements of Asteroids - a theoretical consideration. Comp. Biochem. Physiol. 62A, 639-640.

BINYON, J. & HASLER, B. 1970. Electrophysiology of the starfish radial nerve cord. Comp. Biochem. Physiol., 32, 747-753.

BLOOM, W. and FAWCETT, D.W. 1968. A textbook of histology (9th Edn.). W.B. Saunders Co. London.

BOOLOOTIAN, R.A. & CAMPBELL, J.L. 1964. A primitive heart in the echinoid Strongylocentrotus purpuratus. Science 145, 173-175.

BRUSLÉ, J. 1969. Aspects ultrastructuraux de l'innervation des gonads chez l'ectoile de mer Asterina gibbosa. Z. Zellforsch Mikrosk. Anat., 98, 88-89.

BUCHAMAN, J.B. 1962. A re-examination of the glandular elements in the tube feet and some common British Ophiuroids. Proc. Zool. Soc. London, 138, 645-650.

BUCHANAN, J.B. 1966. The Biology of Echinocardium cordatum (Echinodermata Spatangoidea) from different habits. J. Mar. biol. Ass. U.K., 46, 97-114.

BUCHANAN, J.B. & WOODLEY, J.D. 1963. Extension and retraction of the tube feet of ophiuroids. Nature 197, 616-617.

BULGER, R.E. 1969. The use of potassium pyroantimonate in the localisation of sodium ions in rat kidney tissue. J. Cell. Biol., 40, 79-94.

BURGER, E.H. & MATHEWS, J.L. 1978. Cellular calcium distribution in foetal bones studied with Potassium pyroantimonate. Calcif. Tiss. Res. 26, 181-190.

BURKE, R.D. 1978 . The structure of the nervous system of the pluteus larva of Strongylocentrotus purpuratus. Cell Tiss. Res. 191, 233-247.

BURTON, M.P.M. 1964. Haemal system of regular echinoids. Nature, 204, 1218.

CAMPBELL, A.C; DART, J.K.G; HEAD, S.M. and ORMOND, R.F.G. 1973. The feeding activity of Echinostrephus molaris (de Blanville) in the central Red Sea. Mar. Behav. Physiol. 2, 155-169.

CHAET, A.B. & PHILPOTT, D.E. 1960. Secretory structures in the tube foot of starfish. Biol. Bull., 119, 308-309.

CHAET, A.B. & PHILPOTT, D.E. 1964. A new subcellular particle secreted by the starfish. J. Ult. Res., 11, 354-362.

CHANG, S.C. 1972. Haematoxyglin-Eosin staining of plastic embedded tissue sections. Arch. Pathol. 93, 344-351.

CHIA, F.S. 1969a. Histology of the globiferous pedicellariae of Psammechinus miliaris (Echinodermata Echinoidea). J. Zool. 160, 9-16.

CHIA, F.S. 1969b. Some observations on the locomotion feeding of the sand dollar Dendraster excentricus (Eschscholtz). J. exp. mar. Biol. Ecol., 3, 162-170.

CHIA, F.S. 1975. Selection and elimination of heavy sand particles in juvenile sand dollars. Am. Zool. 15, 789.

CHIEN, P. and KOOPOWITZ, H. 1972. The ultrastructure of neuromuscular systems in Notoplana acticola, a free-living polyclad flatworm. Z. Zellforsch. 133, 277-288.

CLARK, R.B. 1964. Dynamics in metazoan evolution. Clarendon Press, Oxford.

COBB, J.L.S. 1967. The innervation of the ampulla of the tube foot in the starfish Astropecten irregularis. Proc. Roy. Soc., B., 168, 91-99.

COBB, J.L.S. 1968a. The fine structure of the pedicellariae of Echinus esculentus (L.). I. The innervation of the muscles. J.R. Micr. Soc., 88, 211-221.

COBB,J.L.S. 1968b. The fine structure of the pedicellariae of Echinus esculentus (L.). II. The sensory system. J.R. Micr. Soc., 88, 223-233.

COBB,J.L.S. 1969a. The innervation of the oesophagus of the sea urchin Heliocidaris erythrogramma. J. Zellforsch. 98, 323-332.

COBB,J.L.S. 1969b. The distribution of mono-amines in the nervous system of echinoderms. Comp. Biochem. Physiol. 28, 967-971.

COBB,J.L.S. 1970. The significance of the radial nerve cords in Asteroids and Echinoids. Z. Zellforsch. 108,457-474.

COBB,J.L.S. 1978. An ultrastructural study of the dermal papulae of the starfish Asterias rubens with special reference to innervation of the muscles. Cell. Tiss. Res. 187, 515-523.

COBB,J.L.S. & LAVERACK,M.S. 1966. The lantern of Echinus esculentus (L.)
a) I Gross anatomy and physiology 624-640
b) II Fine structure of hyponeural tissue and its connections 641-650
c) III The fine structure of the lantern retractor muscle and its innervation 651-658.
Proc. Roy. Soc. (B), 164, pp as above.

COBB,J.L.S. & LAVERACK,M.S. 1967. Neuromuscular systems in Echinoderms. Symp. Zool. Soc. Lond. 20, 25-51.

COBB,J.L.S. & PENTREATH,V.W. 1976. The identification of chemical synapses in echinoderm nervous systems. Thalassia Jugoslavia 12, 81-85.

COBB,J.L.S. & RAYMOND,A.M. 1979. The basiepithelial nerve plexus of the viscera and coelom of Eleutherozoan Echinodermata. Cell Tiss. Res. 202, 155-163.

COBB,J.L.S. & SNEDDON,E. 1977. An ultrastructural study of the gills of Echinus esculentus. Cell Tiss. Res. 182, 265-274.

COGGESHALL,R.E. 1971. A possible sensory-motor neuron in Aplysia californica. Tissue and Cell 3, 637-648.

COLEMAN,R. 1969a. Ultrastructure of the tube foot sucker of a regular echinoid Diadema antillarum, Philippi. A. Zellforsch., 96, 162-172.

CORRODI,H., HILLARP,N.A. & JONSSON,G. 1964. Fluorescence methods for the histochemical demonstration of monoamines. 3. Sodium borohydride reduction of the fluorescent compounds as a specificity test. J. Histochem. Cytochem. 12, 582-586.

COTTRELL,G.A. & PENTREATH,V.W. (1970). Localisation of catecholamines in the nervous system of a starfish, Asterias rubens, and of a brittlestar, Ophiothrix fragilis. Comp. gen. Pharmac. 1, 73-81.

COWDEN,R.R. & CURTIS,S.K. 1970. Demonstration of protein bound sulphydyl and disulphide groups with Fluorescent mercurials. Histochemie 22, 247-255.

CRAMER,E.B., CARDASIS,C., PEREIRA,G., MILKS,L. & FORD,D. 1978. Ultrastructural localization of cations in the rat Pars distalis under various experimental conditions. Neuroendochrinology 26, 72-84.

DANNEEL,S. & WEISSENFELS,N. 1965. Besseres fixierungsverfahren zur Darstellung des grun plasmas von protozoen und Vertebratenzellen. Mikroskopie. 20, 89-93.

DAVIES,T.T., CRENSHAW,M.A., HEATFIELD,B.M. 1972. The effect of temperature on the chemistry and structure of echinoid spine regeneration. J. Palaeont. 46, 874-883.

DIETRICH,H.F. & FONTAINE,A.R. 1975. A decalcification method for the ultrastructure of echinoderm tissues. Stain Technol. 50, 351-354.

DOLDER,H. 1972. Ultrastructural study of the smooth muscle in the tube feet of the echinoderms, Asterina stellifera and Pentacta peterseni. J. Submicr. Cytol. 4, 221-232.

DOLDER,H. 1975. An ultrastructural and cytochemical study of neuromuscular junctions in Echinoderms. Histochemistry 44, 313-322.

DOYLE,W.L. 1967. Vesiculated axons in haemal vessels of an holothurian Cucumaria frondosa. Biol. Bull. 132, 329-336.

Du BUY,H.G. 1936. Separation of the conducting and contractile elements in the retractor muscle of Thyone briareus. Biol. Bull. 71, 408-409.

DURHAM,J.W. & MELVILLE,R.V. 1966. Classification of the echinoids. Treatise on Invertebrate Palaeontology (R.C. Moore, Ed.) Part II Echinodermata Vol. 3, University of Kansas.

ENGSTER,M.S. & BROWN,S.C. 1972. Histology and ultrastructure of the tube foot epithelium in the Phanerozonian starfish Astropecten. Tissue & Cell. 4, 503-518.

EYLERS,J.P. 1976a. Aspects of skeletal mechanics of the starfish Asterias forbesi. J. Morph. 149, 353-368.

EYLERS,J.P. 1976b. Mechanical properties of holothurian body wall. Thalassia Jugoslavica 12, 111-115.

FALCK,B., HILLARP,N-A., THIEME,G. & TORP,A. 1962. Fluorescence of catecholamines and related compounds condensed with formaldehyde. J. Histochem. Cytochem. 10, 348-354.

FANGE,R. 1969. Pharmacology of echinoderms. In 'Chemical Zoology' (Florkin,M. & Scheer,B.T. Eds.). Vol. III, pp 207-219. Academic Press, New York.

FARMANFARMAIAN,A. 1966. The respiratory physiology of echinoderms. In 'Physiology of Echinodermata'. (R.A. Boolootian, Ed.). pp 245-266. Interscience: New York.

FECHTER,H. 1965. Uber die funktion der Madreporen platte der Echinoidea. Z. vergl. Physiol. 51, 227-257.

FELL,H.B. 1948. Echinoderm embryology and the origin of chordates. Biol. Rev. 23, 81-107.

FELL,H.B. 1962. The evolution of the Echinoderms. Annu. Rep. Smith Inst., 1962, 457-490.

FENNER,D. 1973. The respiratory adaptations of the podia and ampullae of Echinoids (Echinodermata). Biol. Bull. 145, 323-339.

FERGUSON,J.C. 1967. An autoradiographic study of the utilization of free exogenous amino acids by starfishes. Biol. Bull. 133, 317-329.

FERGUSON,J.C. 1969. Feeding activity in Echinaster and its induction with dissolved nutrients. Biol. Bull. 136, 374-384.

FLOOD,P.R. 1966. A peculiar mode of innervation in Amphioxus. Light and electron microscopic studies of the so-called ventral roots. J. Comp. Neur. 126, 181-217.

FLOREY,E. 1974. Nervous control of smooth muscle in the absence of synaptic junctions. Abstract XXVI. Int. Congr. Physiol. Sci. New Delhi.

FLOREY,E. & CAHILL,M.A. 1977. Ultrastructure of Sea-Urchin tube feet. Cell Tiss. Res. 177, 195-214.

FLOREY,E., CAHILL,M.A. & RATHMAYER,M. 1975. Excitatory actions of GABA and of A.Ch. in sea urchin tube feet. Comp. Biochem. Physiol. 51C, 5-12.

FONTAINE,A.R. (1962). Neurosecretion in the Ophiuroid Ophiopholis aculeata, Science, 138, 908-9.

FONTAINE,A.R. & CHIA,F.S. 1968. Echinoderms: An autoradiographic study of Assimilation of dissolved organic molecules. Science, 161,1153-1155.

FORSTER,G.R. 1959. The ecology of Echinus esculentus. Quantitative distribution and rate of feeding. J. Mar. biol. Ass. U.K., 38, 361-367.

FRANKE,W.W., KRIEN,S. & BROWN,R.M. 1969. Simultaneous glutaraldehyde-osmium tetroxide fixation with post osmication. Histochemie., 19, 162-164.

FREEMAN,W.P. & SIMON,S.E. 1964 The histology of holothuroidean muscle. J. cell. comp. Physiol. 63, 25-38.

FUJI,A. 1962. Studies on the biology of the Sea-Urchin V. Food consumption of Strongylocentrotus intermedius. Jap. J. Ecol. 12, 181-186.

FUXE,K. & JONSSON,G. 1967. A modification of the histochemical fluorescence method for the improved localization of 5-hydroxytryptamine. Histochemie. 11, 161-166.

GABE,M. 1966. Neurosecretion. Pergamon Press, London.

GARRONE,R. 1978. Frontiers of matrix biology Vol. 5 Phylogenesis of connective tissue. Morphological aspects and biosynthesis of sponge intercellular matrix. S. Karger. (ISBN 3-8055-2767-5).

GEDDES,P. & BEDDARD,F.E. 1881. Sur l'histologie des pedicellaires et des muscles de l'oursin (Echinus sphaera Forbes). C.R. Acad. Paris, XCII, 308-310.

GEMMILL,J.F. 1914. The development and certain points in the adult structure of the starfish Asterias rubens L. Phil. Trans. R. Soc. (B). 205, 213-294.

GILLOTEAUX,J. 1975. Innervation of the anterior byssal retractor muscle in Mytilus edulis L. II. Ultrastructure of the glio-interstitial cells. Cell Tiss. Res., 161, 511-579.

GISLEN,T. 1924. Echinoderm studies. Zool. Bridr. Uppsala, 9, 1-316.

GOLDING,D.W. 1974. A survey of neuroendocrine phenomena in non-arthropod intertebrates. Biol. Rev. 49, 161-224.

GOMORI,G. 1941. Observations with differential stains in human islets of Langerhans. Amer. J. Path. 17, 395-406.

GOODBODY, I. 1960. The feeding mechanism in the sand dollar (Mellita sexiesperforata (Leske). Biol. Bull., 119, 80-86.

GORDON, I. 1926a. The development of the calcareous test of Echinus miliaris. Phil. Trans. Roy. Soc. B. 214, 259-312.

GORDON, I. 1926b. The development of the calcareous test of Echinocardium cordatum. Phil. Trans. Roy. Soc. B., 215, 255-313.

GORDON, I. 1929. Skeletal development in Arbacia, Echinarachnius and Leptasterias. Phil. Trans. Roy. Soc. B., 217, 289-334.

GRIMSTONE, A.V. & SKAER, R.J. 1972. A guidebook to microscopical. methods. Cambridge, University Press.

GUSTAFSSON, T. & TONEBY, M. 1970. On the role of serotonin and acetylcholine in sea urchin morphogenesis. Exp. Cell. Res. 62, 102-117.

GUSTAFSSON, T., LUNDGREN, B., TREUFELDT, R. 1972. Serotonin and contractile activity in the echinopluteus. Exp. Cell Res. 72, 115-139.

GUSTAFSSON, T. & TONEBY, M. 1971. How genes control morphogenesis. Am. Scient. 59, 452-462.

GUSTAFSSON, T., RYBERG, G. & TREUFELDT, R. 1972b. Acetylcholine and contractile activity in the echinopluteus. Acta Embryol. Exp. 2, 199-223.

HÅKANSON, R., OWMAN, C.H., SPORRONG, B. & SUNDLER, R. 1971. Electron microscopic classification of amine-producing endocrine cells by selective staining of ultrathin sections. Histochemie, 27, 226-242.

HÅKANSON, R., LARSSON, L-I & SUNDLER, F. 1974. Fluorescamine. A novel reagent for the histochemical detection of amino groups. Histochemistry, 39, 15-23.

HAMORI, J. 1963. Electron microscope studies of neuromuscular junctions of endplate type in insects. Acta. biol. Acad. Sci. Hung. 14, 231-245.

HARRISON, G. & PHILPOTT, D. 1966. Subcellular particles in Echinoderm tube feet. J. Ult. Res. 16, 537-547.

HAYAT, M.A. 1970. Principles and Techniques of electron microscopy biological applications. Van Nost. Reinhold, Amsterdam.

HEATFIELD, B.M. & TRAVIS, D.F. 1975. Ultrastructural studies of regenerating spines of the sea urchin Strongylocentrotus purpuratus. Cell types with spherules. J. Morph. 145, 51-72.

HEHN,G. von. 1970. Über den feinbau des hyponeuralen nervensystems des seesternes (Asterias rubens L.). Z. Zellforsch. 105, 137-154.

HIGHNAM,K.C. & HILL,L. 1977. The comparative endocrinology of the Invertebrates. 2nd Edition. Edward Arnold, Lon.

HILGERS, H. & SPLECHTNA, H. 1976. Struktur-und Funktionanalyse ophiocephaler pedizellarien von Sphaerechinus granularis Lam., Echinus acutus Lam., und Paracentrotus lividus Lam. (Echinodermata, Echinoidea). Zoomorphologie 86, 61-80.

HILL,R.B. 1970. Effects of some postulated neurohormones on rhythmicity of the isolated cloaca of a holothurian. Physiol. Zool. 43, 109-123.

HILL,R.B., SANGER,J.W., YANTORNO,R.E. & DEUTSCH,C. 1978. Contraction in a muscle with negligible sarcoplasmic reticulum: The longitudinal retractor of the sea cucumber Isostichopus badionotus (Selenka), Holothuria Aspidochirota. J. exp. Zool. 206, 137-150.

HIRSCH,J.G. & FEDORKO,M.E. 1968. Ultrastructure of human leukocytes after simultaneous fixation with glutaraldehyde and Osmium tetroxide and 'post fixation' in Uranylacetate. J. Cell Biol., 38, 615-627.

HOLLAND,L.Z. & HOLLAND,N.D. 1975. The fine structure of epidermal glands of regenerating and mature globiferous pedicellariae of a sea urchin (Lytechinus pictus). Tissue and Cell, 7, 723-737.

HOLLAND,N.D. 1969. An electron misroscopic study of the papillae of crinoid tube feet. Publ. Staz. Zool. Napoli, 37, 575-580.

HOLLAND,N.D. 1970. The fine structure of the axial organ of the feather star Nemaster rubiginosa. (Ech: Crin.). Tissue & Cell, 2, 625-636.

HOLLAND,N.D. 1971. The fine structure of the ovary of the feather star Nemaster rubiginosa (Ech: Crin.). Tissue & Cell, 3, 161-175.

HOLLAND,N.D. 1976. The fine structure of the embryo during the gastrule stage of Comanthus japonica (Echinodermata: Crinoidea). Tissue & Cell, 8, 491-510.

HUMASON,G.L. 1972. Animal Tissue Techniques. W.H. Freeman, San Francisco.

HUNT,S. 1970. Polysaccharide protein complexes in invertebrates. Academic Press.

HUXLEY,H.E. 1966. The fine structure of striated muscle and its functional significance. Harvey Lecture Series 60, 85-118.

HYMAN,L.H. 1955. The Invertebrates. Vol. IV Echinodermata. McGraw Hill, New York.

IMLAY,M.J. & CHAET,A.B. 1967. Microscopic observations of gamete shedding substance in starfish radial nerves. Trans. Amer. Microsc. Soc. 86, 120-126.

IMMERS,I., LUNDGREN,B. 1972. Aspects of differentiation and function of cilia and adjacent structures of the sea urchin larva. Acta. Embryo. Exp. 2, 177-197.

JACKSON,D.S. & BENTLEY,J.P. 1968. Collagen-Glycosaminoglycan interactions. In: Treatise on collagen Vol. 2. Biology of Collagen (Ed. B.S. Gould) Part A. Academic Press, London.

JANGOUX,M. & SCHALTIN,P. 1977. Le complexe axial de Psammechinus miliaris (Gmelin) (Echinodermata, Echinoidea). Arch. Zool. exp. gen. 118, 285-303.

JENSEN,H. 1975. Ultrastructure of the Dorsal Haemal Vessel in Sea Cucumber Parastichopus tremulus (Echinodermata: Holothuroidea). Cell Tiss. Res. 160, 355-369.

JENSEN,M. 1972. The ultrastructure of the echinoid skeleton. Sarsia, 48, 39-48.

JENSEN,M. 1974. The Strongylocentrotidae (Echinoidea), a morphologic and systematic study. Sargia, 57, 113-148.

JORDAN,H. 1914. Über 'reflexarme' Fiere. IV. Die Holothurien. Mitteil. Die Holothurien also hohlorganartige Tiere und die Tonusfunktion ihrer Muskulatur. Zool. Jahrb. Abt. 3. 34, 365-436.

JORDAN,H. 1919. Über reflexarme Tiere IV. Die Holothurien. 2. Mitteil. Die Reizbarkeit und Einfluss des zentral Nervensystems suf die Muskulatur und die muskelähnlichen Fasern der Haut (auf Erregbarkeit und Tonusfunktion). Zool. Jahrb., Abt. 3, 36, 109-156.

JOSEPHSON,R.K. 1975. Extensive and intensive factors determining the performance of striated muscles. J. exp. Zool. 194, 135-154.

JUORIO,A.V. & ROBERTSON,H.A. 1977. Identification and distribution of some monoamines in tissues of the sunflower star, Pycnopodia helianthoides (Echinodermata). J. Neurochem. 28 (573-579).

KAWAGUTI,S. 1964a. Electron microscopic structures of the podial wall of an Echinoid with special reference to the nerve plexus and the muscle. Biol. J. Okayama Univ., 10, 1-12.

KAWAGUTI,S. 1964b. Electron microscopy on the intestinal wall of the Sea-Cucumber with special attention to its muscle and nerve plexus. Biol. J. Okayama Univ. 10, 39-50.

KAWAGUTI,S. 1965a. Electron microscopy on the radial nerve of the starfish. Biol. J. Okayama Univ. 11, 41-52.

KAWAGUTI,S. 1965b. Electron microscopy on the ovarian wall of the echinoid with special references to its muscles and nerve plexus. Biol. J. Okayama Univ. 11, 66-74.

KAWAGUTI,S. 1965c. Electron microscopy on the ampulla of the echinoid. Biol. J. Okayama Univ. 11, 75-86.

KAWAGUTI,S. 1966. Electron microscopy on the body wall of the Sea-Cucumber with special attention to its mucous cells. Biol. J. Okayama Univ. 12, 35-45.

KAWAGUTI,S. & IKEMOTO,N. 1965. Electron microscopy on the longitudinal muscles of the Sea-Cucumber. pp 124-131 in Molecular Biology of Muscular contraction. (Ed. S. Ebashi) Igaku Shuin Ltd., Tokyo.

KAWAGUTI,S. & KAMISHIMA,Y. 1964a. Electron microscopic structure of Iridophores of an echinoid, *Diadema setosum*. Biol. J. Okayama Univ. 10, 13-22.

KAWAGUTI,S. & KAMISHIMA,Y. 1964b. Electron microscopic study on the integument of the Echinoid, *Diadema setosum*. Annot. Zool. Jap., 37, 147-152.

KAWAGUTI,S. & KAMISHIMA,Y. 1965. Electron microscopy on the spine muscle of the echinoid. Biol. J. Okayama Univ. 11, 31-40.

KAWAGUTI,S., KAMISHIMA,Y. & KOBASHI,K. 1965. Electron microscopy on the radial nerve of the Sea-urchin. Biol. J. Okayama Univ. 11, 87-95.

KENDRICK-JONES,J., COHEN,C., SZENT-GYÖRGI,A.G. & LONGLEY,W. Paramyosin: molecular length and assembly. Science, 163, 1196-1198.

(cont.)

KERKUT, G.A. 1954. The mechanics of co-ordination of the starfish tube feet. Behav. 6, 206-232.

KIERNIK, E. 1906. Beitrag zur histologie der echiniden insbesondere der muskeln. Zool. Anz., 29, 610-614.

KLEIN, R.L., SHYKE-CHONG, Y., THURESON -KLEIN, A. 1972. Critique on the K-pyroantimonate method for semiquantitative estimation of cations with electron microscopy. J. Histochem. Cytochem. 20, 65-78.

LANE, B.P. & EUROPA, D.L. 1965. Differential staining of ultrathin sections of epon embedded tissues for light microscopy. J. Histochem. Cytochem. 13, 579-582.

LARSSON, L.-I., SUNDLER, F., & HAKANSON, R. 1975. Fluorescamine as a histochemical reagent. Demonstration of polypeptide hormone-secreting cells. Histochemistry, 44, 245-251.

LAWRENCE, J.M. 1975. On the relationship between marine plants and sea urchins. Oceanogr. mar. Biol. Ann. Rev. 13, 213-286.

LAWRENCE, J.M. 1976. Covering response in sea urchins. Nature 262, 490-491.

LECLERC, M. 1974. L'organe axial et ses relations avec la sexualité et l'immunité chez les Asterides. Ann. Sci. Nat. Zool. 16, 285-359.

LECLERC, M. & DELAVAULT, R. 1971. Presence de fibres nerveuses dans la paroi du sinus axial et dans la paroi coelomique chez Asterina gibbosa Pennat (Echinoderma, Asteride). C.R. Acad. Sci. Paris, Serie D., 272, 3311-13.

LEVINE, R.J.C., ELFVIN, M., DEWEY, M.M. and WALCOTT, B. 1976. Paramyosin in invertebrate muscles. II. Content in relation to structure and function. J. Cell Biol. 71, 273-279.

LEWIS, J.B. 1958. The biology of the tropical sea-urchin Tripneustes esculentus (Leske) in Barbados, British West Indies. Can. J. Zool., 36, 607-621.

LEWIS, J.B. 1964. Feeding and digestion in the tropical sea-urchin Diadema antillarum. Can. J. Zool., 42, 549-557.

LOVEN, S. 1883. On Pourtelasia a genus of Echinoidea. Kongl. Svenska Vetensk-Akad. Handl. 19, 1-95.

LOWY, J., MILLMAN, B.M., HANSON, J. 1964. Structure and function of smooth tonic muscles of lamellibranch molluscs. Proc. Roy. Soc. B., 160, 525-563.

MACKIE, G.O., SPENCER, A.N. & STRATHMANN, R. 1969. Electrical activity associated with ciliary reversal in echinoderm larvae. Nature, 223, 1384-1385.

MACRAE, E.K. 1963. Observations on the fine structure of pharyngeal muscle in the planarian Dugesia tigrina. J. Cell Biol. 18, 651-662.

MALANGA, C.J. 1974. Effects of dopamine on anaerobic metabolism and ciliary activity in bivalve gills. Comp. gen. Pharmac. 5, 51-59.

MALANGA, C.J. 1975. Dopaminergic stimulation of frontal ciliary activity in the gill of Mytilus edulis. Comp. Biochem. Physiol. 51C, 25-34.

MALANGA, C.J. & YOUNG, S.I. 1978. The metabolic fate of dopamine in the ciliated gill epithelium of bivalve molluscs. Comp. Biochem. Physiol. 60C, 129-136.

MARTINEZ, J.L. 1976. Histologia y ultrastructura de la cuticula de los podios de Ophiothrix fragilis (Echinodermata, Ophiuroidea). Biol. R. Soc. Espanola Hist. Nat. (Biol.) 74, 167-181.

MARTINEZ, J.L. 1977a. Estructura y ultraestructura del epitelio de los podios de Ophiothrix fragilis (Echinodermata, Ophiuroidea). Biol. R. Soc. Espanola Hist. Nat. (Biol). 75, 275-301.

MARTINEZ, J.L. 1977b. Histologia y ultraestructura del tejido conectivo de los podios de Ophiothrix fragilis (Echinodermata, Ophiuroidea). Biol. R. Soc. Espanola Hist. Nat. (Biol.). 75, 303-313.

MARTINEZ, J.L. 1977c
Ultrastructura del tejido nervioso podial de Ophiothrix fragilis (Echinodermata, Ophiuroidea). Biol. R. Soc. Espanola Hist. Nat. (Biol.) 75, 315-333.

MARTINEZ, J.L. 1977d. Ultrastructura del tejido muscular y del epitelio celomico de los podios de Ophiothrix fragilis. (Echinodermata, Ophiuroidea). Biol. R. Soc. Espanola Hist. Nat. (Biol.), 75, 335-348.

MARUYUMA, K. & MATSUMIYA, H. 1957. The contractile proteins from tube feet of a starfish. J. Biochem. (Tokyo), 44, 537-542.

MATHEWS, M.B. 1975. Connective tissue. Macromolecular structure and evolution. Springer-Verlag.

MATSUMURA, T. 1974. Collagen fibrils of the Sea Cucumber, Stichopus japonicus.: purification and morphological study. Conn. Tiss. Res. 2, 117-125.

MATUKAS, U.J., PANNER, B.J., & ORBISON, J.L. 1967. Studies on the ultrastructural identification and distribution protein-polysaccharide in cartilage matrix. J. Cell. Biol. 32, 365-377.

MELVILLE, R.V. & DURHAM, J.W. 1966. Skeletal morphology. Treatise on Invertebrate Palaeontology Part A, Echinodermata 3, Volume 1. Ed. R.C. Moore. Geological Society of America & University of Kansas Press.

MENDES, E.G., ABBUD, L. & ANCONA-LOPEZ, A.A. 1970. Pharmacological studies on the invertebrate non-striated muscles - I. The response to drugs. Comp. gen. Pharmac. 1, 11-22.

MENTEN, D.N. & EIKEN, A.Z. 1970. The structure of the integument of the Sea Cucumber, Thyone briareus. J. Morph. 131, 17-36.

MEYERS, D.B., HIGHTON, T.C. & RAYNS, D.G. 1969. Acid mucopolysaccharides closely associated with collagen fibrils in normal human synovium. J. Ult. Res. 28, 203-213.

MEYERS, D.B., HIGHTON, T.C. & RAYNS, D.G. 1973. Ruthenium red-positive filaments interconnecting collagen fibrils. J. Ult. Res. 42, 87-92.

MEYER, D.L. 1971. The collagenous nature of problematical ligaments in crinoids (Echinodermata). Mar. Biol. 9, 235-241.

MILL, P.J. and KNAPP, M.F. 1970. Neuromuscular junction in the body wall muscle of earthworm Lumbricus terrestris. L. J. Cell. Sci. 7, 263-271.

MILLOTT, N. 1966. A possible function for the axial organ of echinoids. Nature 209, 594-596.

MILLOTT, N. 1967. The axial organ of echinoids: Re-interpretation of its structure and function. Symp. Zool. Soc. Lon. 20, 53-63.

MILLOTT, N. 1969. Injury and the axial organ of echinoids. Experientia 25, 756-757.

MILLOTT, N. & COLEMAN, R. 1969. The podial pit - a new structure in the Echinoid Diadema antillarum Philippi. Z. Zellforsch. 95, 187-197.

MILLOTT, N. & TAKAHASHI, K. 1963. The shadow reaction of Diadema antillarum. IV Spine movements and their implications. Phil. Trans. B., 246, 437-469.

MILLOTT, N. & VEVERS, H.G. 1964. Axial organ and fluid circulation in Echinoids. Nature, 204, 1216-1217.

MISCHOR, B. 1975. Zur morphologie und Regeneration der Hohlstacheln von Diadema antillarum Philippi und Echinothrix diadema (L.) (Echinoidea: Diadematidae). Zoomorphologie 82, 243-258.

MOSS, M.L. & MEEHAN, M.M. 1967. Sutural connective tissues in the test of an echinoid Arbacia punctulata. Acta anat. 66, 279-304.

MOTOHIRO, T. 1960. Mucoprotein in marine products - Parts I, II & III. Bulletin of the Japanese Society of Scientific Fisheries 26, 1171-1182.

NAITOH, Y. & ECKERT, R. 1974. The control of ciliary activity in protozoa. In 'Cilia and Flagella' (M.A. Sleigh, Ed.) Academic Press, London.

NICAISE, G. 1973. The gliointerstitual system of molluscs. Int. Rev. Cytol. 34, 251-332.

NICHOLS, D. 1959a. The histology and Activities of the tube feet of Echinocyamus pusillus. Q.J.M.S., 100, 539-555.

NICHOLS, D. 1959b. The histology of the tube feet and Clavulae of Echinocardium cordatum. Q.J.M.S. 100, 73-87.

NICHOLS, D. 1959c. Changes in the Chalk Heart-Urchin Micraster interpreted in relation to living forms. Phil. Trans. Roy. Soc. B., 242, 347-437.

NICHOLS, D. 1960. The histology and activities of the tube feet of Antedon bifida. Q.J.M.S. 101, 105-117.

NICHOLS, D. 1961. A comparative histological study of the tube feet of two Regular Echinoids. Q.J.M.S., 102, 157-180.

NICHOLS, D. 1966. Functional morphology of the water vascular system. In 'Physiology of the Echinodermata' (R.A. Boolootian, Ed.) pp 219-244. Interscience: New York.

NICHOLS, D. 1967. The origin of echinoderms. Symp. Zool. Soc. Lond., 20, 209-229.

NICHOLS, D. 1968. Echinoderms. Hutchinsons University Library.

NICHOLS, D. 1972. The water vascular system in living and fossil echinoderms. Palaeontology 15, 519-538.

NICHOLS, D. & CURREY, J.D. 1968. The secretion, structure, and strength of echinoderm calcite. In: Cell structure and its interpretation Eds. S.M. McGee Russel & K.F.A. Ross. pp 251-261. Arnold (Lon.).

NØRREVANG, A. & WINGSTRAND, K.G. 1970. On the occurrence and structure of choanocyte-like cells in some echinoderms. Acta Zoologica, 51, 249-270.

O'CONNELL, M.G., ALENDER, C.B. & WOOD, H.N. 1974. A fine structural study of venom gland cells in globiferous pedicellariae from Strongylocentrotus purpuratus. J. Morph., 142, 411-432.

OBINATA, T., IKEDA, M., HAYASHI, T. 1974. The native actin filaments for Sea Urchin muscle. Int. J. Biochem. 5, 875-884.

OBINATA, T., SHIRAO, T. & MURAKAMI, S. 1975. Sea urchin paramyosin. Int. J. Biochem. 6, 569-574.

OKAZAKI, K. 1960. Skeleton formation of sea urchin larvae. II. Organic matrix of the spicule. Embryologia 5, 283-320.

OLDFIELD, S.C. 1975. Surface fine structure of the globiferous pedicellariae of the Regular Echinoids, Psammechinus miliaris Gmelin. Cell Tiss. Res. 162, 377-385.

OLDFIELD, S.C. 1976. Surface ornamentation of the echinoid test and its ecological significance. Palaeobiology, 2, 122-130.

OLSON, M. 1938. The histology of the retractor muscles of Thyone briareus Leseur. Biol. Bull. 74, 342-347.

ORKAND, R.K. 1977. Glial Cells. In: Handbook of Physiology. Section 1: The Nervous System, Vol. 1, Part 1. (Ed. Kandel, E.R.). American Physiological Society, Bethesda, Maryland.

OSBORNE, M.P., FINLAYSON, L.H. & RICE, M.J. 1971. Neurosecretory endings associated in the striated muscle in three insects (Schistocerca, Carausius and Phormia) and a frog (Rana). Z. Zellforsch. 116, 391-404.

OSBORNE, N.N. 1971. Occurrence of GABA and taurine in the nervous systems of the dogfish and some invertebrates. Comp. gen. Pharmac., 2, 433-438.

OZAKI, H. 1974. Localisation and multiple forms of acetyl cholinesterase in sea-urchin embryos. Dev. Growth Diff. 16, 267-279.

PAINE, V.L. 1926. Adhesion of the tube feet in starfishes. J. exp. Zool. 45, 361-366.

PANTIN, C.F.A. 1969. Notes on microscopical technique for Zoologists. Cambridge, University Press.

PAPARO, A. & AIELLO, E. 1970. Glio-inhibitory effects of branchial nerve stimulation in the mussel, Mytilus edulis. Comp. gen. Pharmac., 1, 241-250.

PARKER, G.H. 1927. Locomotion and righting movements in Echinoderms, especially in Echinarachnius. Am. J. Psychol. 39, 167-180.

PAUL, C.R.C. 1972. Morphology and function of exothecal pore structures in cystoids. Palaeontology 15, 1-28.

PAUL, C.R.C. 1976. Respiration rates in primitive (fossil) echinoderms. Thalassia Jugoslavica 12, 277-286.

PAUL, C.R.C. 1977. Evolution of primitive echinoderms. In 'Patterns of evolution as illustrated by the fossil record' (A. Hallam, Ed.) pp 123-158. Elsevier Scientific: Oxford.

PEARSE, A.G.E. 1972a & b. Histochemistry Theoretical and Applied. Vol. I & II. Churchill Livingstone (Lon. & Edin.).

PEEBLES, F. & FOX, D.L. 1933. The structure, functions and general reactions of the marine sipunculid worm Dendrostoma zostericola. Bull. Scripps. Inst. Oceanogr. tech. 3, 201-234.

PENTREATH, V.W. & COBB, J.L.S. 1972. Neurobiology of Echinodermata. Biol. Rev. 47, 363-392.

PENTREATH, V.W. & COTTRELL, G.A. 1968. Acetylcholine and cholinesterase in the radial nerve of Asterias rubens. Comp. Biochem. Physiol., 27, 775-785.

PENTREATH, V.W. & COTTRELL, G.A. (1971). 'Giant' neurons and neurosecretion in the hyponeural tissue of Ophiothrix fragilis Abildgaard. J. exp. mar. Biol. Ecol., 6, 249-264.

PEQUIGNAT,E. 1966. 'Skin digestion' and epidermal absorption in irregular and regular urchins and their probable relation to the outflow of spherule-coelomocytes. Nature, 210, 397-399.

PERPEET,C. & JANGOUX,M. 1973. Contribution a l'etude des pieds et des ampules ambulacraires d'Asterias rubens (Echinodermata, Asteroidea). Forma et Functia, 6, 191-209.

PHILPOTT,D.E., KAMLBROCK,M. & SZENT-GYORGY,A.G. 1960. Filamentous organization of molluscan muscles. J. Ult. Res. 3, 254-269.

PITELKA,D.R. 1974. Basal structures attached to cilia. In: Cilia and Flagella. (M.A. Sleigh, Ed.) pp 437-469. Academic Press, London.

PLESCH,B. 1977a. An ultrastructural study of the musculature of the pond snail Lymnaea stagnalis (L.). Cell Tiss. Res. 180, 317-340.

PLESCH,B. 1977b. An ultrastructural study of the innervation of the musculature of the pond snail Lymnaea stagnalis (L.) with reference to peripheral neurosecretion. Cell Tiss. Res. 183, 353-369.

PROSSER,C.L. & JUDSON,C.L. 1952. Pharmacology of haemal vessels of Stichopus californicus. Biol. Bull. 102, 249-251.

PRUSCH,R.D. 1977. Solute secretion by the tube foot epithelium in the starfish Asterias forbesi. J. exp. Biol. 68, 35-43.

PUCCI-MINAFRA,I., GALANTE,R. & MINAFRA,S. 1978. Identification of collagen in the aristotle's lanternae of Paracentrotus lividus. J. Submicr. Cytol. 10, 53-63.

QUINN,B.G. 1965. Predation in Sea Urchins. Bull. Mar. Sci., 15, 259-264.

RAMBOURG,A., HERNANDEZ,W. & LEBLOND,C.P. 1969. Detection of complex carbohydrates in the Golgi apparatus of rat cells. J. Cell Biol. 40, 395-414.

RAUP, D.M. 1960. Ontogenetic variation in the crystallography of echinoid calcite. J. Palaeont. 34, 1041-1050.

RAUP, D.M. 1965. Crystal orientations in the echinoid apical system. J. Palaeont. 39, 934-951.

RAUP, D.M. 1966. The Endoskeleton. In 'Physiology of Echinodermata'. (R.A. Boolootian, Ed.). Interscience: New York.

REESE, E.S. 1966. The complex behaviour of Echinoderms. In 'Physiology of Echinodermata' (R.A. Boolootian, Ed.). Interscience: New York.

REYNOLDS, E.S. 1963. The use of lead citrate at high pH as on electron opaque stain for electron microscopy. J. Cell Biol. 17, 208-210.

ROBERTSON, H.A. & JUORIO, A.V. 1976. Octopamine and some related non-catecholic amines in invertebrate nervous systems. Int. Rev. Neurobiol. 19, 173-224.

ROBERTSON, J.D. 1949. Ionic regulation in some massive invertebrates. J. exp. Biol. 26, 182-200.

ROMANES, G.J. & EWART, J.C. 1881. Observations on the locomotor system of Echinodermata. Phil. Trans. Roy. Soc., 172, 829-885.

ROSENBLUTH, J. 1965. Ultrastructure of somatic muscle cells in Ascaris lumbricoides. II. Intermuscular junctions, neuromuscular junction and glycogen stores. J. Cell Biol. 26, 579-591.

ROSENBLUTH, J. 1972. Myoneural junctions of two distinct types of earthworm body wall muscle. J. Cell Biol. 54, 566-579.

RUBIN, W.P. 1974. Calcium in the secretory process. Plenum: New York.

RUDE, S., COGGESHALL, R.E. & Van ORDEN, L.S. 1969. Chemical and ultrastructural identification of 5-HT in an identified neuron. J. Cell Biol., 41, 832-854.

RYBERG,E. 1974. The localization of biogenic amines in the echinopluteus. Acta Zool. 55, 179-189.

RYBERG,E. 1977. The nervous system of the early echinopluteus. Cell Tiss. Res. 179, 157-167.

SANDEMAN,D.C. 1965. Electrical activity in the radial nerve cord and ampullae of Sea Urchins. J. Exp. Biol. 43, 247-256.

SANNES,P.L., KATSUYAMA,T. & SPICER,S.S. 1978. Tannic acid metal salt sequences for light and electron microscopic localization of complex carbohydrates. J. Histochem. Cytochem., 26, 55-61.

SCHLECHNER,J. & LUCERO,J. 1968. A light and electron microscopic investigation of the digestive system of the ophiuroid Ophioderma panamensis (Brittlestar). J. Morph. 124, 451-482.

SCHLOTE,F.E. 1963. Neurosekretartige Grana in den peripheren Nerven und in den Nerv-Muskel-Verhindungen von Helix pomatia. Z. Zellforsch. 60, 325-347.

SELYE,H. 1965. The Mast Cells. Butterworths, Washington.

SERAFINI-FRACASSINI,A. & SMITH,J.W. 1974. The structure and biochemistry of cartilage. Churchill Livingstone: Edinburgh and London.

SERVETTAZ,F. & GONTCHAROFF,M. 1976. Etude Cytochemique des Cellules Présumées Neurosécretrices dans le Systeme Nerveux Central des Héteronémertes Lineidae. Gen. Comp. Endocr. 30, 285-291.

SHELKOVNIKOV,S.A., STARSHINOVA,L.A., ZEIMAL,E.V. 1977. Two kinds of cholinoreceptors on the non-visceral muscle of some echinodermata. Comp. Biochem. Physiol. 58C, 1-12.

SILK,M.H. & SPENCE,I.M. 1969. Ultrastructural studies of the blood fluke Schistosoma mansoni. III. Nerve Tissue and sensory structures. S. Afr. J. Med. Sci. 34, 93-104.

SMITH,A.B. 1978a. A comparative study of the life style of two Jurassic irregular echinoids. Leth. 11, 57-66.

SMITH,A.B. 1978b. A functional classification of the coronal pores of regular echinoids. Palaeontology,21, 759-789.

SMITH, G.N. & GREENBERG, M.J. 1973. Chemical control of the evisceration process in Thyone briareus. Biol. Bull. 144, 421-436.

SMITH, J.E. 1937. The structure and function of the tube feet in certain echinoderms. J. Mar. biol. Ass., 22, 345-357.

SMITH, J.E. 1945. The role of the nervous sytem in some of the activities of the starfish. Biol. Rev. 20, 29-43.

SMITH, J.E. 1946. The mechanics and innervation of the starfish tube feet - ampulla system. Phil. Trans B., 232, 279-310.

SMITH, J.E. 1947. The activities of the tube feet of Asterias rubens. Q.J.M.S., 88, 1-14.

SMITH, J.E. 1950a. The motor nervous system of the starfish Astropecten irregularis (Pennant), with special reference to the innervation of the tube feet and ampulla. Phil. Trans. Roy. Soc. B., 234, 521-558.

SMITH, J.E. 1950b. Some observations on the nervous mechanisms underlying the behaviour of starfish. S.S.E.B. 4, 196-220.

SMITH, J.E. (1965). Echinodermata. In 'Structure and Function in the Nervous systems of Invertebrates. (Bullock, T.H. & Horridge , G.A.) Vol. II, pp 1519-1558. W.H. Freeman & Co. London.

SMITH, J.E. 1966. The form and functions of the nervous system. In 'Physiology of Echinodermata' (R.A. Boolootian, Ed.) pp 503-511. Interscience: New York.

SMITH, J.W., PETERS, T.J. & SERAFINI-FRACASSINI, A. 1967. Observations on the distribution of the protein polysaccharide complex and collagen in bovine articular cartilage. J. Cell Sc. 2, 129-136.

SOMLYO, A.P. & SOMLYO, A.V. 1976. Ultrastructural aspects of activation and contraction of vascular smooth muscle. Fed. Proc. 35, 1288-1293.

De SOUZA SANTOS, H. 1966. The ultrastructure of the mucous granules from starfish tube feet. J. Ult. Res., 16, 259-268.

De SOUZA SANTOS, H. 1966. Ultrastructure of a mucous fluid cell found in the tube feet of the starfish Asterina stellifera. Experientia, 22, 812.

De SOUZA-SANTOS, H. & SILVA SASSO, W. 1968. Morphological and histochemical studies on the secretory glands of starfish tube feet. Acta. anat., 69, 41-51.

De SOUZA-SANTOS, H. & SILVA SASSO, W. 1970. Ultrastructural and histochemical studies on the epithelium revestment layer in the tube feet of the Starfish Asterina stellifera. J. Morph. 130, 287-296.

De SOUZA-SANTOS, H. & SILVA SASSO, W. 1973. Ultrastructural and histochemical studies on the mucous granules in the tube feet of the Starfish Echinaster brasiliensis. Experientia., 29, 473-474.

De SOUZA-SANTOS, H. & SILVA SASSO, W. 1974. Ultrastructural and histochemical observations of the external epithelium of echinoderm tube feet. Acta. anat., 88, 22-33.

SPURR, A.R. 1969. A low-viscosity epoxy resin embedding medium for electron microscopy. J. Ult. Res., 26, 31-43.

SQUIRE, J.M. 1971. General model for the structure of all myosin-containing filaments. Nature 223, 457-462.

STANG-VOSS, C. 1971. Zur ultrastruktur der Blutzellen wirbellosen tiere. VI. Uber die Hämocyten von Psammechinus miliaris (Echinoidea). Z. Zellforsch., 122, 76-84.

STOTT, F.C. 1955. The food canal of the Sea-urchin Echinus esculentus and its functions. Proc. Zool. Soc. Lond., 125, 63-86.

STOTT, R.S.H., HEPBURN, H.R., JOFFE, I. & HEFFRON, J.J.A. 1974. The mechanical defensive mechanism of a Sea-Cucumber. S. Afr. J. Sci., 70, 46-48.

SUGI, H. & SUZUKI, S. 1978. Ultrastructural and physiological studies on the longitudinal body wall muscle of Dolabella auricularia. I. Mechanical response and ultrastructure. J. Cell Biol. 79, 454-466.

SUZUKI, S. & SUGI, H. 1978. Ultrastructural and physiological studies on the longitudinal body wall muscle of Dolabella auricularia. II. Localization of intracellular calcium and its translocation during mechanical activity. J. Cell Biol. 79, 467-478.

SWEENEY, D. 1963. Dopamine: Its occurrence in molluscan ganglia. Science, 139, 1051.

TAKAHASHI, K. 1964. Electrical responses to light stimuli in the Isolated Radial Nerve of the Sea Urchin Diadema setosum (Leske). Nature, 201, 1343-1344.

TAKAHASHI, K. 1966. Muscle physiology. In 'Physiology of Echinodermata' (R.A. Boolootian, Ed.) pp 513-527.

TAKAHASHI, K. 1967a. The catch apparatus of the Sea-Urchin spine: I. Gross histology. J. Foc. Sci. Tokyo Univ., 11, 109-120.

TAKAHASHI, K. 1967b. The catch apparatus of the Sea-Urchin spine: II. Responses to stimuli. J. Foc. Sci. Tokyo Univ., 11, 121-130.

TANAKA, K., NISHI, C., TAKAYA, M. & UCHIYAMA, T. 1972. A hexosamine-containing polyfucose sulphate-protein complex from Stichopus japonicus Selenka. J. Biochem. 72, 1265-1267.

THUM, A.B. & ALLEN, J.C. 1976. Reproductive ecology of the lamp urchin Echinolampas crassa (Bell), 1880 from a subtidal biogenic ripple train. Trans. Rg. Sci. S. Afr., 42, 23-33.

TONEBY, M. 1977a. Determination of 5-Hydroxytryptamine in early echinoderm embryos. Comp. Biochem. Physiol., 58C, 77-83.

TOSEBY, M. 1977b. Functional aspects of 5-Hydroxytryptamine in early embryogenesis of the Sea Urchin Paracentrotus lividus. Wilhelm Roux's Archives 181, 247-259.

TRANZER, J.P., THOENEN, H., SNIPES, R.C. & RICHARDS, J.G. 1969. Recent developments on the ultrastructural aspect of Adrenergic Nerve endings in various experimental conditions. Prog. Brain Res., 31, 34-36.

TRANZER, J.P. & RICHARDS, J.G. 1976. Ultrastructural cytochemistry of biogenic amines in nervous tissue: methodological improvements. J. Histochem. Cytochem. 29, 1178-1193.

TRUMP, B.F. & BULGER, R.E. 1966. New ultrastructural characteristics of cells fixed in a Glutaraldehyde-Osmium mixture. Lab. Invest. 15, 368-382.

TSUCHIYA, T. and AMEMIYA, S. 1977. Studies on the radial muscle of an echinothuriid sea-urchin, Asthenosoma - I. Mechanical responses to electrical stimulation and drugs. Comp. Biochem. Physiol. 57C, 69-73.

TWAROG, B.M. 1976. Aspects of smooth muscle function in molluscan catch muscle. Physiol. Revs. 56, 829-838.

UEXKÜLL, J. von. 1903. Der biologische Bauplan des Sipunculus. Z. Biol. 44, 269-344.

UNGER, H. 1962. Experimentelle und histologische Untersuchungen über Wirkfactoren aus den Nervensystem von Asterias glacialis. Zool. Jb. Physiol., 69, 481-536.

VANDEN BOSSCHE, J.P. & JANGOUX, M. 1976. Epithelial origin of starfish coelomocytes. Nature, 261, 227-228.

VENABLE, J.H. & COGGESHALL, R. 1965. A simplified lead citrate stain for use in electron microscopy. J. Cell Biol. 25, 407-408.

VEVERS, H.G. 1967. The histochemistry of the echinoid axial organ. Symp. Zool. Soc. Lond., 20, 65-74.

VOGEL, H.G. 1975. Measurement of some viscoelastic properties of rat skin following repeated load. Conn. Tiss. Res. 4, 163-168.

WALTER, M.F. & SATIR, P. 1978. Calcium control of ciliary arrest in mussel gill cells. J. Cell Biol. 79, 110-120.

WARSHAWSKY, H. & MOORE, G. 1967. A technique for the fixation and decalcification of rat incisorsfor electron microscopy. J. Histochem. Cytochem., 15, 542-547.

WATANABE, H. 1969. Electron microscopic observations on the innervation of smooth muscle in the guinea pig vas deferens. Acta. Anat. Nippon 44, 189-202.

WEBER, J.N. 1969. The incorporation of magnesium into the skeletal calcites of echinoderms. Am. J. Sci. 267, 537-566.

WEBER, J.N. 1973. Temperature dependence of magnesium in echinoid and asteroid skeletal calcite: A reinterpretation of its significance. J. Geol. 81, 543-556.

WEBER, W. & GROSMANN, M. 1977. Ultrastructure of the Basiepithelial Nerve plexus of the Sea Urchin Centrostephanus longispinus. Cell Tiss. Res. 175, 551-562.

WEIHE, E., HARTSCHUH, W., METZ, J. & BRUHL, U. 1977. The use of ionic Lanthanum as a diffusion tracer and as a marker of calcium binding sites. Cell Tiss. Res. 178, 285-302.

WELSH, J.H. (1966). Neurohormones and neurosecretion. In 'Physiology of Echinodermata' (R.A. Boolootian, Ed.), pp 545-560. Interscience: New York.

WELSH, J.H. 1972. Handbook der experimentallen Pharmacologie. XXXIII. Ed. H. Blaschko & E. Muscholl, Chaps. IV. 79-109. 'Catecholamines in the Invertebrates'.

WENDELAARBONGA, S.E. 1970. Ultrastructure and histochemistry of neurosecretory cells and neurohaemal areas in the pond snail Lymnaea stagnalis (L.). Z. Zellforsch., 108, 190-224.

WILKIE, I.C. 1978a. Nervously mediated change in the mechanical properties of Brittlestar ligament. Mar. Behav. Physiol., 5, 289-306.

WILKIE, I.C. 1978b. Functional morphology of the autotomy plane of the Brittle star Ophiocomina nigra (Abildgaard) (Ophiuroidea, Echinodermata). Zoomorphologie 91, 289-305.

WILKIE, I.C. 1979. The Juxtaligamental cells of Ophiocomina nigra (Abildgaard) (Echinodermata: Ophiuroidea) and their possible role in Mechano-effector function of collagenous tissue. Cell Tiss Res. 197, 515-530.

WINKELMAN, L. 1976. Comparative studies of paramyosins. Comp. Biochem. Physiol. 55B, 391-397.

WISSOCQ, J. 1970. Evolution de la musculature longitudinale dorsale et ventrale au cours de la stolonisation de Syllis amica Quatrefages (Annelide Polychaete). 1. Muscles du ver asexuel et muscles du stolon. J. Microscopie. 9, 355-388.

WOOD, J.G. 1966. Electron microscopic localisation of amines in central nervous tissue. Nature, 209, 1131-1133.

WOOD, J.G. 1967. Cytochemical localisation of 5-hydroxytryptamine (5HT) in the central nervous system (CNS). Anat. Rev., 157, 343-344.

WOODLEY, J.D. 1967. Problems in the ophiuroid water vascular system. Symp. Zool. Soc. Lon., 20.

WYMAN, L.C. & LUTZ, B.R. 1930. The action of adrenaline and certain drugs in the isolated holothurian cloaca. J. exp. Zool. 57, 441-453.

ZUCKERKANDL, E. 1950. Coelomic pressures in Sipunculus nudus. Biol. Bull. 98, 161-173.

STUDIES ON THE WATER VASCULAR SYSTEM OF REGULAR ECHINOIDS

CONTENTS - PART 2

Fig. 1

Madreporite, E. chloroticus

g   Gonopore

Scale 500µ

Fig. 2

Madreporite, Holopneustes

t   Tubercle (attachment site for spine)

arrow   Granule ("   "   " pedicellaria)

Scale 500µ

Fig. 3

Madreporite, E. mathaei

Scale 500µ

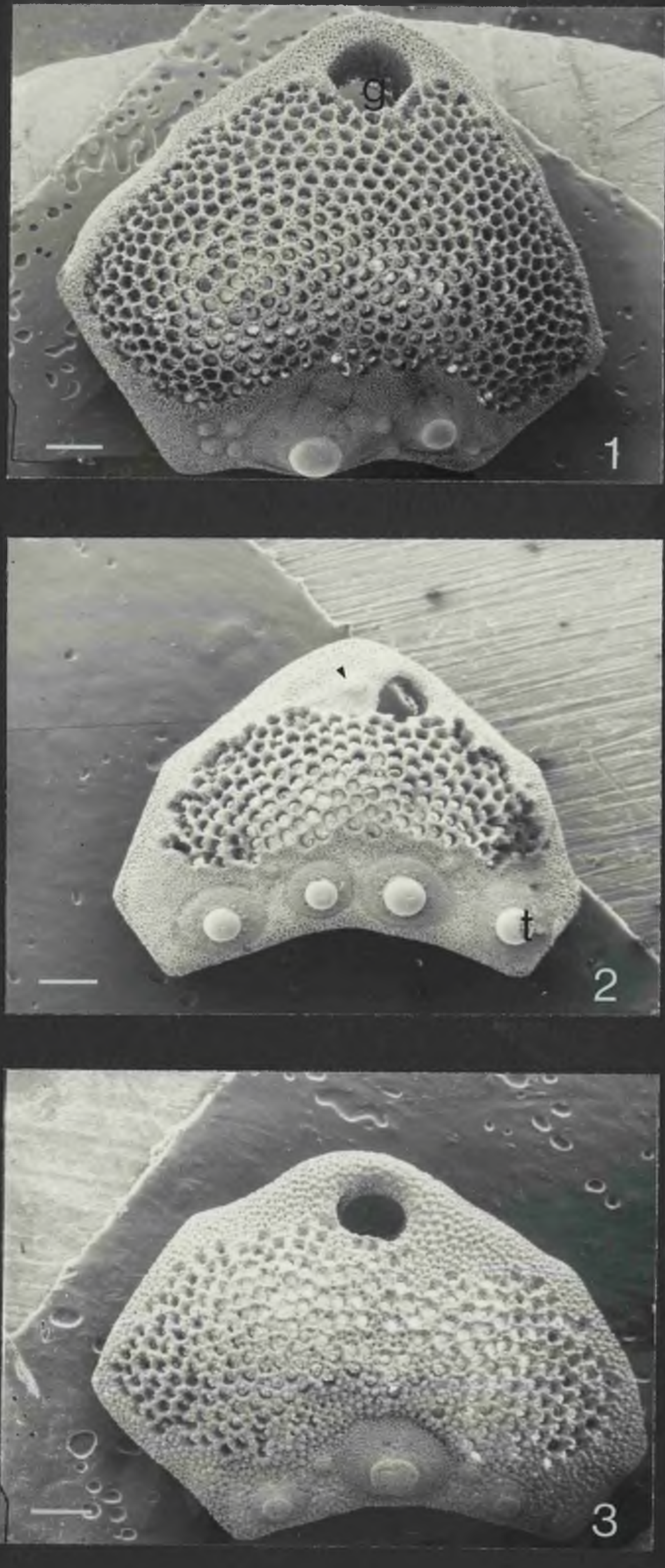
g
1
t
2
3

Fig. 4

Hydropores - external, *E. chloroticus*

Scale 100µ

Fig. 5

Madreporite - internal, *D. setosum*

The depression (d) lying between the gonopore and the hydroporiferous area accommodates the madreporic vesicle.

Scale 200µ

Fig. 6

Madreporite - internal, *E. esculentus*

Note differences in the stereom structure of the ridge (r) and the Hydroporiferous area (Ha) which it delineates from the remainder of the madreporite.

Scape 100µ

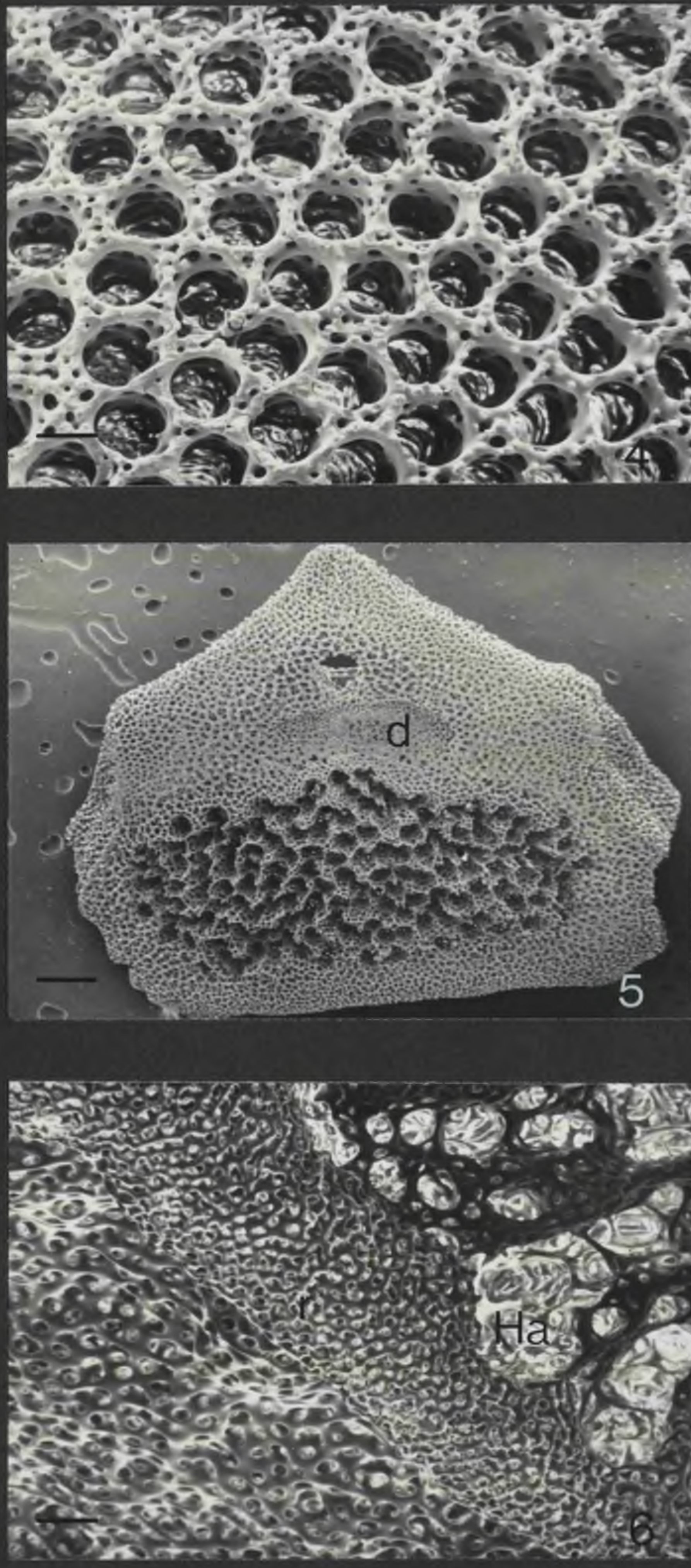
4
d
5
r
Ha
6

Fig. 7

Hydropores - internal, _E. chloroticus_

Note the jagged vertical trabeculae.

Scale 50μ

Fig. 8

TTF plate, _D. setosum_

A single pore (p) provides an exit for the passage of the terminal tube foot.

g Granule

Scale 100μ

Fig. 9

TTF plate, _E. chloroticus_

t Tubercle

Scale 200μ

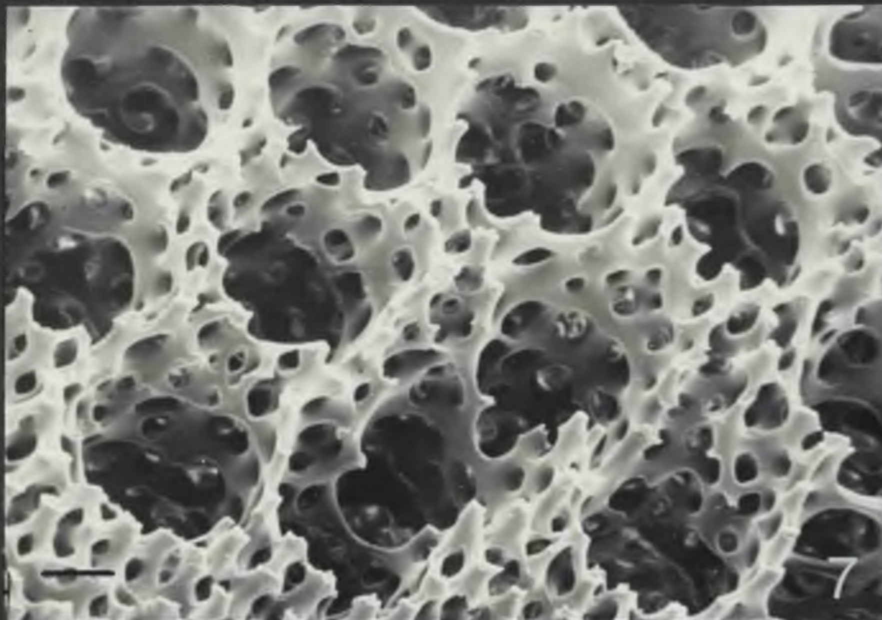
7

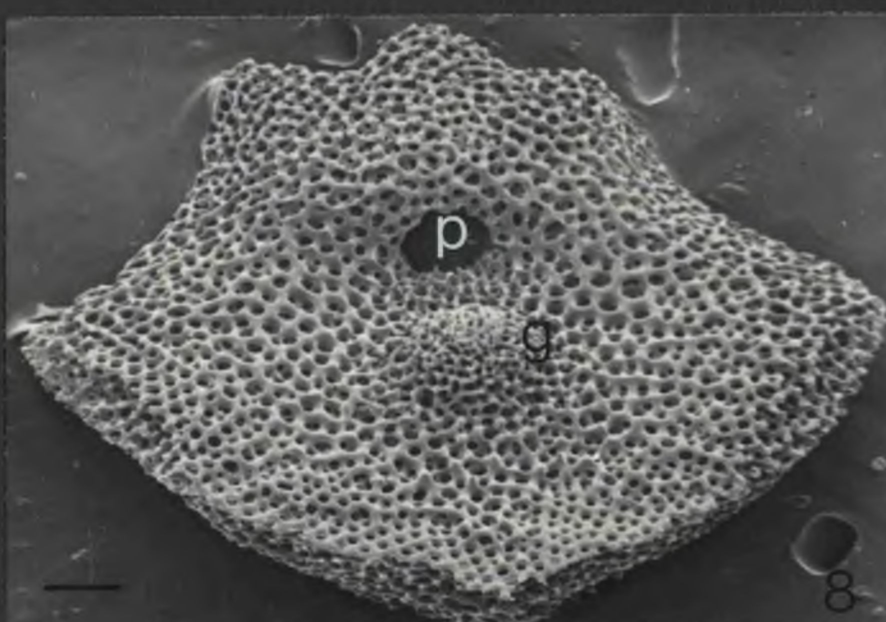
p
g
8


t
9

Fig. 10

TTF plate - internal, *D. setosum*

Note the canal leading to the pore (p)

Scale 100µ

Fig. 11

TTF plate - internal, *E. chloroticus*

Note the absence of a canal leading to the pore

Scale 100µ

Fig. 12

Apical region of a single ambulacrum, *E. mathaei*

Note decrease in size of isopores adapically.

p Perradial suture

a Adradial suture

Scale 500µ

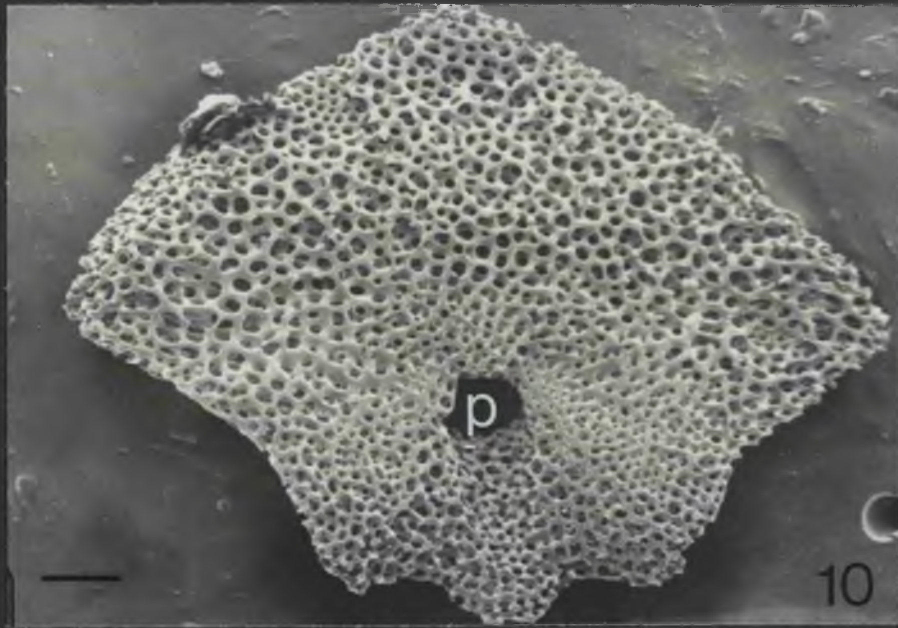
p
10

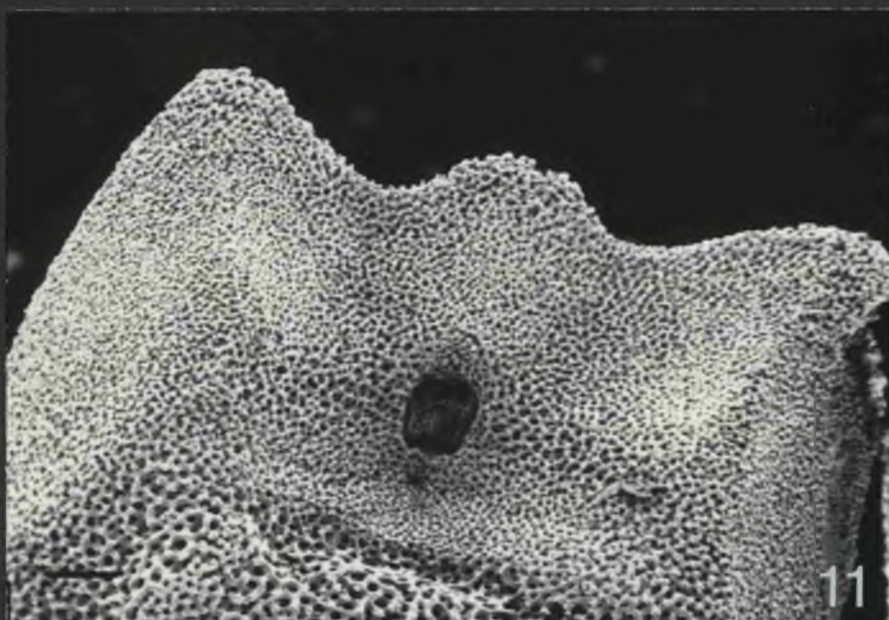
11

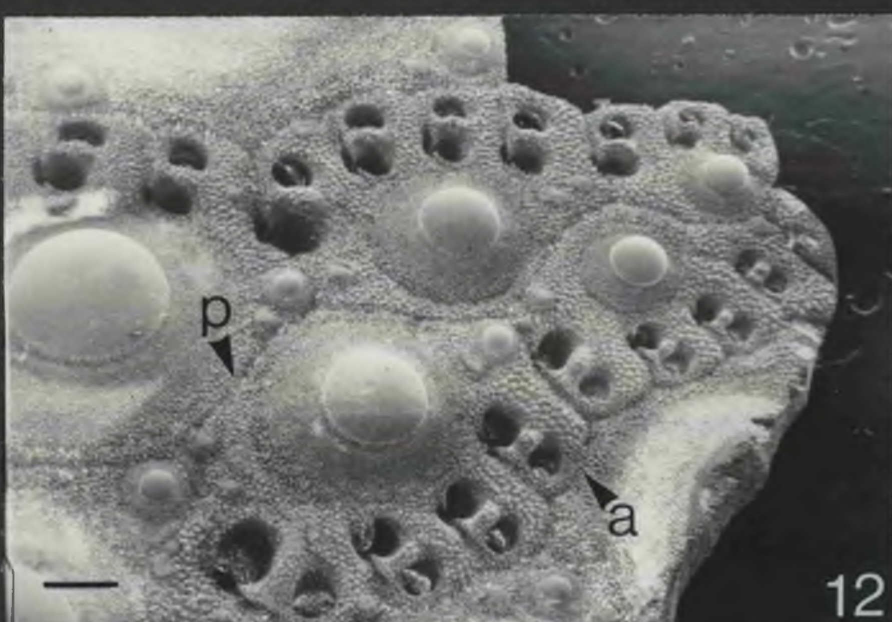
p
a
12

Fig. 13

Apical end of an ambulacrum, _S. droebachiensis_

The penultimate tube foot passes through a considerably reduced pore pair.

Scale 100µ

Fig. 14

Ambital isopore, _E. chloroticus_

Ap Adradial pore

Pp Perradial pore

Arrow indicates passage of neural groove along the transverse adoral suture.

Scale 200µ

Fig. 15

Isopores - internal, _A. lixula_

Note the canal (c) which passes into the perradial pore.

Ap Adradial pore

Scale 200µ


13

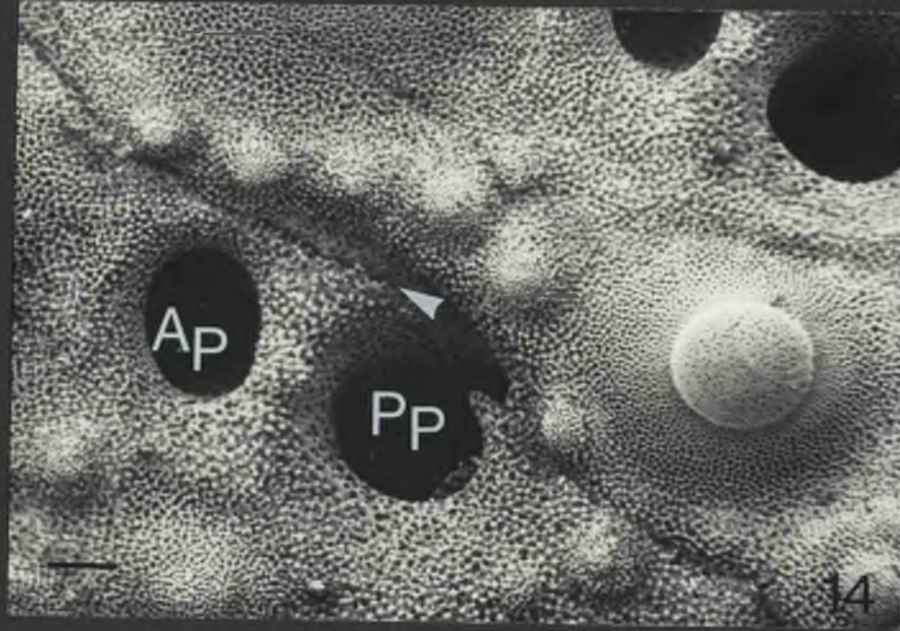
Ap
Pp
14

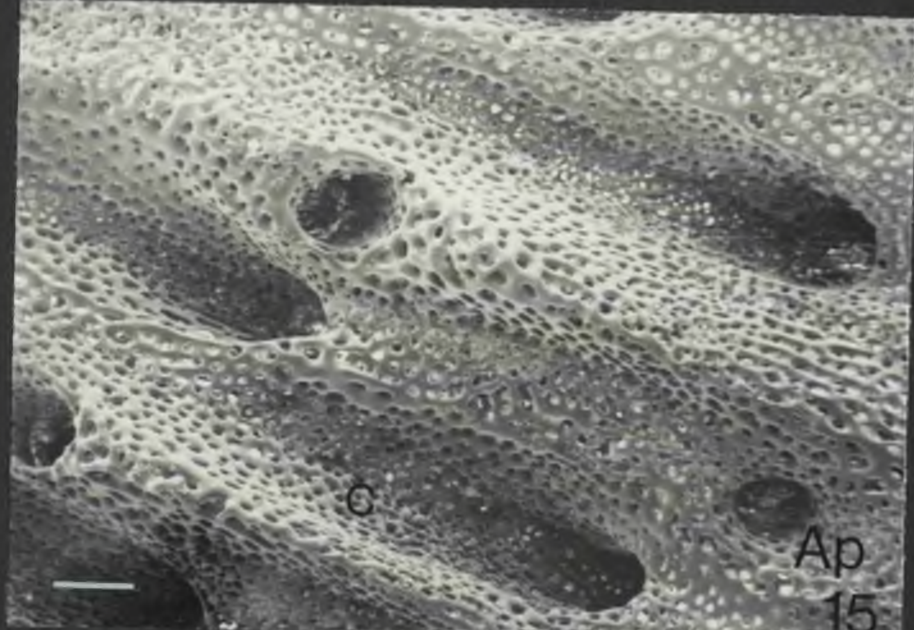
c
Ap
15

Fig. 16

Simple echinoid plates, *E. esculentus*

A single demiplate (d) occurs between two primary (p) plates.

Arrow indicate sutures

Scale 1mm

Fig. 17

Complex echinoid plates, *S. purpuratus*

Six demiplates (d) occur between two primary (p) plates.

Arrows indicate sutures

Scale 1mm

Fig. 18

An uncompounded plate, *S. profundii*

Note the well developed neural canal (n) associated with the perradial pore.

Scale 100μ


P
P
d
16


d
p
p
17

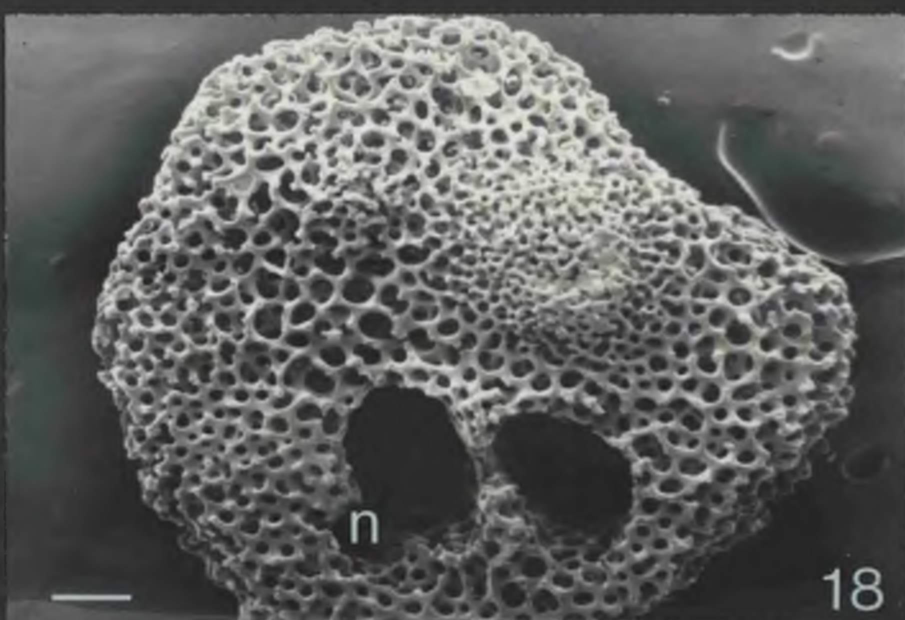
n
18

Fig. 19

Ambital isopores, *D. setosum*

Arrows indicate the progressive closure of the neural notch within the rostrum (r).

Scale 100µ

Fig. 20

Ambulacrum - internal, *A. lixula*

Arrows indicate sutures

Scale 500µ

Fig. 21

PTP plate, *Holopneustes*

Scale 100µ

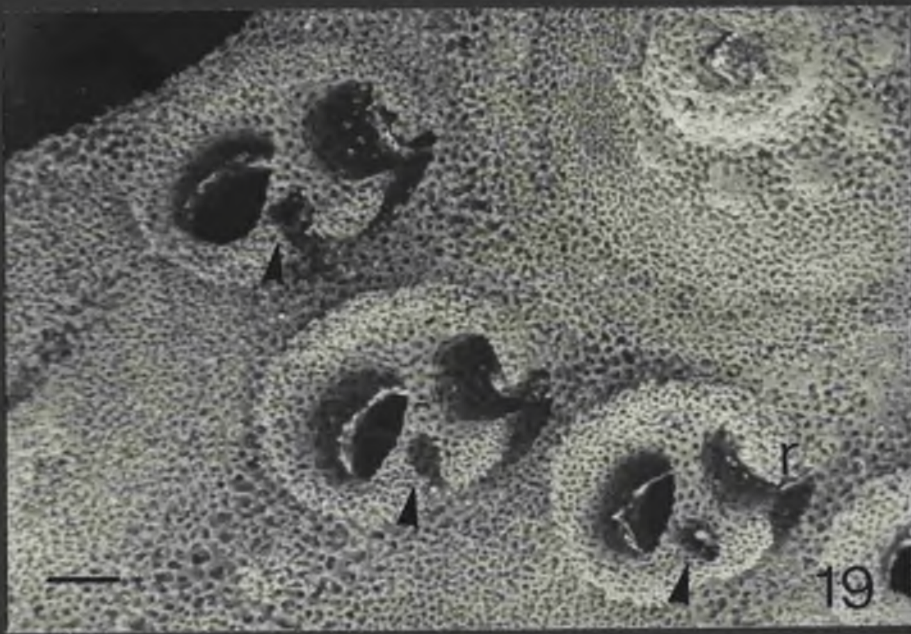
r
19


20

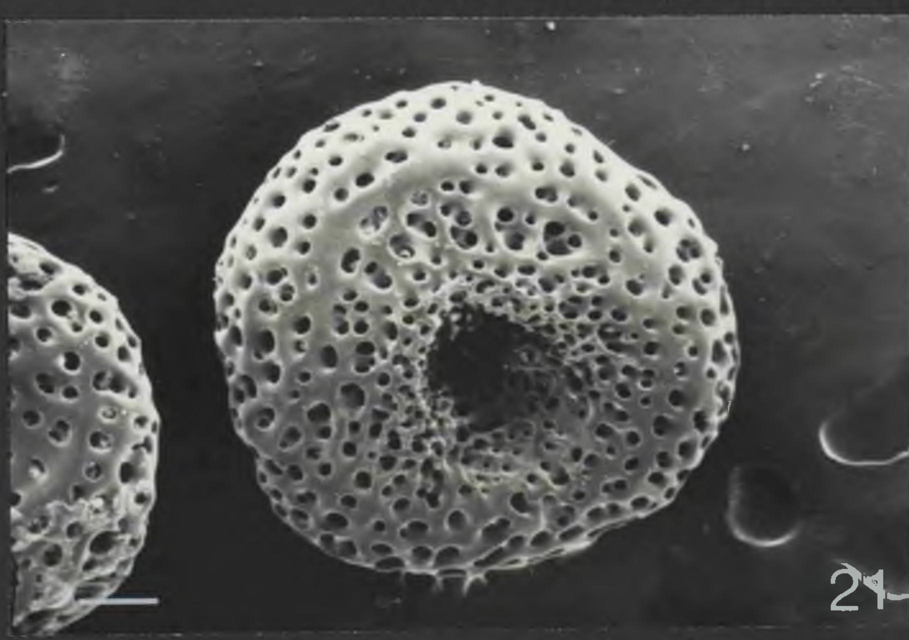
21

Fig. 22

PTF plate - internal, *Holopneustes*

Scale 100μ

Fig. 23

PTF plate, *S. profundii*

g Granule

r Rostrum

Scale 200μ

Fig. 24

PTF plate, immature *E. esculentus*

g Granule

Scale 100μ


22

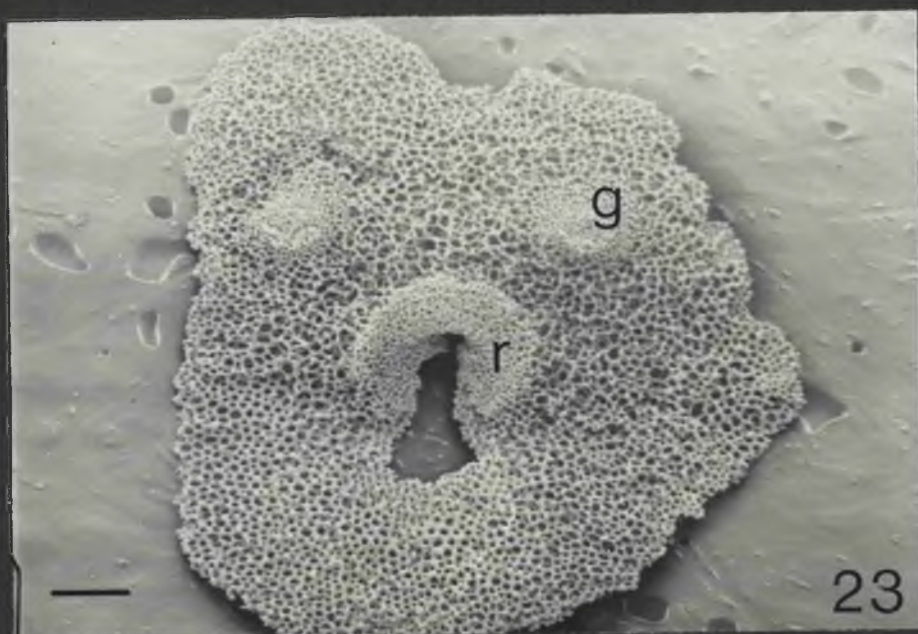
g
r
23

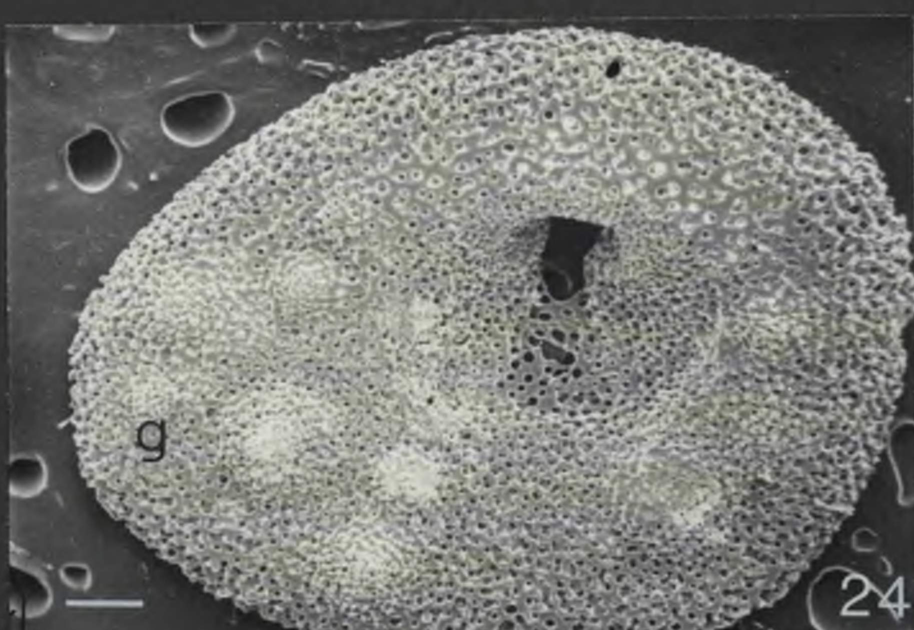
g
24

Fig. 25

PTF plate, mature *E. esculentus*

Arrows indicate evaginations which form the interporal partition.

t Tubercle

Scale 500μ

Fig. 26

PTF Interporal partition, mature *E. esculentus*

Arrow indicates a trabecula which fuses the two finger-like evaginations.

Scale 20μ

Fig. 27

PTF pore - internal *P. miliaris*

Note the incomplete formation of an interporal partition.

Scale 100μ


t
25

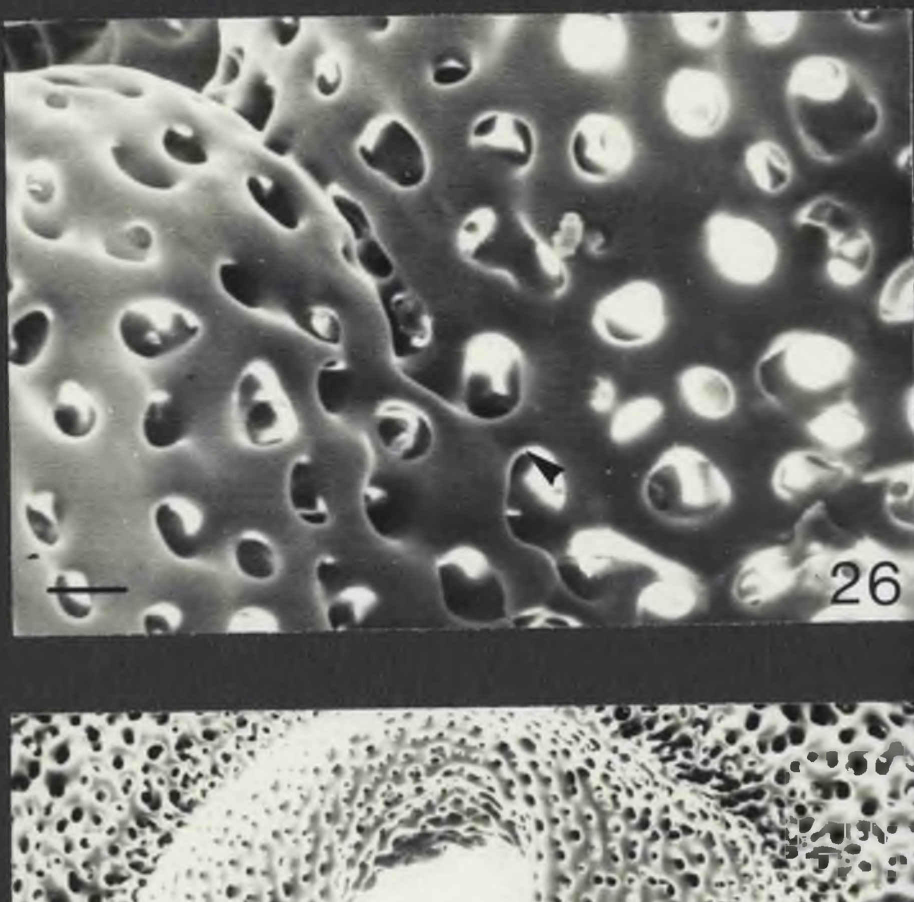
26

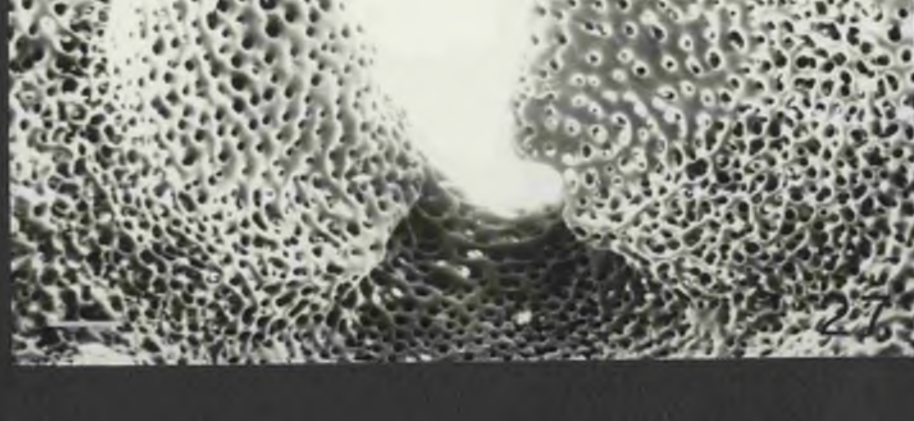
27

Fig. 28

PTF plate, D. setosum

Arrows indicate the development of a pair of interporal partitions.

Scale 500μ

Fig. 29

PTF plate - internal, D. setosum

Arrow indicates a complete interporal partition.

Note the canal (c) which passes into the adoral pore.

Scale 100μ

Fig. 30

PTF plate, E. chloroticus

A well developed interporal partition (Ip) forms a complete pore pair.

Scale 200μ

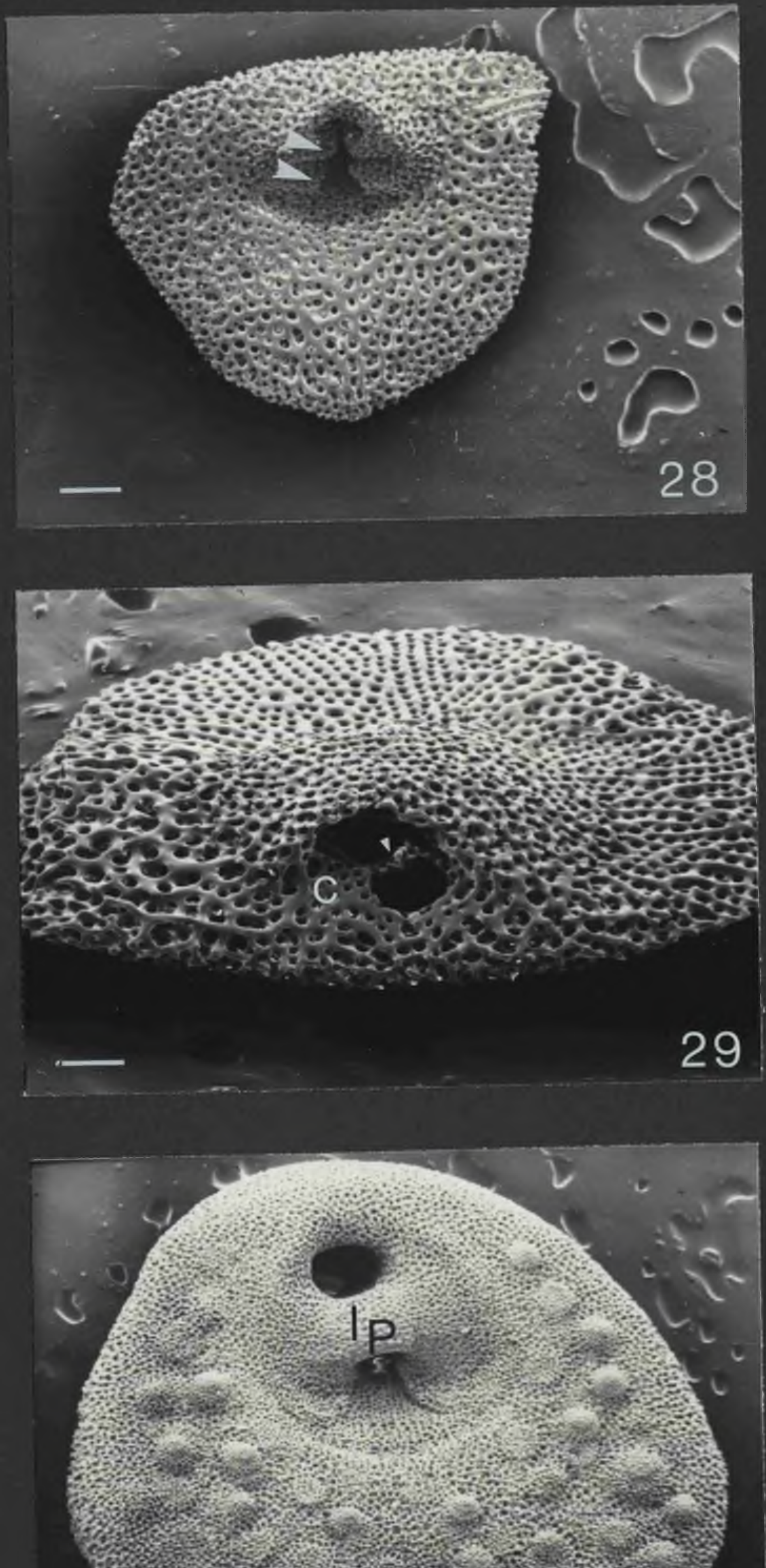
28
c
29
lp
30

Fig. 31

PTF plate, *S. pallidus*

Note the hypertrophy of the interporal partition.

Scale 500μ

Fig. 32

PTF plate, *A. lixula*

Arrow indicates the perpendicularly orientated adoral pore.

Scale 500μ

Fig. 33

Relationship of disk elements to the tube foot stem, *A. lixula*

s Stem

f Frame ossicle (note increase in size distally)

r Rosette ossicle

Scale 50μ


31


32

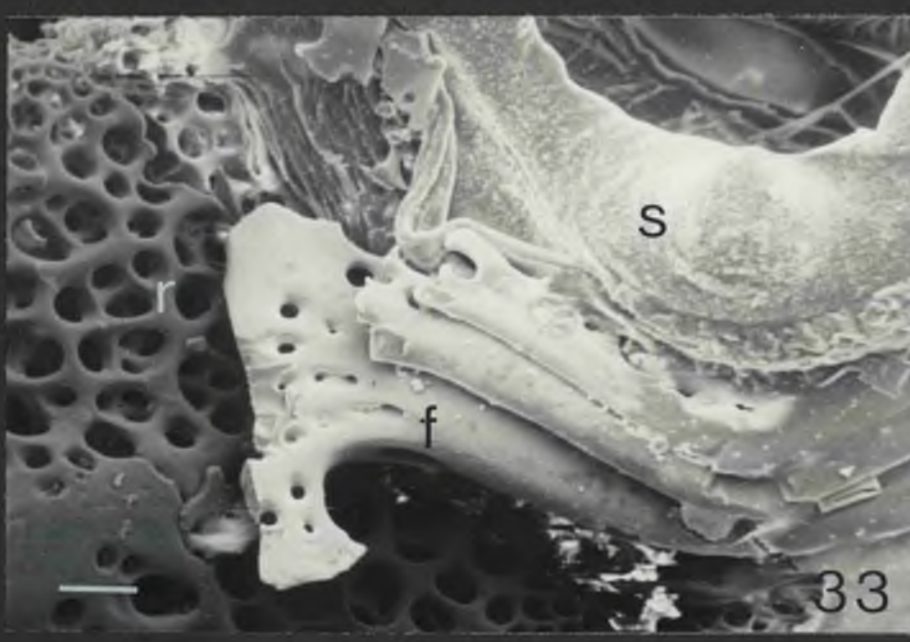
s
r
f
33

Fig. 34

Distal frame ossicle, E. mathaei

Tf Terminal flange

Scale 50μ

Fig. 35

Proximal frame ossicle, A. lixula

Scale 20μ

Fig. 36

Proximal and distal frame ossicles, E. esculentus

m Main shaft

s Small shaft

Scale 20μ

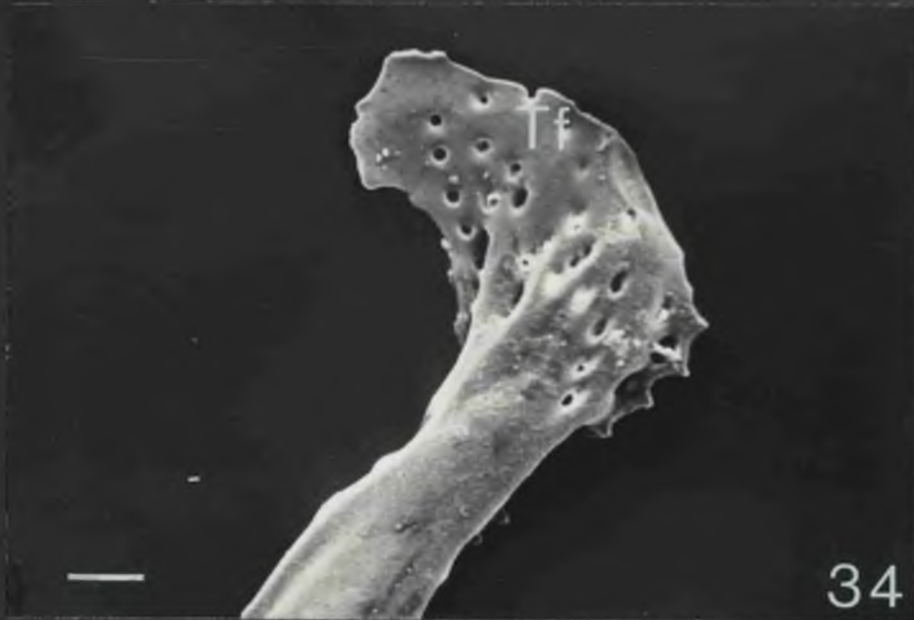
ff
34

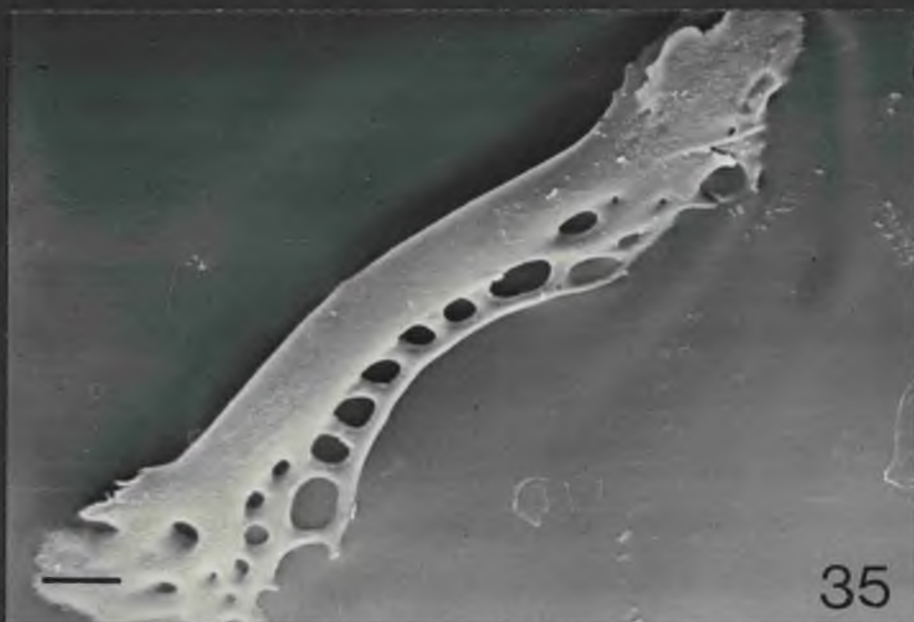
35


m
s
36

Fig. 37

ATF rosette ossicles - distal, *E. esculentus*

Note that the ossicles interlock such that the lumen (l) of the tube foot can pass through the rosette.

Scale 100μ

Fig. 38

ATF rosette ossicle - distal, *E. chloroticus*

Note the enlarged trabeculae which form the projections.

Scale 50μ

Fig. 39

ATF rosette ossicle - proximal, *A. lixula*

Scale 50μ

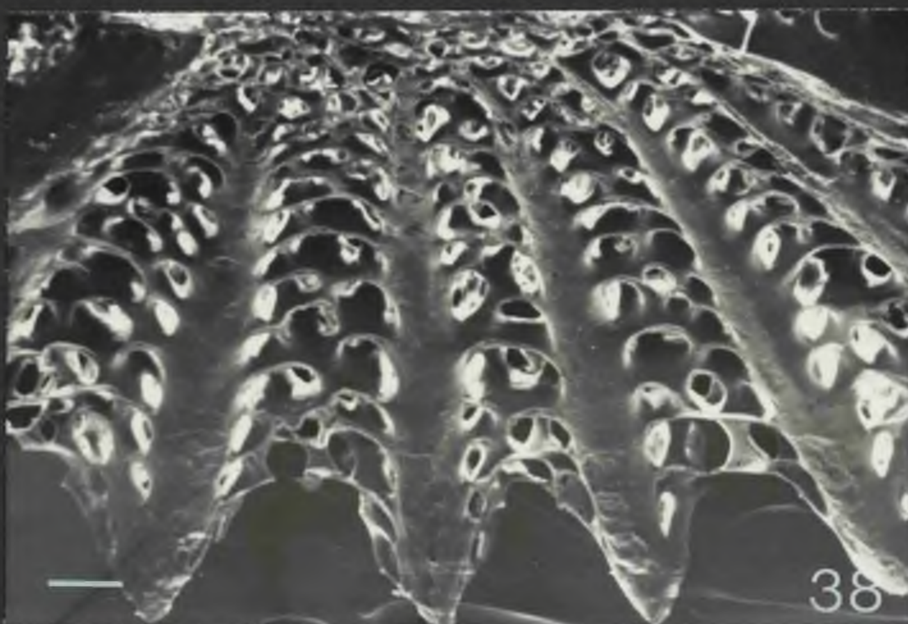

Fig. 40

ATF rosette ossicle - distal, A. lixula

Scale 50μ

Fig. 41

PTF rosette ossicle - proximal, A. lixula

Note flattened profile

Scale 100μ

Fig. 42

PTF rosette ossicle - proximal, E. esculentus

Scale 100μ

Fig. 43

Rudimentary PTF rosette ossicle, A. lixula

Scale 50μ

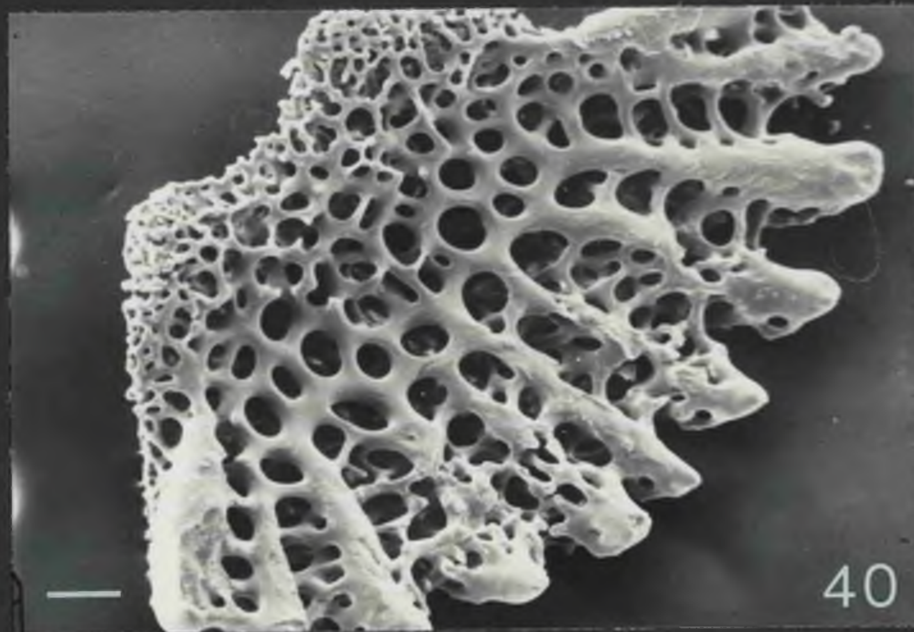
40

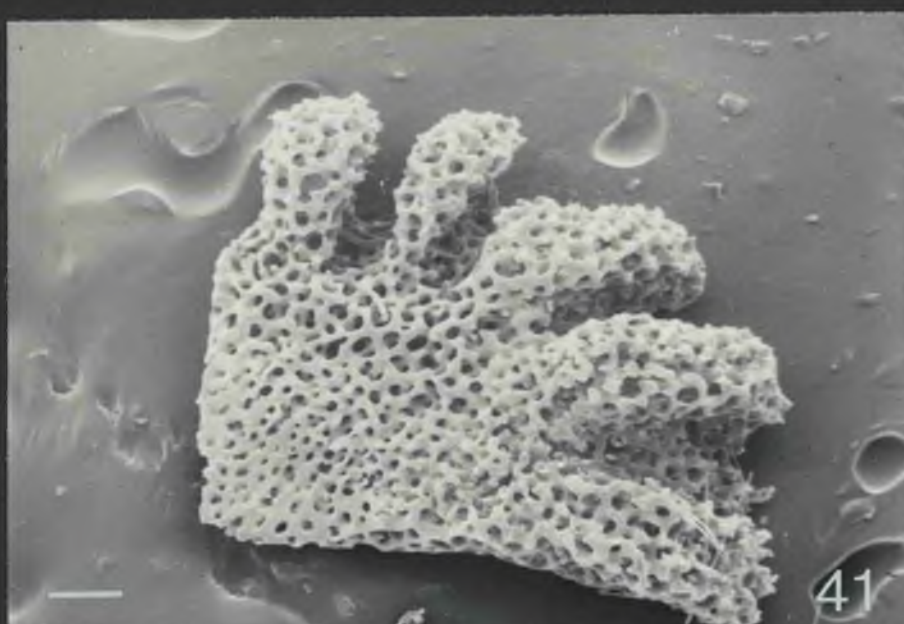
41

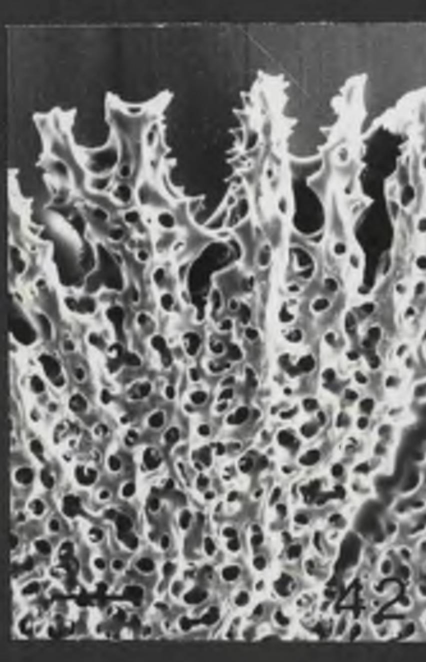
42

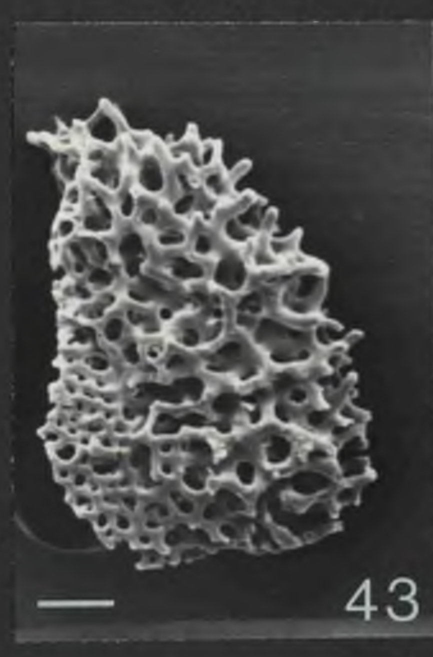
43

Fig. 44

Granule microstructure - PTF plate

__P. miliaris__

Scale 30μ

Fig. 45

Tubercle microstructure - Madreporite

__E. chloroticus__

Scale 55μ


44

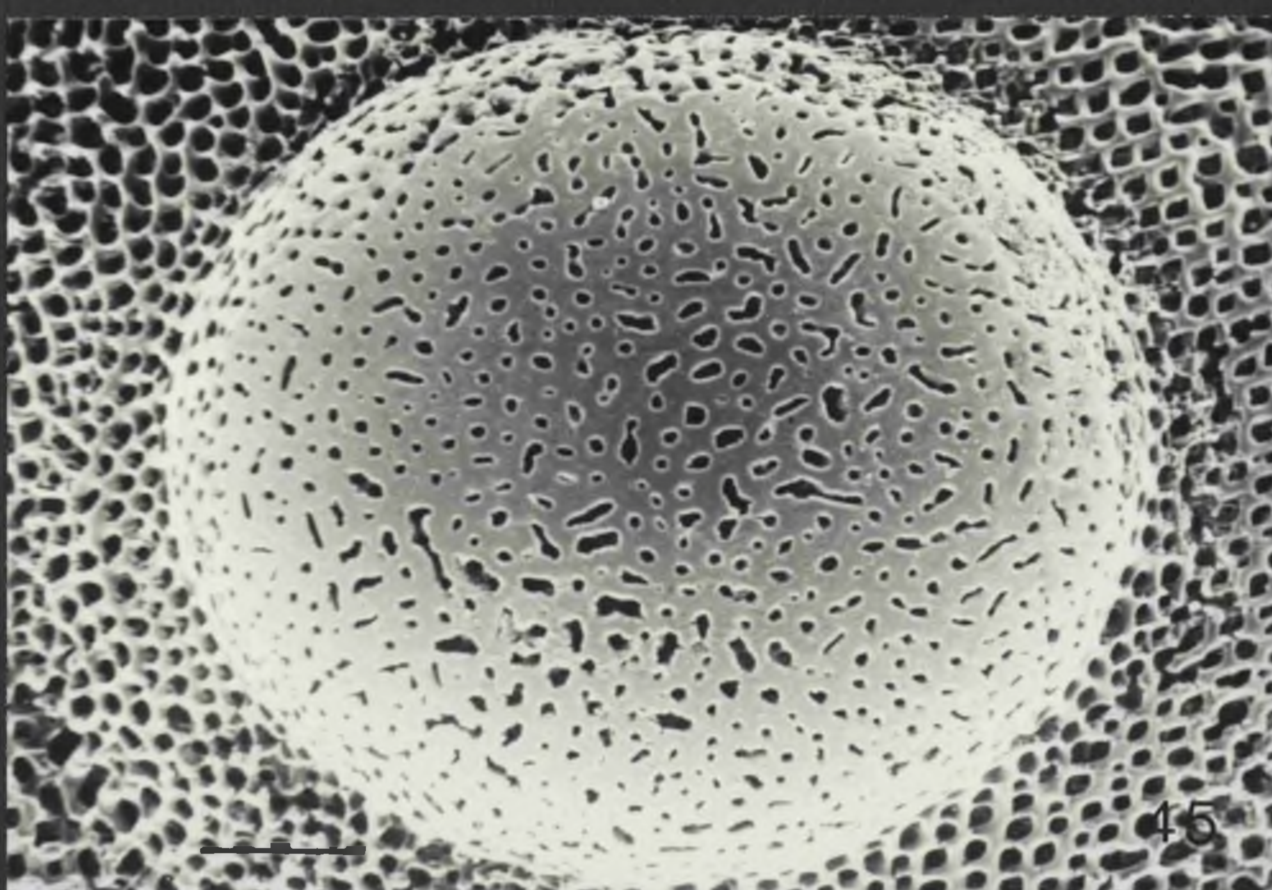
45

Fig. 46

T.S. madreporic canals

The section passes through the upper canal at a more proximal level - note the difference in the endothelia and the presence of intensely staining secretory cells.

Semithin. Azure/MB

Scale 20µ

Fig. 47

T.S. madreporic canals

The section passes through more distal levels of the canals - note the progressive thickening of the endothelia

C Cilia.

Semithin Azure/MB

Scale 20µ

Fig. 48

In distal regions of the madreporic canal long cilia project towards the opening of the canal.

Note the electron dense precipitate on the microvilli.

Scale 1µ

Fig. 49

Some cells within the distal endothelia show intense β (white arrow) or γ (black arrow) metachromasia.

C Cilia M Microvilli

Semithin Azure/MB

Scale 10µ

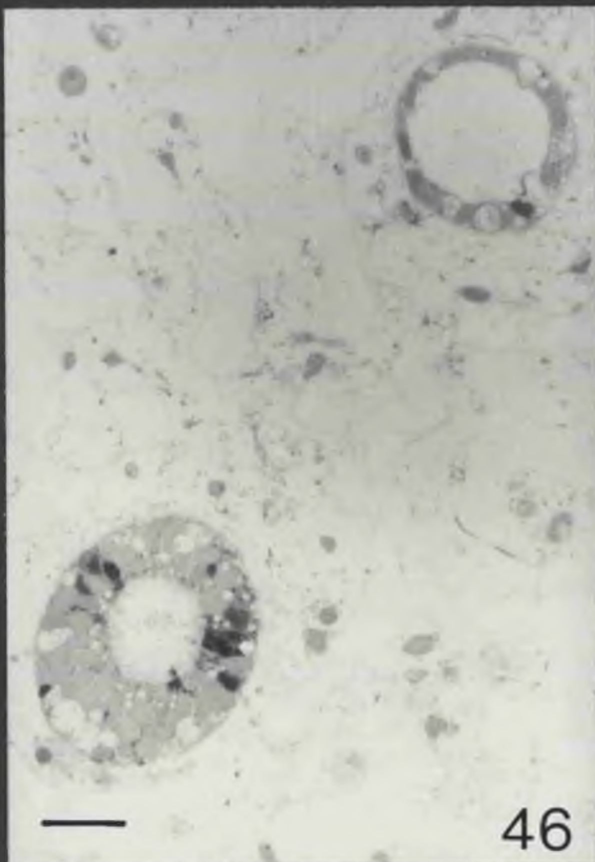
46

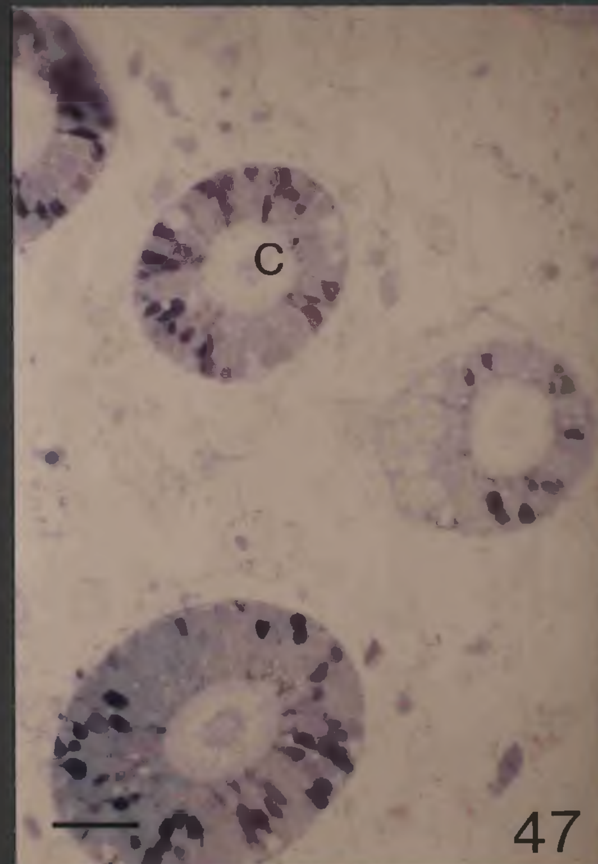
c
47

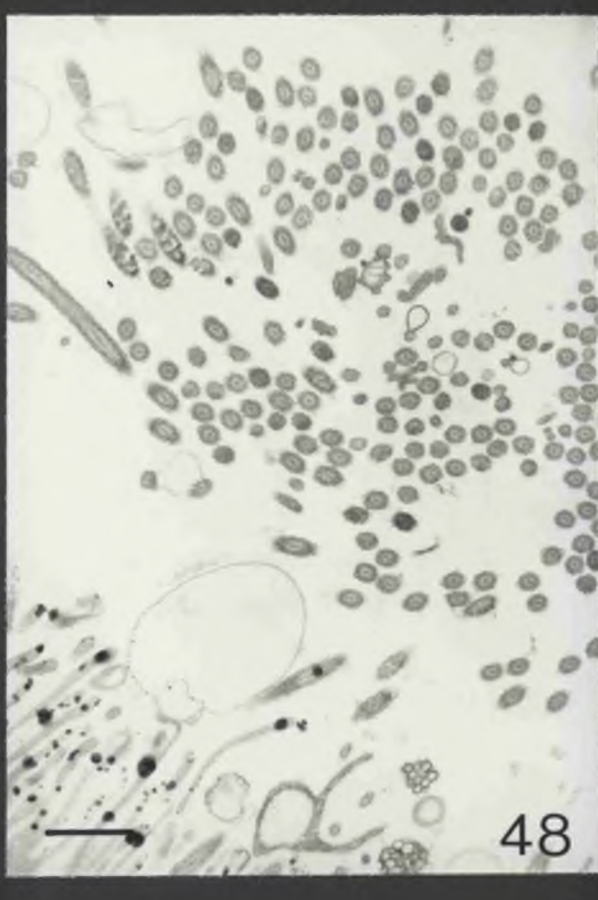
48

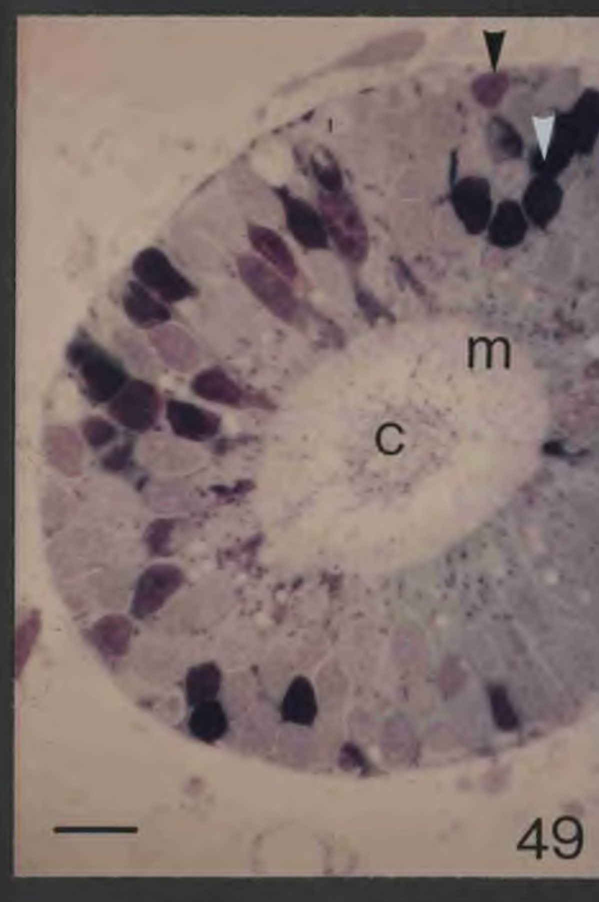
m
c
49

Fig. 50

Inner layer of the axial organ.

a   Axial sinus

e   Endothelial cell

m   Muscle

Scale 2.5μ

Fig. 51

Relationship between inner muscle cell (axial organ) and the connective tissue. Note the bifurcation of the muscle cell (B).

b   Basal lamina

i   Interdigitation

h   Hemidesmosome

Scale 1μ

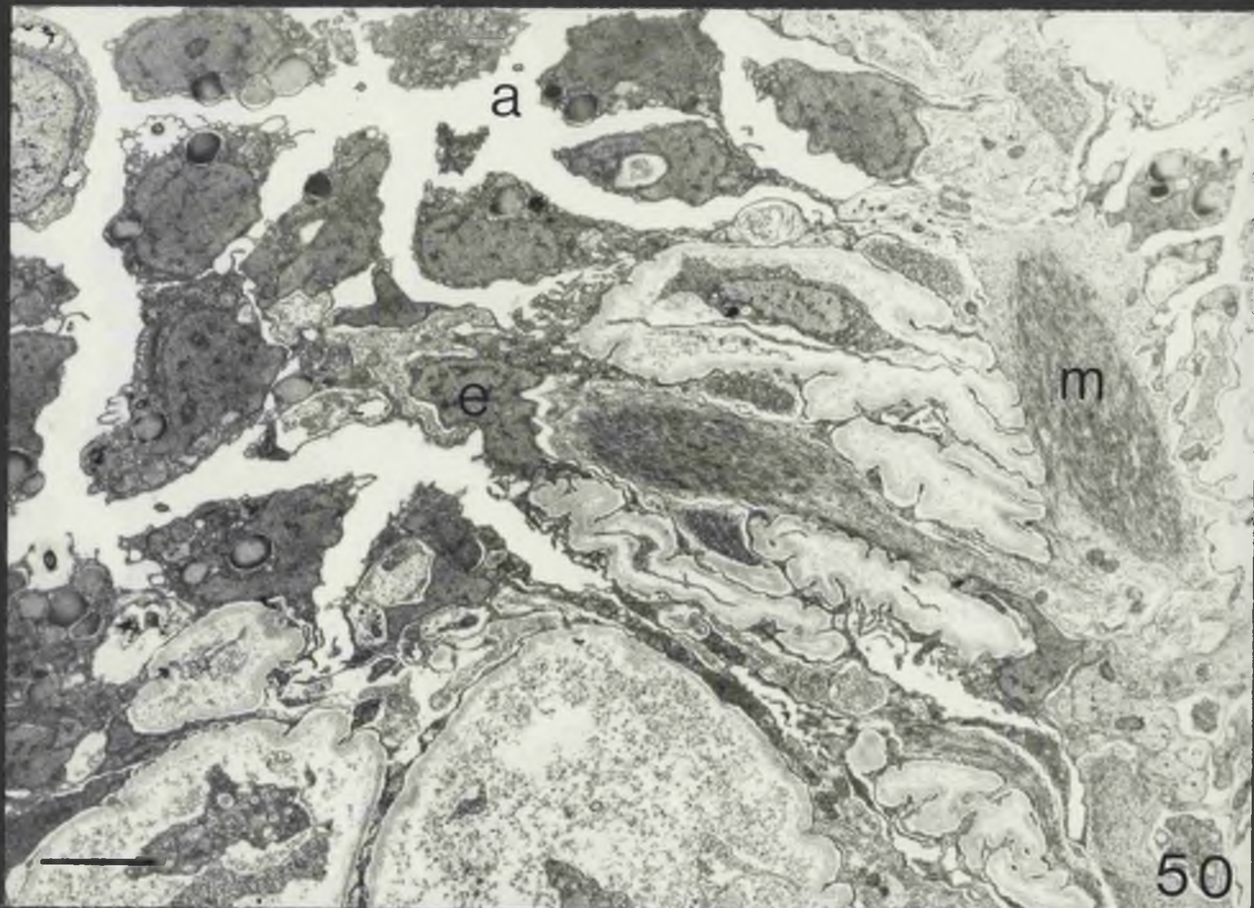
a
e
m
50

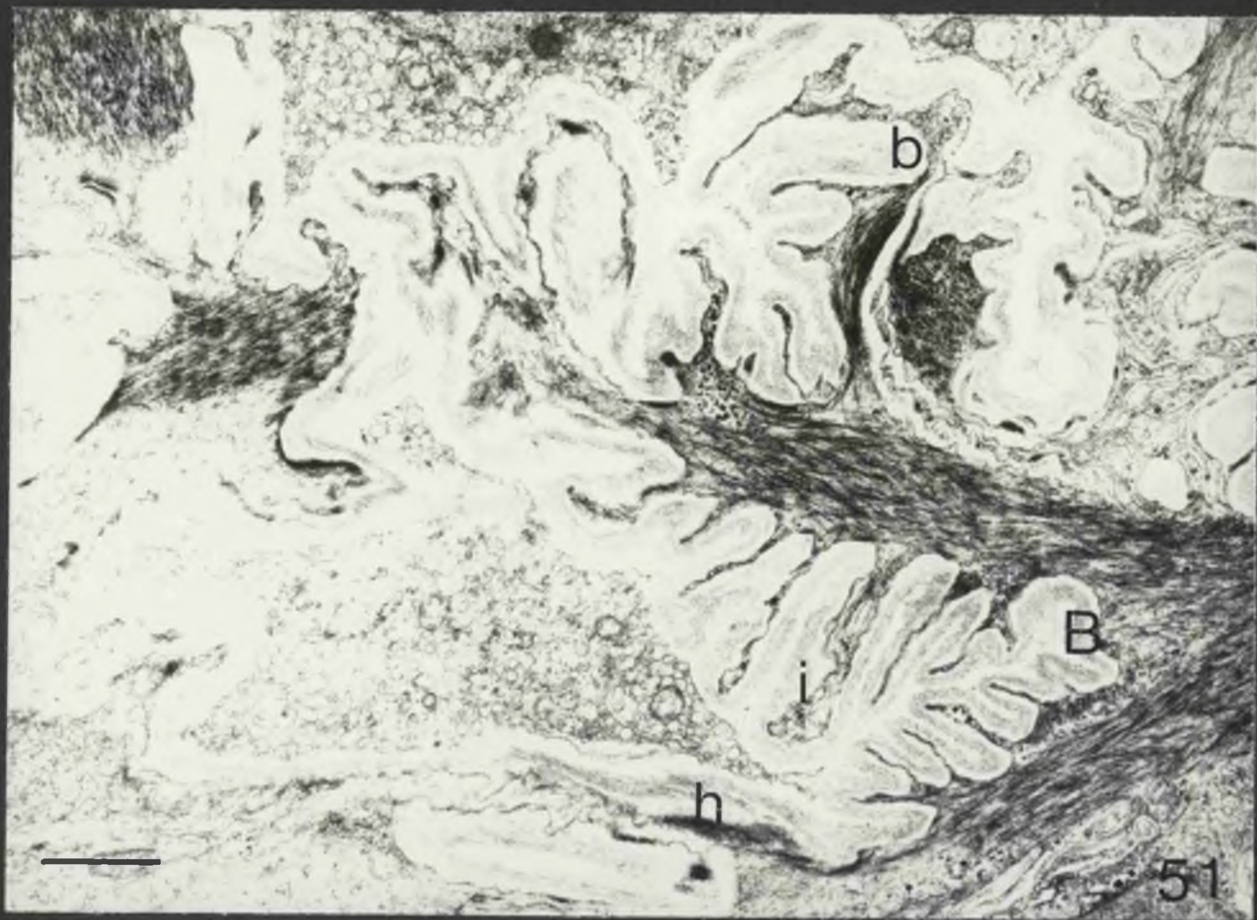
b
B
i
h
51

Fig. 52

The basal lamina separating the inner muscle layer from the connective tissue is composed of numerous fine filaments (f).

Scale 1μ

Fig. 53

Phagocytic cells within the connective tissue of the axial organ.

p Pseudopodia

Scale 1μ


f
52


p
53

Fig. 54

Some amoebocytes (n) appear to be necrosing as they pass through the connective tissue into the axial sinus.

Scale 1μ

Fig. 55

LISG axons (L) innervating inner muscle cells (M) of the axial organ.

l	LISG
S	Sarcolemmal extension over LISG axon
arrow	Neurotubule

Scale 200nm.

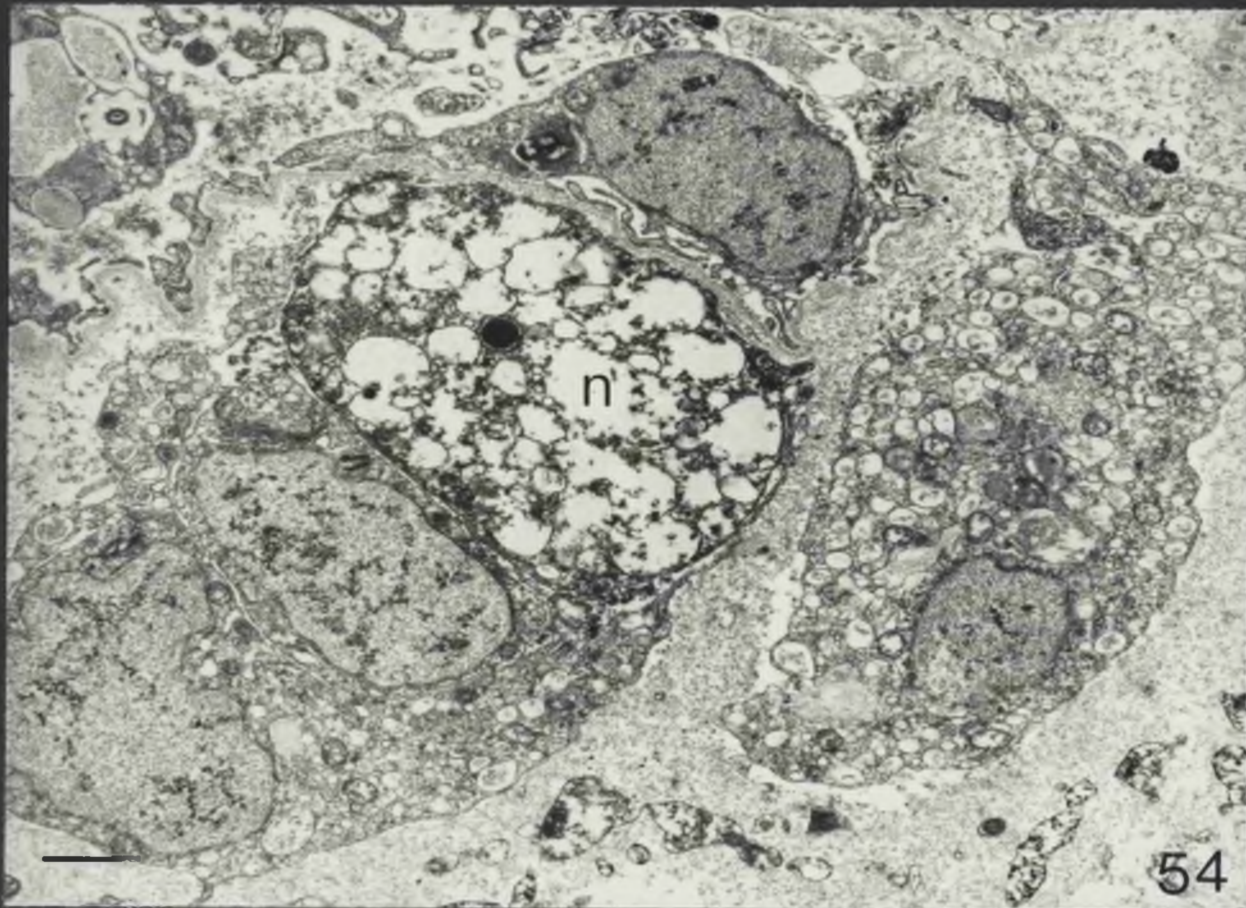
n
54

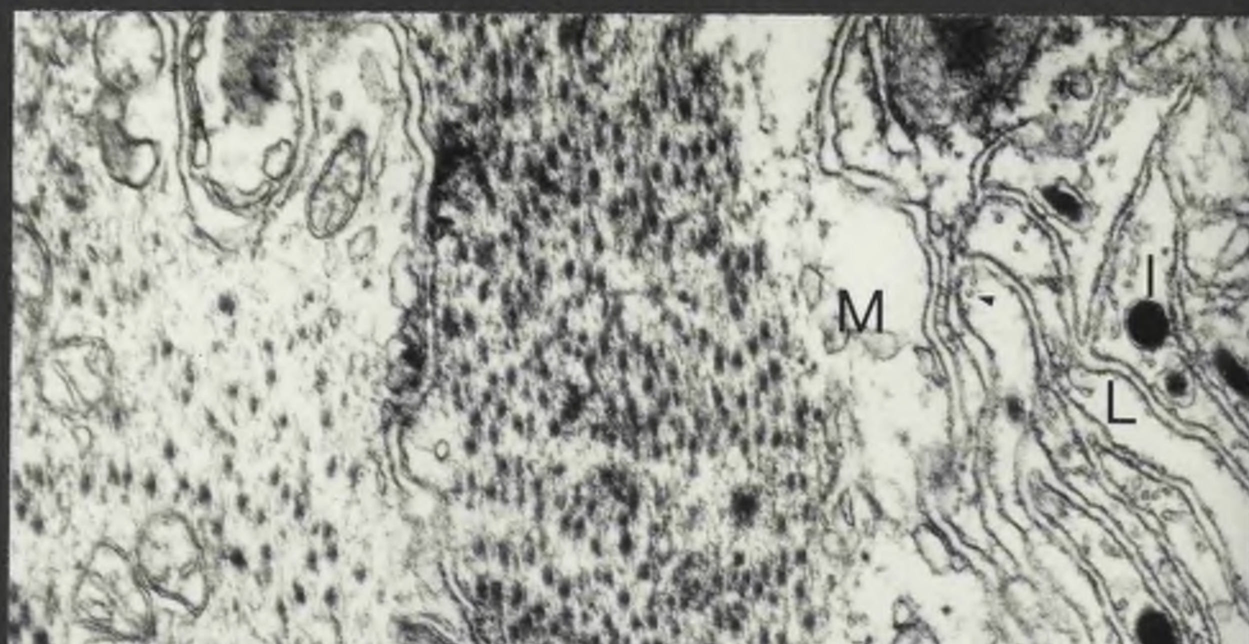
M
l
L
S
55

Fig. 56

Mitochondria (M) in the condensed state were frequently observed in muscle cells after aldehyde fixation.
In some regions of the inner muscle layer LDSG axons form a distinct plexus (P).

Scale 400nm.

Fig. 57

Variation of LDSGs within the connective tissue.

Scale 150nm.

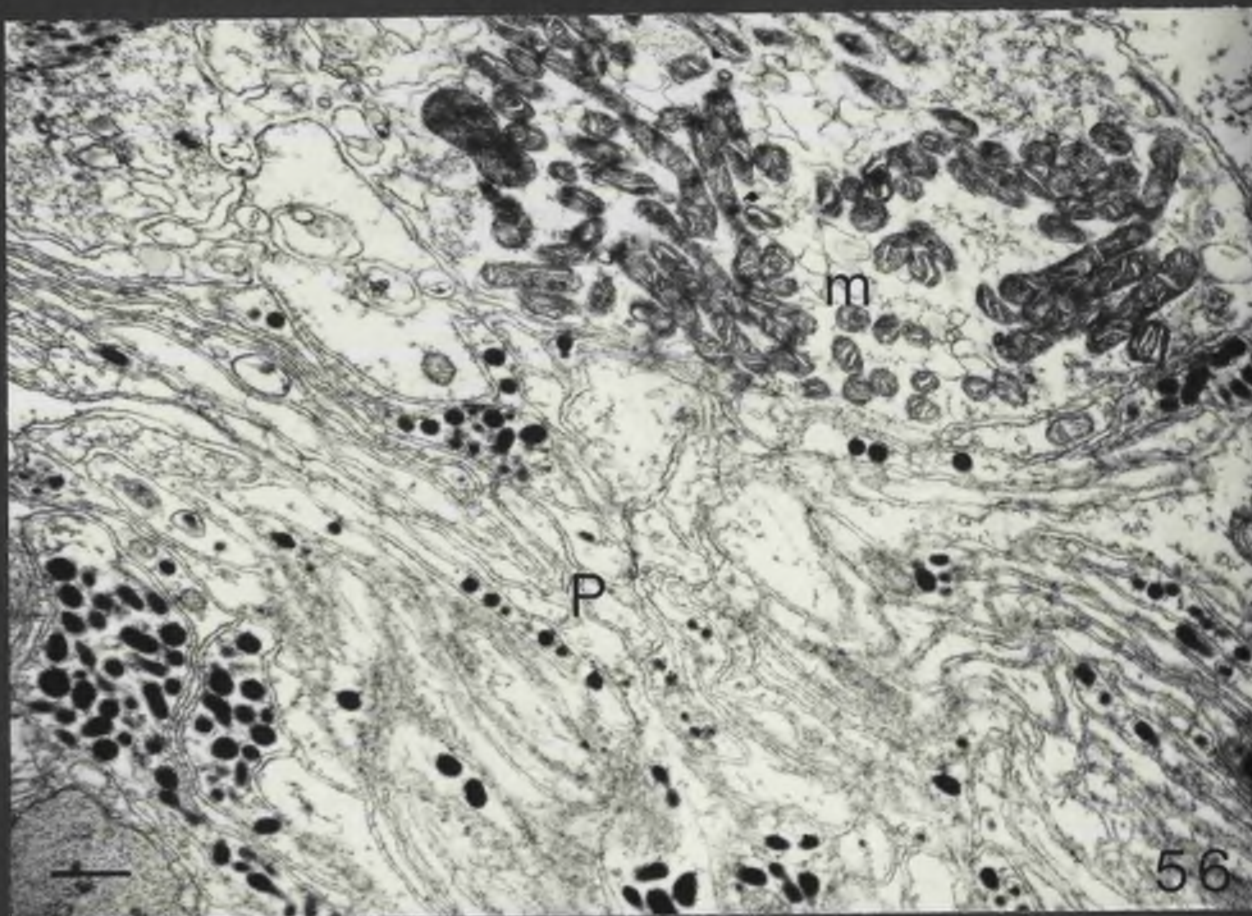
m
P
56

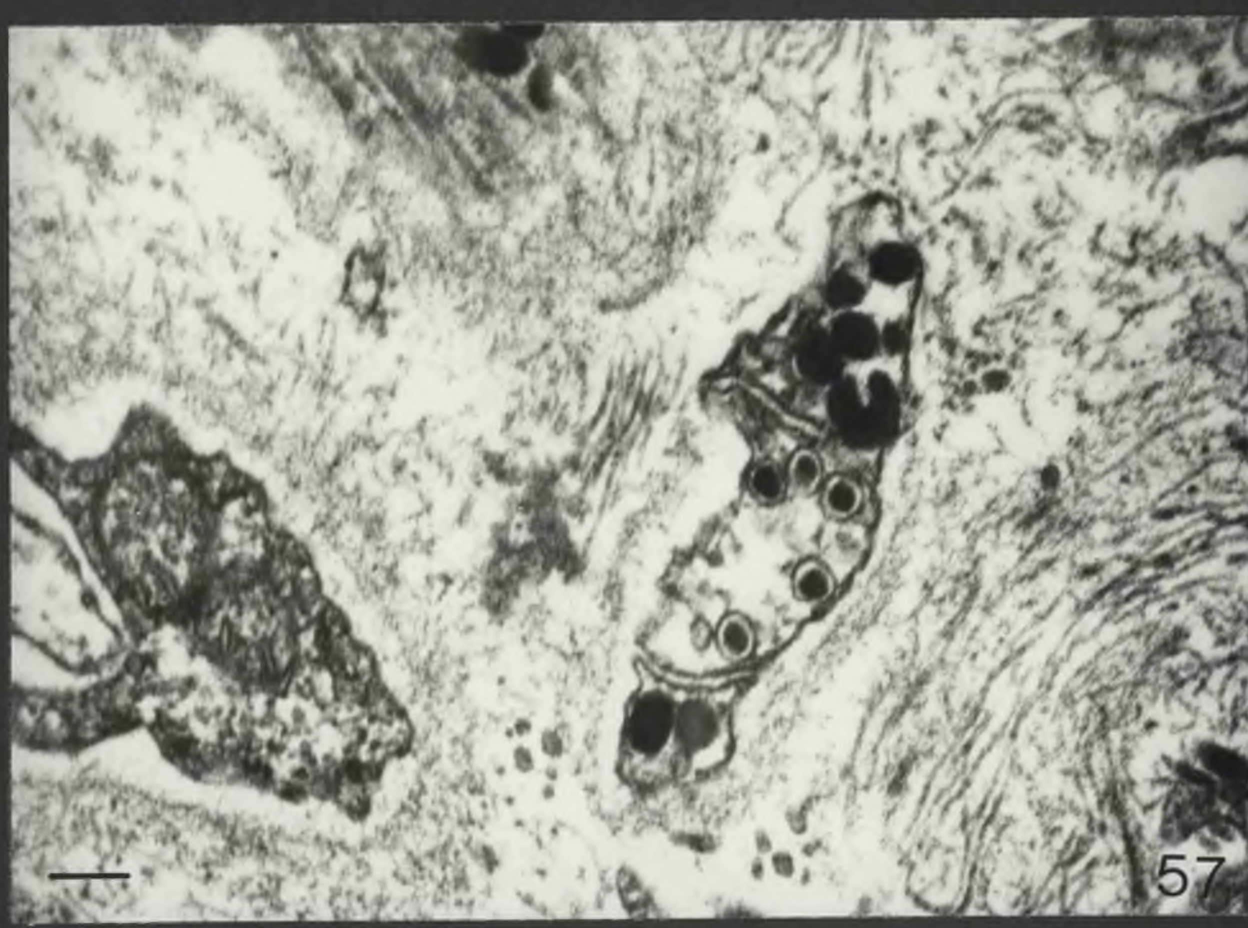
57

Fig. 58

T.S. Axial organ, prepared for localisation of biogenic monoamines.

The more intense fluorescence is specific (s) and occurs within the basiepithelial plexus. The less intense fluorescence is non-specific (N).

a Axial sinus

m Mesentery

S Stone canal

Scale 20μ

Fig. 59

Colour photomicrography clearly shows the difference between specific (S) and non-specific fluorescence (n).

Scale 25μ

Fig. 60

Na-monoborohydride reduction extinguishes specific fluorescence.

Scale 25μ

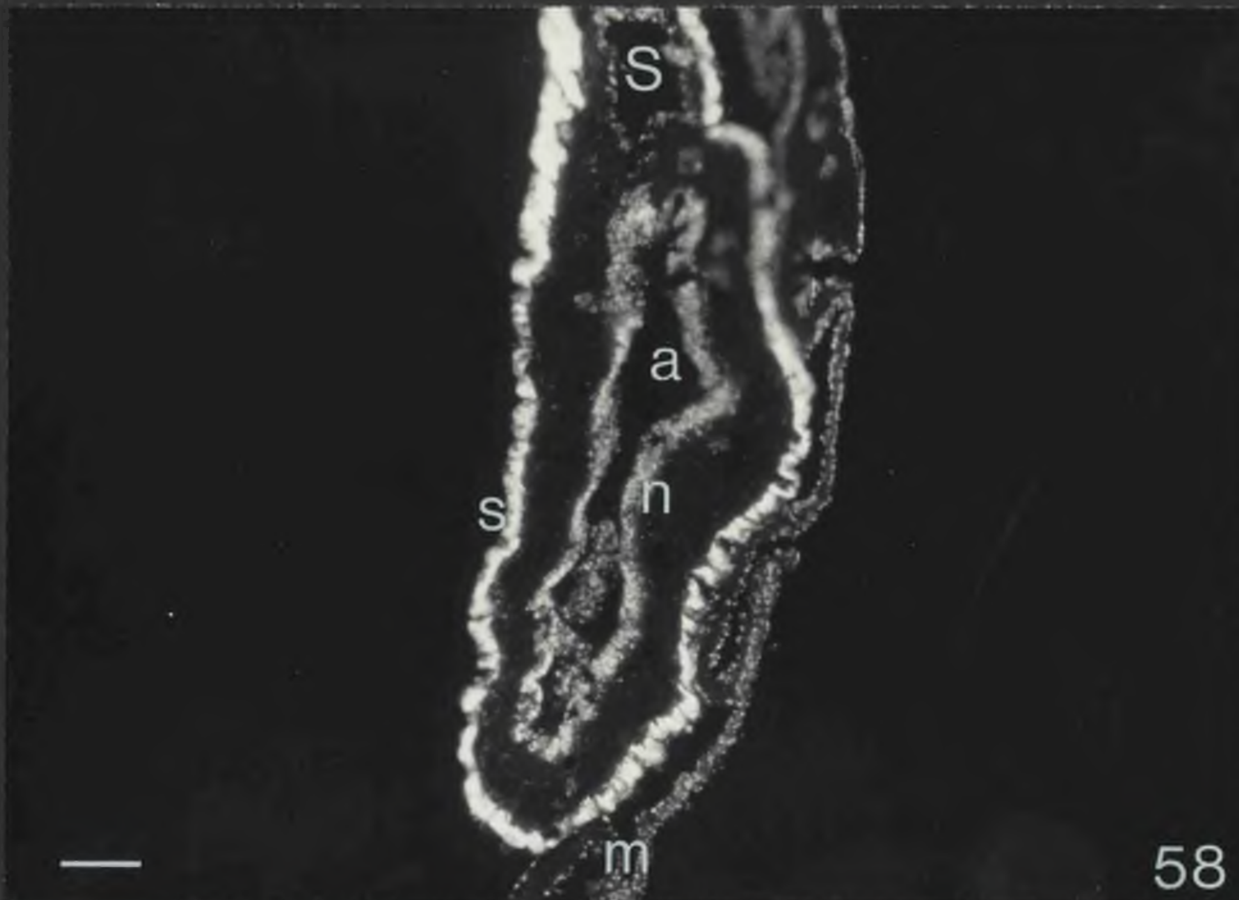
S
a
s
n
m
58

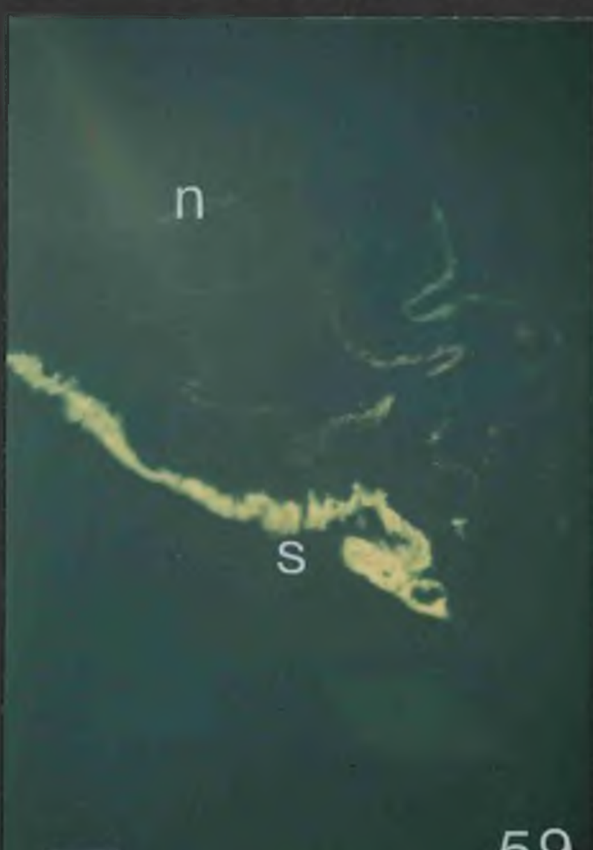
n
s
59


60

Fig. 61

T.S. axial complex, prepared for histochemical localisation of biogenic monoamines.

Note thickening of the nerve plexus in region of stone canal (S).

a autofluorescent bodies

Scale 20μ

Fig. 62

Arrows indicate axon bundles within the outer epithelia of the axial complex. Similar bundles are not observed within the endothelia (e) lining the axial sinus.

Scale 20μ

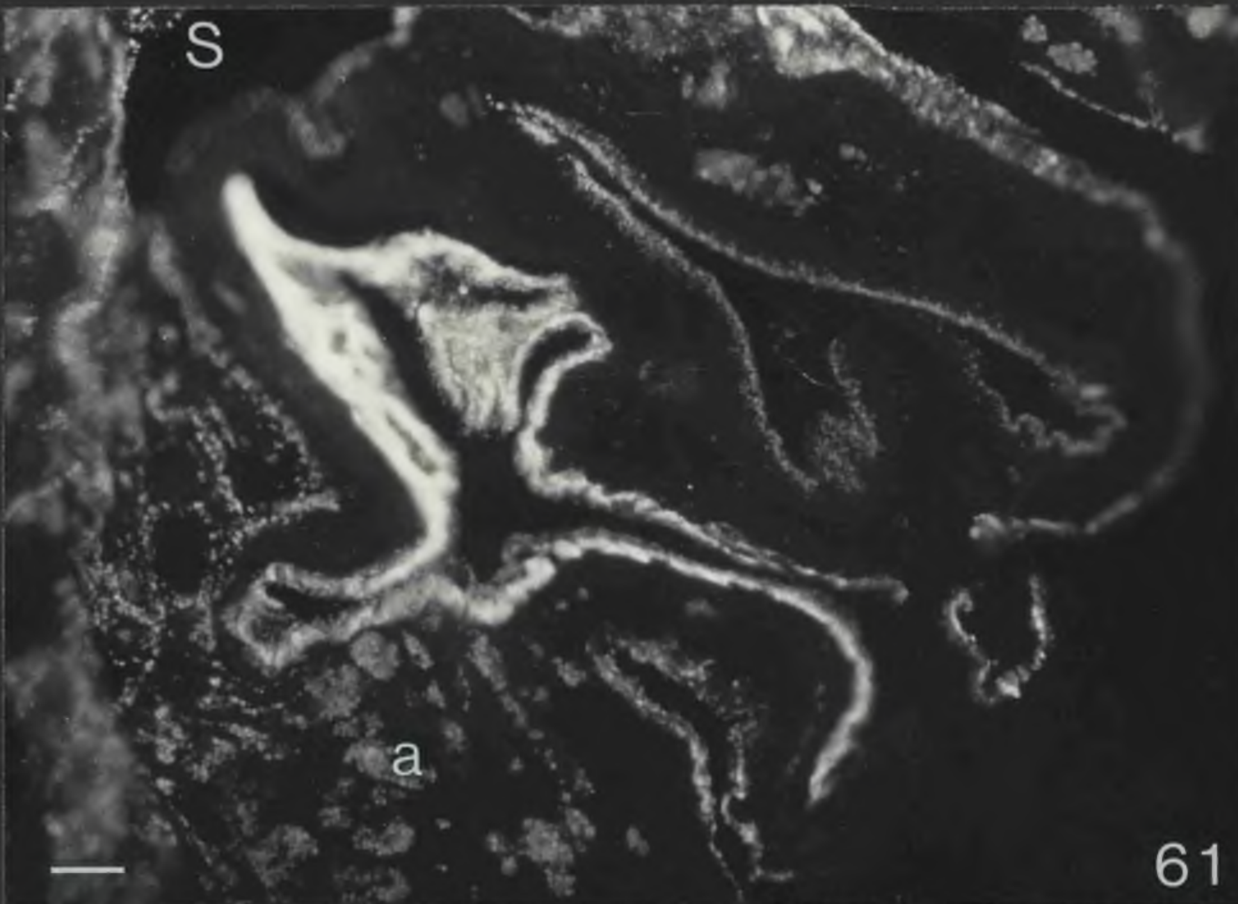
S
a
61

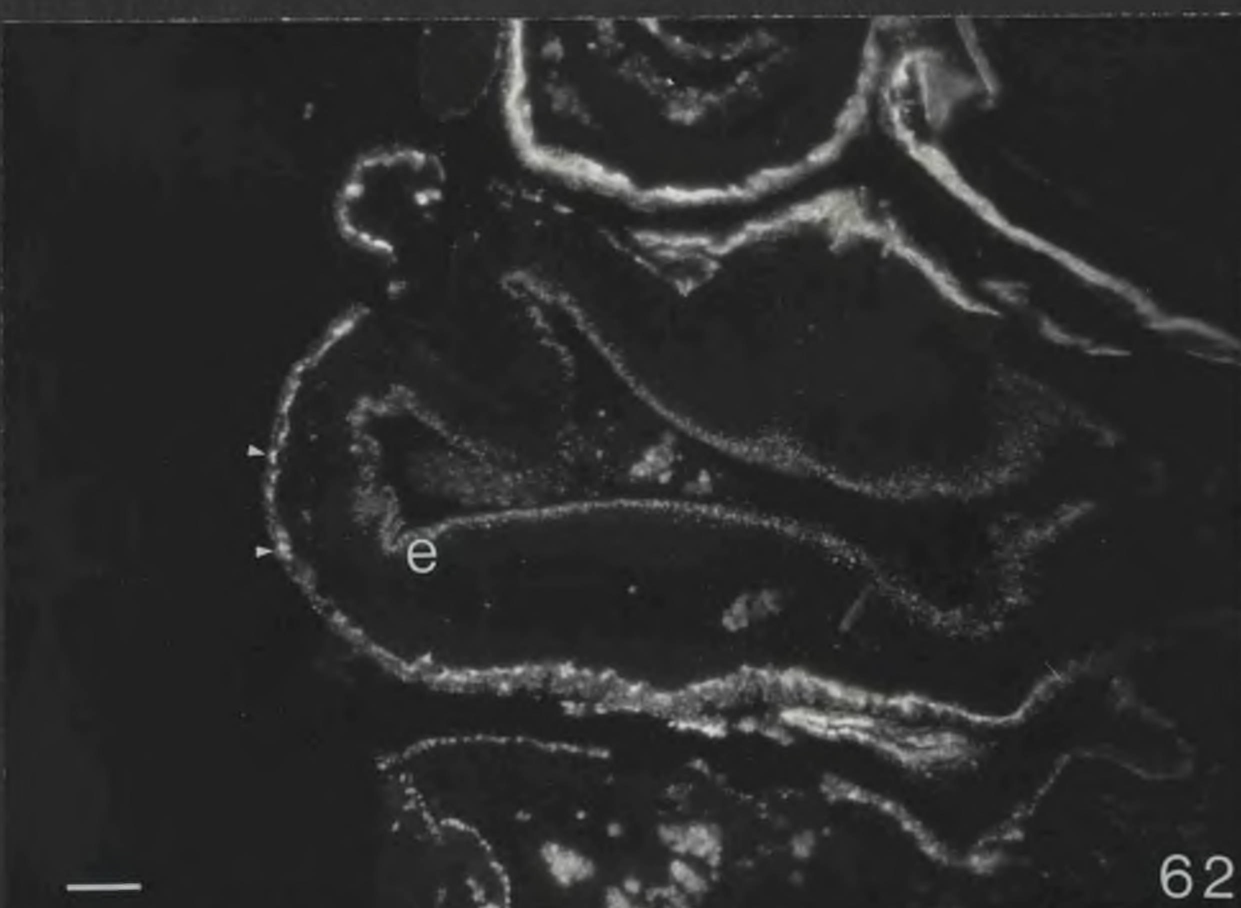
e
62

Fig. 63

T.S. proximal region of axial complex showing extensive aminergic nerve plexus around axial haemal vessel (h) and stone canal (S).

Scale 20µ

Fig. 64

T.S. inner layer of stone canal

a Amoebocyte

e Endothelial process

M Muscle cell body

Note that myofilaments occur within small extensions (arrow) in addition to the perinuclear region.

Scale 1µ

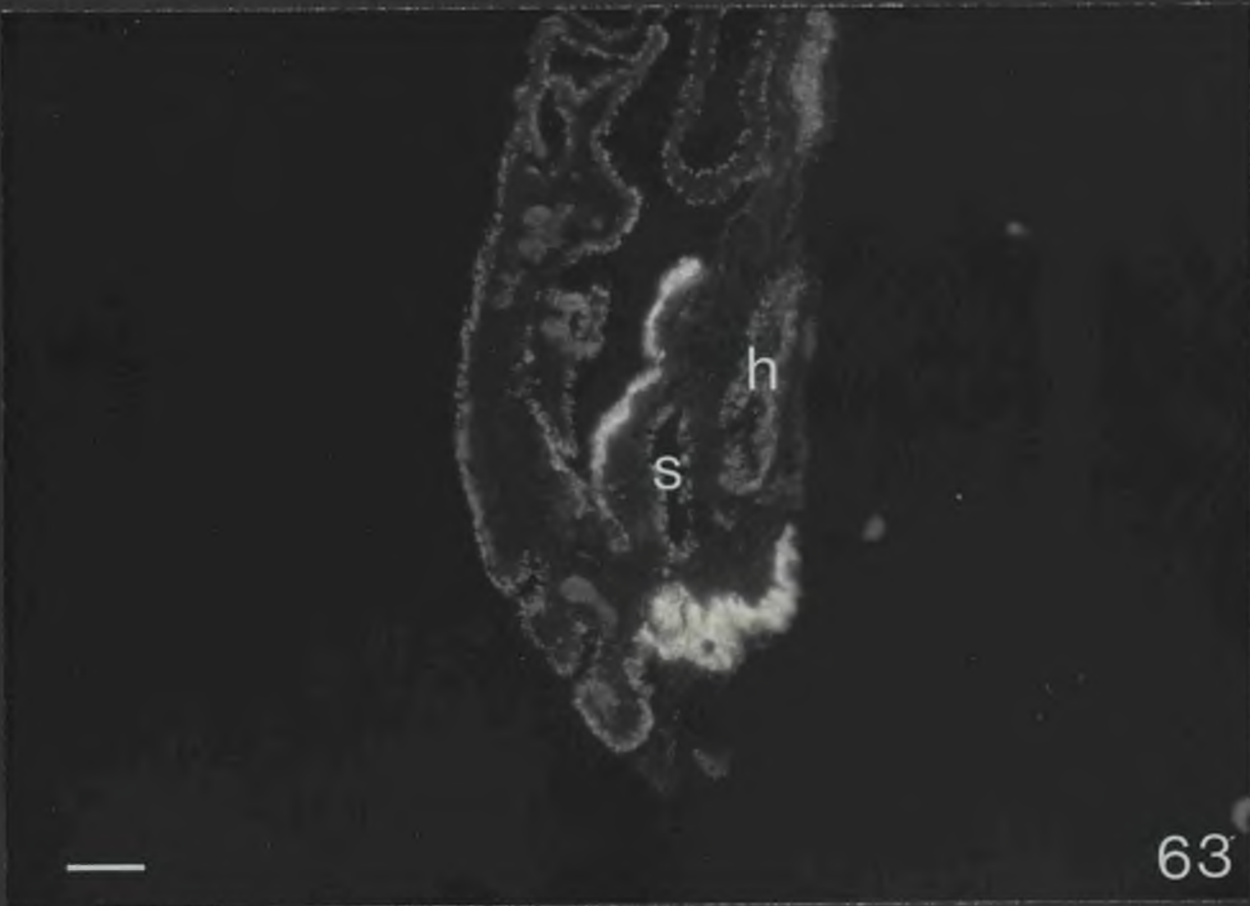
h
s
63

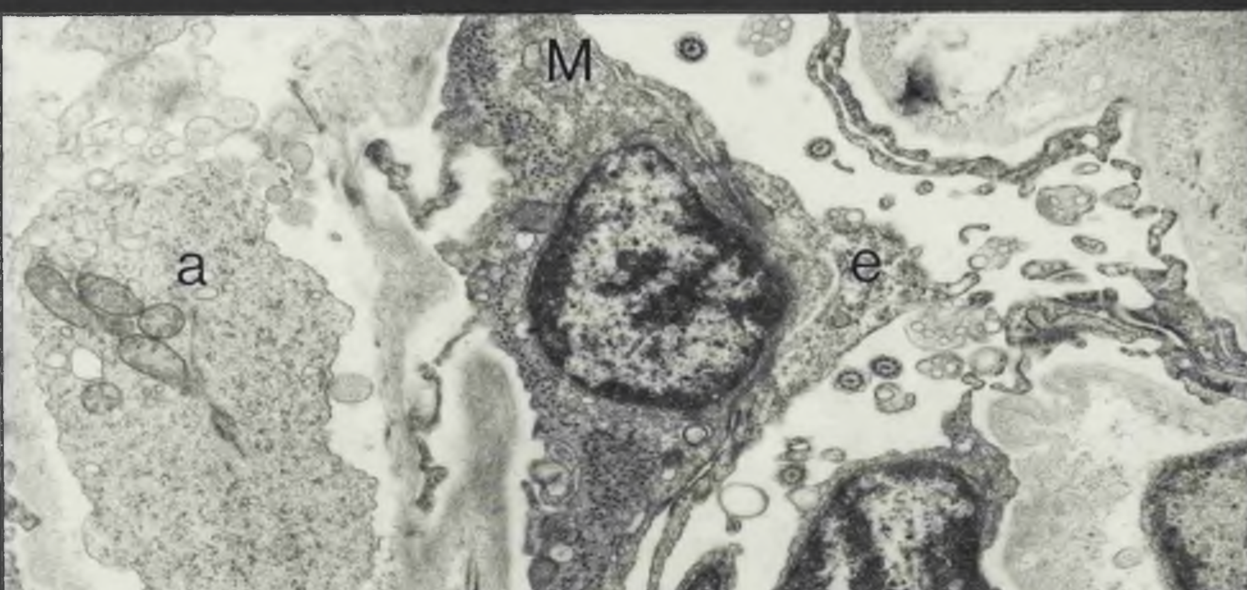
M
a
e
64

Fig. 65

Degenerating muscle cells(M) passing into the lumen of the stone canal.

Scale 400nm

Fig. 66

The outer epithelium (e) of the polian vesicles is underlain by numerous basiepithelial axons ([illegible]) containing DCVs.

Scale 1μ

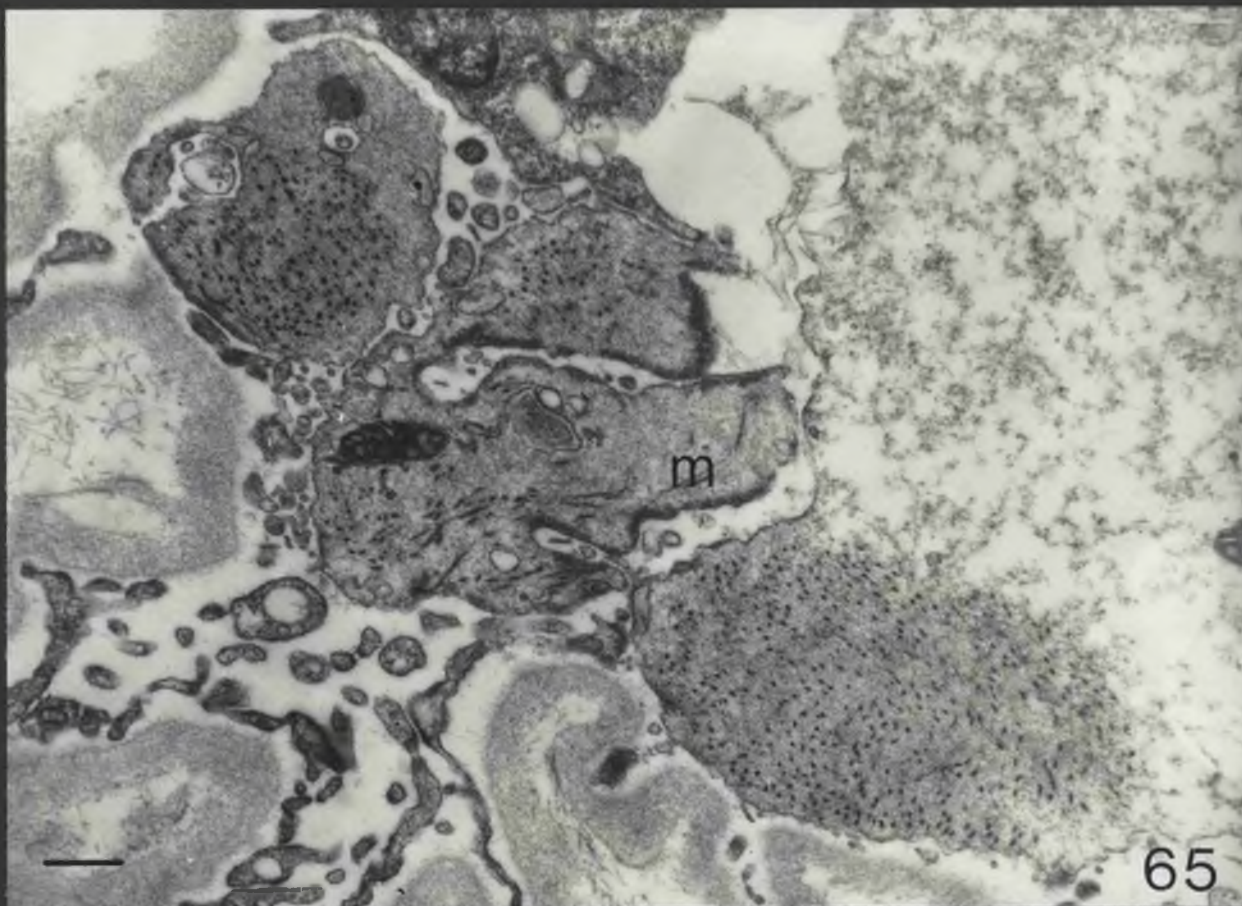
m
65

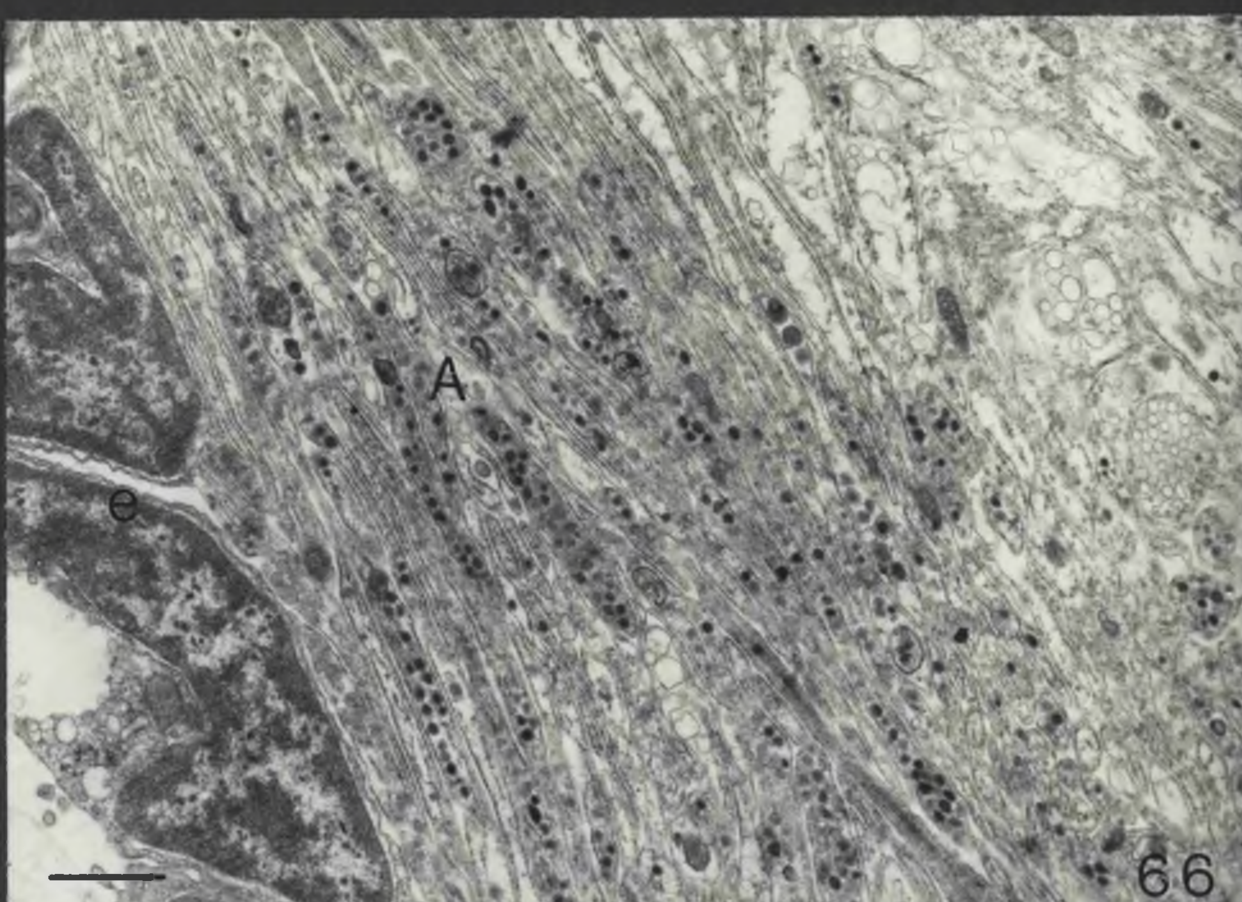
A
e
66

Fig. 67

Amoebocyte (a) and fibrocyte (f) within the connective tissue matrix of a polian vesicle.

Scale 2µ

Fig. 68

One type of amoebocyte (similar to above) is characterised by vacuoles surrounded with electron dense granular material (g). Another type of amoebocyte, the morula cell (m) is characterised by large electron opaque spherules containing dense bodies and lamella structures (arrow) probably representing lytic bodies at different stages of activity.

Scale 1µ

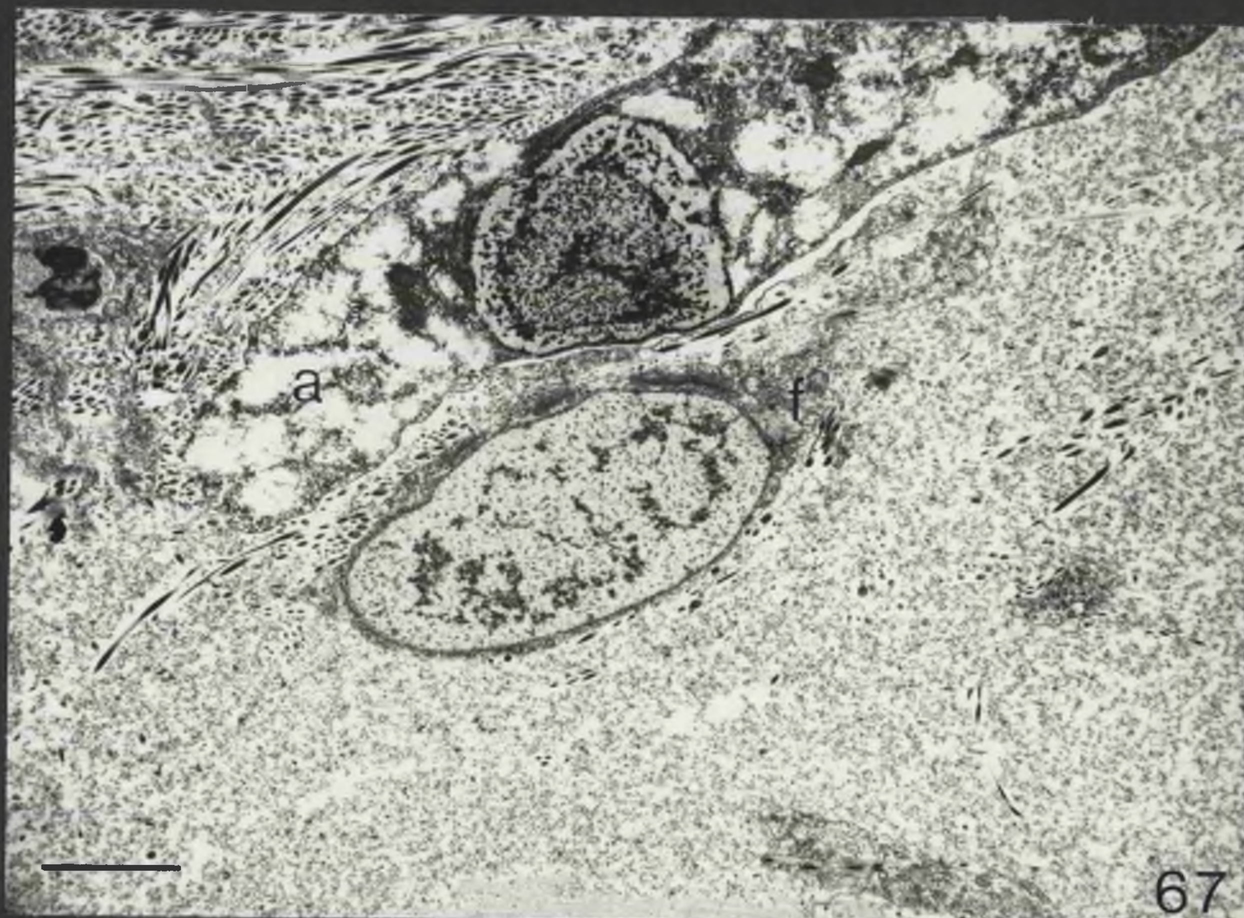

67

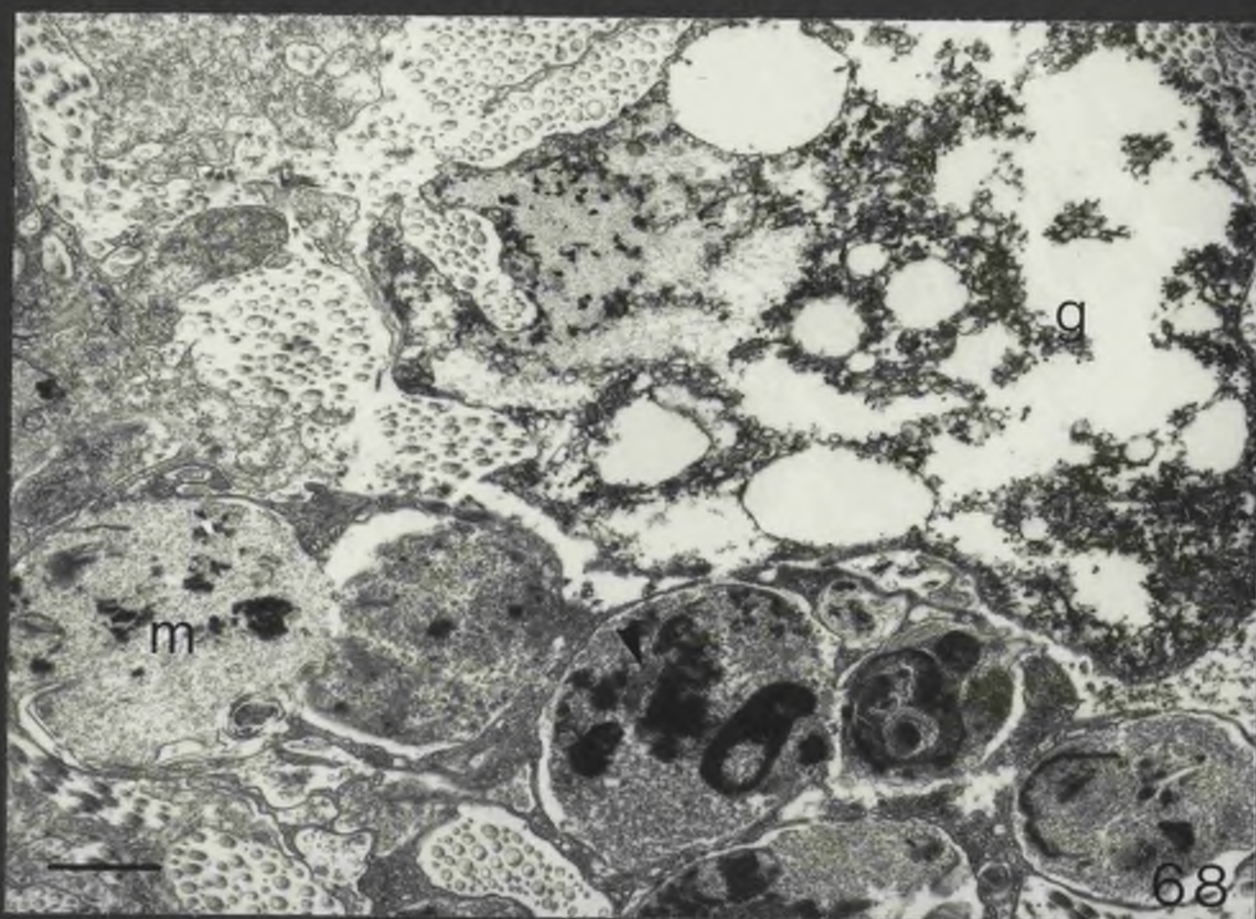

68

Fig. 69

Amoebocytes (A) and vacuolar processes (V) passing into the lumen of the polian vesicle.

Scale 1μ

Fig 70.

Outer epithelia of the descending branch of the radial water canal.

B Basal collar structure - note the ring, spokes radiating from peripheral doublets, and terminal dense bodies

f Fuzz coat

l Lamellae forming collar around cilium

Scale 1μ

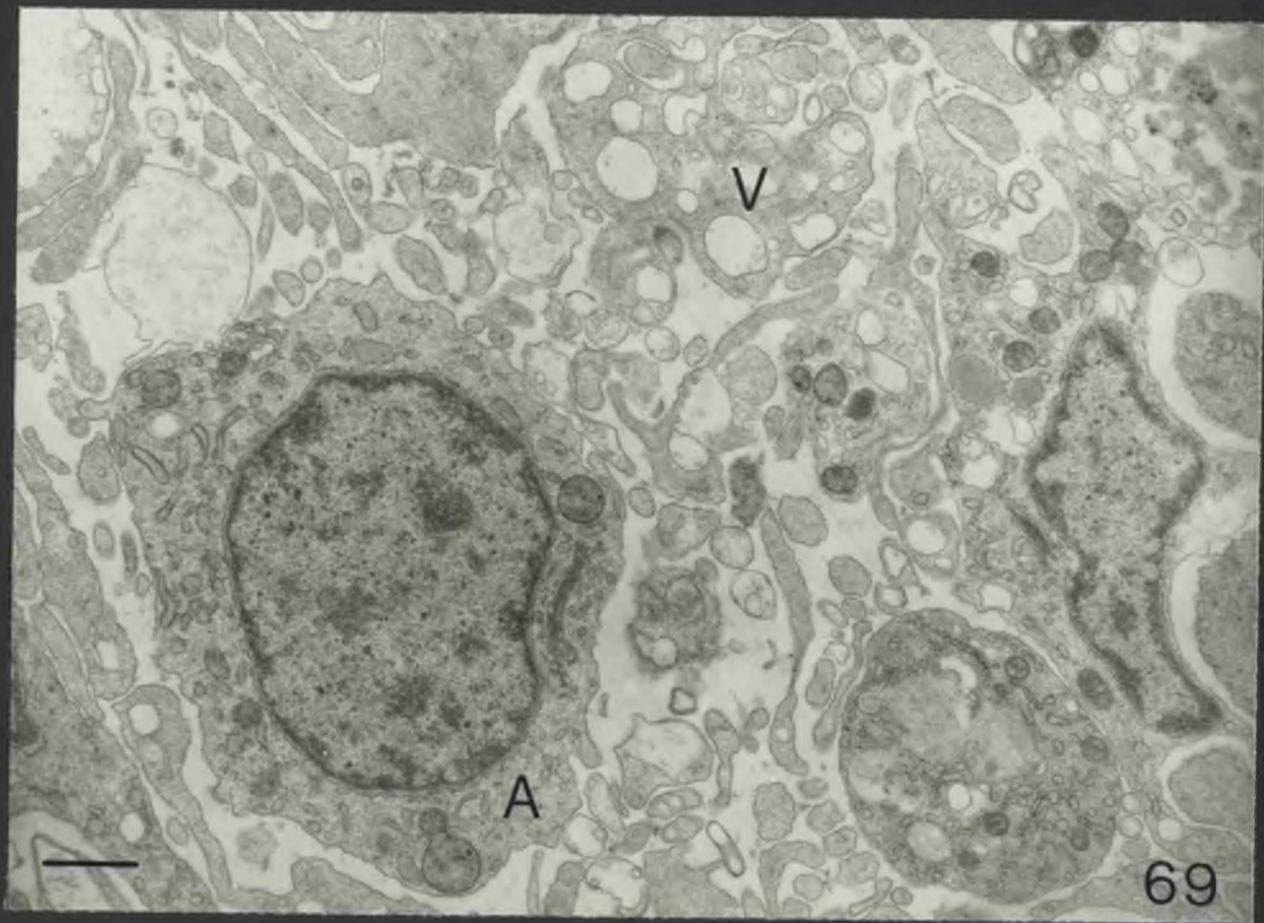
V
A
69

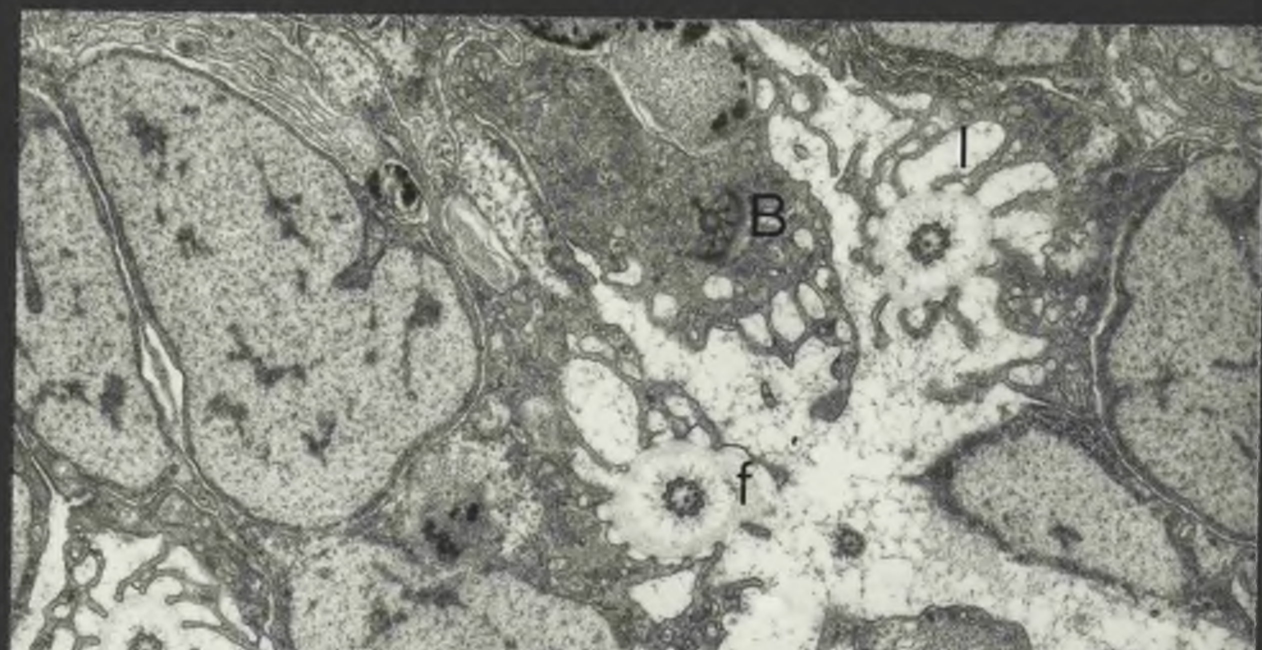
I
B
f
70

Fig. 71

Choanocyte cells - outer epithelia of radial water canal

l	Radial lamella with microvillous ending
v	Vacuole

Scale 300nm

Fig. 72

Ciliary basal apparatus of choanocyte cell.

c	Centriole
f	Filaments extending from fuzz coats
r	Rootlet
arrow	Peripheral tubules

Scale 500nm

Inset: Transition zone is of the type II Metazoan form (PITELKA 1974)

Arrow indicates basal plate

Scale 1u

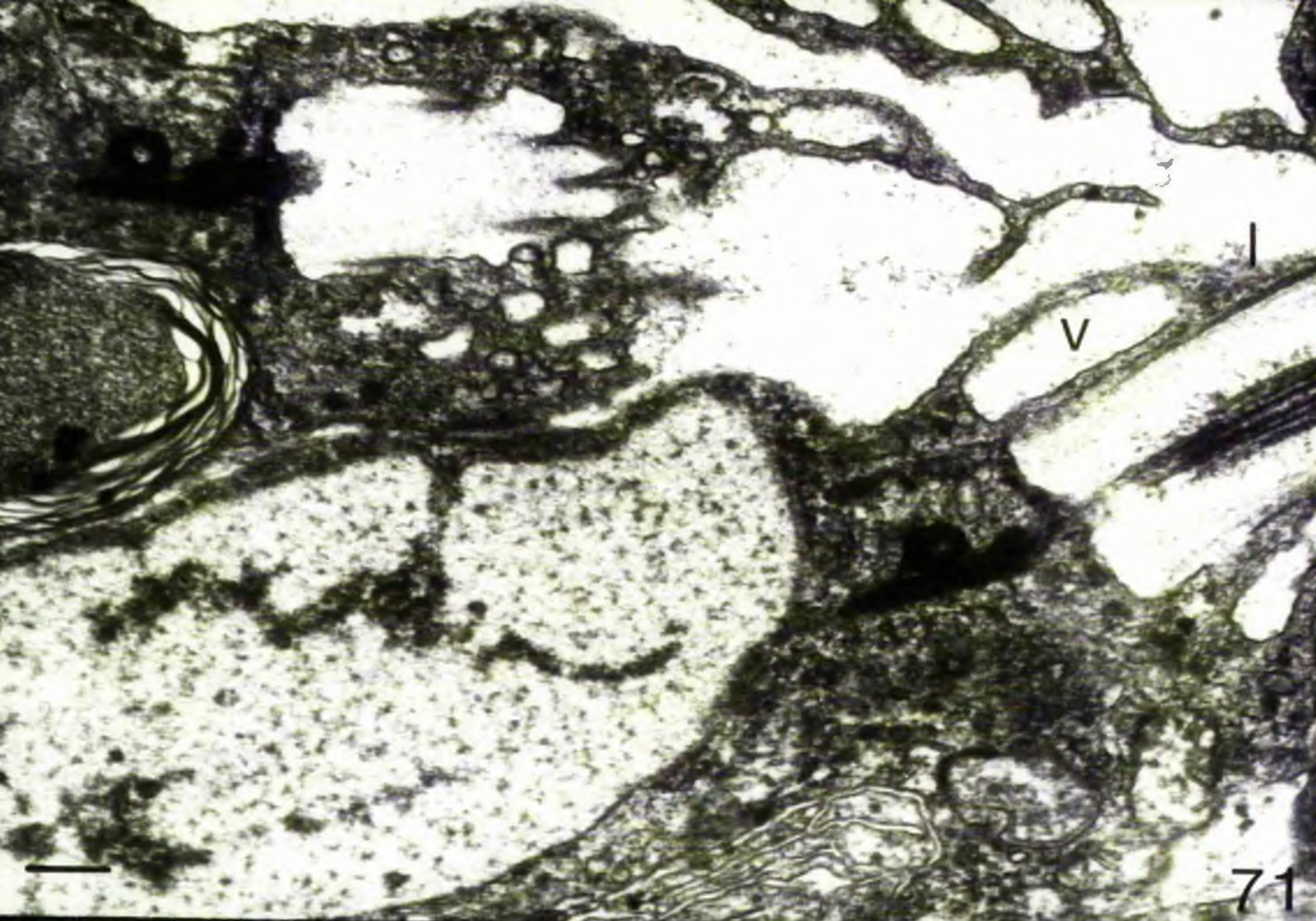

l
v
71

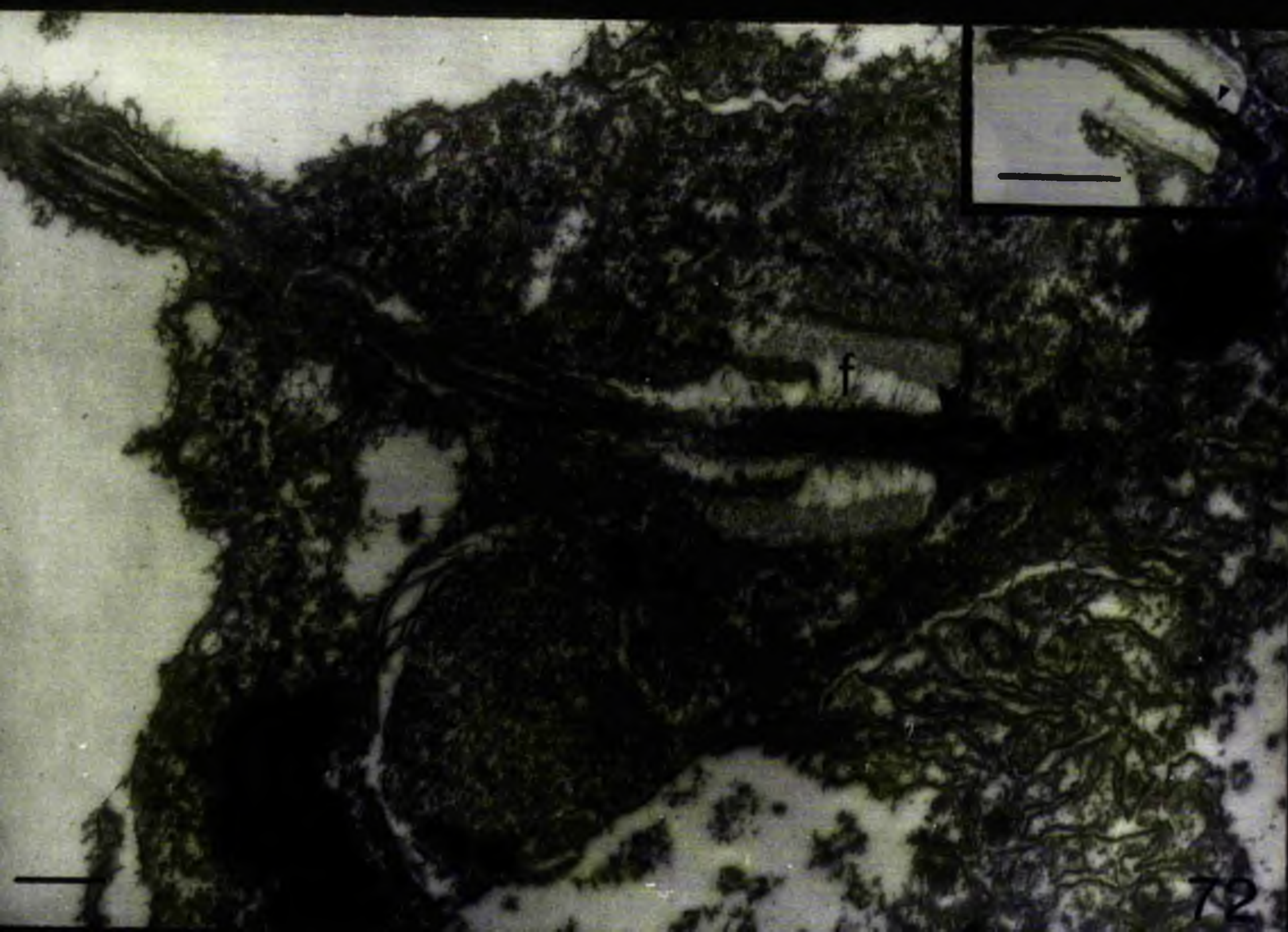

f
72

Fig. 73

Basiepithelial plexus, radial water canal.

A Axon bundle

E Epithelia

Scale 1μ

Fig. 74

Two axon bundles separated by an epithelial process (e) which is anchored to the basal lamina by means of a 'foot' (F). Note the difference in ultrastructure between the epithelial process and the axons.

Scale 500nm


E
A
73

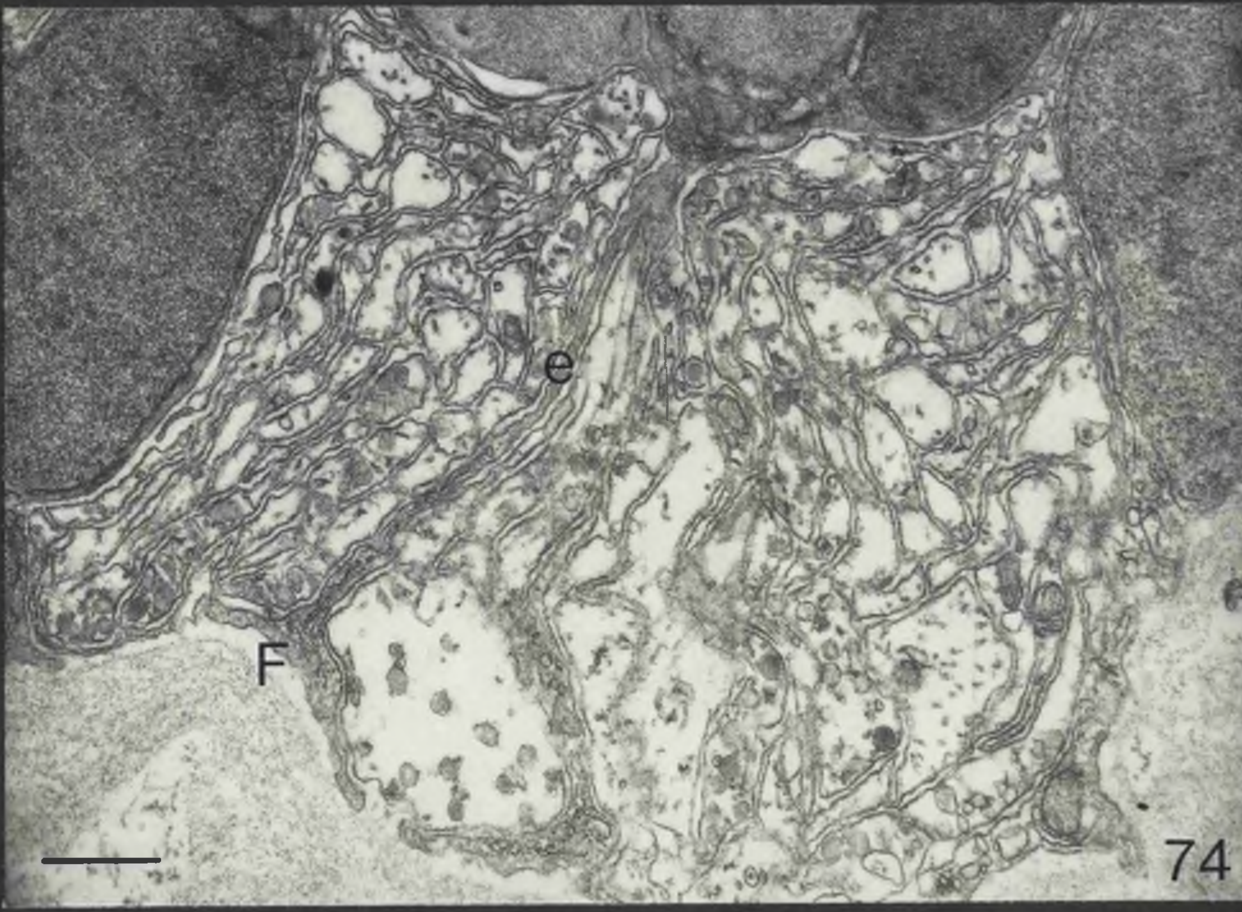
e
F
74

Fig. 75

A tract (T) of very small basiepithelial axons passing between an epithelial cell body and the basal lamina.

Scale 150nm

Fig. 76

A single axon forming synaptoid contacts (S) on two adjacent epithelial cells. It is also possible to interpret this micrograph as two synaptoid contacts on a single cell(?)

Scale 300nm

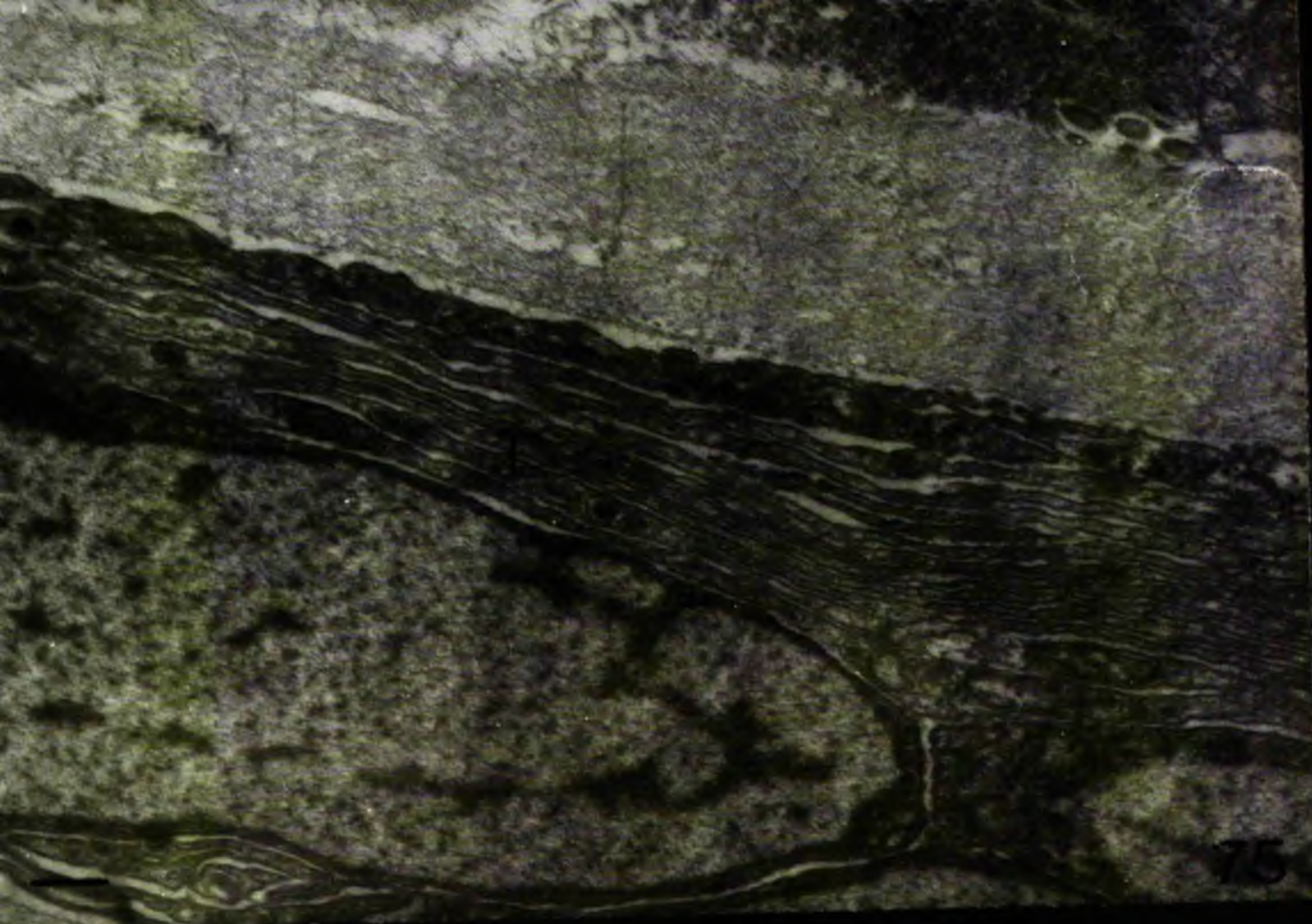
75

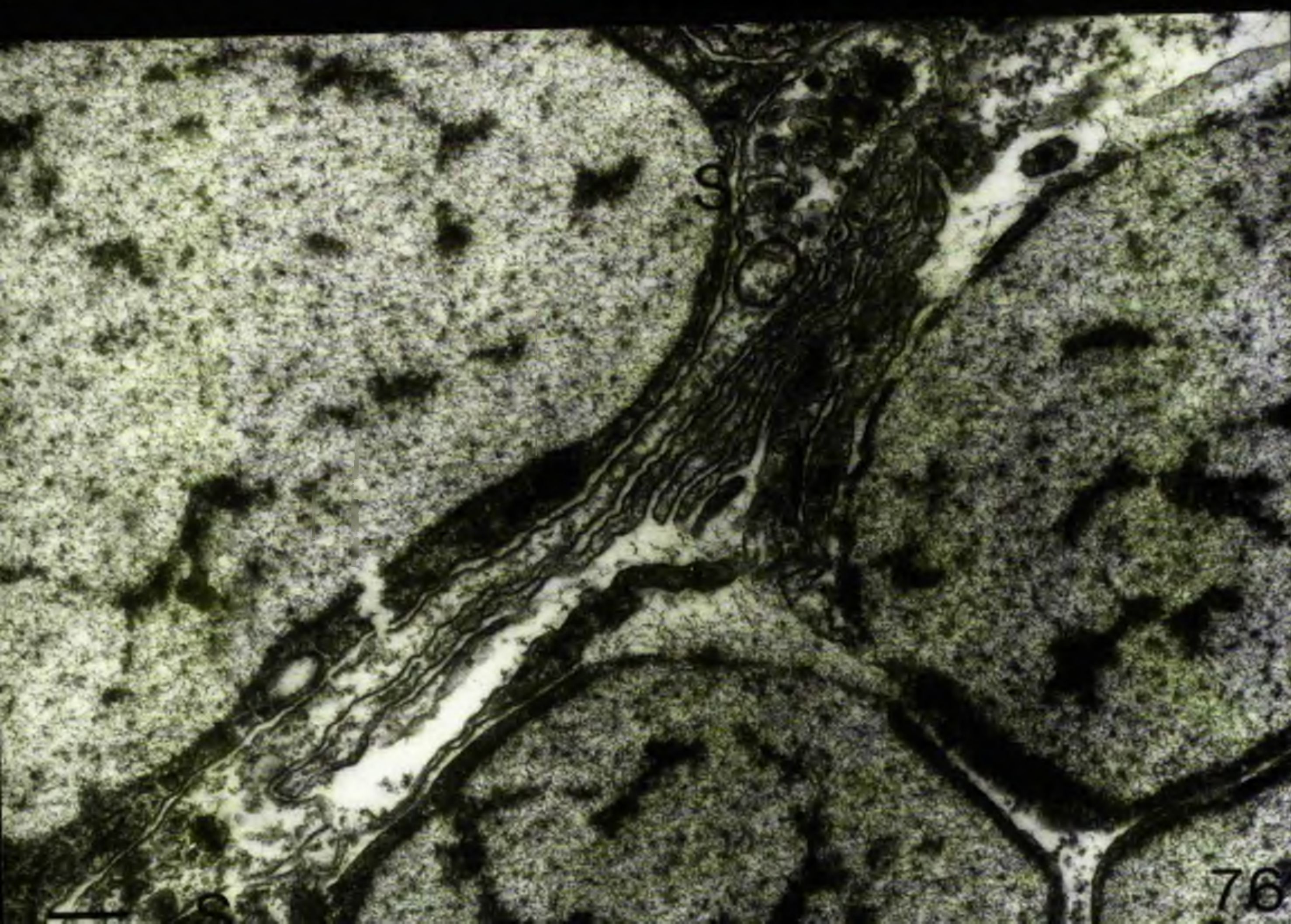

76

Fig. 77

Synaptoid varicosity containing LCVs (L) and CVs (C).

Scale 150nm

Fig. 78

Varicosity (V) containing several LCVs and CVs abutting against the epithelial cell.

Scale 300nm

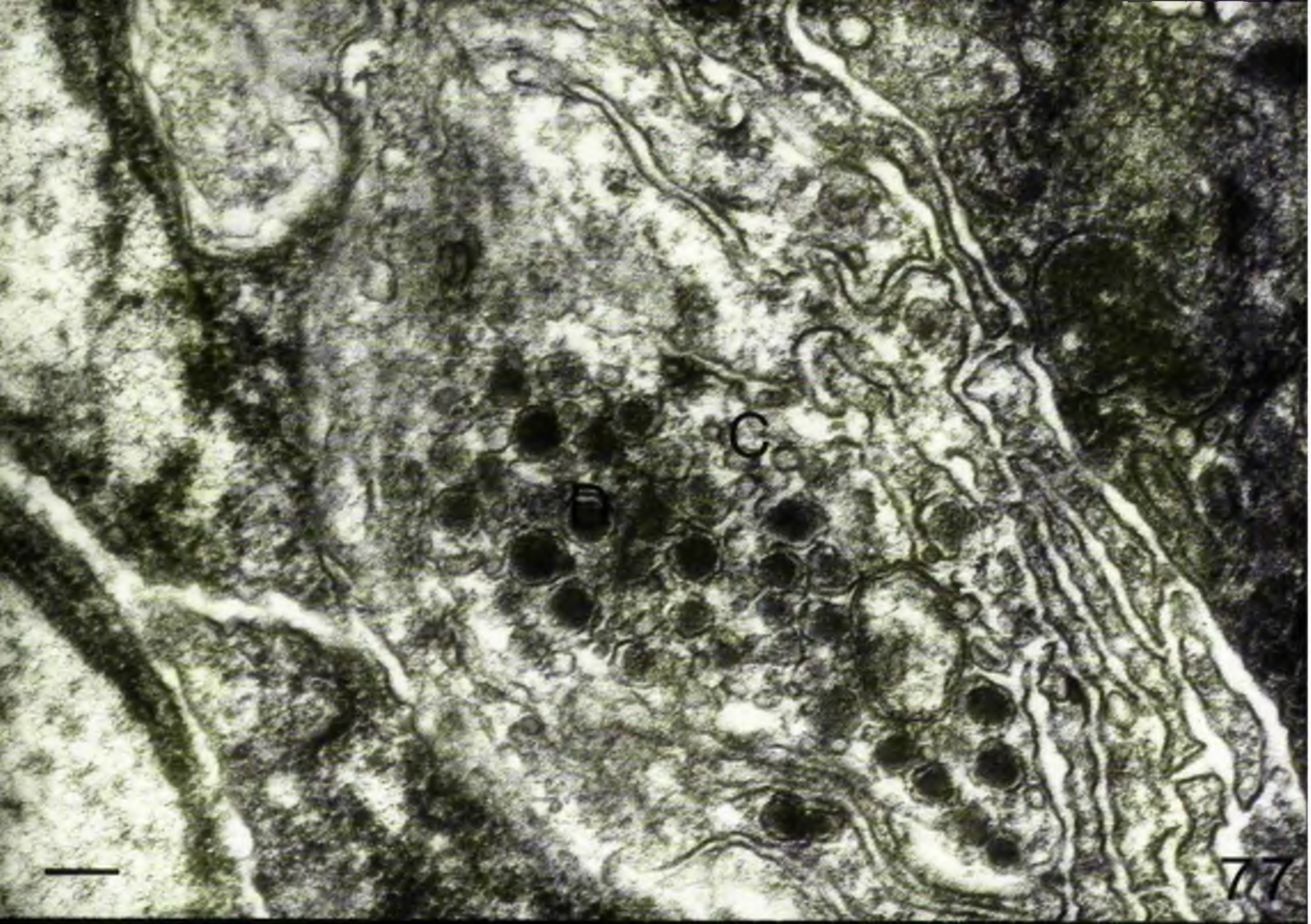

77

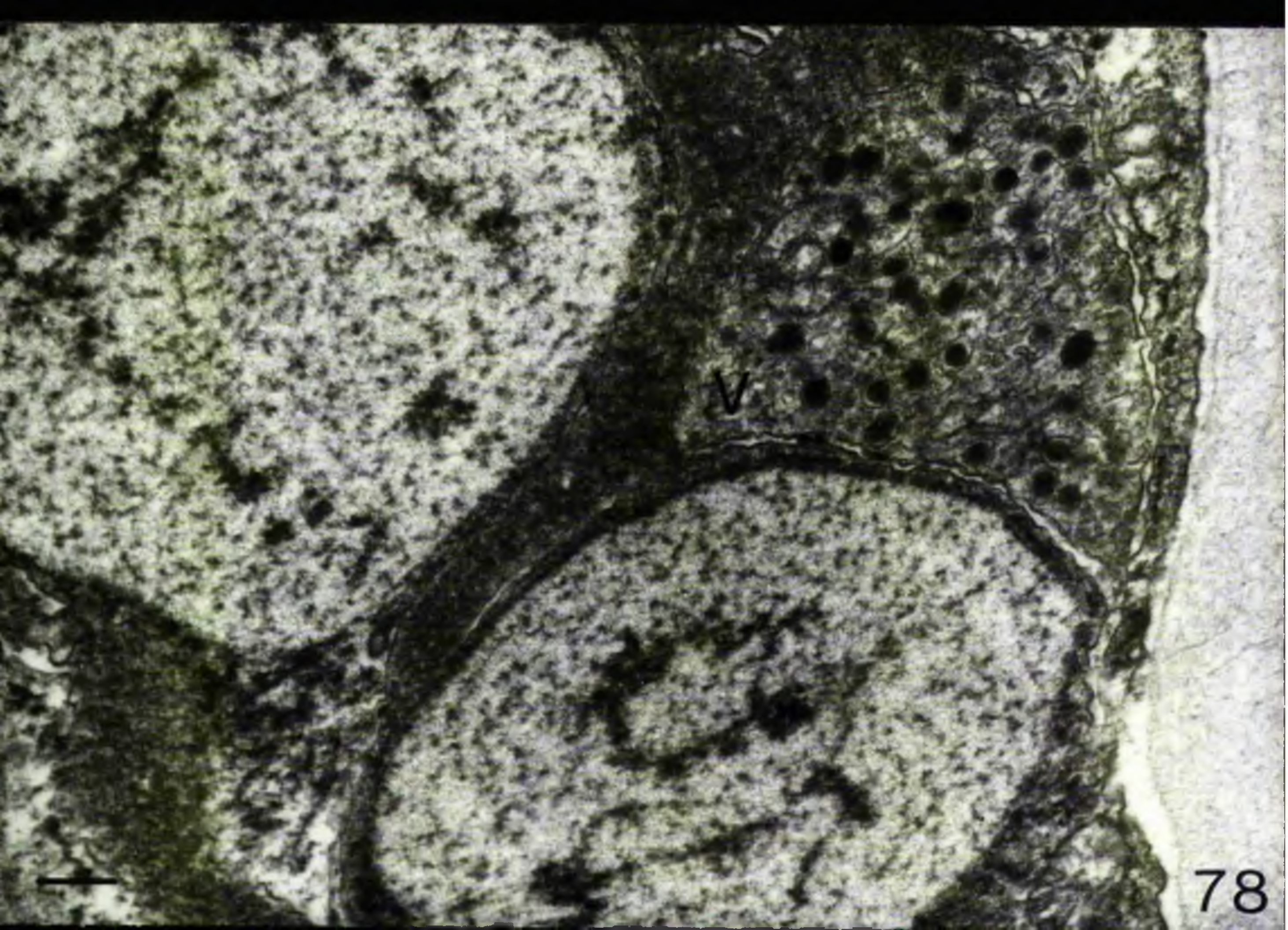

78

Fig. 79

Synaptoid contact between varicosity and epithelial cell. Note the epithelial process (e) which extends over the varicosity.

Scale 500nm

Fig. 80

Septate junction (J) between adjacent epithelial cells.

Scale 120nm

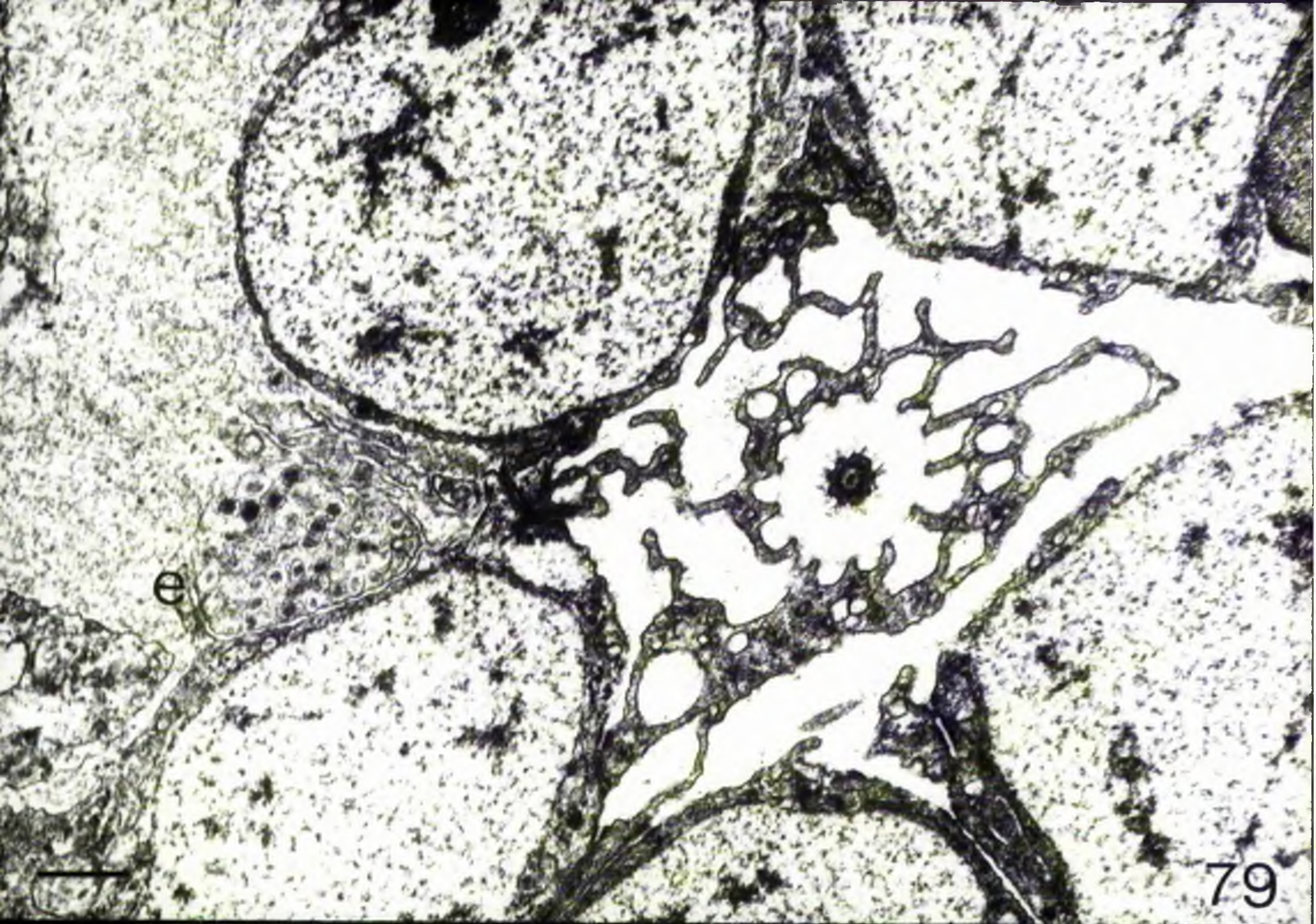

79

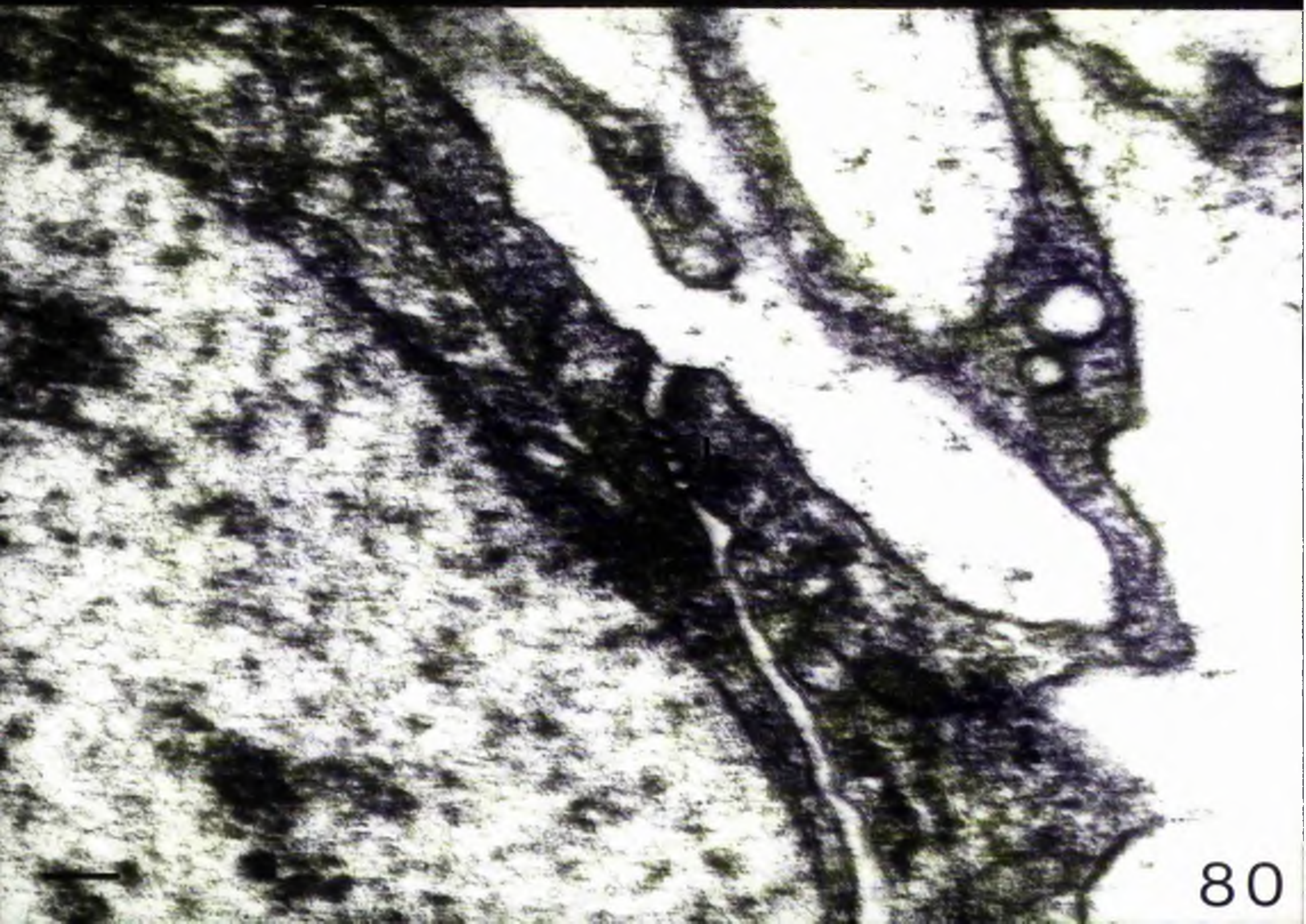
80

Fig. 81

Morula cell (M) within the connective tissue of the radial water canal.

S Spherules

Scale 1μ

Fig. 82

Fibrocyte

Arrows indicate fibrils within the connective tissue matrix and within the cytoplasm of the fibrocyte.

The latter appear to show a transverse striation.

Scale 400nm

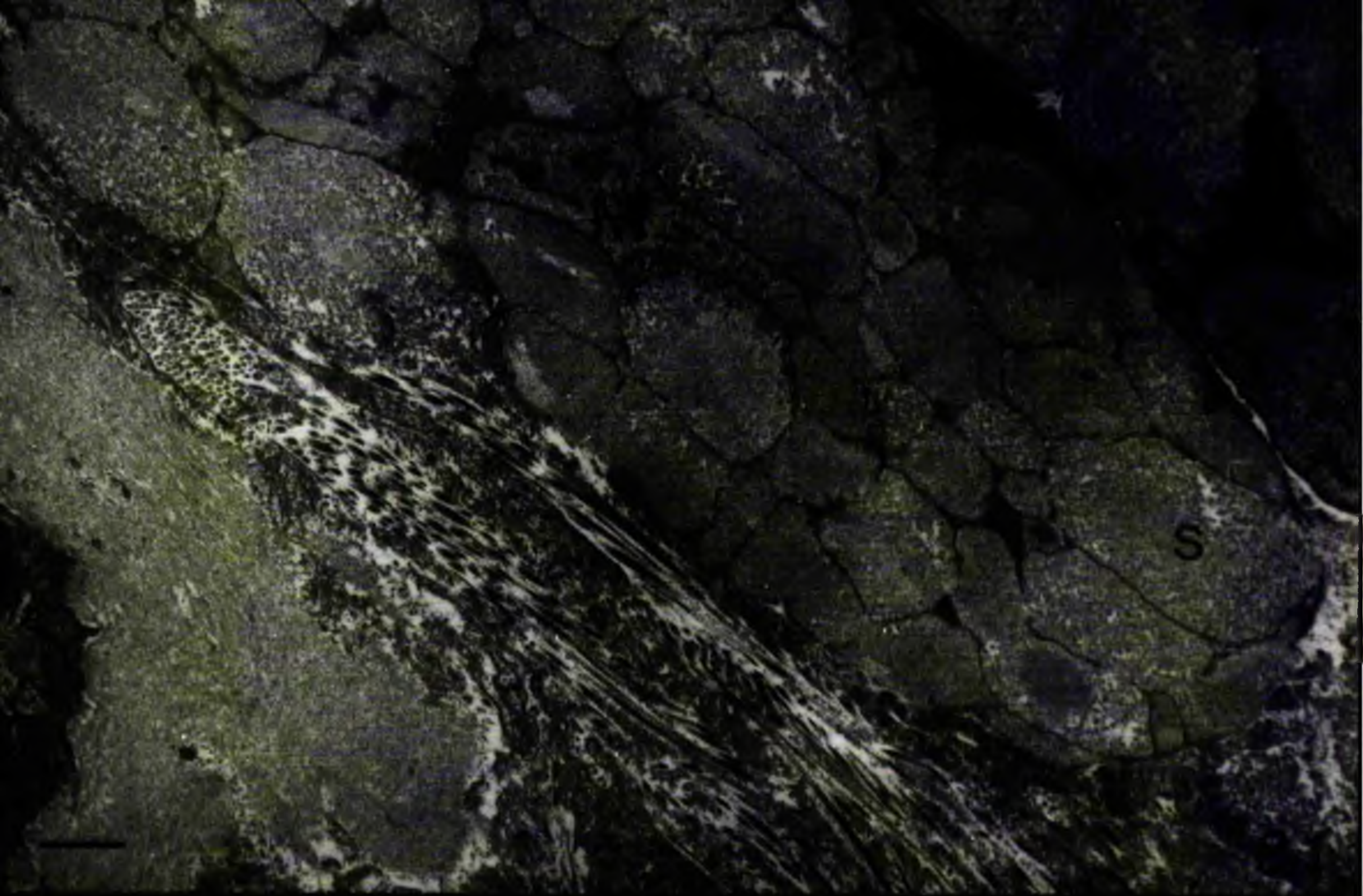

82

Fig. 83

Variation in diameter of collagen filaments (C)

Note that the repeat period of the transverse striation is constant in all filaments.

Scale 150nm

Fig. 84

Longitudinal muscle cells of the mesentery supporting the descending branch of the radial water canal.

Arrow indicates hemidesmosome between muscle cell and basal lamina.

Scale 600nm

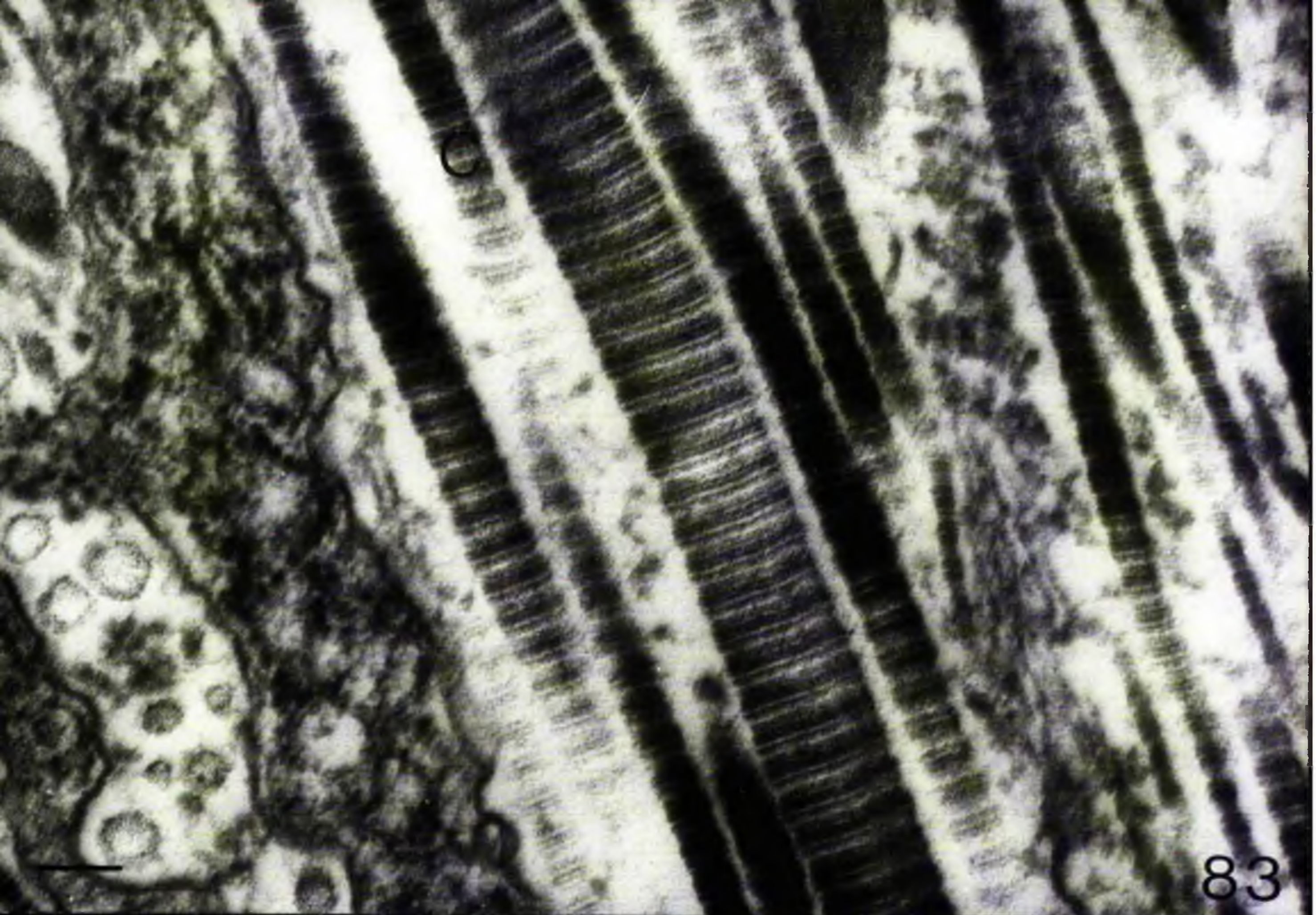

83

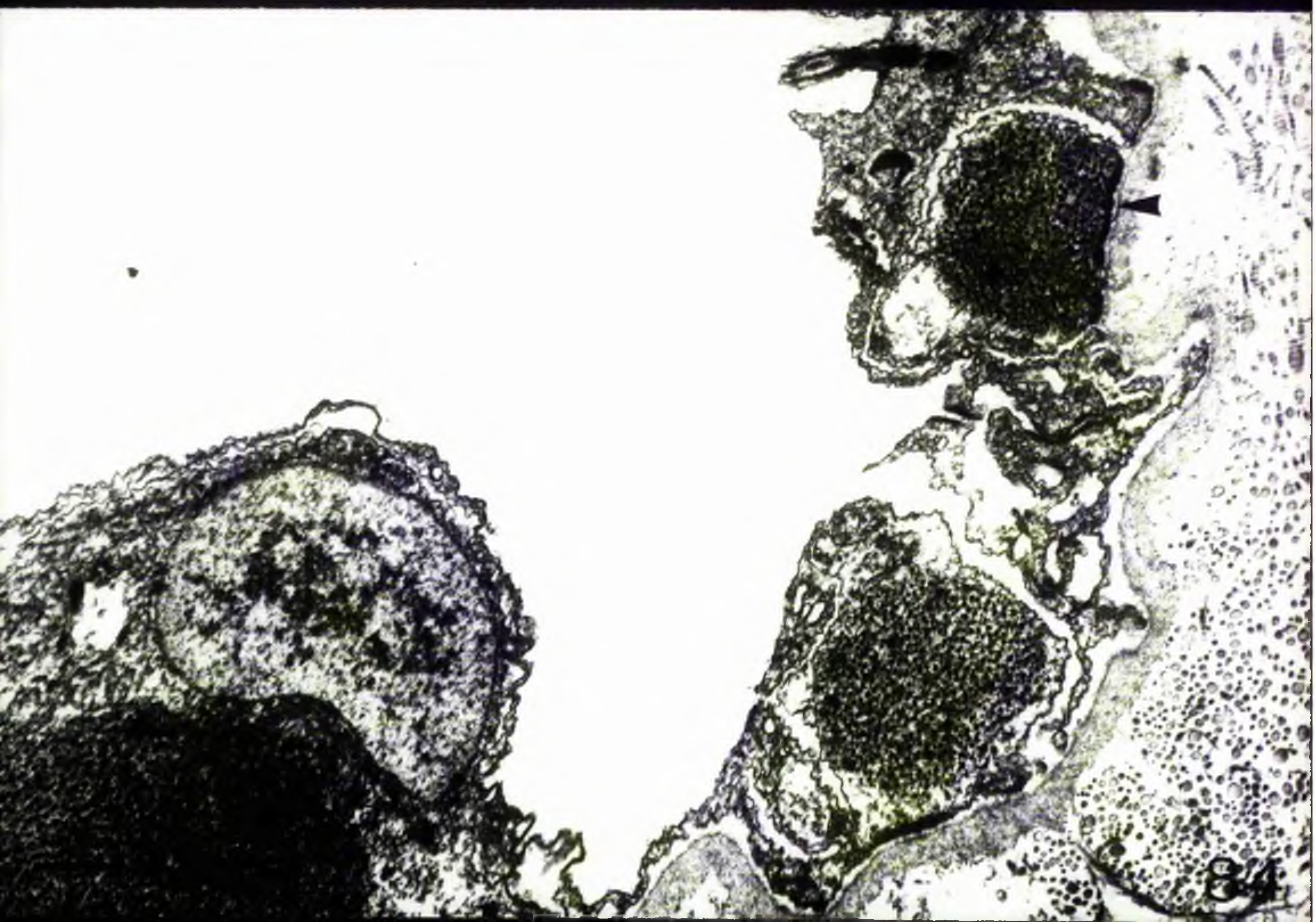
84

Fig. 85

Axon bundle (A) passing through the connective tissue of the water canal mesentery.

Scale 250nm


A

Fig. 86

T.S. PTF disk passing through rosette (r).

b Basiepithelial plexus (proximal to rosette)

Paraffin section, Azan

Scale 40µ

Fig. 87

T.S. PTF disk proximal to rosette.

t Tube foot nerve

Paraffin section, Azan

Scale 40µ

Fig. 88

PTF disk : distal epithelia

s Secretory granule

Scale 300nm

Fig. 89

PTF disk : proximal epithelia

s Secretory granule

Note the process containing neurotubules (arrow) passing between two vacuolated epithelial cells.

Scale 400nm


b
r
86

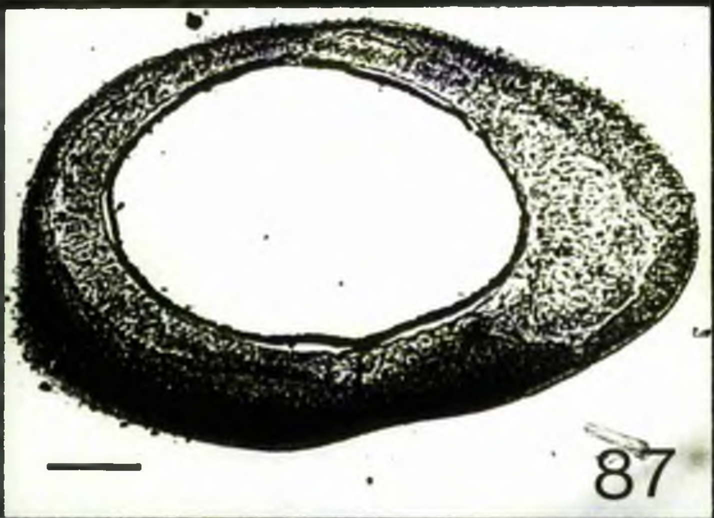
87


s
88

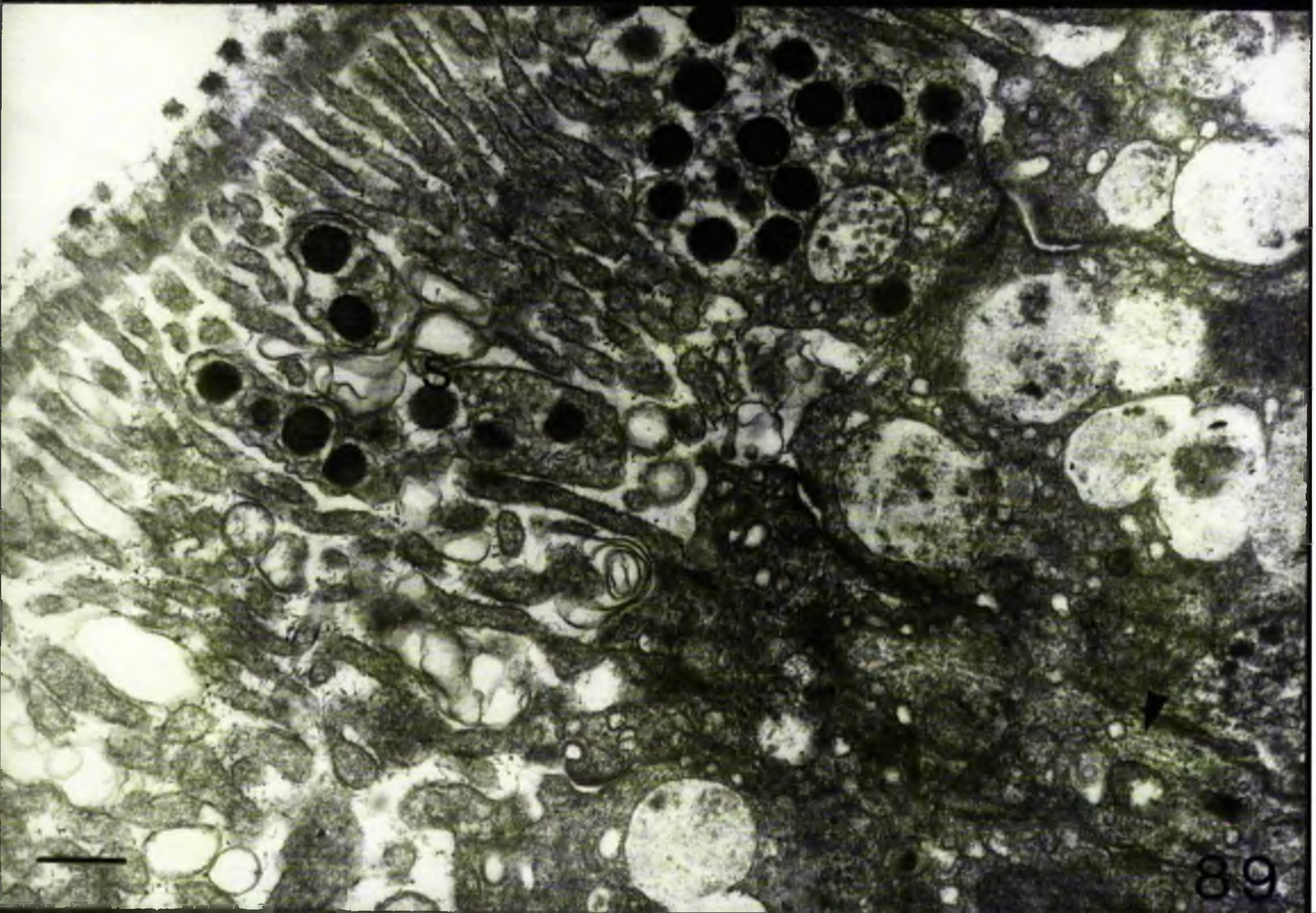
s
89

Fig. 90

PTF disk - proximal epithelium

Secretory process (P) releasing secretory granules between microvilli.

Note the cilium (C), and the electron dense band (B) across distal region of microvilli.

Scale 200nm

Fig. 91

Distal secretory cell (D)

Scale 400nm

Fig. 92

Distal secretory process (P)

Scale 400nm

C
P
B
90

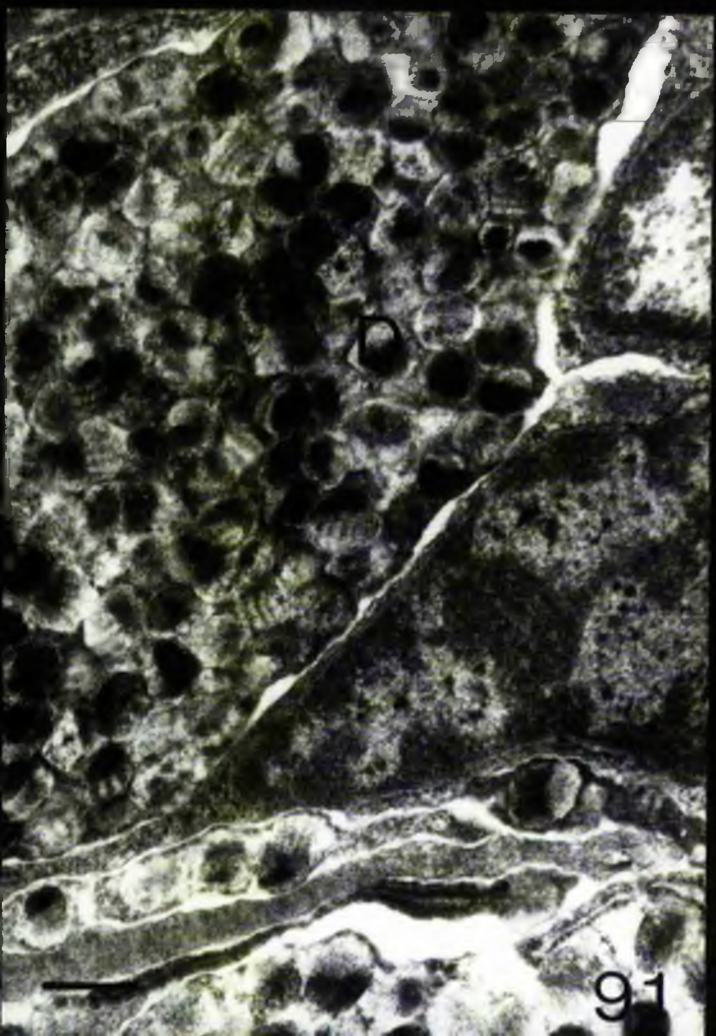

D
91

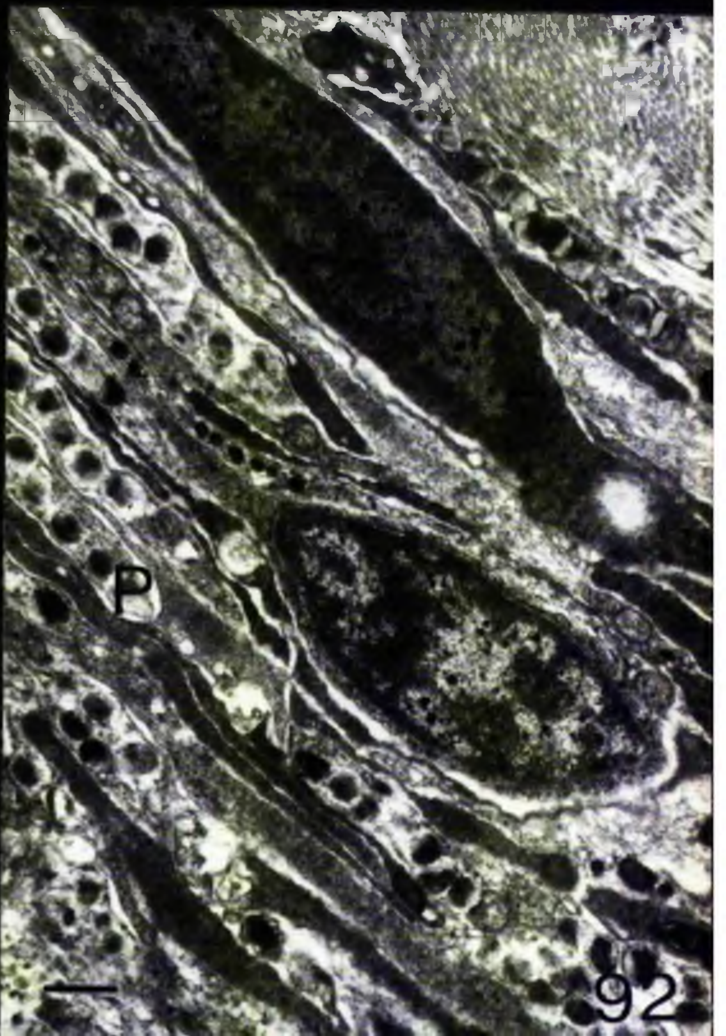

P
92

Fig. 93

Sagittal section PTF disk

P Proximal epithelia (Metachromatic)

D Distal epithelia (Basophilic)

Semithin, Azure/M.B.

Scale 30µ

Fig. 94

Proximal epithelial cell process (e)

I Intermediate junction

Arrow Intercellular channel

Scale 300nm

Fig. 95

Neurosensory dendrites (d) terminating within epithelia at edge of PTF disk

C Cilium

Arrow Neurotubules

Scale 350nm


D
P

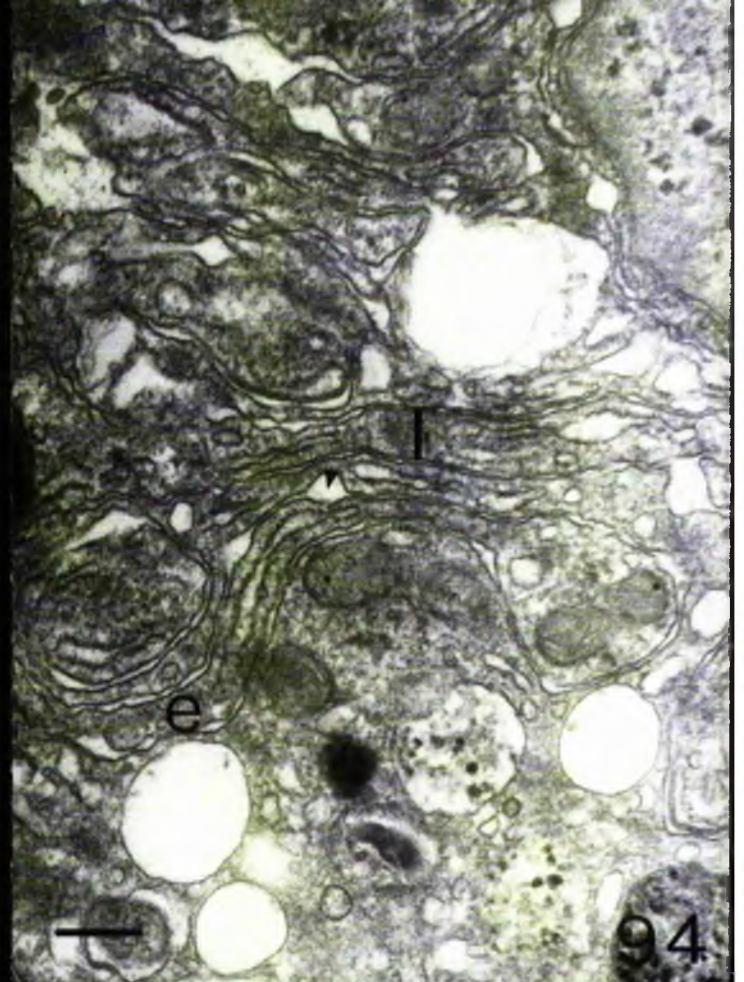
I
e
94

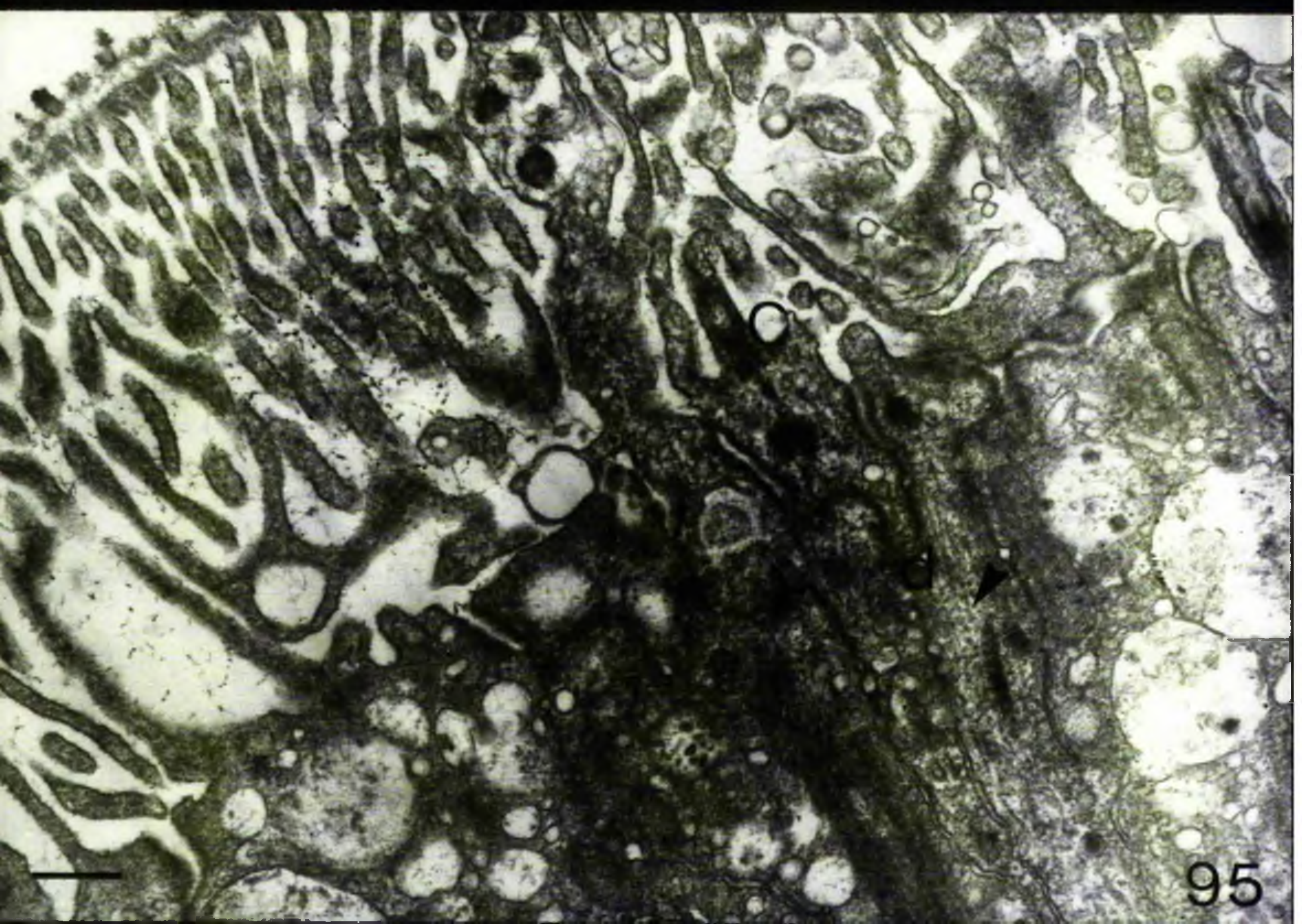
c
d
95

Fig. 96

PTF disk - distal surface

All detail is obscured by a mucous coat

Scale 15μ

Fig. 97

PTF disk - distal surface

After EDTA treatment some mucous is removed revealing cilia (arrow).

Scale 4μ

Fig. 98

T.S. edge of PTF disk

b Basiepithelial plexus

n Neurosensory cell somata

r Rosette ossicle projection

(Note metachromatic collagen filaments around Rosette projections)

Semithin, Azure/M.B.

Scale 20μ

Fig. 99

Neurosensory somata (N)

Scale 1μ

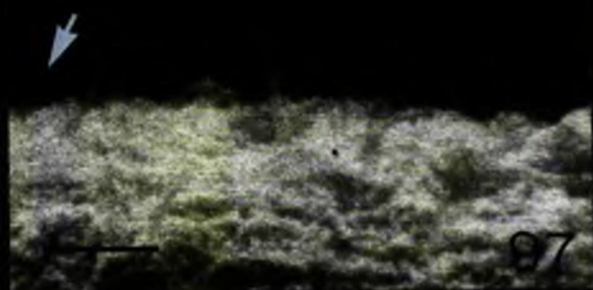
97

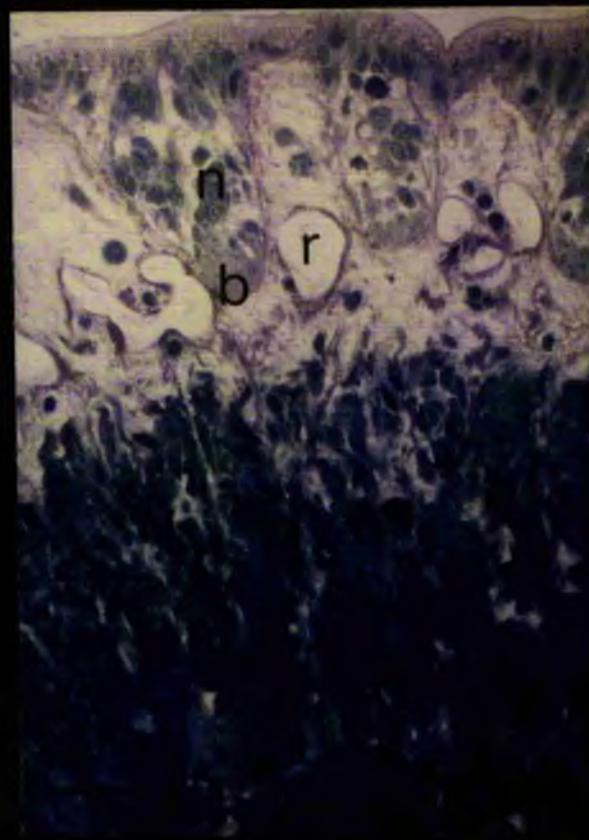
n
r
b

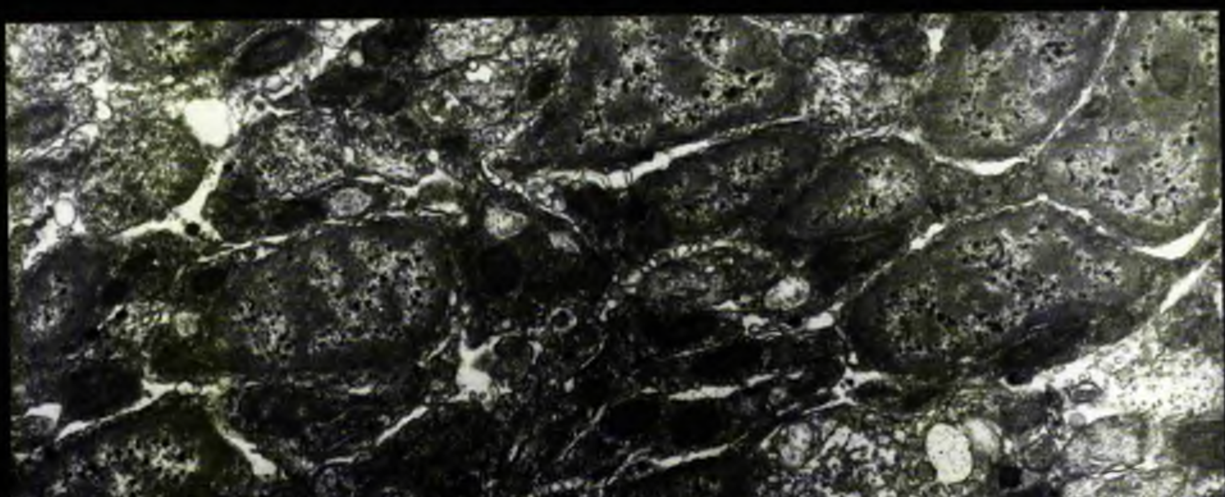
N
99

Fig. 100

Sensory axons (S) projecting into the basiepithelial plexus.

Scale 600nm

Fig. 101

Sensory axons

C Cluster of granular material and neurotubules

Arrow Neurotubule

Scale 200nm

Inset

Sensory axons semithin basiepithelial plexus

Arrow [illegible]

Scale 300nm

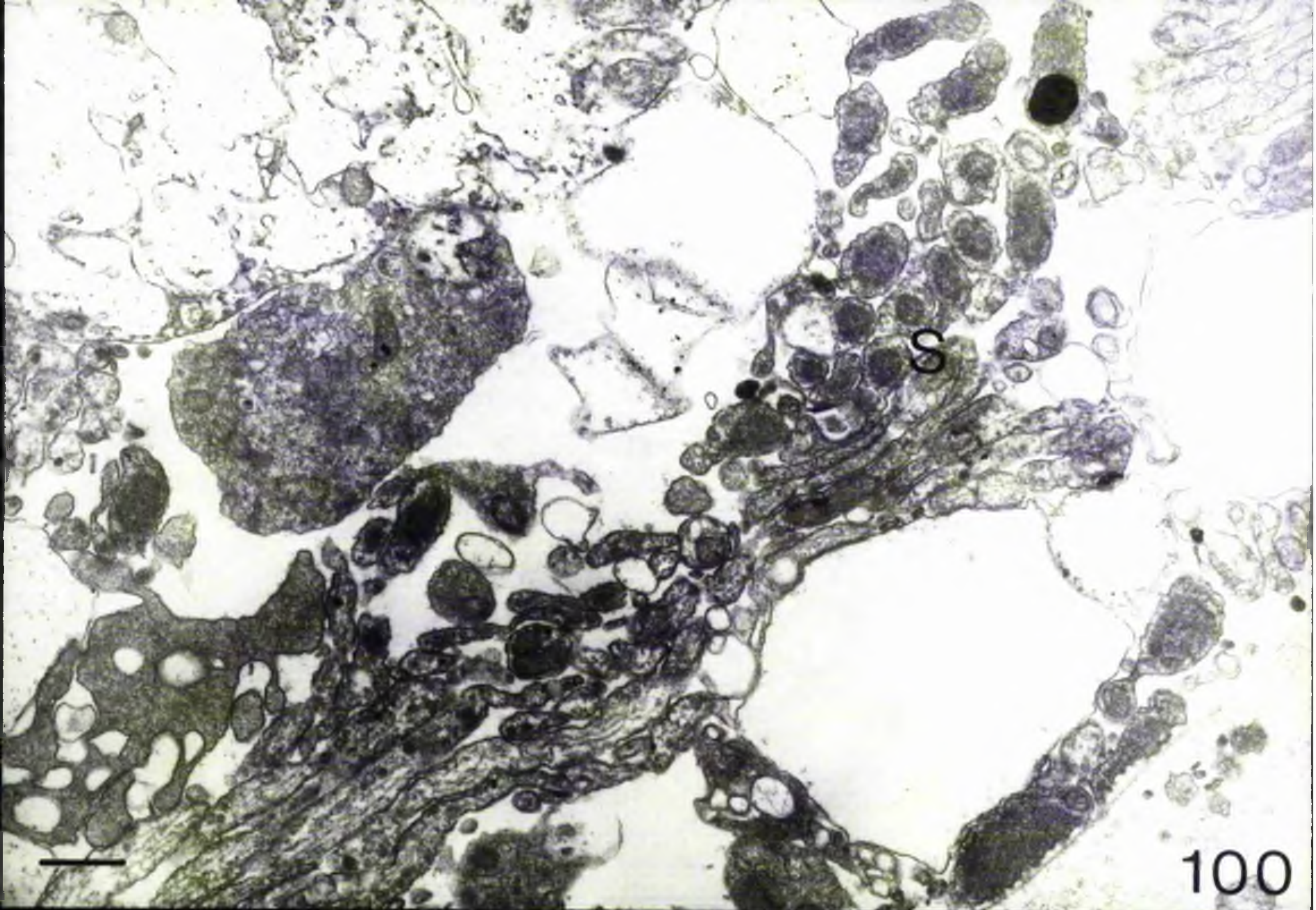

100

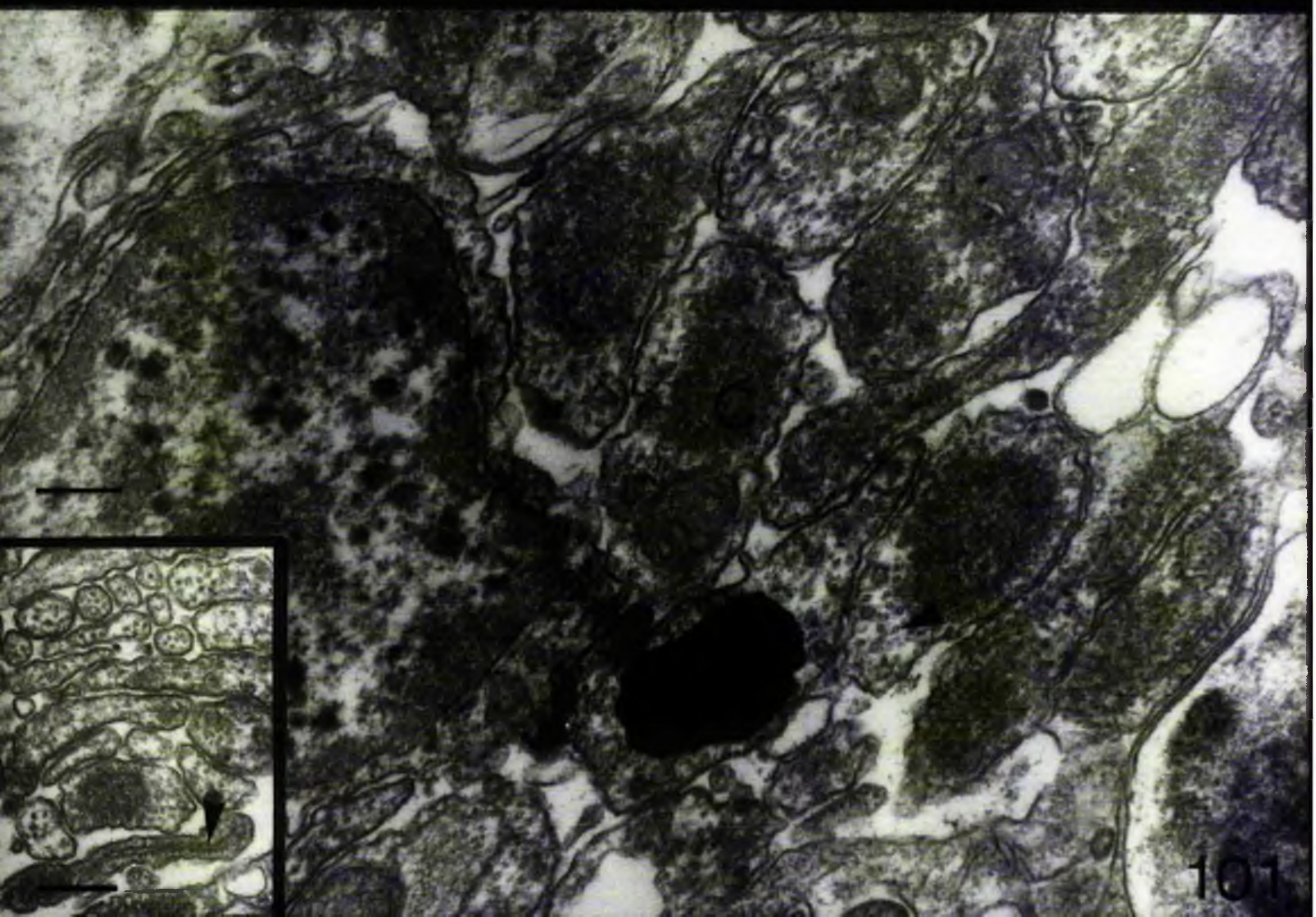

101

Fig. 102

PTF disk: Connection between the distal disk plexus and the proximal disk plexus (P)

D Distal plexus - circumferential tract

R " " - radial tract

Semithin, Azure/M.B.

Scale 20µ

Fig. 103

T.S. PTF disk (section at level shown in Fig. XXVI)

D Disk connective tissue sheath

DL Disk levator muscles

S Stem connective tissue sheath

SR Stem retractor muscles

Semithin, Tol. B.

Scale 20µ

Fig. 104

PTF disk - distal epithelium

B Basiepithelial plexus

C Connective tissue sheath (mainly circular collagen bundles)

D Disk levator muscle

Note that the secretory granules are similar to PTF dsik secretory granules (distal).

Scale 500nm

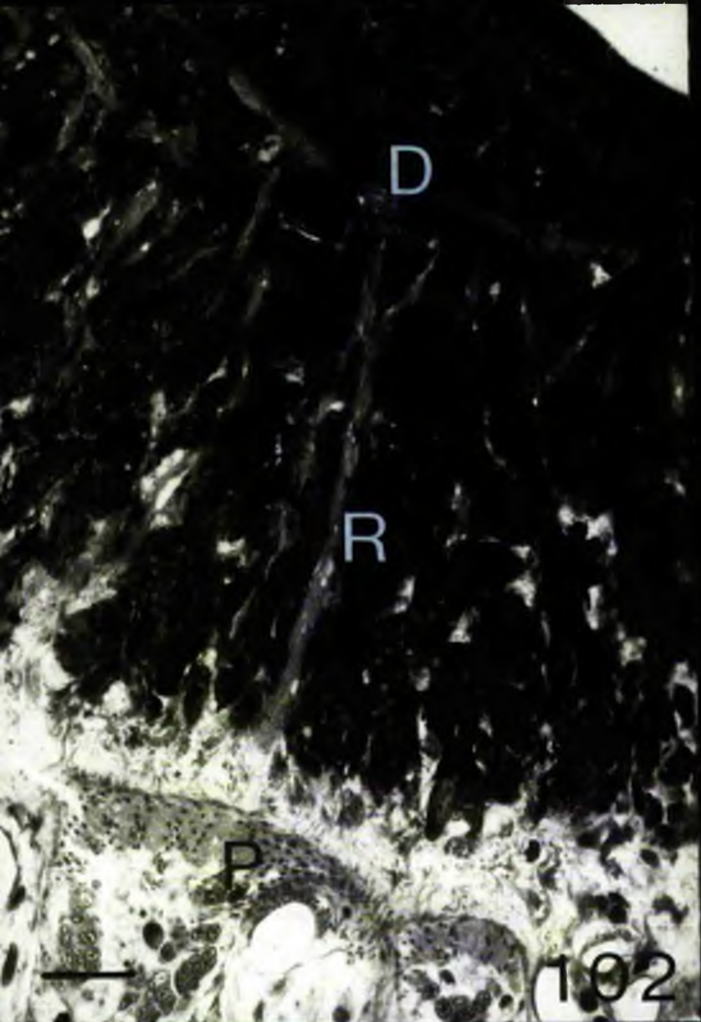
D
R
P
102

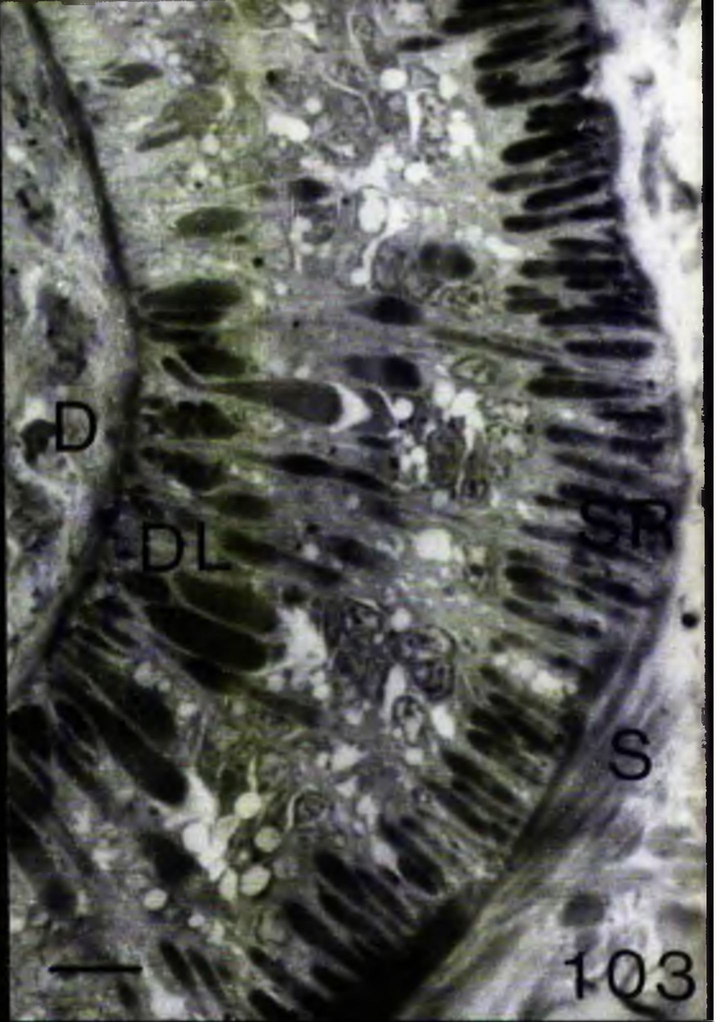
D
DL
SR
S
103

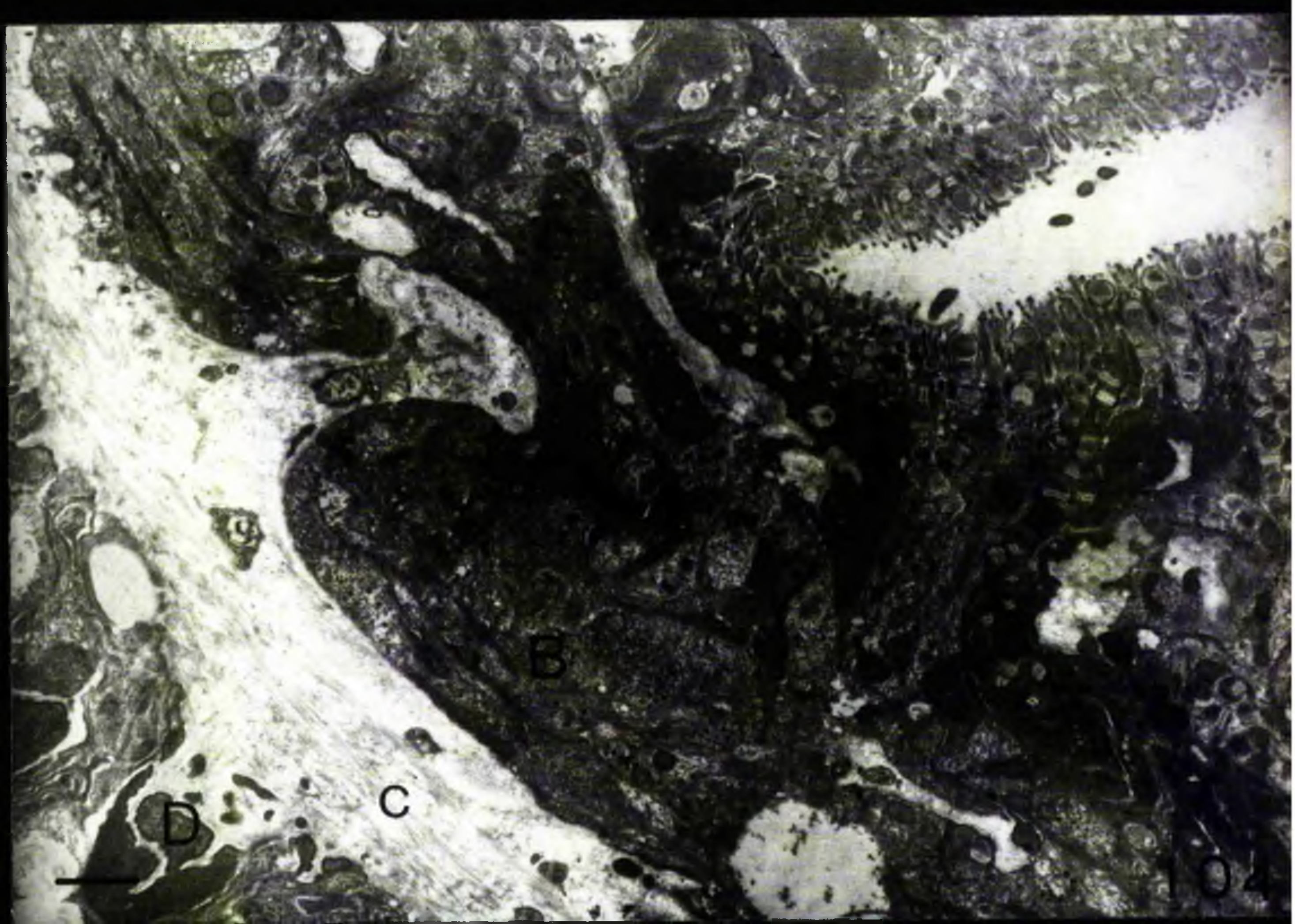
B
D
C
104

Fig. 105

Disk levator muscle - disk wall

a Attachment process of basal lamina

Scale 200nm

Fig. 106

Disk levator muscle - stem wall

h Hemidesmosome

I Type I fibre

II Type II fibre

Scale 250nm

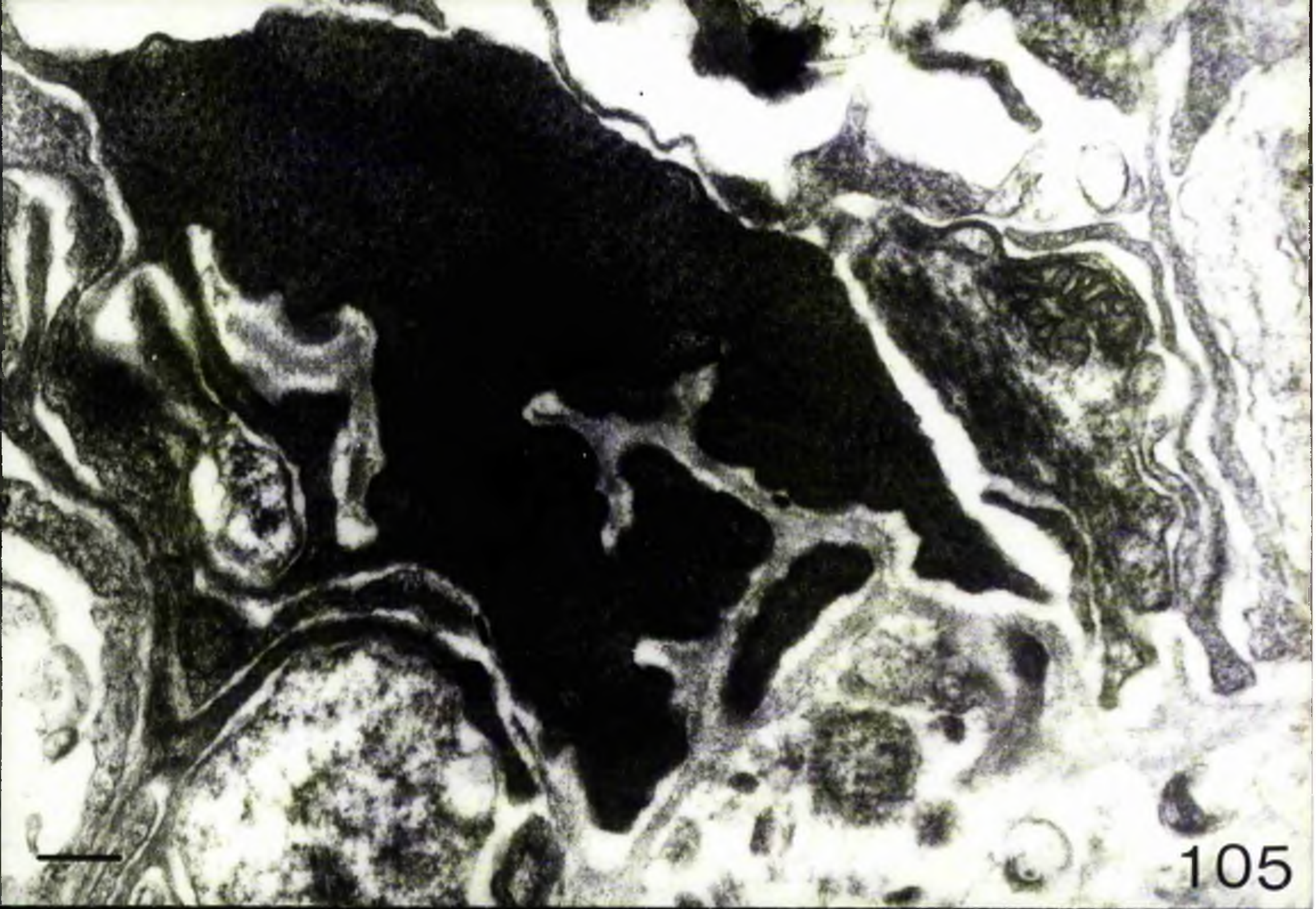

105

106

Fig. 107

Type II disk levator muscle

L LDSG axon

m Mitochondrion (note particles on cristae)

s Subsurface cisterna

Large arrow Thick filament

Small arrow Thin filament

Scale 200nm

Fig. 108

Sarcolemmal extension (S) from Type I muscle fibre

Large arrow Intramitochondrial dense body

Small arrow Subsurface cisterna

Note enveloping sheath (e) around LDSG axon

Scale 600nm

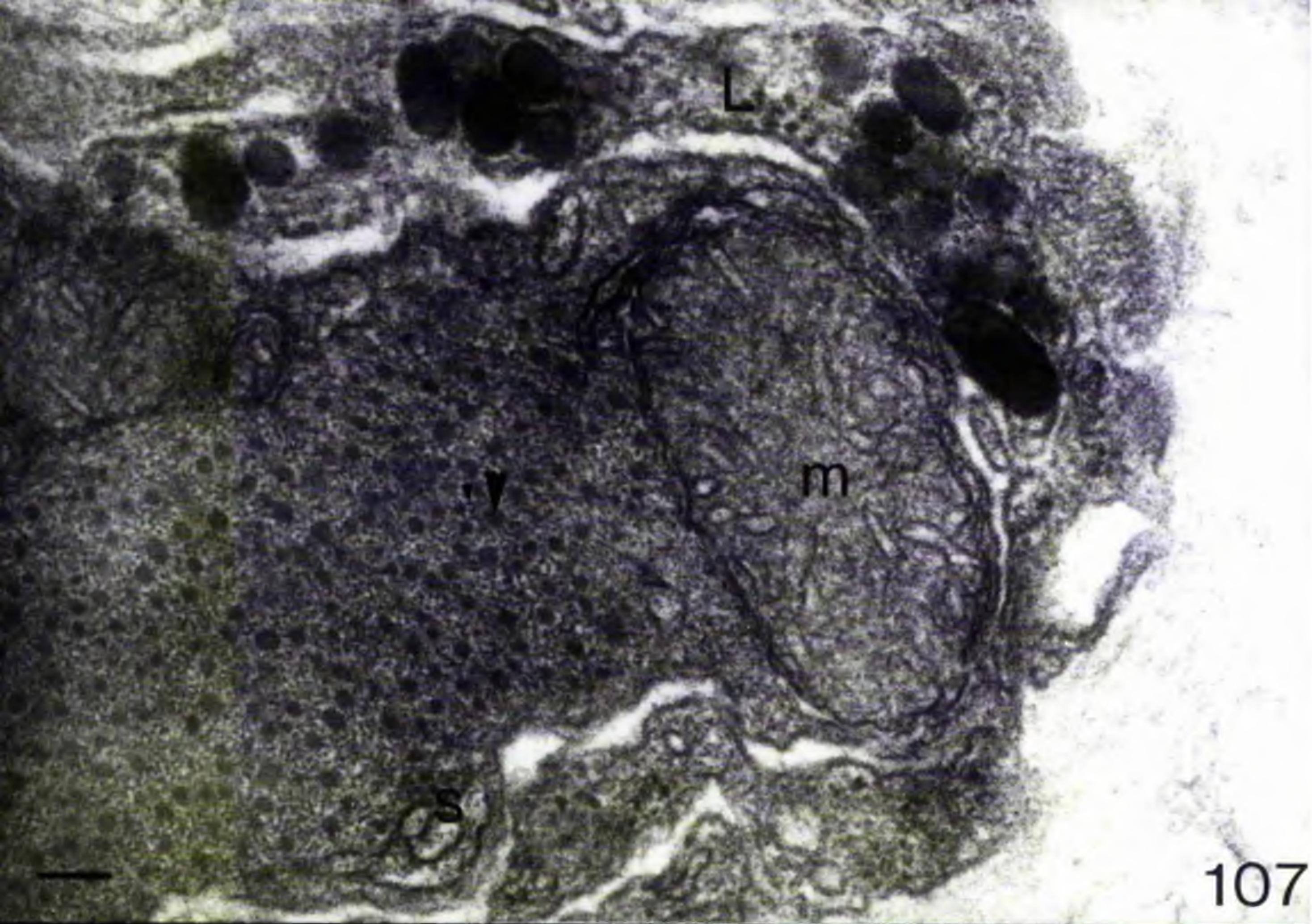

107

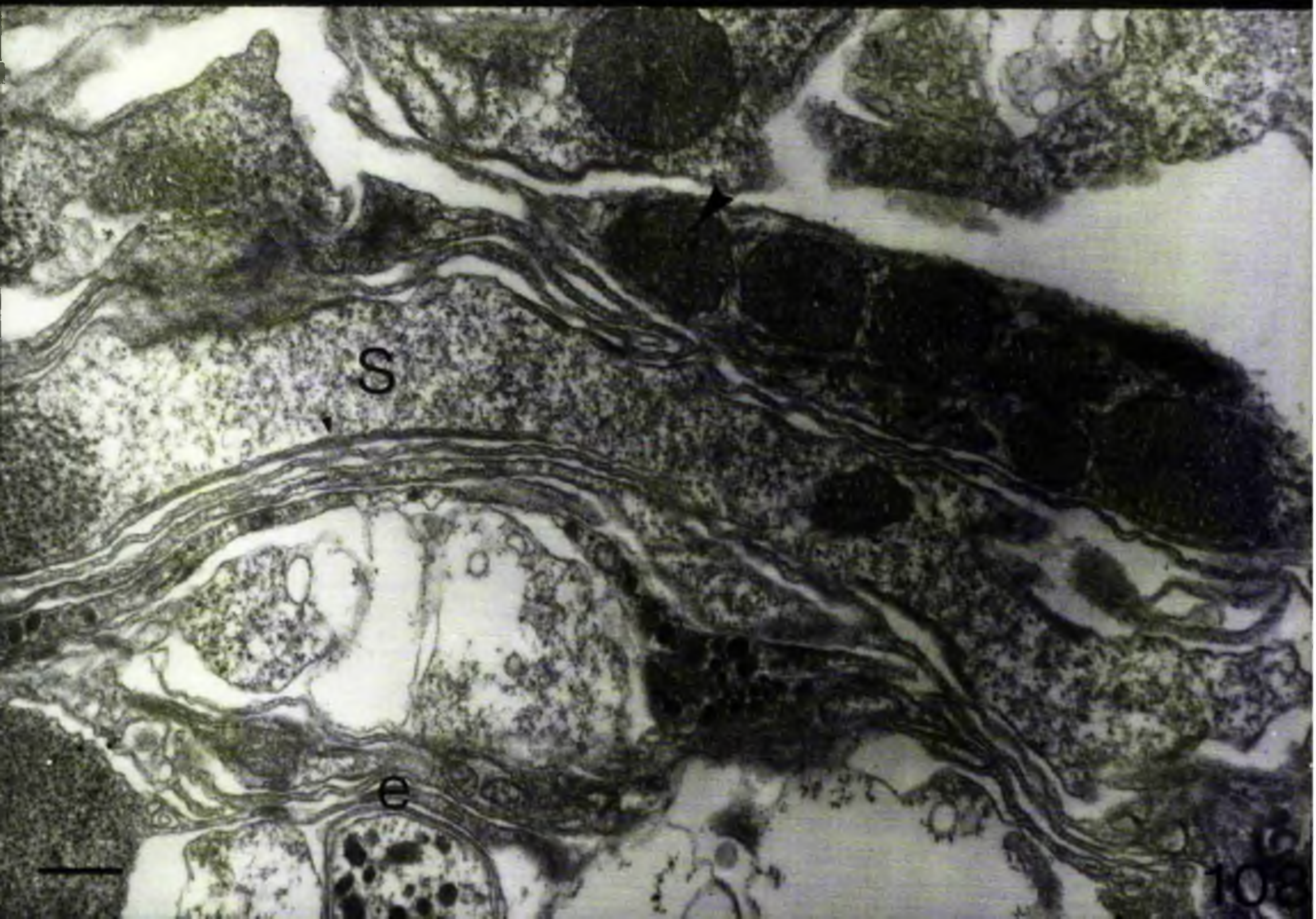

108

Fig. 109

Epithelial processes within the stem can be distinguished from axons due to the presence of tonofilaments (t).

Scale 1μ

Fig. 110

Row of cilia projecting from tube foot stem.

Scale 500nm

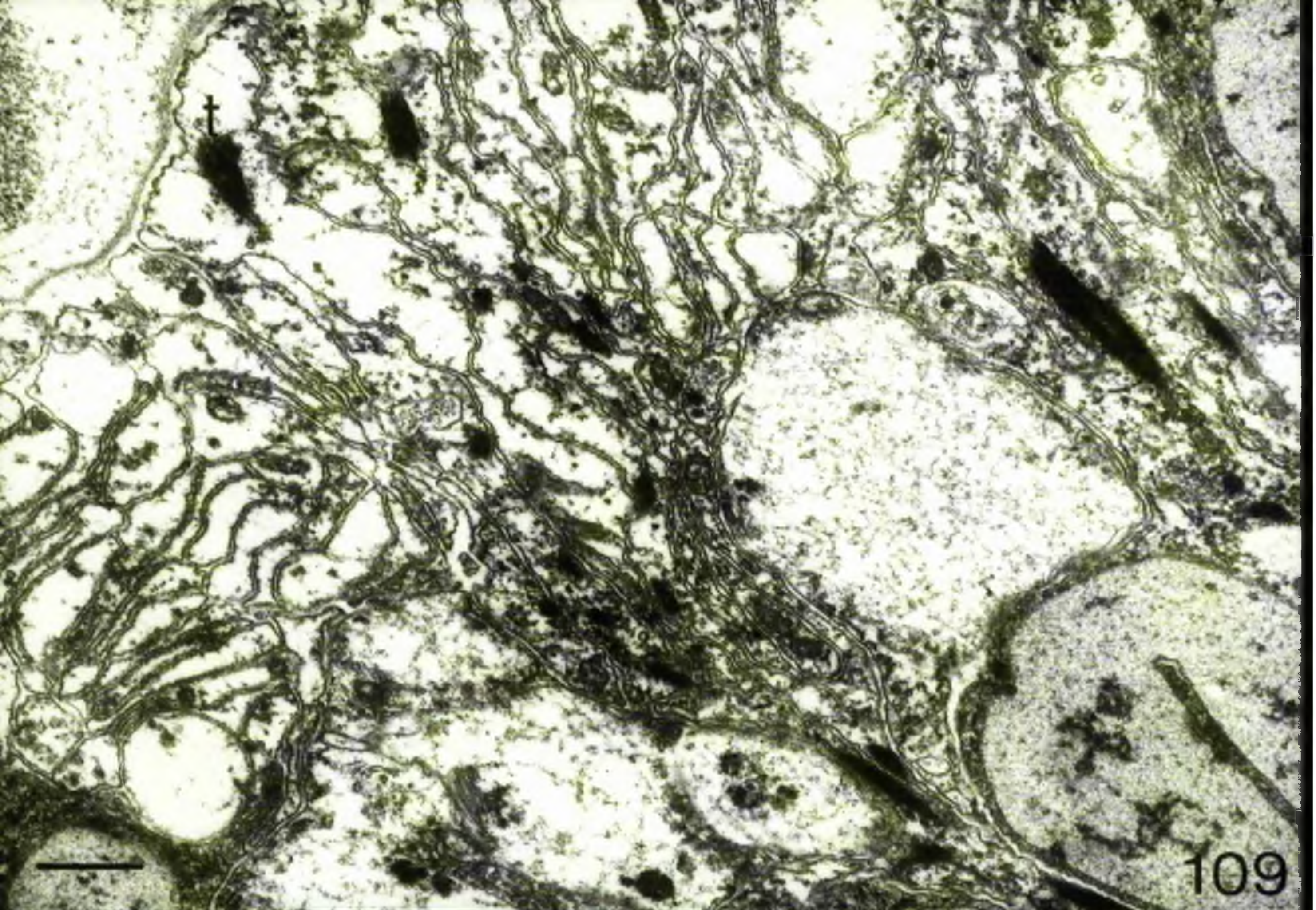

109


110

Fig. 111

Neurosensory (N) cells within stem epithelia.

a Axon extending to basiepithelial plexus

b Basal apparatus at distal end of dendrite

v Vacuolated epithelial cell

arrows Two dendrites from one soma

Scale 2μ

Fig. 112

Two neurosensory cells (N)

a Axon

d Dendrite

Scale 2μ

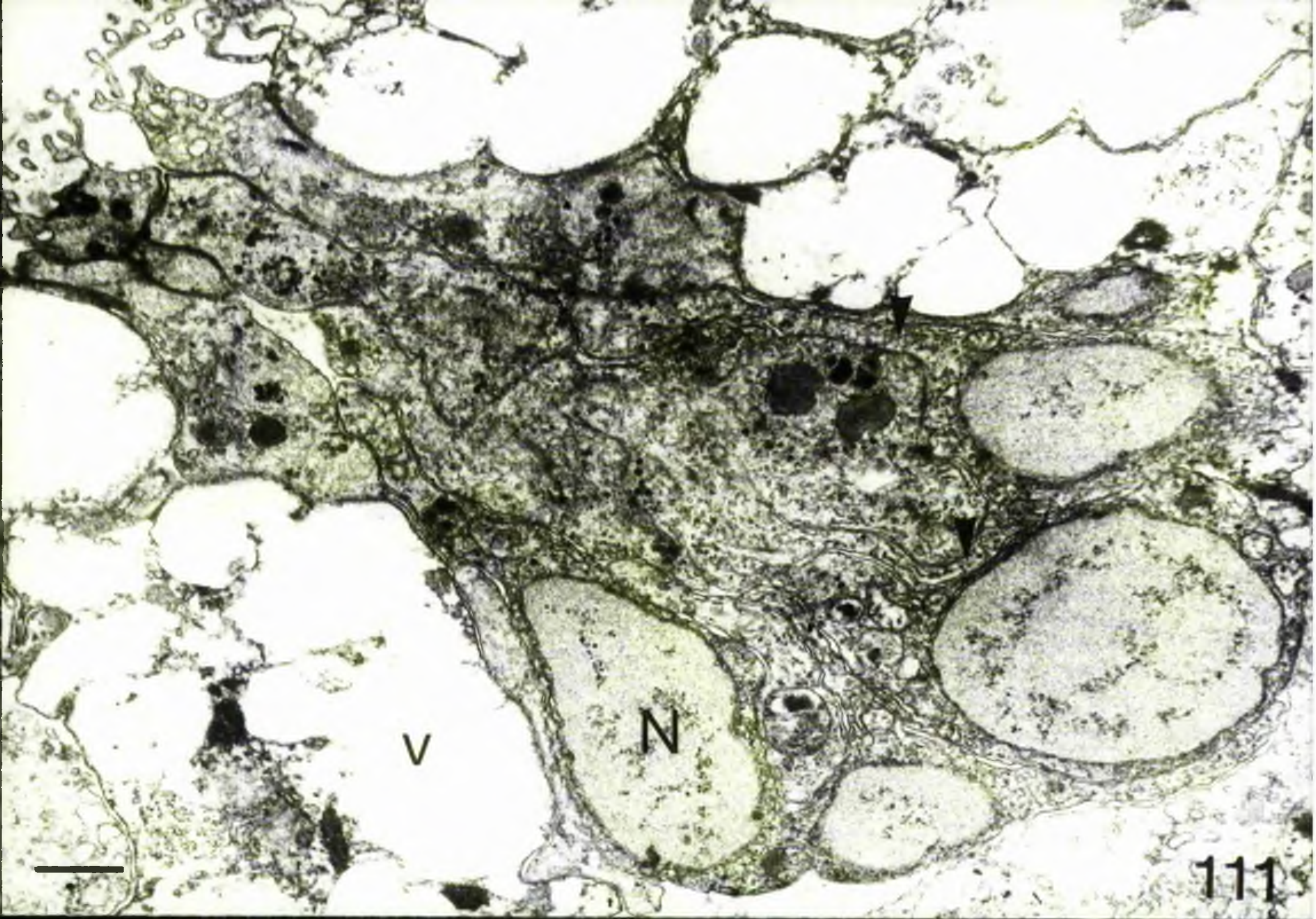
V
N
111

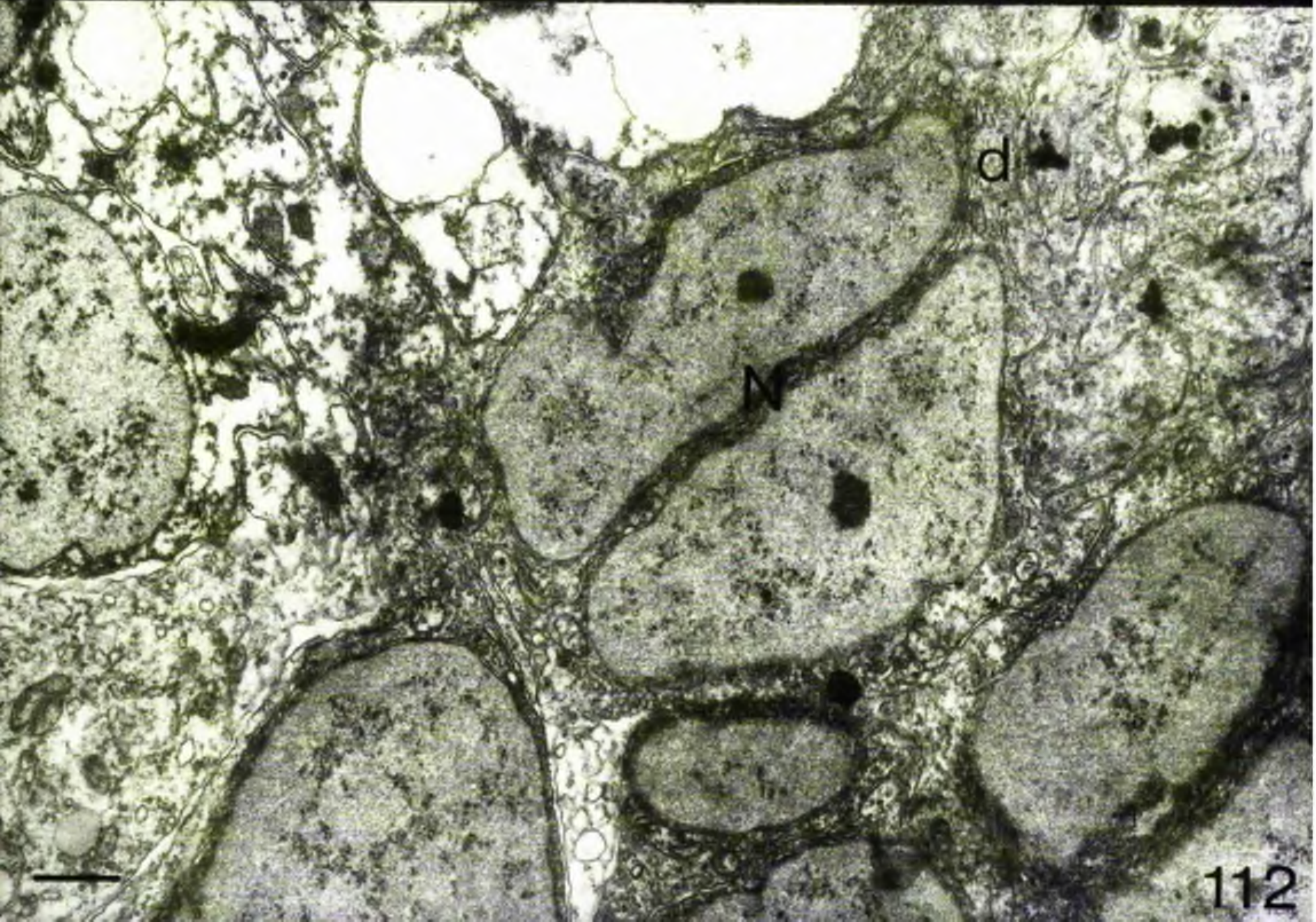
d
N
112

Fig. 113

Tube foot stem: basiepithelial plexus

c CV

d DCV

Note synaptoid cleft contains dense material (arrow)

Scale 400nm

Fig. 114

Thickening of basiepithelial plexus (arrows) forms tube foot nerve (N).

Semithin, Tol. B.

Scale 7μ

Fig. 115

Axons after Fix. I (no Glut.)

Scale 400nm

Fig. 116

Axons after Fix II (Glut. prefix)

Note the improved preservation of neurotubules (arrow)

Scale 800nm

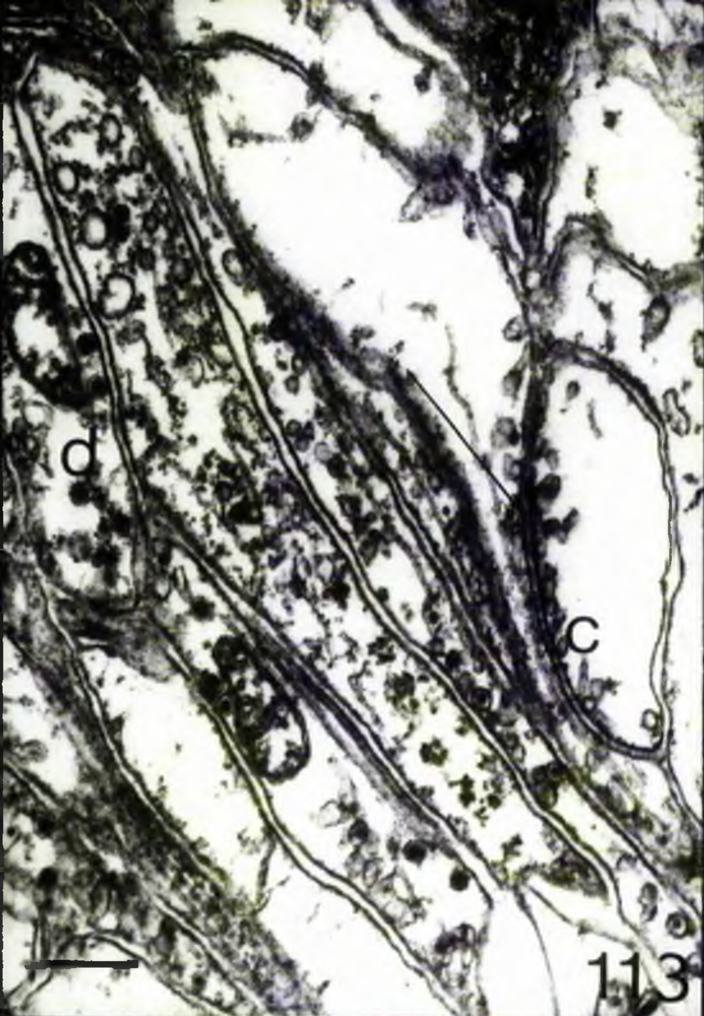
d
c
113

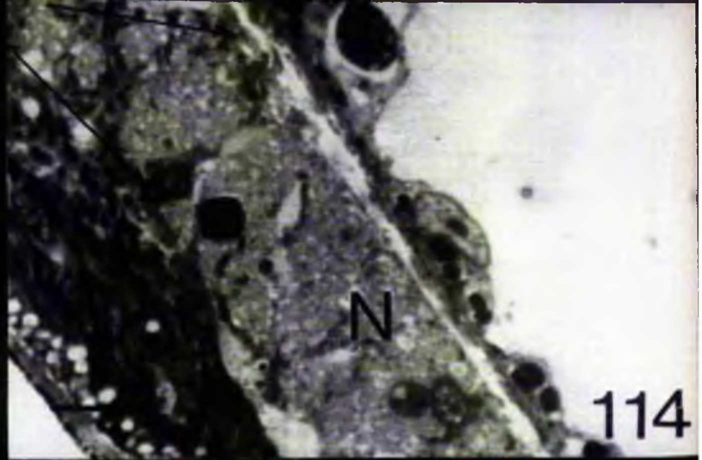
N
114

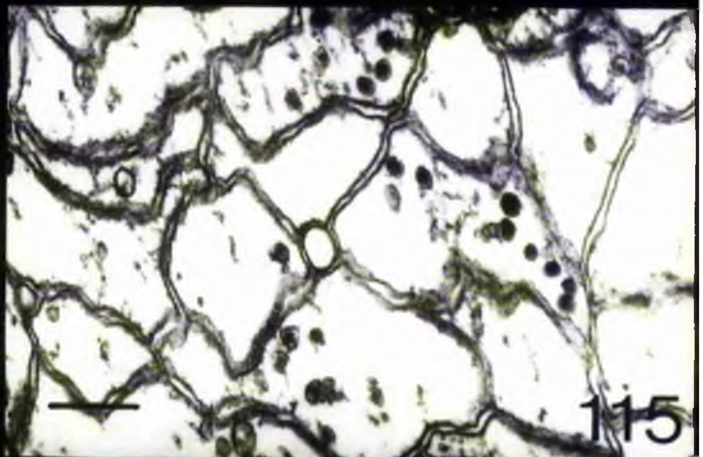
115

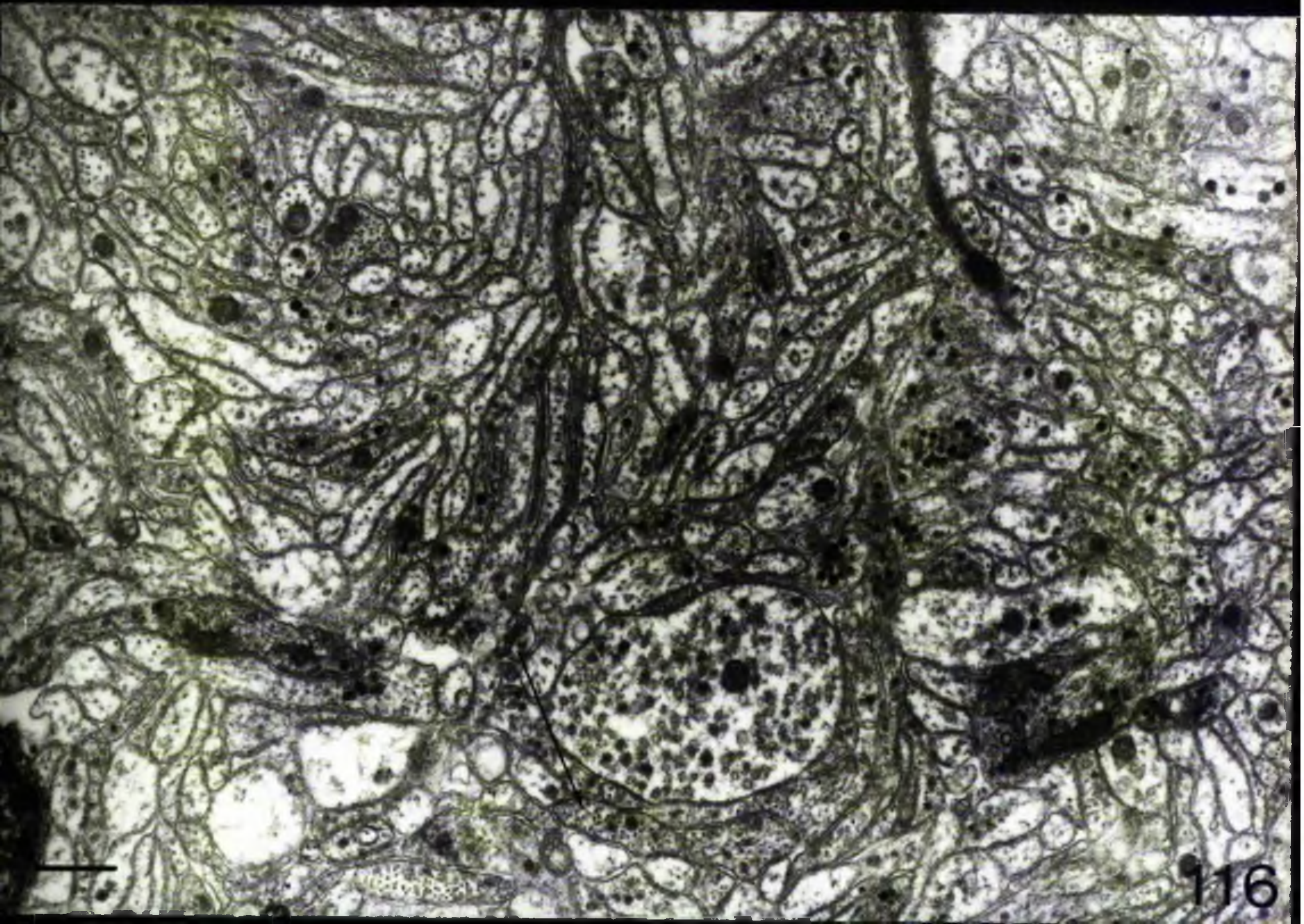
116

Fig. 117

T.S. ATF stem, prepared for fluorescence localisation of monoamines.

S Specific fluorescence from tube foot nerve

N Non-specific fluorescence from epithelia

Scale 30µ

Fig. 118

As above - after Na-monoborohydride reduction.

Note that fluorescence persists in the epithelia and (faintly) in the endothelia.

Scale 30µ

Fig. 119

T.S. wall of ATF stem.

C Connective tissue - outer amorphous, inner longitudinal (l) and circular (c)

E Epithelia

M Muscle

Semithin, Tol. B.

Scale 10µ

Fig. 120

T.S. Collageno-muscular junction (extended ATF)

C Circular collagen bundles

L Longitudinal collagen bundles

M Muscle

Arrows LDSG processes

Scale 1.5µ

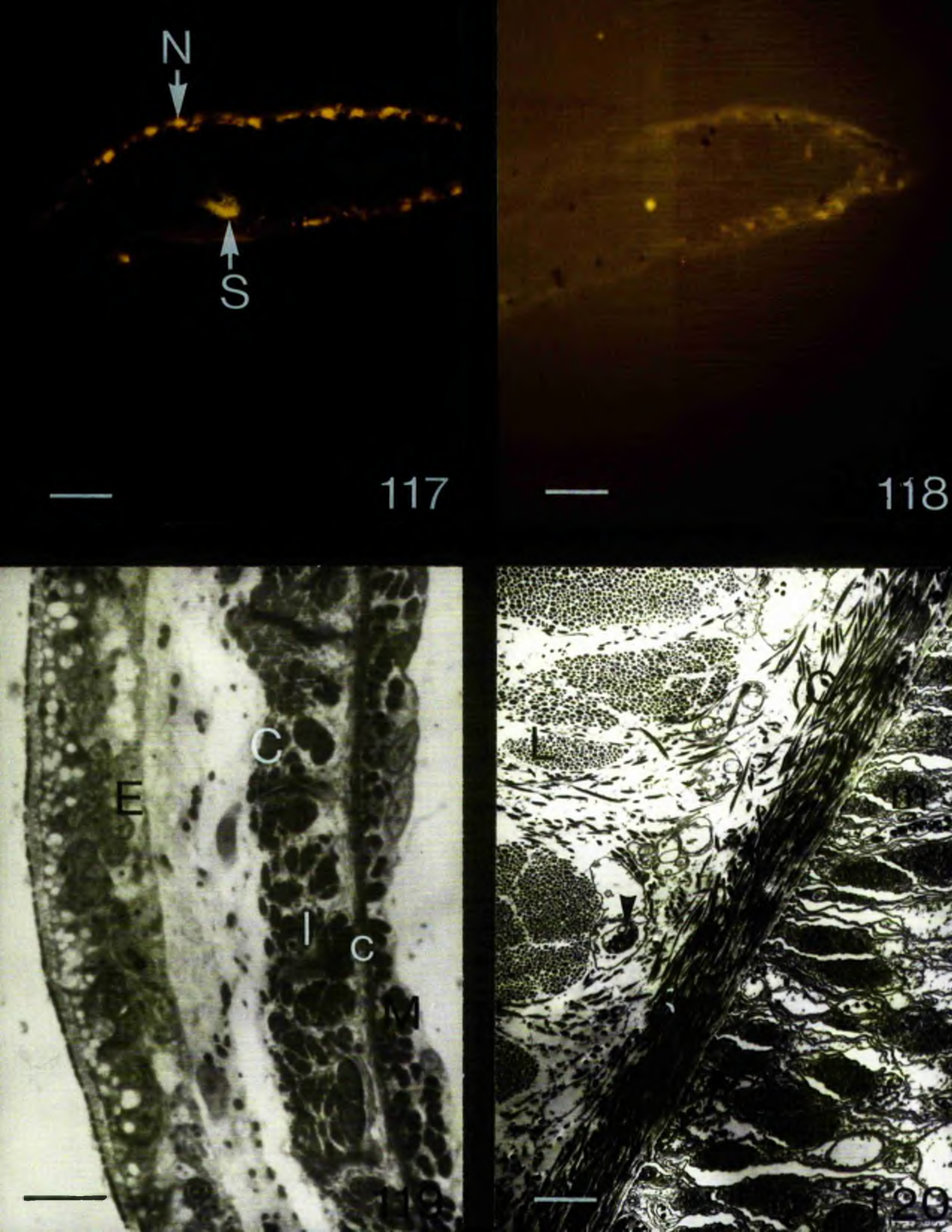
N
S
117
118
C
E
I
c
M
L
m
120

Fig. 121

Circular connective tissue layer.

Note the fine filaments (arrow) interweaved among the collagen filaments.

L LDSG axon containing LDSG and CV

R Radial collagen filaments

Scale 500nm

Fig. 122

T.S. connective tissue sheath (ATP - contracted)

Note sections of longitudinal collagen filaments are more oblique (arrow).

Scale 1.5μ

Fig. 123

Longitudinal collagen filaments (note variation in diameter)

Scale 500nm


121


122

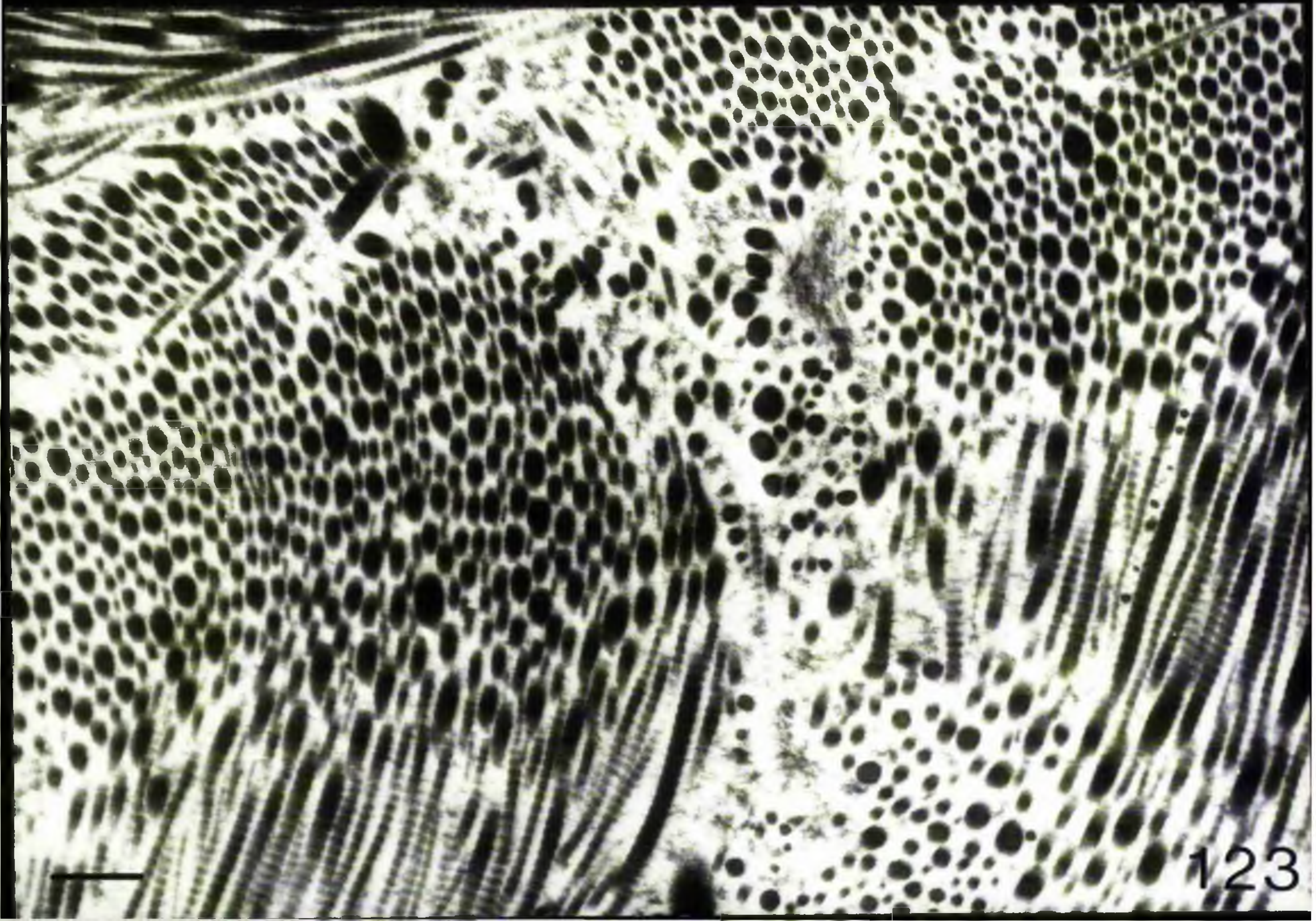
123

Fig. 124

ATF Stem retractor musculature; contracted.

E Endothelial cell bodies

Semithin, M.Blue

Scale 20µ

Inset

ATF Stem retractor musculature; extended.

Same magnification

Fig. 125

The TF musculature (M) decreases in thickness adjacent to the TF nerve (N).

Note that the connective decreases in thickness in this region (arrow): only the circular layer is present.

Semithin, M.Blue

Scale 10µ

Fig. 126

L.S. ATF collageno-muscular junction.

e Lateral evagination of muscle fibre into circular connective tissue layer

arrow Basal lamina

Scale 250nm

Fig. 127

ATF retractor muscle fibres

Note the interdigitating sarcolemmal extensions (S).

Fix 1

Scale 500nm

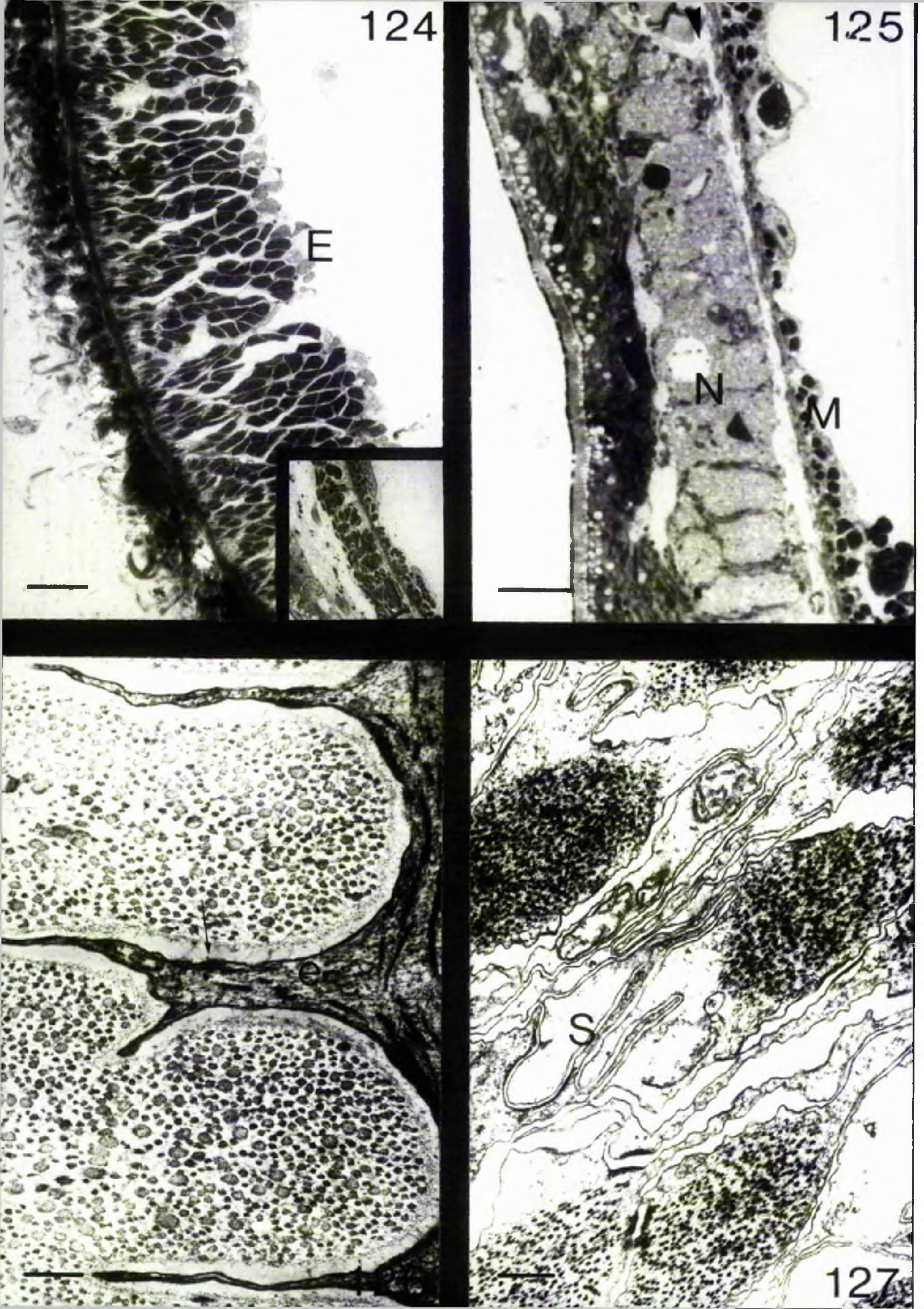
124
E
125
N
M
e
S
127

Fig. 128

The myofilament array is not highly ordered.

Large arrow   A rare orbit of thin filaments around a thick filament

Small arrow   Subsurface cisternae. Fix. II

Scale 400nm

Fig. 129

LDSG axon (L) adjacent to muscle fibre

Note that thin myofilaments are poorly preserved due to lack of Glut. fix. Fix. I.

Scale 120nm

Fig. 130

Z-bodies (Z) appear to form points of attachment for thin myofilaments.

Note vacuolar cisternae (v).

Scale 300nm

Fig. 131

Straight desmosome between two muscle fibres.

Scale 300nm

Fig. 132

Irregular desmosomes between muscle fibres.

Scale 300nm

Fig. 133

Intermediate junction (arrow) adjacent to straight desmosome.

Scale 300nm

Fig. 134

Hemidesmosome (arrow) between muscle fibre and endothelial process.

Scale 300nm

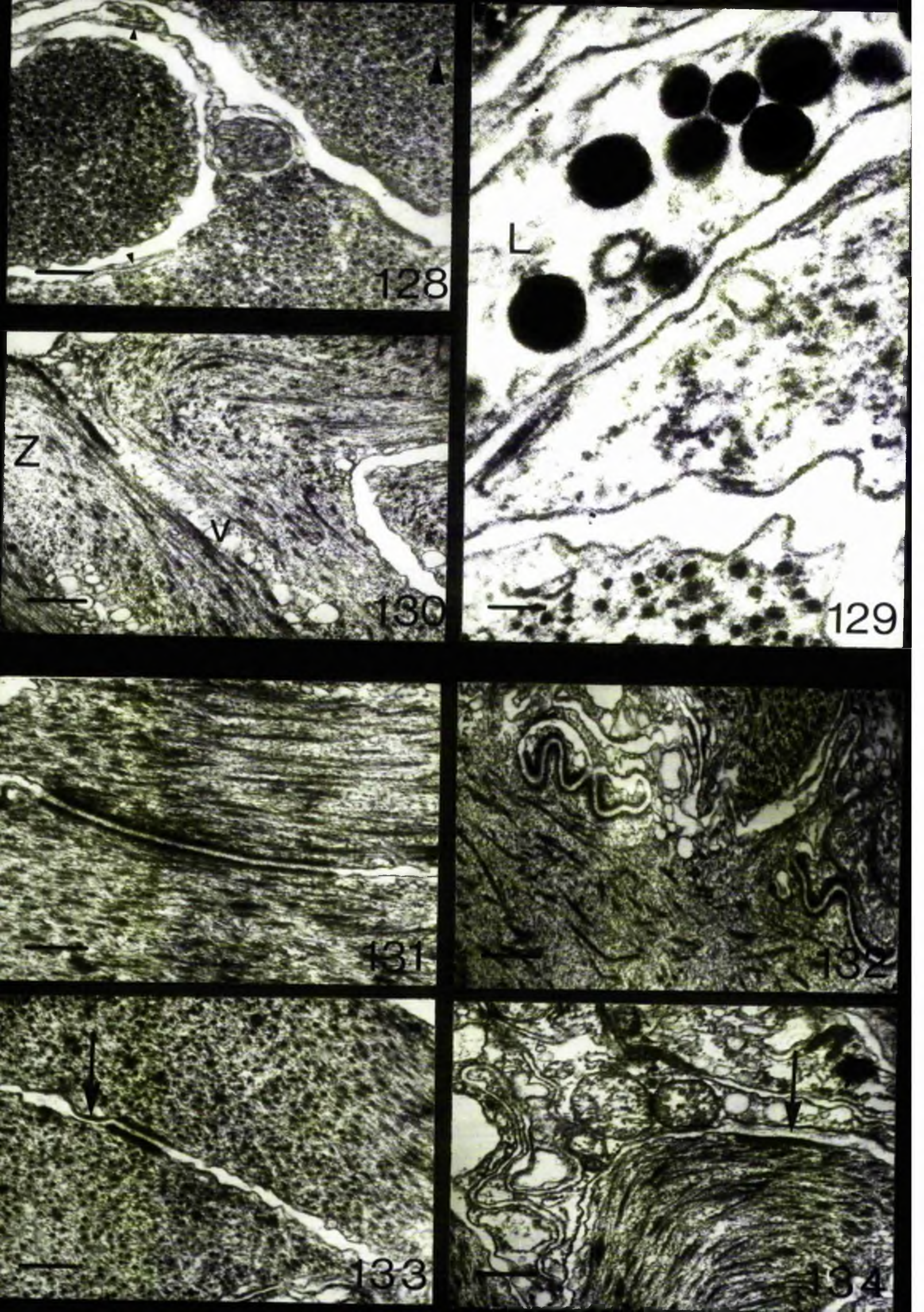
128
L
129
Z
V
130
131
132
133
134

Fig. 135

Muscle fibre/endothelial process septate junctions (J).

Arrow indicates granular structure in cytoplasmic matrix subjacent to transverse link forming junction.

Scale 300nm

Inset

Muscle/muscle septate junction (arrow) adjacent to desmosome.

Scale 200nm

Fig. 136

TF musculature at a level proximal to pore-pair.

Note the appearance of modified muscle processes - muscle tails (T).

C Connective tissue

M Muscle fibre - probably distal region of muscle tail since microtubules (arrow) occur within the sarcoplasm.

Scale 500nm

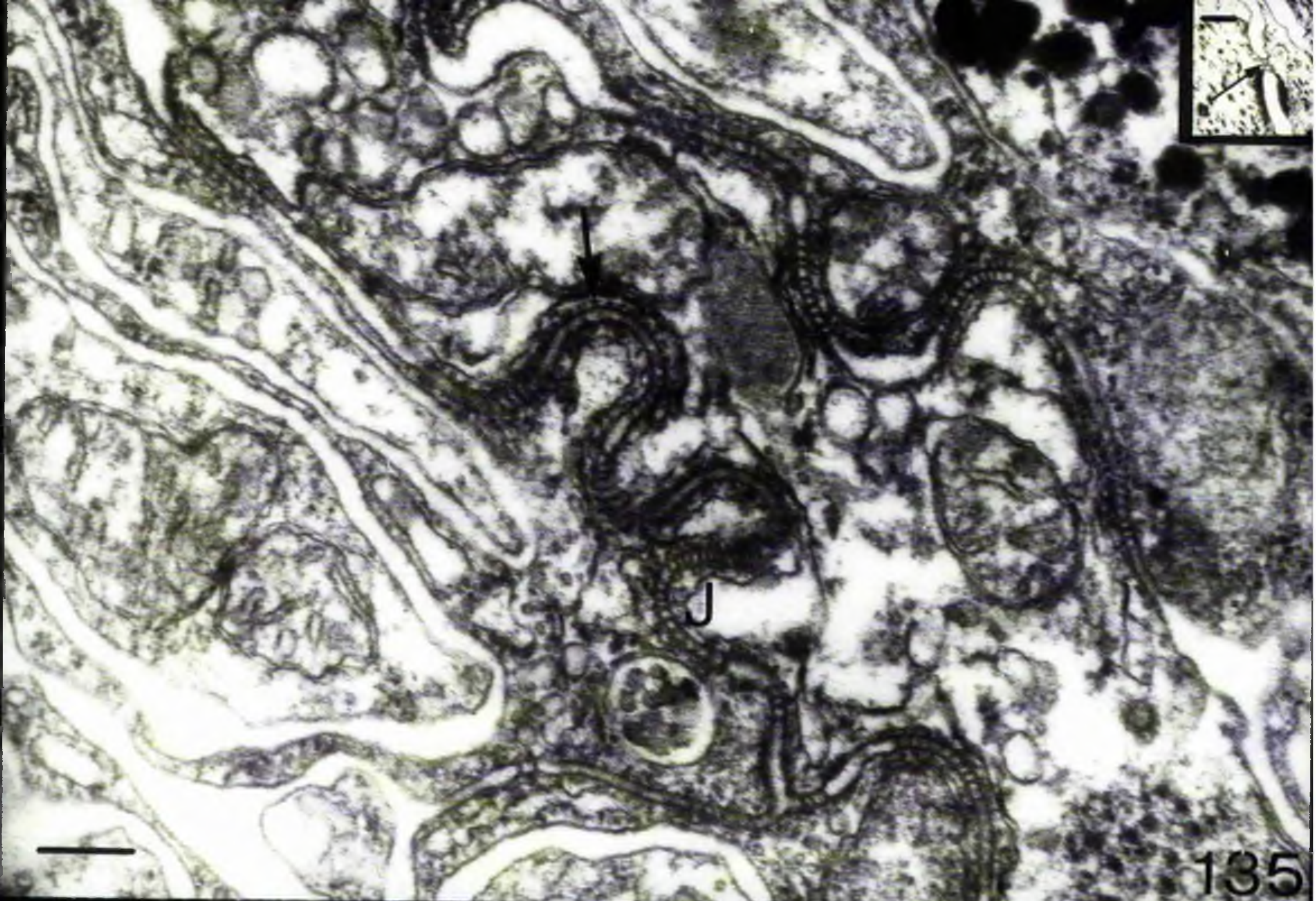

135

136

Fig. 137

Muscle tails entering the intraporal region.

Thick filaments disappear, leaving clear sarcoplasm containing mitochondria (m) and microtubules (arrow).

Scale 400nm

Fig. 138

TS PTF stem proximal to pore pair.

Bundles of muscle tails (e.g. a & b) have a similar appearance to axons within the adjacent tube foot nerve. Note the artefactual sinus between nerve and connective tissue.

Semithin, M. Blue.

Scale 20µ

Fig. 139

Bundle a from Fig. 138.

Scale 1µ

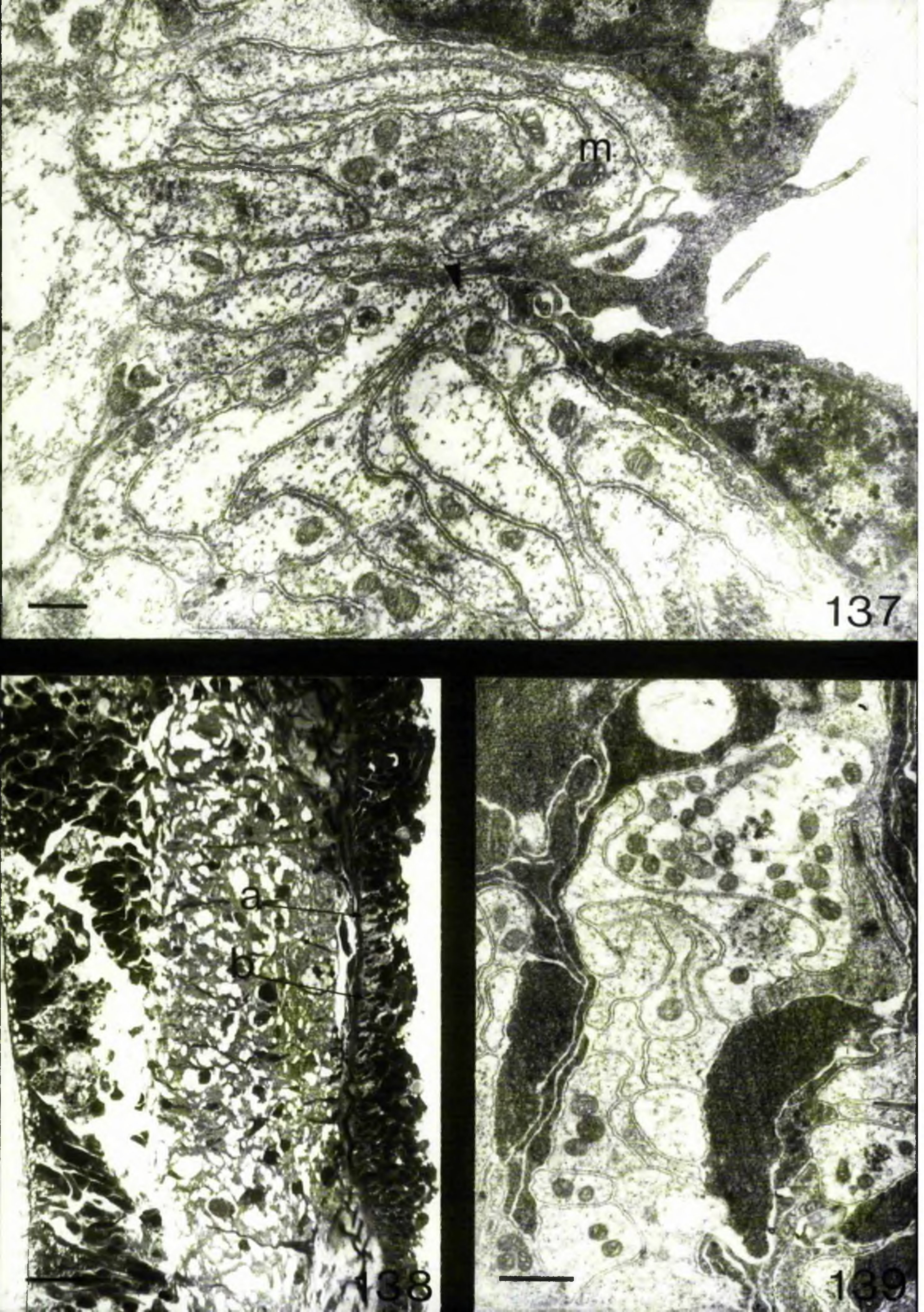
m
137
a
b
138
139

Fig. 140

Bundle b from Fig. 139.

Scale 1μ

Fig. 141

TS PTF stem proximal to pore pair.

Note the nerve (N) is in contact with the connective tissue (c)

Arrow Muscle tail bundle

Semithin, Azure/M.B.

Scale 20μ

Fig. 142

A connective tissue layer always separates basiepithelial

axons (A) from muscle tails (T).

Scale 500nm


140

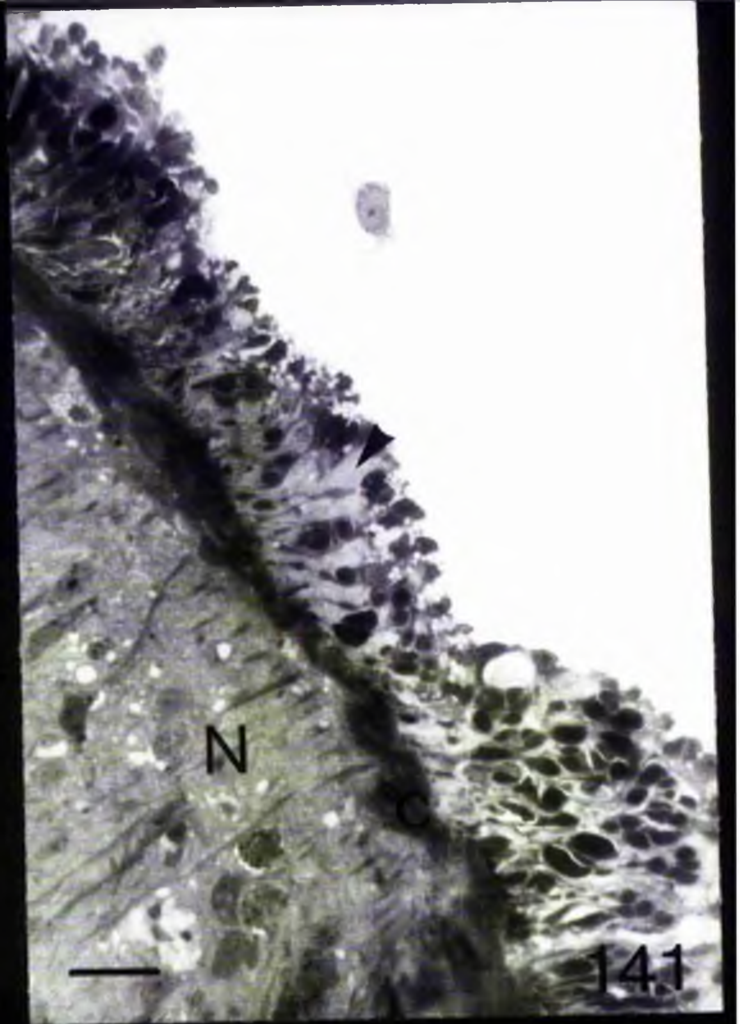
N
C
141

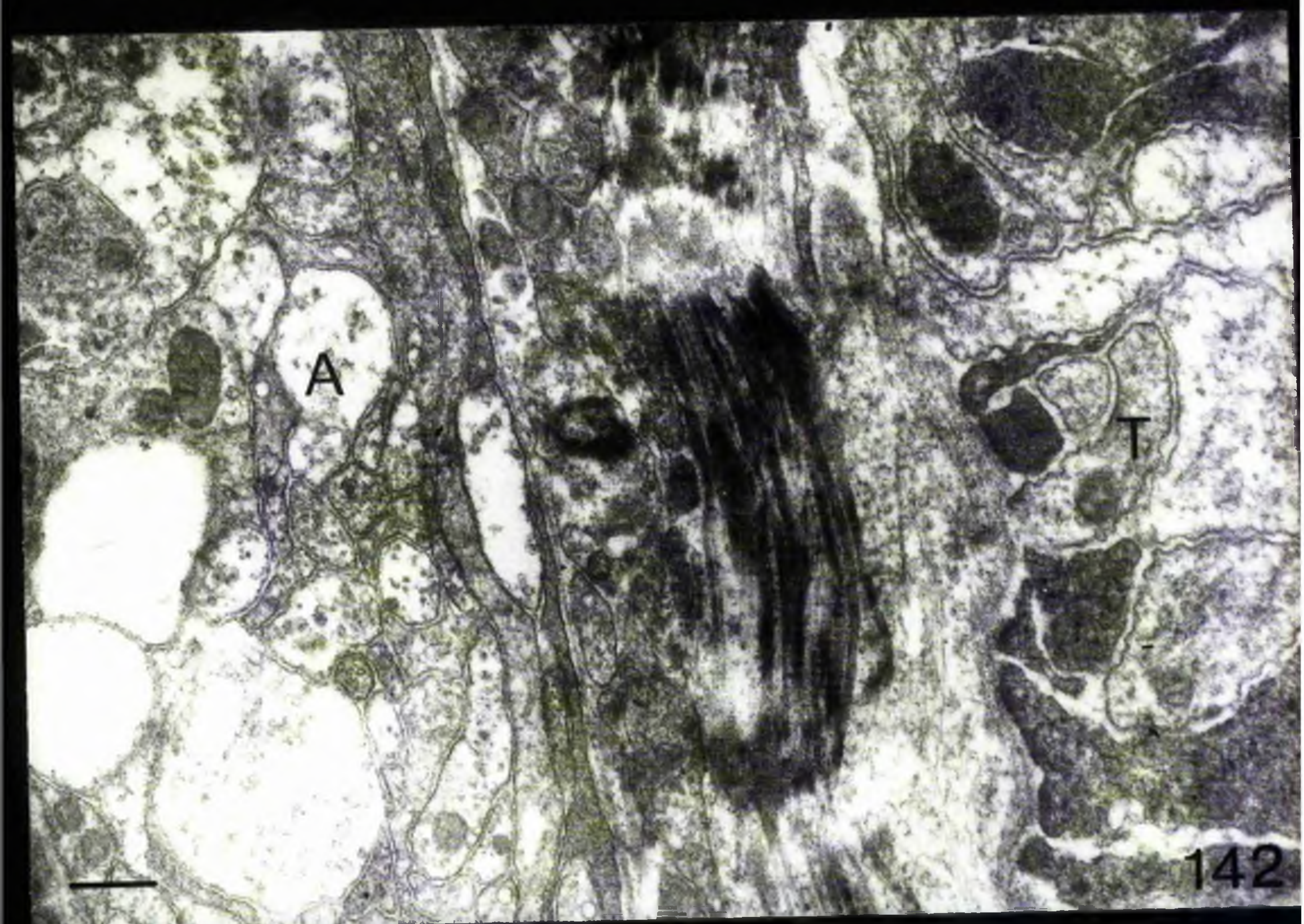
A
T
142

Fig. 143

T.S. PTF stem passing through interporal partition (I).

A thin connective tissue layer (arrow) still separates the T.F. nerve (lateral nerve) from the musculature. Muscle tail bundles are smaller and more diffuse at this level.

Semithin, Tol. B.

Scale 20μ

Fig. 144

The musculature only extends into the perradial pore (P). The adradial pore (A) does not contain any musculature, nor any nervous tissue.

Semithin, Tol. B.

Scale 20μ

Fig. 145

A morula-type amoebocyte (M) passing through the connective tissue of the intraporal region. Note the varicosities containing CV (arrow)

Scale 1μ


I


A
P
144


M
145

Fig. 146

Type I neurone somata, probably aminergic (A), containing numerous DCV (D).

Neurone somata were only observed within intraporal regions of the tube foot nerve.

Scale 1μ

Fig. 147

Type II neurone soma (N), bipolar and non-aminergic.

Note the well developed golgi complexes (g), and two processes (arrows).

Scale 500nm

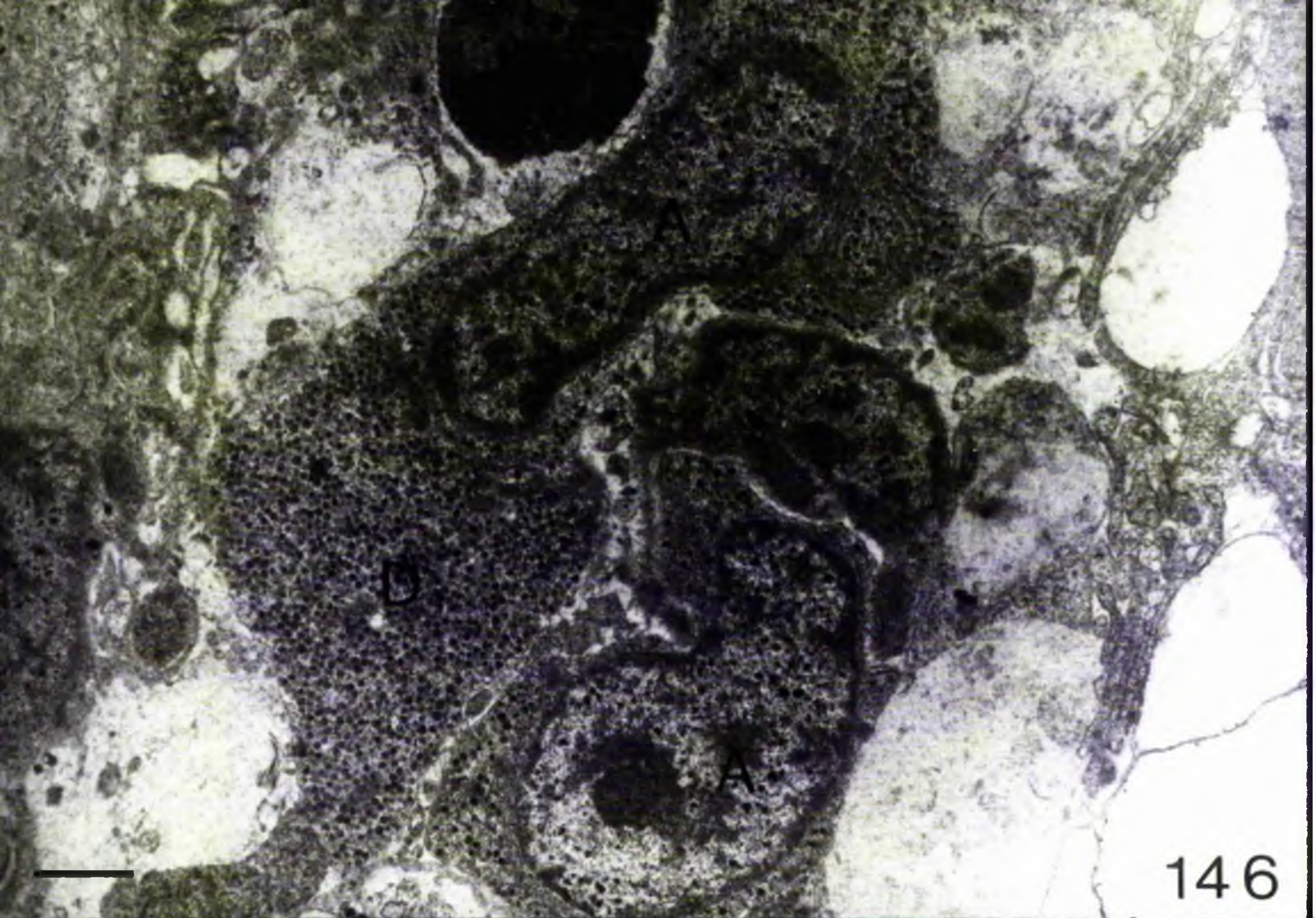

146

147

Fig. 148

Type I neurone soma containing DCV which possess a well developed core (arrow).

Scale 400nm

Fig. 149

Type I neurone soma containing DCV which possess a reduced core (arrow).

Note the extensive neurofilaments (n).

Scale 400nm

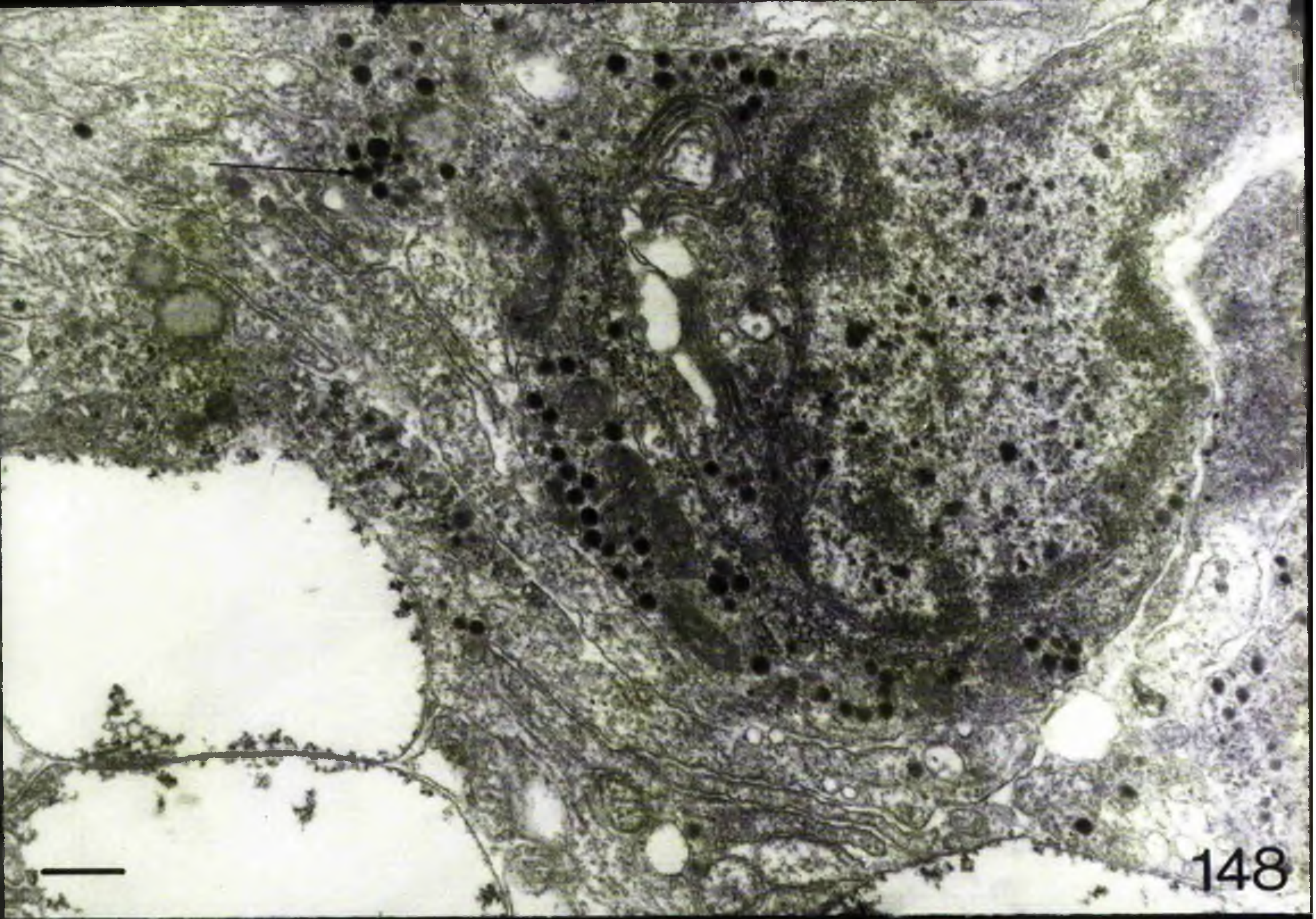

148

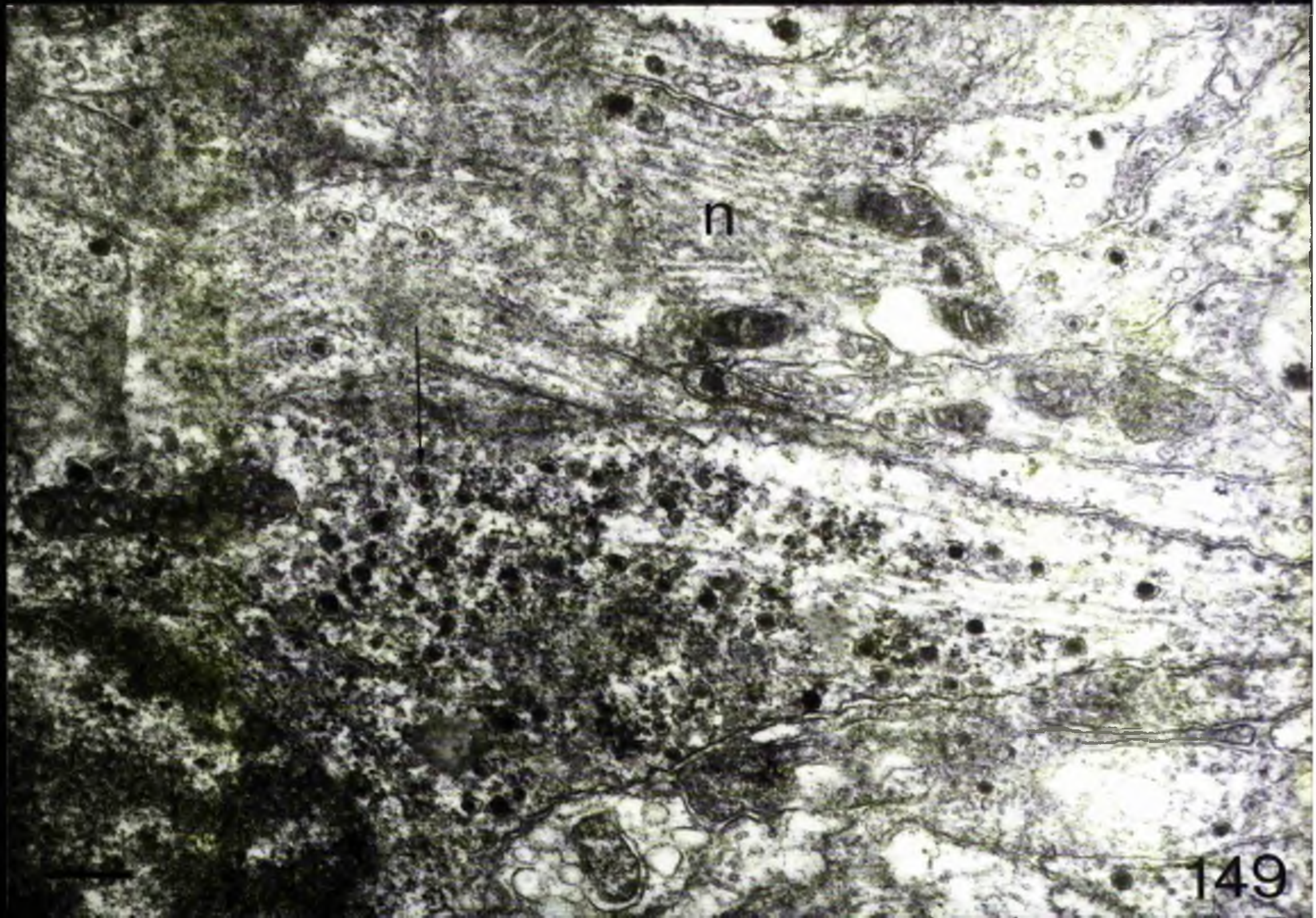

149

Fig. 150

Peristomial ampulla muscle fibre.

Note the evagination of the basal lamina (b) into the muscle.

Scale 250nm

Fig. 151

Mitochondrion cluster within ampulla muscle fibre.

Note the close packing of the mitochondria (arrow).

Scale 250nm

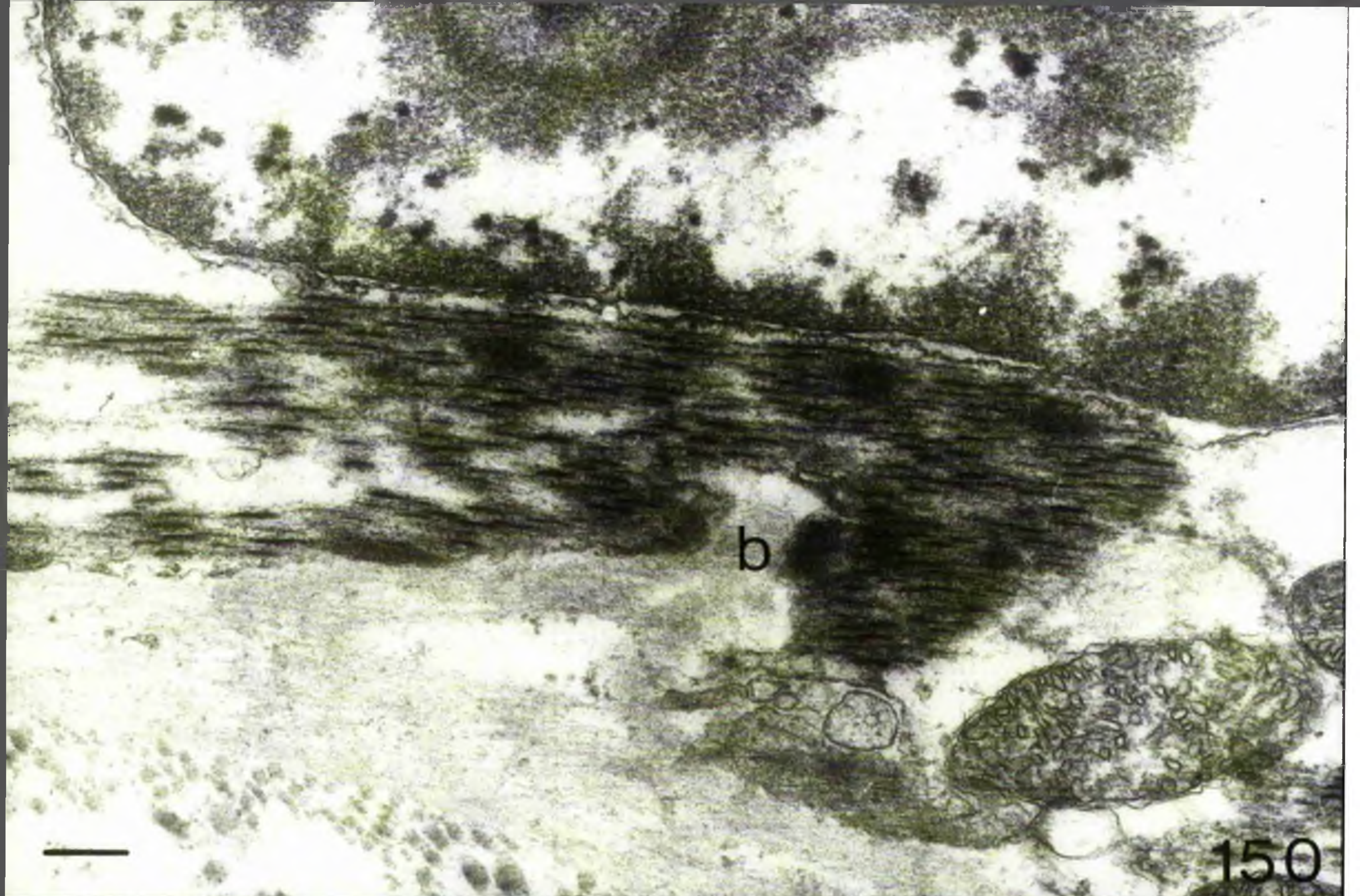
b
150


151

Fig. 152

T.S. ATF stem.

AB-CEC [$MgCl_2$] = OM

Without the presence of electrolytes, alcianophilia occurs in all tissues, particularly the muscle layer (arrow).

Scale 20μ

Fig. 153

T.S. ATF stem.

AB-CEC [$MgCl_2$] = 0.2M

Addition of low electrolyte level decreases alcianophilia in the muscle layer but not within the circular connective tissue (large arrow) nor the endothelia (small arrow).

Scale 20μ

Fig. 154

T.S. ATF stem.

AB-CEC [$MgCl_2$] = 1.0M

High levels of electrolytes abolish alcianophilia in the muscle layer but not within the connective tissue (particularly circular layer-arrow) and endothelia.

Scale 20μ

Fig. 155

ATF collagen filaments.

PA-Bi

Small arrows Transverse belts

Large arrow Outer coat

Scale 200nm

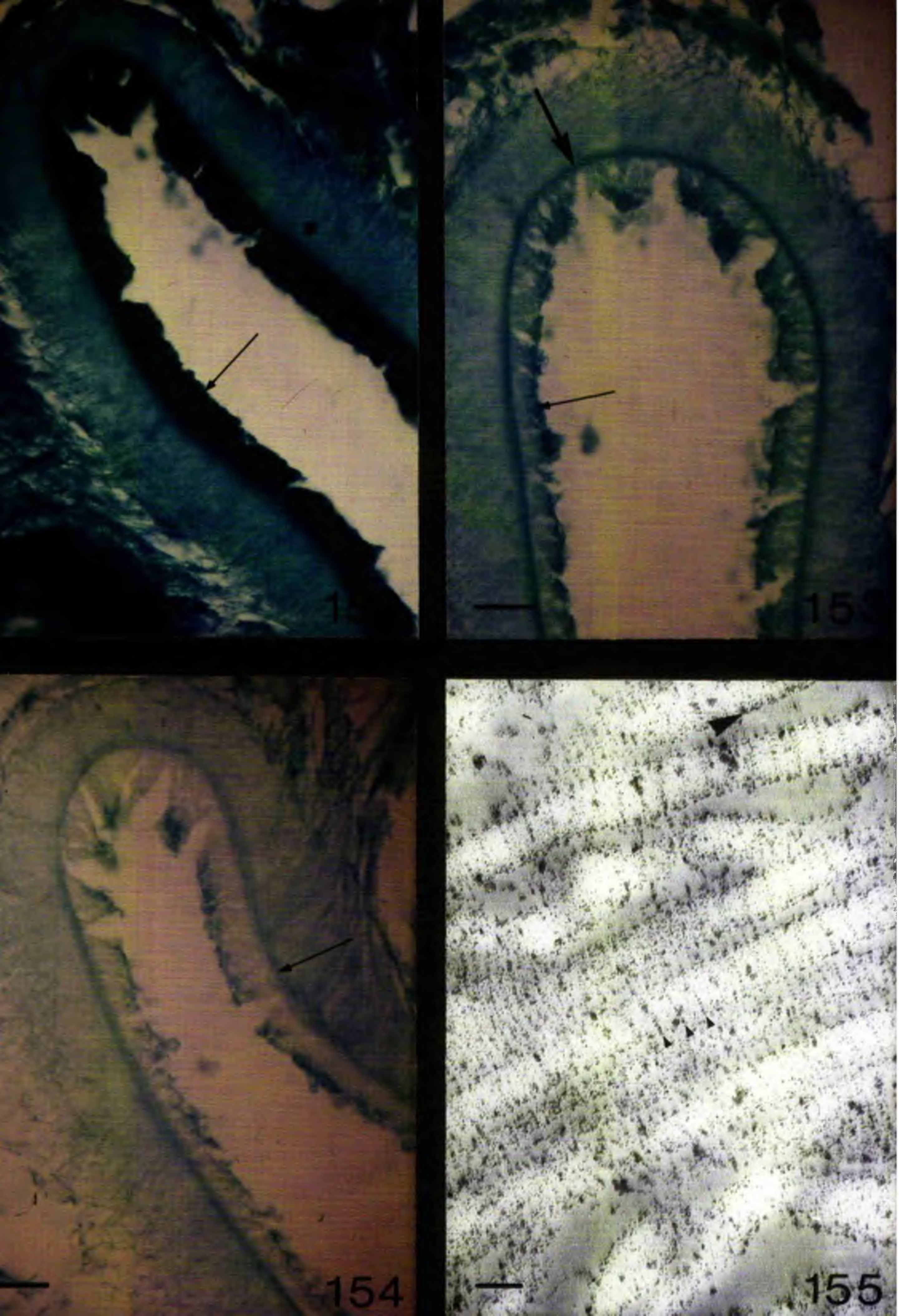
154
155

Fig. 156

ATF collagen filaments. PA-Bi

Small arrows   Fine lateral filaments

Scale 200nm.

Fig. 157

PA-Bi Control

Scale 200nm.

Fig. 158

PTF plate

Semithin, Azure/BF.

Collagen filaments interweaving among the stereom (s) show intense fuchsinophilia (arrow).

Scale 20μ

Fig. 159

The tissue within the stereom (termed stroma) contains a variety of amoebocytes (a), amorphous connective tissue and collagen bundles (arrow) wrapping around skeletal trabeculae (t).

Note the LDSG process (L).

Scale 1.5μ

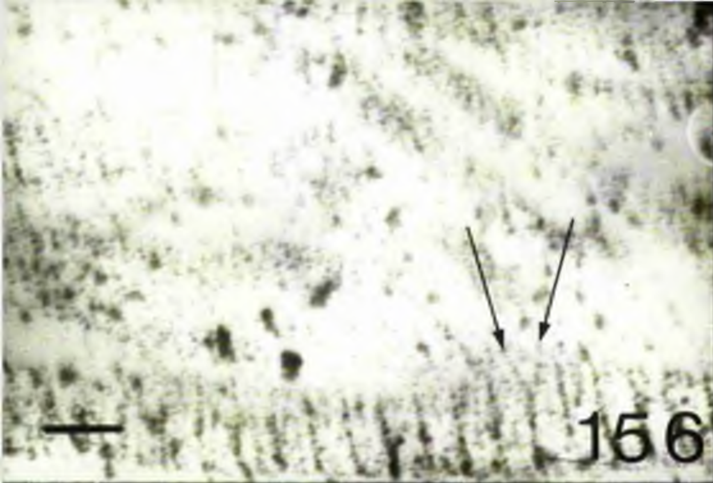
156

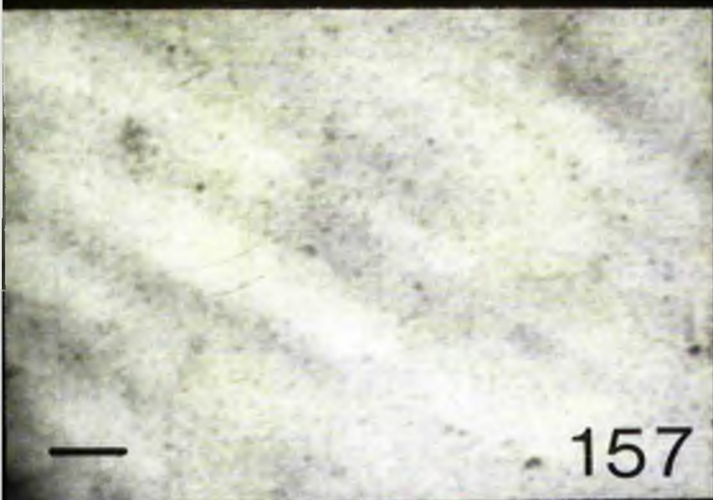
157

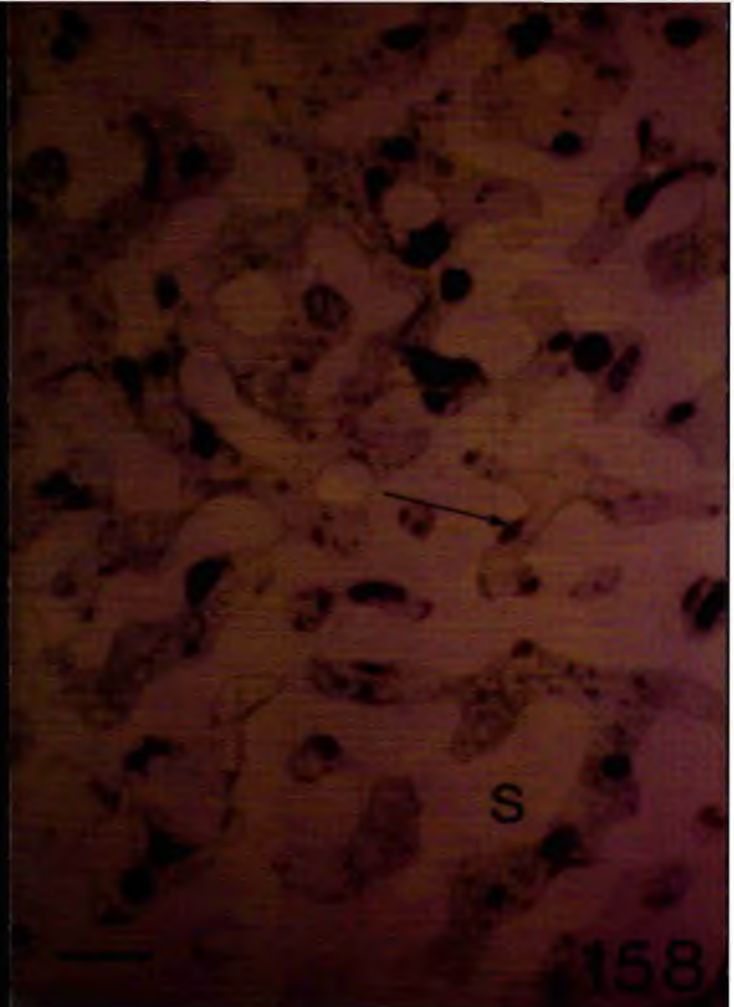

158

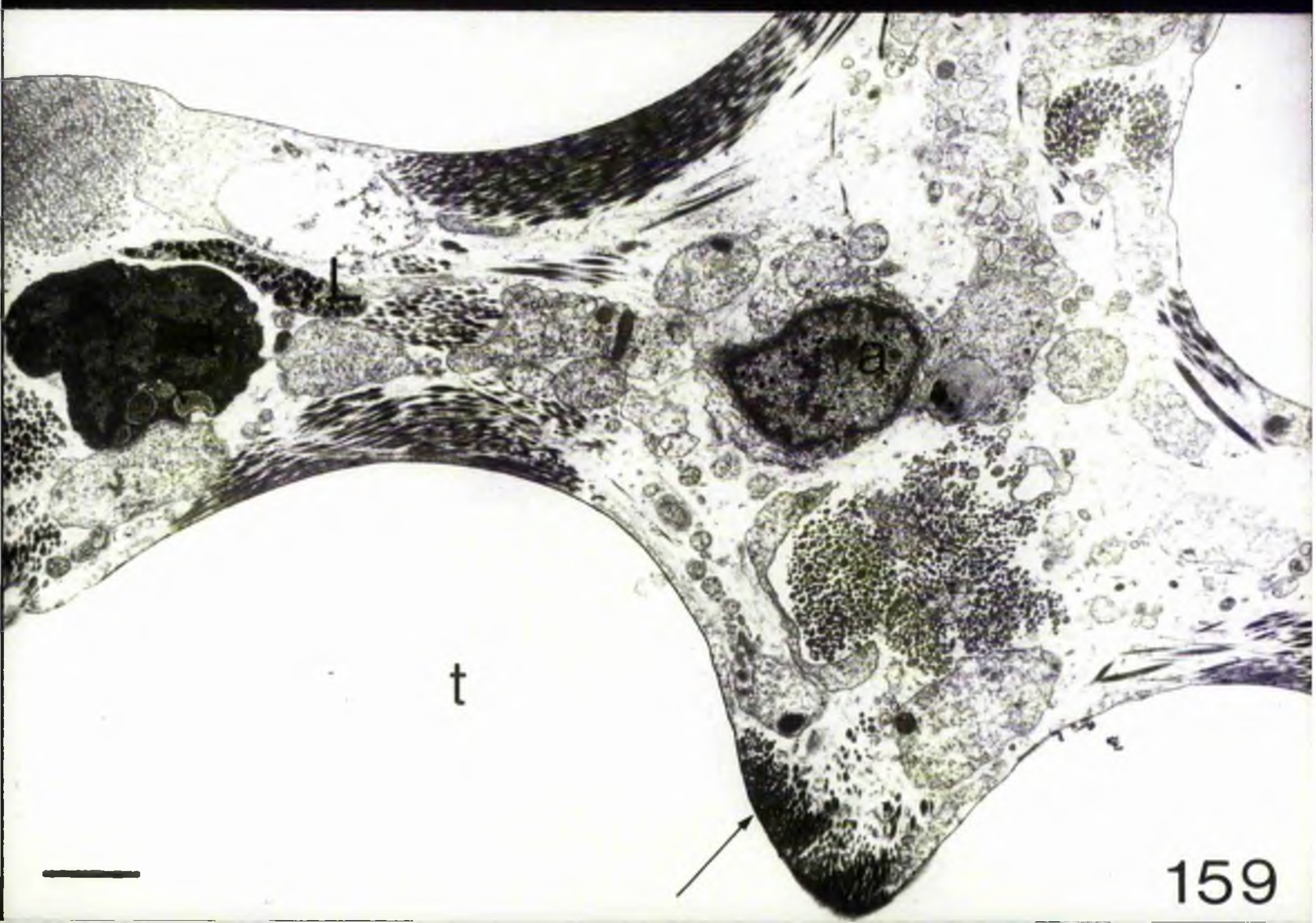

159

Fig. 160

Collagen filaments (F) wrapping round a trabecula (t).

Note the trabecular surface is smooth.

b Basal lamina

Scale 300nm

Fig. 161

Collagen filaments (F) inserted onto a trabecula (t).

Note the interweaving fibrils (arrow) and the irregular trabecular surface.

Scale 300nm

Fig. 162

LDSG cell soma within ATF connective tissue.

Note the cisternae of RER(R) aligned parallel to the nuclear membrane. Fix III.

Scale 600nm

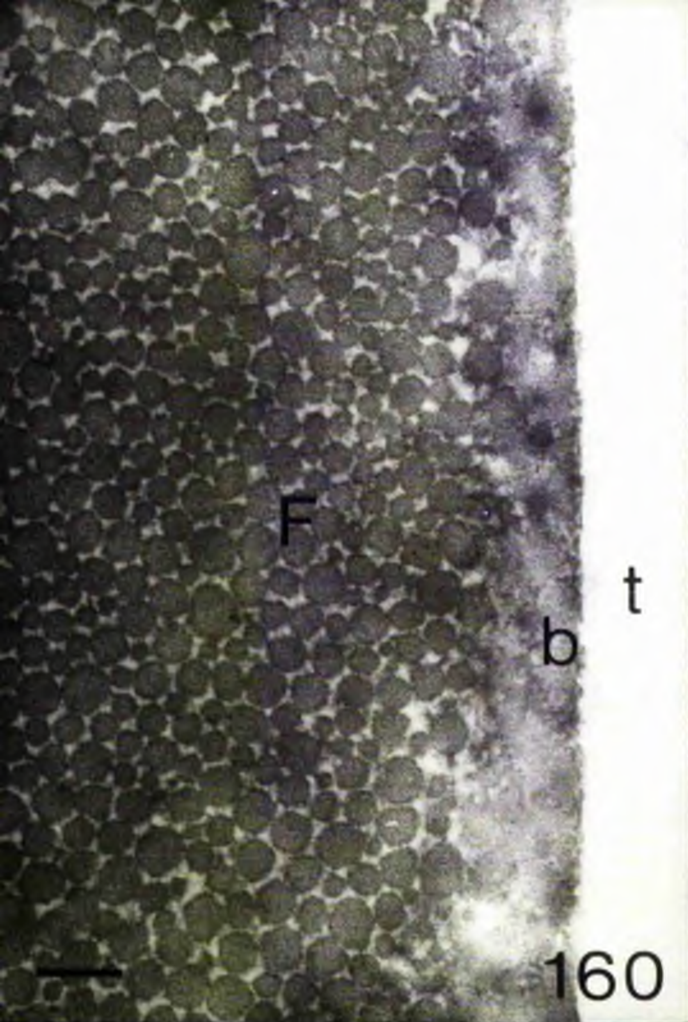
F
t
b
160


F
t
161

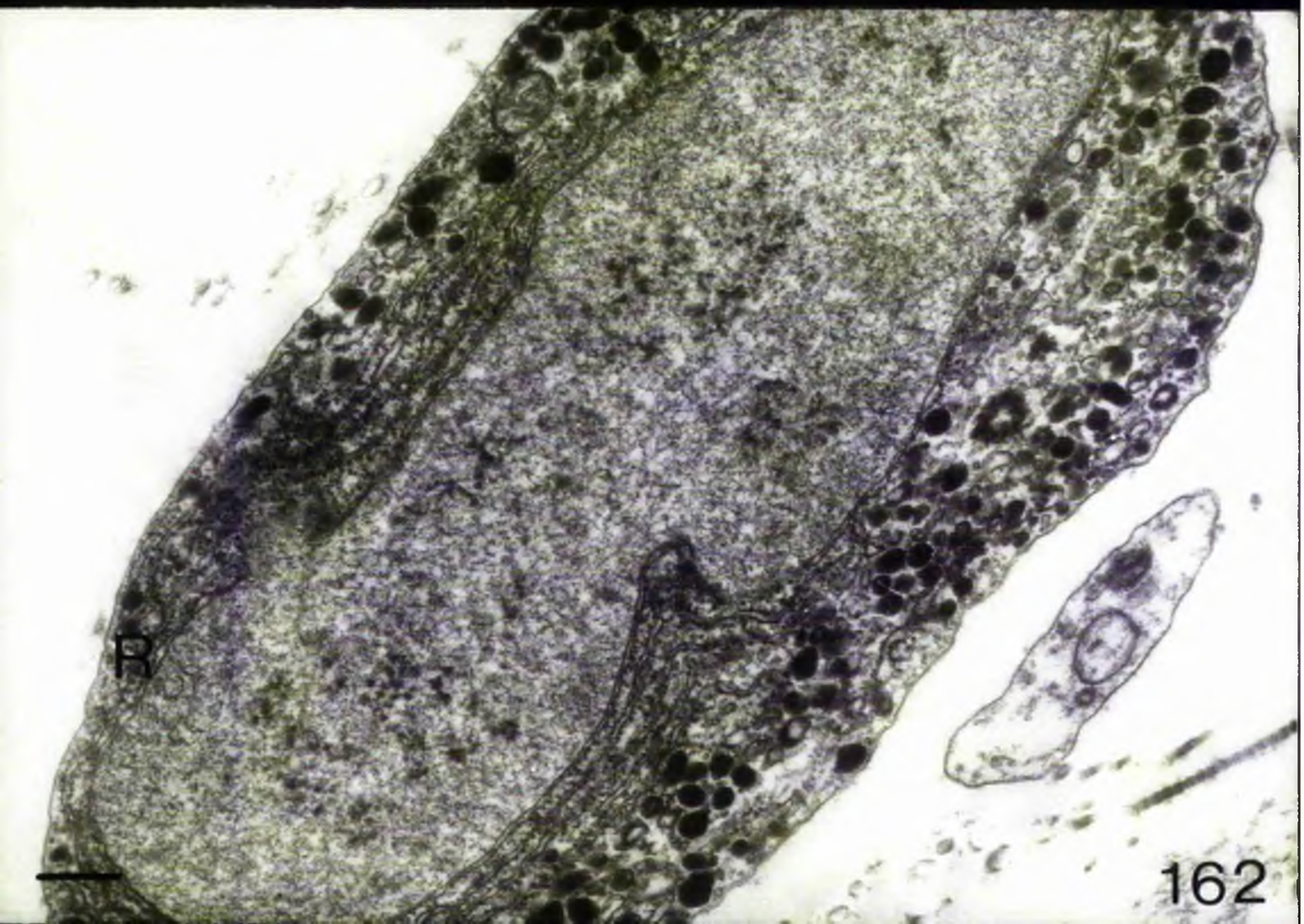
R
162

Fig. 163

LDSG cell soma within ATF musculature - Fix. I.

Note the ruptured RER (arrow) and intense osmiophilia of the LDSGs.

Scale 1μ

Fig. 164

LDSG processes (L) tunnelling through muscle cell (m).

Note the sheath (sarcolemmal?) which surrounds one of the LDSG processes (arrow). Fix. I.

Scale 250nm

Fig. 165

The LDSG plexus within the TF musculature terminates against the connective tissue sheath (C).

Note the variation in shape and size of LDSGs.

Scale 250nm

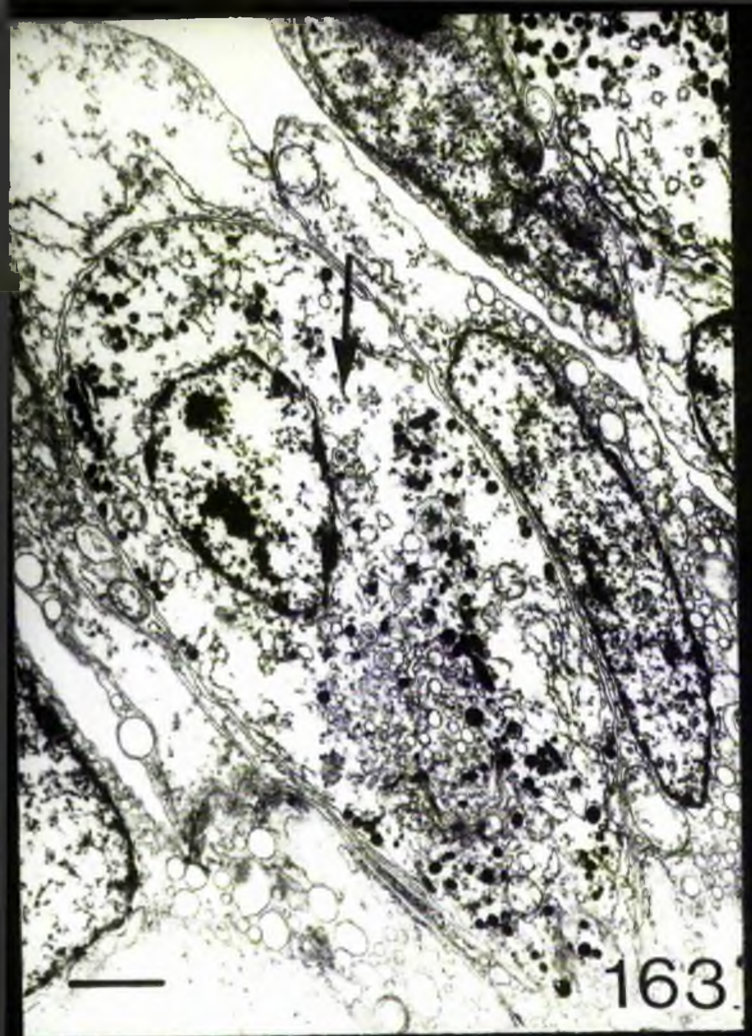
163

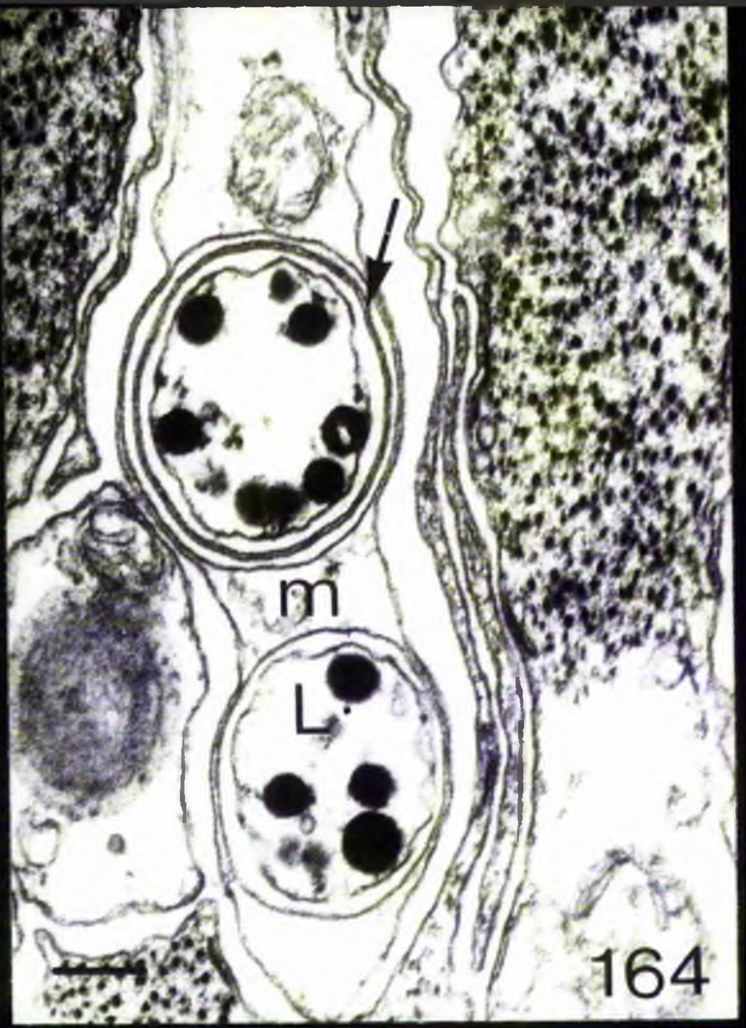
m
L
164

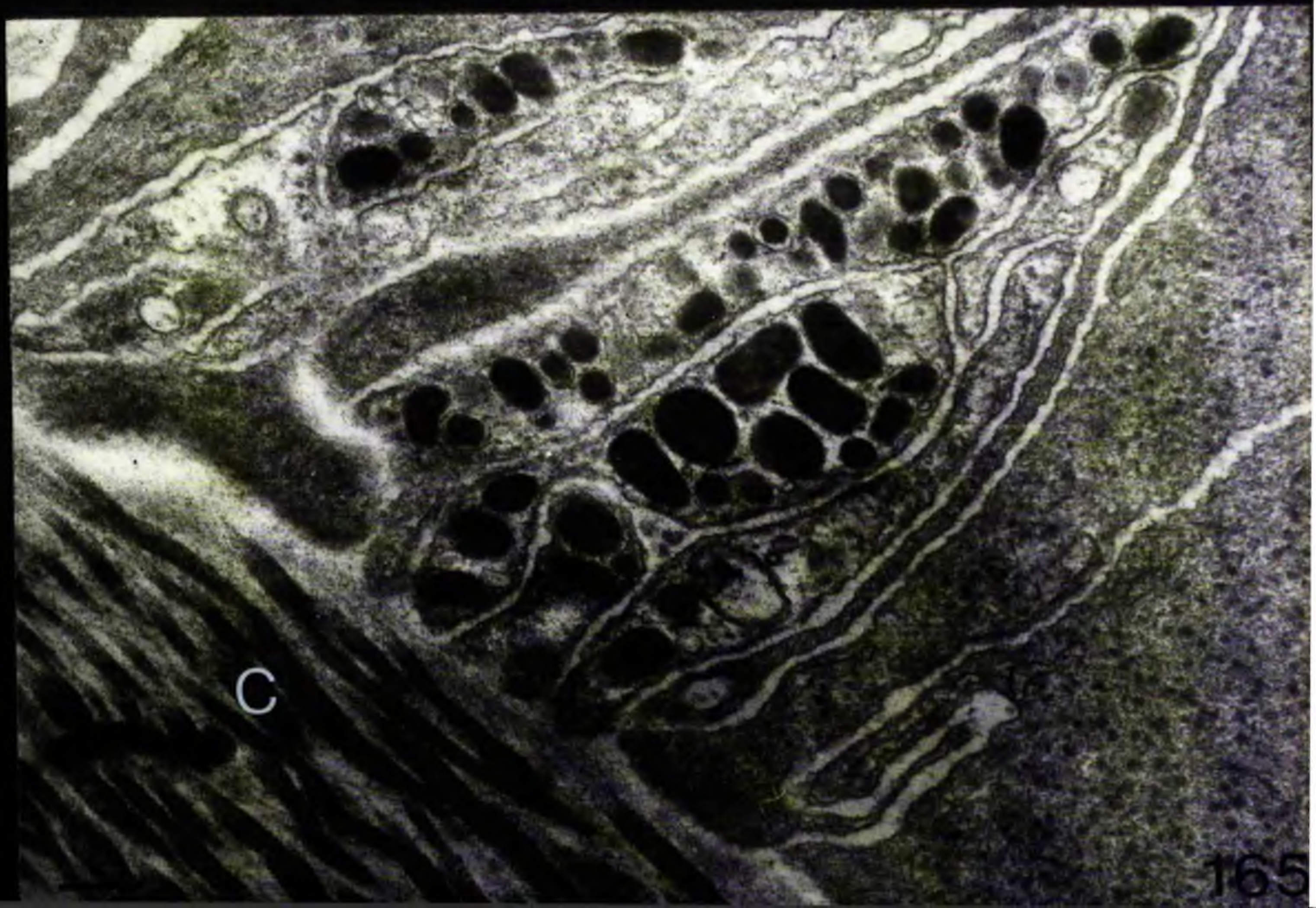
C
165

Fig. 166

Possible synaptoid contact between CV-containing basiepithelial axon (a) and LDCG process (l) within connective tissue.

Scale 300nm

Fig. 167

Terminations of LDCG axons accompany lateral evaginations (e) of the muscle fibre into the connective tissue.

Note the spurious lack of electron density of the collagen filaments (arrow).

Scale 300nm

Fig. 168

ATF muscle layer.

The small LDCG processes show intense, non-metachromatic basophilia (arrows). C Connective tissue (metachromatic)

Semithin, Tol. Blue

Scale 10µ

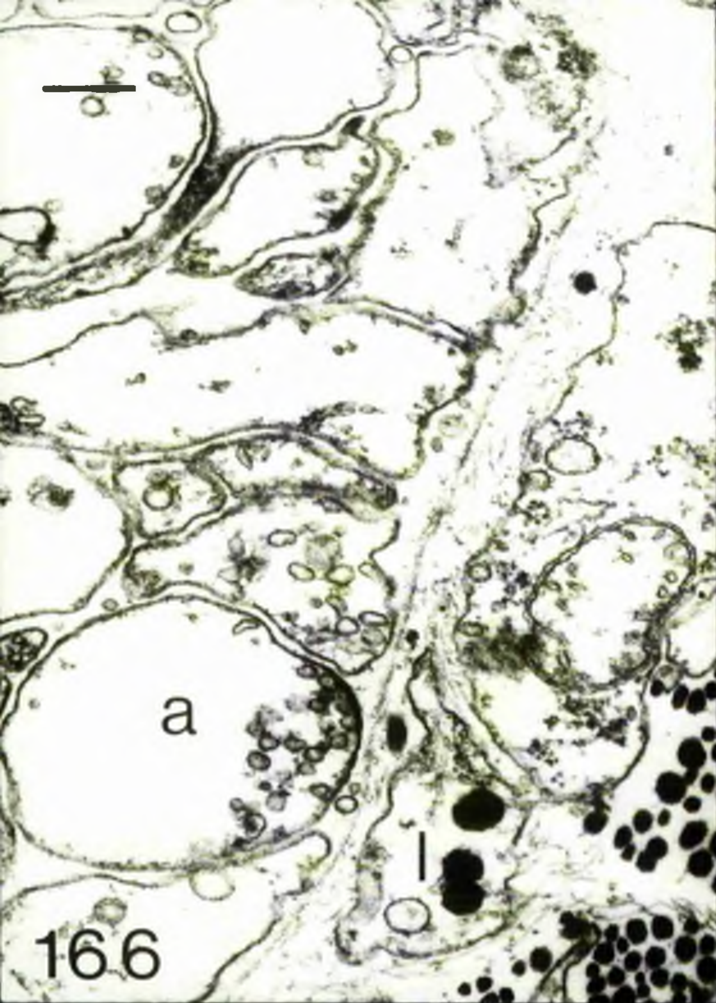
a
l
166


c
168

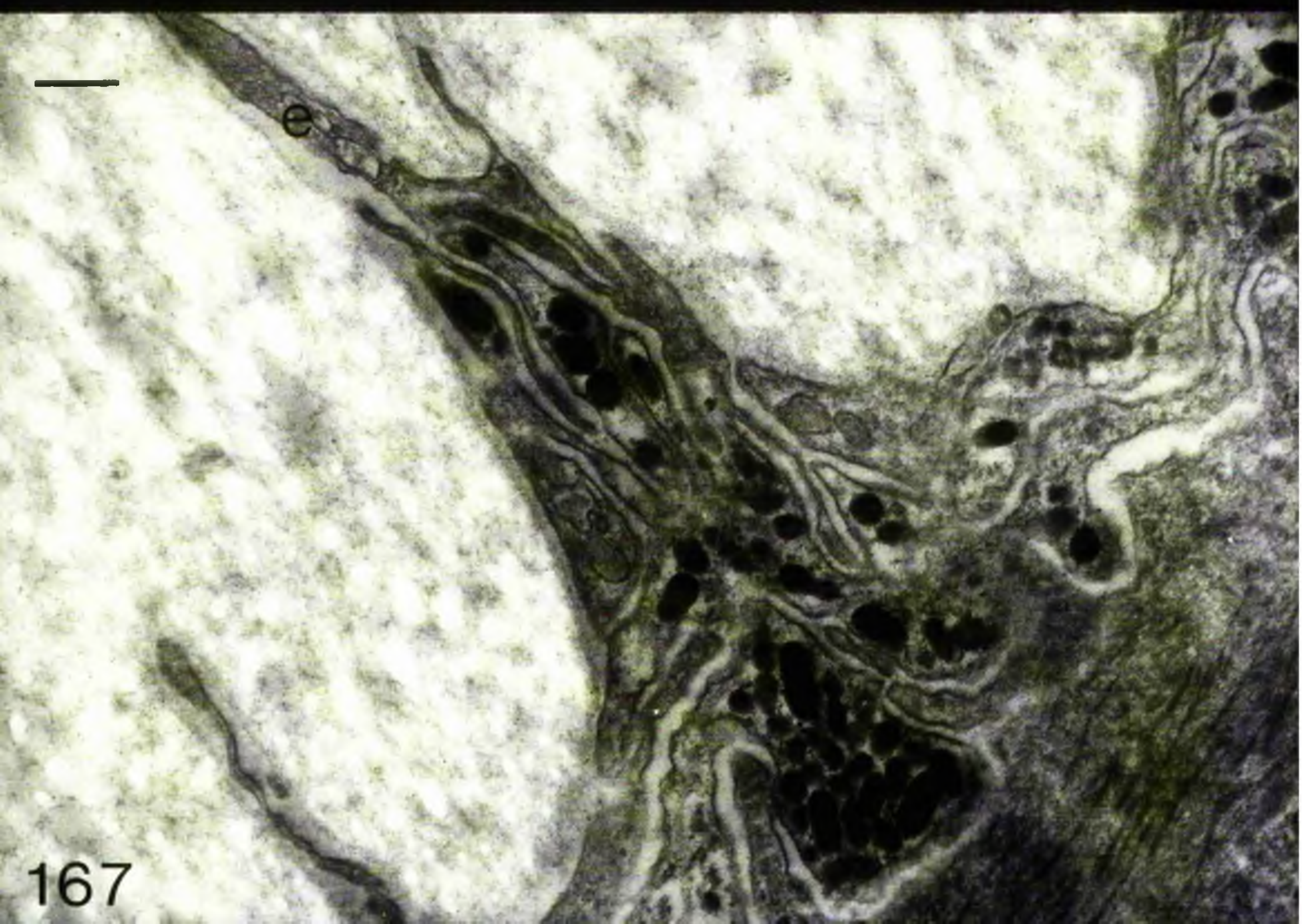
e
167

Fig. 169

Basophilic granules within a LDSG cell soma (arrow).

Semithin, Tol. Blue

Scale 10μ

Fig. 170

Several basophilic LDSG processes (arrow) terminate against the connective tissue.

Semithin, Azure/A.F.

Scale 10μ

Fig. 171

ATF: Paraffin section, AB-PAS.

Blue alcianophilic cell bodies (nuclei) within endothelia and alcianophilic outer connective tissue layer (i.e. non-collagenous zone).

Purple Schiff $+^{ve}$/alcianophilic

m Muscle, c Connective tissue, arrow Schiff $+^{ve}$ cell body.

Scale 30μ

Fig. 172

ATF: Paraffin section, PAS

c Connective tissue m Muscle arrows LDSG process.

Scale 10μ

Fig. 173

ATF: Paraffin section, PAS - Control

Scale 30μ

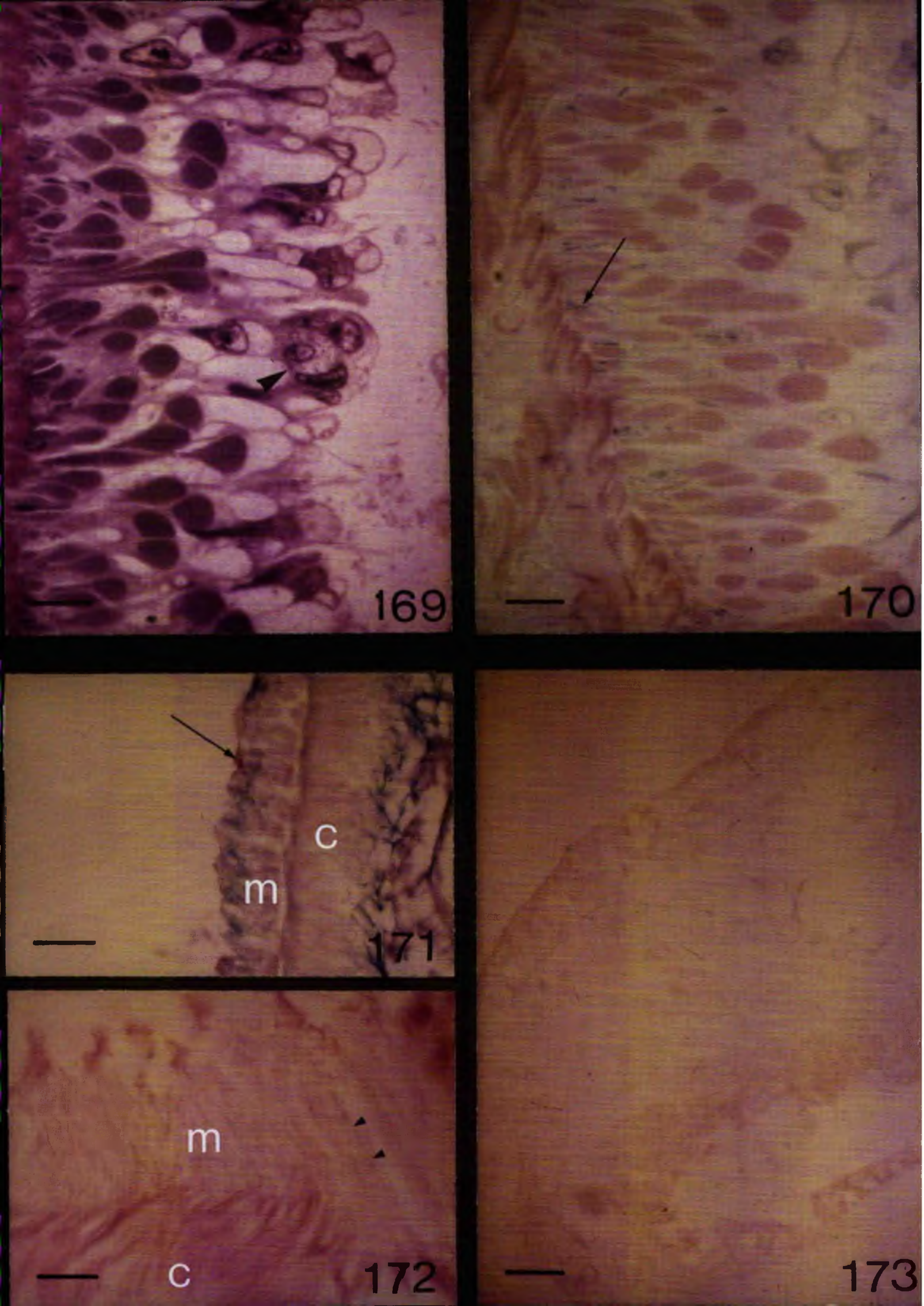
169
170
c
m
171
m
c
172
173

Fig. 174

ATF: Semithin, PAS/Haem.

Schiff $+^{ve}$ reaction in cuticle (small arrow) and LDCG cells (large arrow).

Scale 30µ

Fig. 175

ATF: Semithin, PAS/Haem.

Schiff $+^{ve}$ reaction in LDCG cell soma and process (large arrow)

Note processes terminating against connective tissue (small arrow).

Scale 10µ

Fig. 176

ATF: Semithin, PAS/Haem.

Schiff $+^{ve}$ LDCG processes (arrow)

Scale 10µ

Fig. 177

LDCG cell soma: PA-Cr-Ag

Silver precipitation occurs over LDCGs (l), nucleus (n) and ribosomes (arrow indicates ribosomes on RER).

Scale 400nm

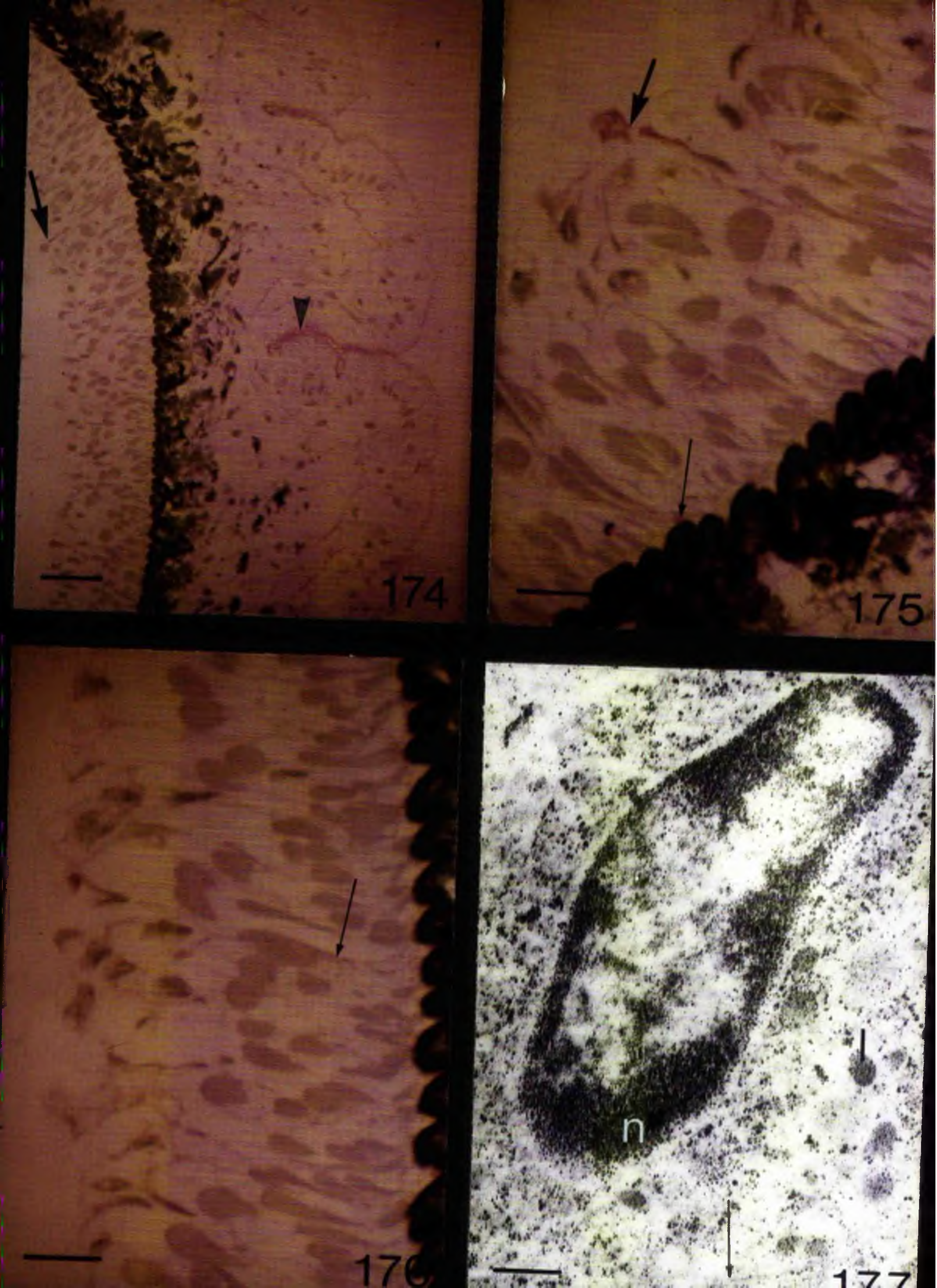
174
175
n

Fig. 178

PTP muscle layer: PA-Cr-Ag.

Intense silver precipitation occurs over LDSGs (l) and a slight background precipitation also occurs over muscle cells (m).

Scale 200nm

Fig. 179

LDSGs: PA-Cr-Ag.

Precipitation of silver is restricted to the granule, very little occurs within the LDSG cell cytoplasm.

p Precipitation over collagen filaments.

Scale 70nm

Fig. 180

LDSGs: PA-Bi

Similar to PA-Cr-Ag method

The Bismuth precipitate is finer than the silver.

Scale 60nm

Fig. 181

LDSG process/connective tissue: PA-Cr-Ag Control

Scale 150nm

Fig. 182

LDSG process/muscle layer: PA-Bi Control

Scale 150nm

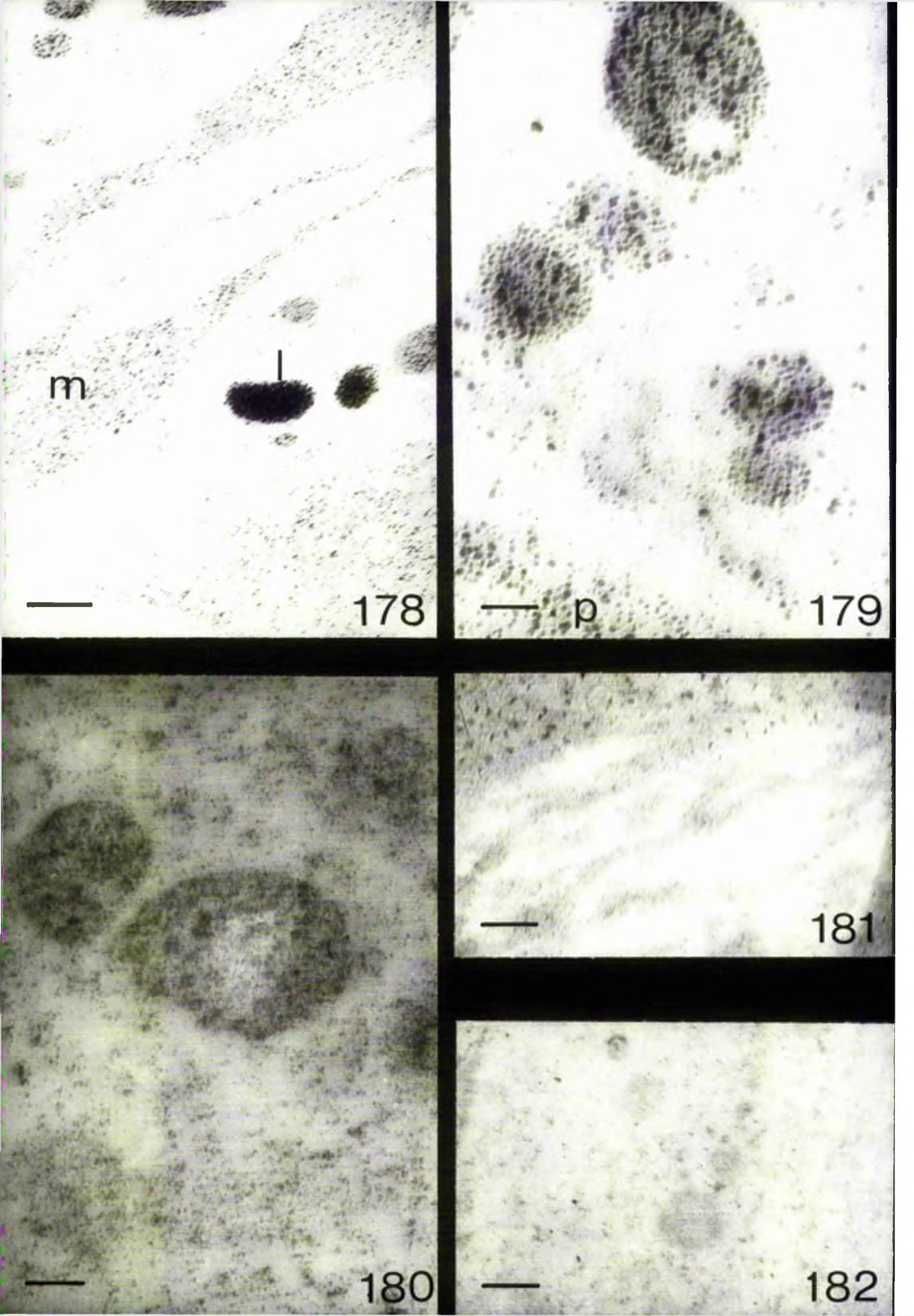
m
178
p
179
180
181
182

Fig. 183

ATF cuticle: PA-Cr-Ag.

Silver precipitation occurs in a coat around epithelial microvilli (small arrow - T.S. microvillus, large arrow - L.S. microvillus).

Scale 70nm

Fig. 184

LDSG processes within connective tissue of ATF disk.

arrow Neurotubules

Scale 750nm

Fig. 185

LDSG process and small muscle fibre (arrow) within spine catch apparatus.

Scale 500nm

Fig. 186

The catch apparatus consists of large bundles of collagen filaments receiving a considerable LDSG innervation.

Scale 750nm

Inset Catch apparatus.

LDSG processes (arrow) are basophilic in contrast to the metachromatic collagen.

Semithin, Azure/M.B.

Scale 10μ

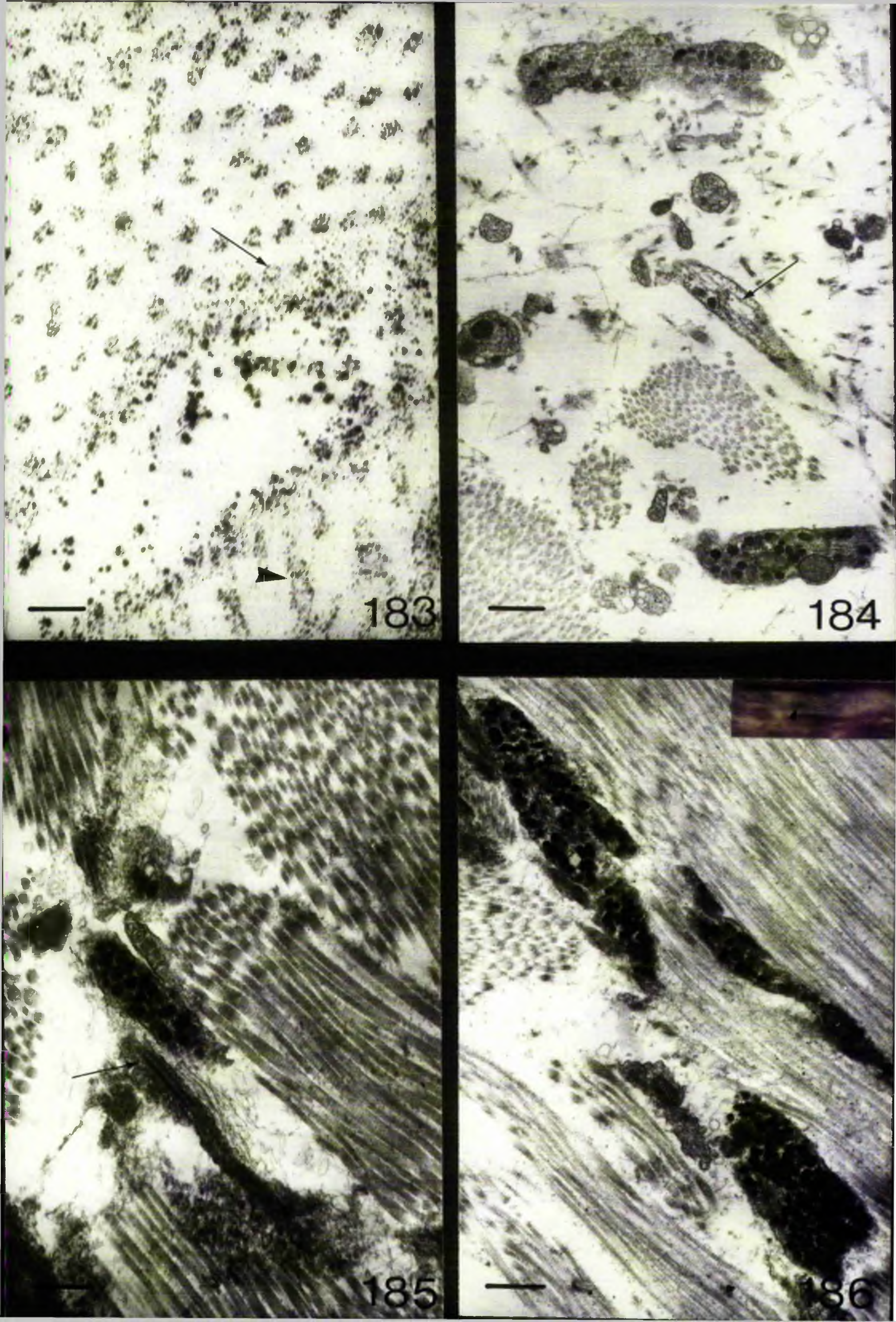
183
184
185
186

Fig. 187

Spine tubercle.

LDSG process adjacent to four axons of an unknown type.

Scale 500nm

Fig. 188

Spine tubercle.

Small LDSG process surrounded by four axons of an unknown type. Note the neurotubules (arrows) occurring in both types of axon.

Scale 500nm

Fig. 189

Spine tubercle.

LDSG cell soma.

Scale 2μ

Fig. 190

ATF musculature: K-ant.

Sb precipitation on:

Muscle cisternae (arrow)

" sarcolemma (s)

Degranulating LDSGs (l)

Scale 400nm


187


188


189

190

Fig. 191

ATP: K-ant.

m Mitochondria in muscle process

s Subsurface vesicles in muscle

Scale 300nm

Fig. 192

ATP: K-ant.

Arrow Subsurface cisternae in muscle

Scale 300nm

Fig. 193

ATP: K-ant.

Arrow Cisternae in muscle

Scale 300nm

Inset: EDTA treatment removes Pb precipitate.

Fig. 194

ATP: K-ant.

l LDSG process

m Muscle

arrow Intense precipitate on LDSG

Scale 300nm

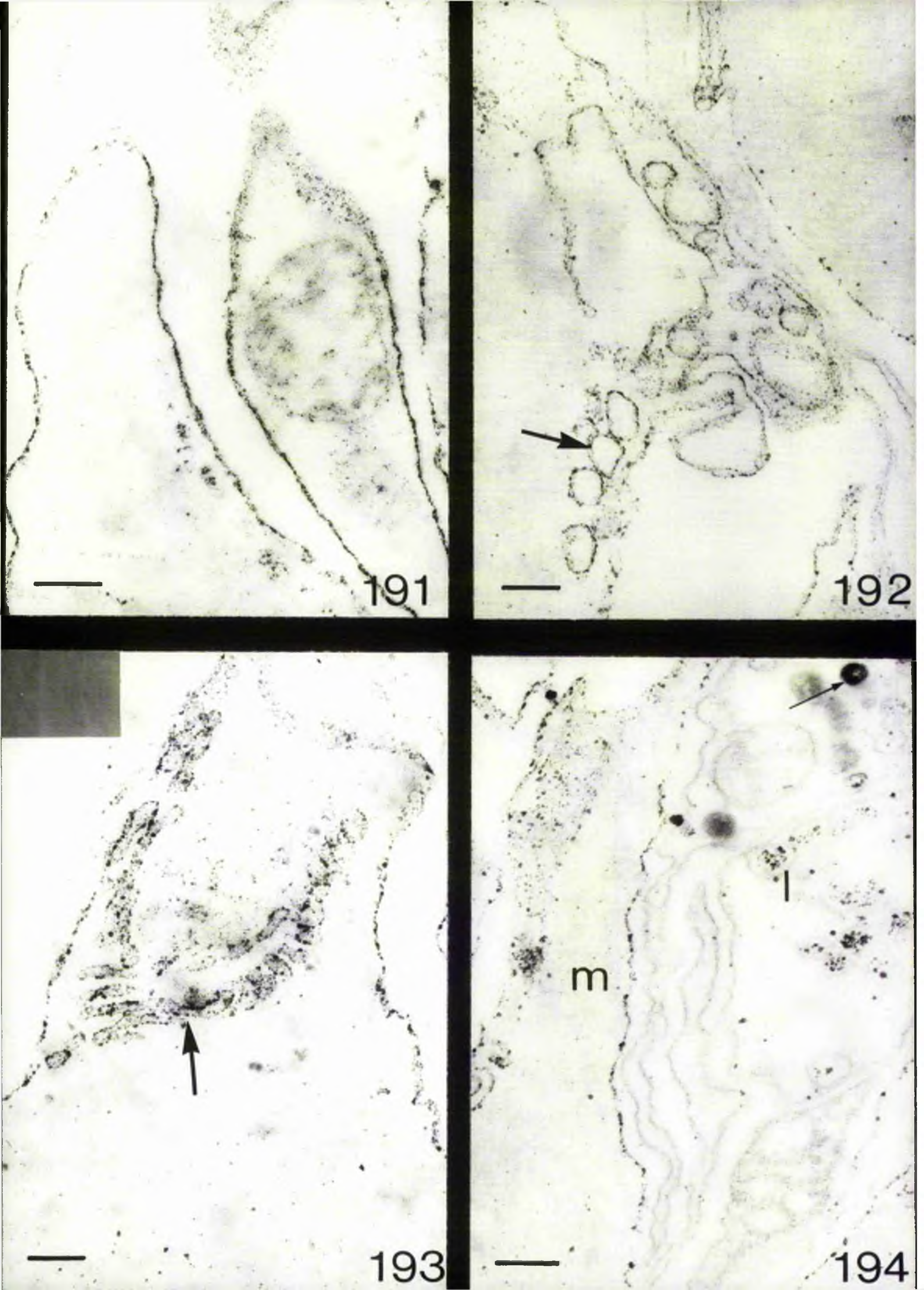
191
192
193
l
m
194

Fig. 195

X-ray spectrum: Subsurface cisternae precipitate

Distinct Sb and Ca peaks at 3.6 & 3.7 KeV.

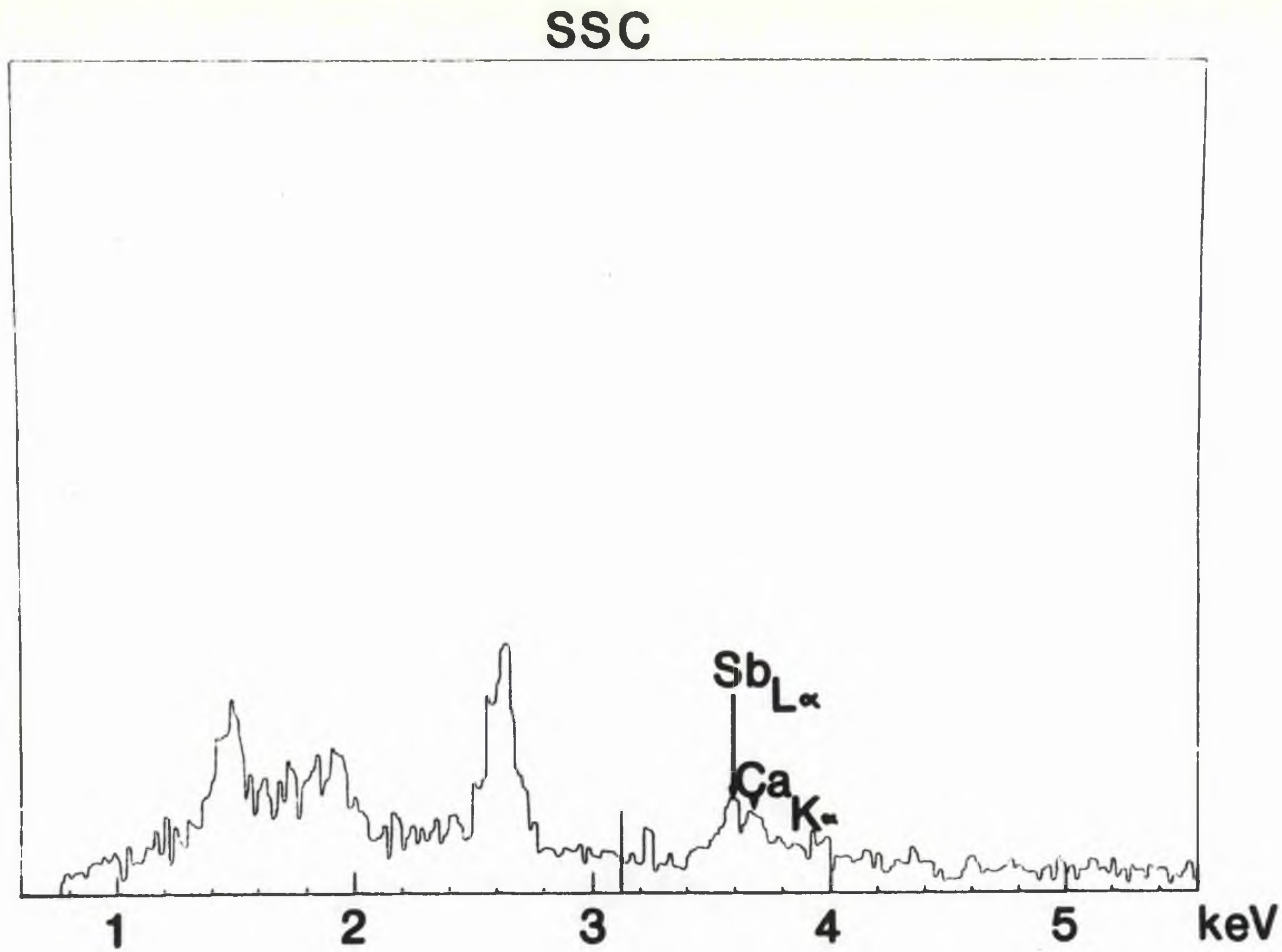
SSC
Sb Lα
Ca Kα
1
2
3
4
5
keV

Fig. 196

X-ray spectrum: Subsurface cisternae precipitate

Ca peak is skewed, but quite distinct from Sb.

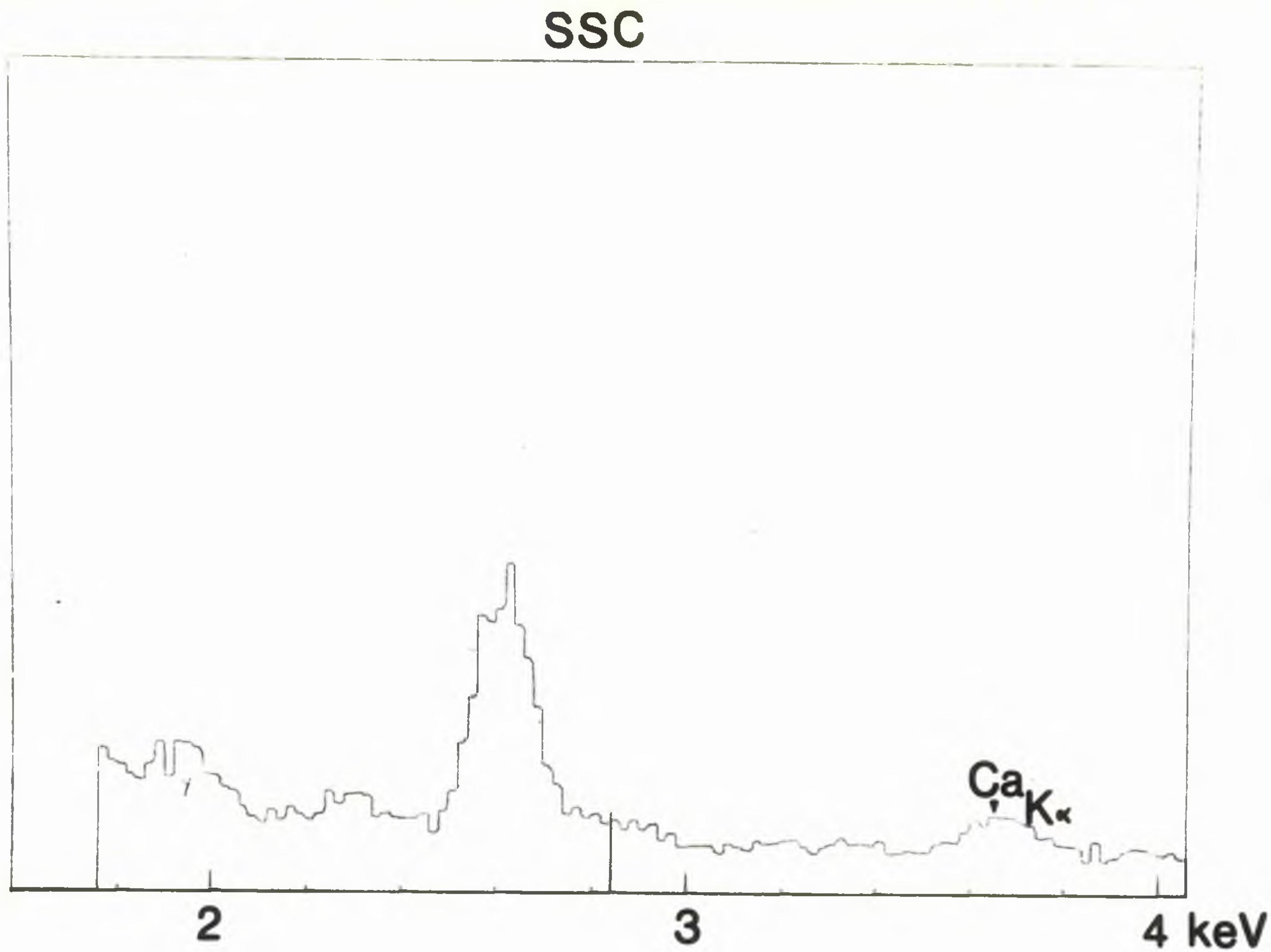
SSC
Ca Kα
2
3
4 keV

Fig. 197

X-ray spectrum: LDSG precipitate

High levels of Os, S, Cl.

Distinct K, Sb and Ca peaks.

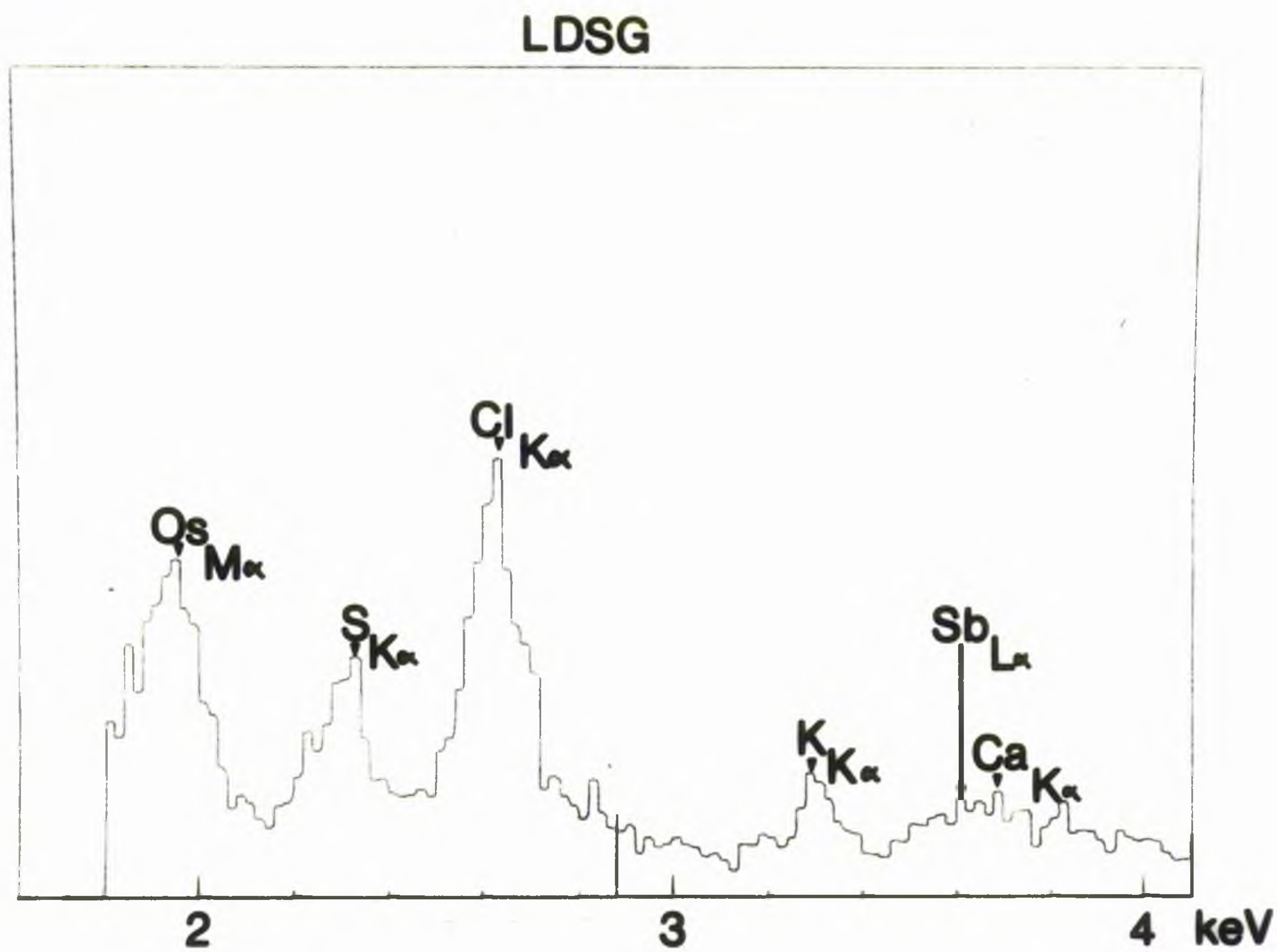
LDSG
Os Mα
S Kα
Cl Kα
K Kα
Sb Lα
Ca Kα
2
3
4
keV

Fig. 198

X-ray spectrum: LDSG precipitate

$Ca_{K\alpha}$ peak is quite distinct from Sb_{L_α} and $Sb_{L\beta_1}$ peaks.

LDSG

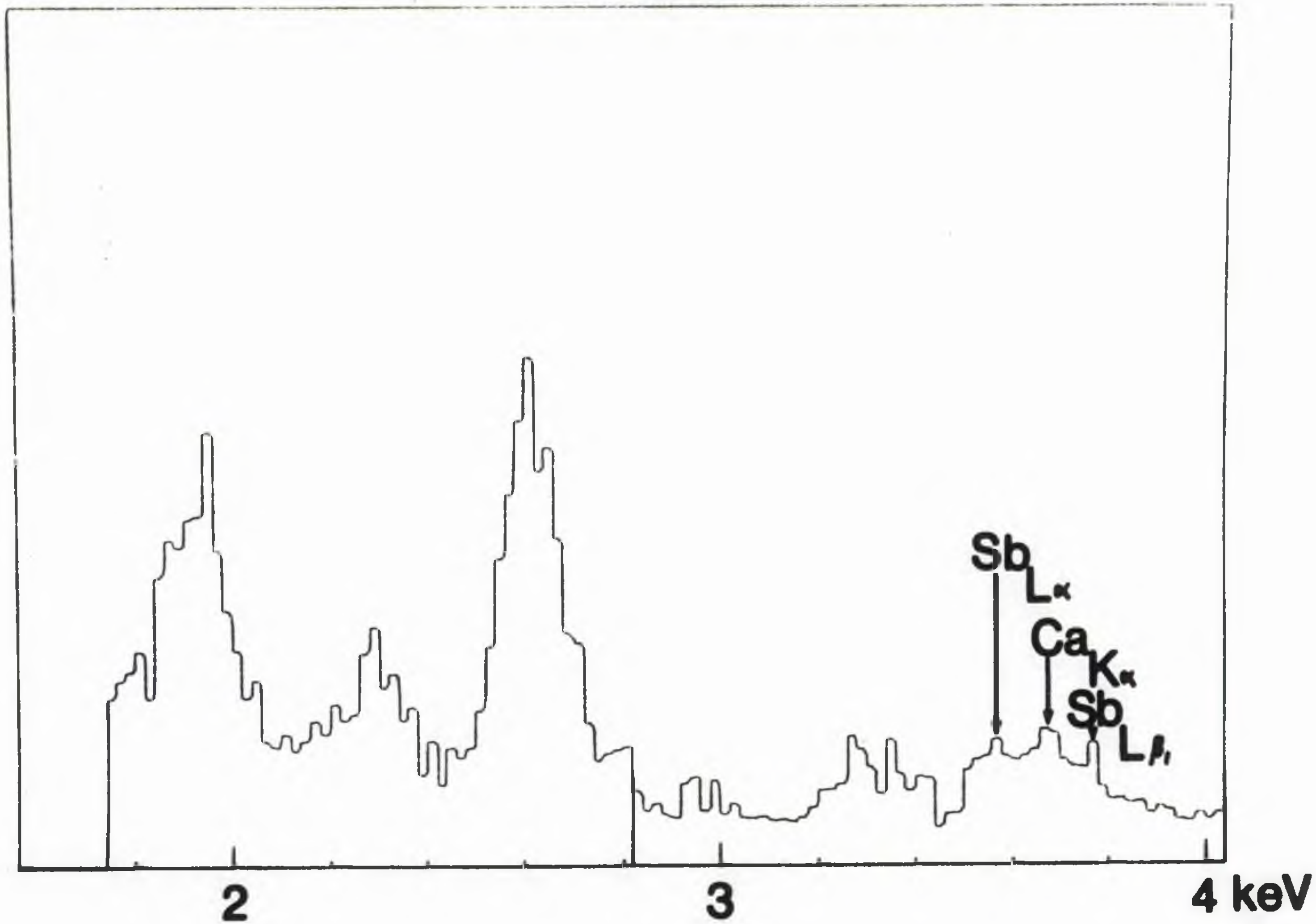

Fig. 199

X-ray spectrum: sarcolemma precipitate

Arrow:- One large peak at 3.6/3.7KeV; distinct Ca peak not visible.

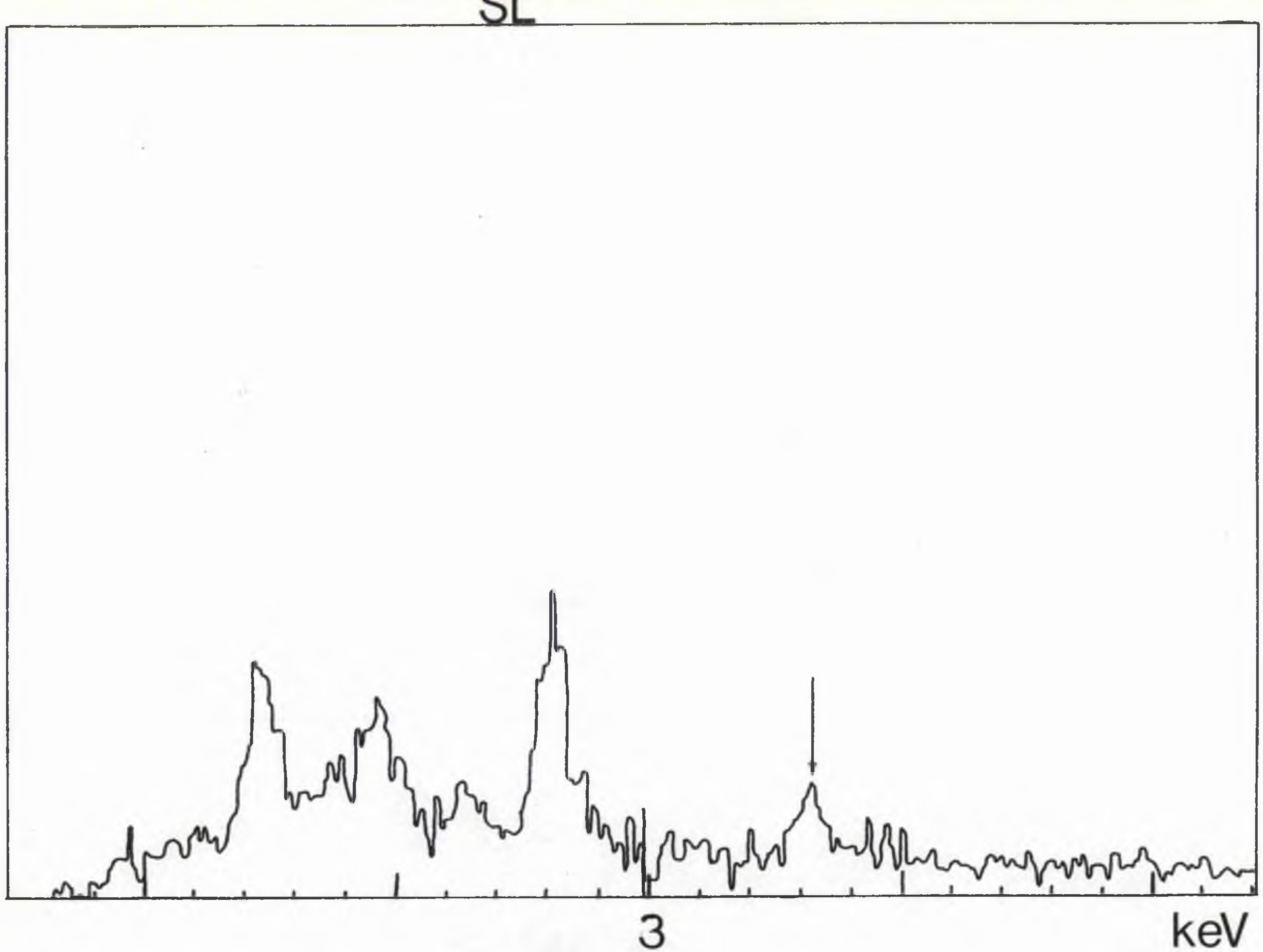
SL
3
keV